Polyploidy and high mountain environments. Evolutionary processes at different scales in the subtribe Leucanthemopsidinae (Compositae, Anthemideae)

Dissertation zur Erlangung des

Doktorgrades der Naturwissenschaften (Dr. rer. nat.)

der Fakultät für Biologie und vorklinische Medizin

der Universität Regensburg

vorgelegt von

Salvatore Tomasello

aus

Palermo, Italien

im Dezember 2014

Das Promotionsgesuch wurde eingereicht am: 18.12.2014

Die Arbeit wurde angeleitet von: Prof. Dr. Christoph Oberprieler

Unterschrift:

Table of Contents

Chapter 1

General Introduction

1.1 Polyploidy

Polyploidy, the presence of three or more complete chromosome sets in an organism (Grant 1981), has long been recognised as a prominent phenomenon in plants. Since many of the world's major agricultural crops (e.g., wheat, oats, cotton, potato, and coffee) have a polyploid origin, plant polyploidy is also of substantial importance to humans. While pregenomics estimates of the number of polyploid plant species ranged between 30-35% (Stebbins 1950), 47% (Grant 1963, 1981), and 70-80% (Lewis 1980), a more recent work inferred the 35% of flowering plants to be neo-polyploid (Wood et al. 2009). However, based on modern whole-genome sequencing techniques it became clear that even diploid lineages have experienced in the past whole genome duplications (WGD), as demonstrated first in *Brassica* (Lagercrantz 1998) and *Arabidopsis* (Vision et al. 2000; Bowers et al. 2003). Based on these findings, the evolutionary history of all angiosperms is considered to be characterised by multiple rounds of genome duplications (Jaillon et al. 2007; Tang et al. 2008; Fawcett et al. 2013).

Although definitions can slightly change with the criteria used, concerning the formation of new polyploids two major types of polyploidy can be distinguished (Stebbins 1947): autopolyploidy and allopolyploidy. Autopolyploids arise via genome duplication within a single individual (or individuals of the same population), which translates into a substantial equality of the genomes involved in the polyploid formation. On the other hand, allopolyploidization occurs through genome doubling subsequent to hybridization between different species, which contribute distinct genomes to the newly formed polyploid (Stebbins 1947; Grant 1975). A main difference between these two types of polyploidy is the behaviour of chromosome during meiosis: While in the first case, chromosomes form multivalents during chromosome pairing of meiosis, in the latter the formation of bivalents prevent

recombination between parental genomes (Ramsey & Schemske 2002). A third and intermediate type is the so called "segmental allopolyploidy", which involves hybridization between genetically distinct races or populations of the same species, and which can therefore lead to the formation of both bivalents and multivalents during chromosome paring (Stebbins 1971; Levin 2002).

There is an on-going discussion about the evolutionary importance of polyploidy, being it rather suggested as a major driving force of plant evolution by some authors (e.g., Soltis & Soltis 2009) or considered a "dead-end" in the evolutionary path (Stebbins 1950, 1971; Mayrose et al. 2011). As a consequence, the recent years have witnessed a renewed interest in different aspects of polyploidy in plants, including questions on the mechanism of polyploid formation and establishment (Ramsey & Schemske 1998, 2002; Husband 2004; Baack & Stanton 2005), on the frequency of recurrent polyploidisation (Leitch & Bennet 1997; Liu & Wendel 2003; Osborn et al. 2003), on population genetics of polyploids (Husband & Schemske 1997; Cook & Soltis 2000; Jørgensen et al. 2011), and on the ecological effects of plant polyploidy (Bayer et al. 1991; Segraves & Thompson 1999; Thompson et al. 2004; Arvanitis et al. 2007; Raabová et al. 2008; Sonnleitner et al. 2010, 2013).

1.2 Mountain and alpine environments

Mountain environments are found where, along an altitudinal gradient, the natural vegetation changes progressively from lowland and montane forest formations, to dwarf-shrubs, grass-, sedge-, and moss-heath formations, and finally to open and frozen ground (Nagy & Grabherr 2009). The term "alpine" is more specifically used for the vegetation types growing above the "treeline", although this boundary is often blurred and fragmented over several hundred meters of altitude (Körner 1995), and may be totally absent in arid mountains (Nagy & Grabherr 2009). More precisely, the treeline is the imaginary line connecting the highest spots, where small stature trees are naturally found in a mountain range, and above of which trees are not able to grow (Hermes 1955; Grabherr et al. 2003; Körner 2003). As the altitude increases, common climatic features of the "alpine life zone" are a decrease in temperature, atmospheric pressure, and air moisture (as consequence of the reduced pressure), as well as an increase in solar radiation (see Körner 2003). A shortened vegetative period due to winter snow coverage is also an additional feature in high elevations

areas of the northern hemisphere temperate mountains, while an accentuated seasonality and summer drought is a characteristic of mountain and alpine environments in mediterranean regions (i.e., oro-mediterranean).

A total area of 4 x 10^6 km^2 of vegetation-covered land falls within the "alpine life zone", which constitutes roughly the 3% of the global land area (Körner 1995). There, about the 4% of the total Earth's flora is found (Heywood 1995). The global latitudinal distribution of the alpine life zone is strongly asymmetric, with 82% of the total alpine area being found in the Northern Hemisphere. Temperate alpine environments represent 55% of the whole alpine life zone (Körner 1995).

Geographical isolation, glaciation and a varied history of species migration and/or evolution led to high degrees of taxonomic richness and genetic complexity in high mountain floras. The total alpine flora of the World is around 8,000-10,000 species, with the majority of alpine taxa being members of the Compositae (Asteraceae) and Poaceae families (Körner 1995). The European Alps are inhabited by approximately 650 truely alpine taxa (Ozenda 1993). The West-East orientation, the more pronounced fragmentation and the greater isolation of the Eurasian mountain ranges from arctic environments caused them to show greater regional variation and speciation compared to mountains in other regions of the world (Körner 1995). Concerning the origins, current alpine floras in most cases are considered to be the product of a mix between ancestral elements (mostly of Tertiary origin), immigrants (of various ages), and new evolutionary lineages (Mexmüller 1954; Billings 1974; Ozenda 1988; Körner 1995). Glaciation, fragmentation (as a product of the orogenesis and glaciation), possibility of migration within altitudinal belts, and the speed of tectonic uplift represent the major selective forces at the continental scale in high mountain environments (Agakhanjanz & Breckle 1995; Körner 1995).

1.3 Polyploidy in high mountain environments

Polyploidy is a particularly important speciation mechanism in plants, and the 15% of all speciation events occurring in plants involves an increase on the number of complete chromosome sets (Wood et al. 2009). This is particularly true in Palearctic species that were strongly influenced by the ice ages (Burnier et al. 2009). The climatic oscillations of the Pleistocene caused substantial changes in ecosystems, dramatic modifications of the European landscape and latitudinal/altitudinal shifts of species distributions (Lang 1994; van

Andel & Tzedakis 1996). In the case of high-mountain organisms, the Quaternary glacial periods, causing downshifts of vegetation belts and the dominance of cold-resistant species over vast geographical areas, created the possibility of genetic exchange and species migrations among presently isolated mountain ranges, e.g., the Alps and the Carpathians (Pawłowski 1928).

High frequencies of polyploids in high latitude and high altitude environments were noted quite early (Tischler 1935, Löve & Löve 1949). However, only few studies tried to assess the incidence of polyploidy in alpine regions, often with contrasting results. Indeed, high fequency of polyploids (63.6%) was observed by Löve & Löve (1967) in the alpine zone of Mt. Washington, and Morton (1993) reported a polyploid incidence of 52.9% in the flora of Cameroon Mountains. By contrast, no significantly higher occurrence of polyploids was reported for the flora of the Hengduan Mountains (22%; Nie et al. 2005), and for the Spanish alpine flora (23%; Loureiro et al. 2013). In the Swiss Alps, Favarger (1957) did not find any difference between the frequency of polyploids in areas above the snow limit and the surrounding lowlands. The supposed higher frequency of polyploids in area heavily influenced by glaciation has been attributed to either the enhanced colonisation abilities of polyploids (e.g., Stebbins 1950, 1985; Ehrendorfer 1980), the increased production of unreduced gametes under environmental stress (Ramsey & Schemske 1998; Otto & Whitton 2000; Mable 2004), or being a consequence of higher hybridisation frequencies (and allopolyploid formation) in areas under influence of strong climatic oscillations during the Pleistocene and Holocene (Palme et al. 2004; Vamosi & McEwen 2012).

The importance of WGD for speciation in areas affected by climatic oscillations was stressed by Stebbins (1984, 1985) in his “secondary contact” hypothesis. Following this author, the species range oscillation having occurred during the alternating cold and warm Pleistocene periods may have helped to produce new contact zones between partially differentiated populations of the same species, giving rise to “intra-specific” hybridization accompanied by polyploidization.

1.4 The subtribe Leucanthemopsidinae

The subtribe *Leucanthemopsidinae* Oberpr. & Vogt (Compositae, Anthemideae) was described by Oberprieler et al. (2007a) based on phylogenetic evidences (Oberprieler & Vogt 2000; Oberprieler 2005; Oberprieler et al. 2007a). It consists of four genera, the three annual

Table 1.1: List of the taxa included in the subtribe Leucanthemopsidinae following Heywood (1975) and Euro+Med (Greuter 2006-2009).

	Ploidy	Altitudinal zone
Castrilanthemum debeauxii (Degen et al.) Vogt & Oberpr.	2*x*	mid-montane (1300-1900 m)
Prolongoa hispanica G.López & C.E.Jarvis	2*x*	colline (300-700 m)
Hymenostemma pseudoanthemis (Kunze) Willk.	2*x*	lowland (<300 m)
Leucanthemopsis alpina (L.) Heywood		
subsp. *alpina*	2*x* 4*x* 6*x*	alpine (2600-3800 m)
subsp. *cuneata* (Pau) Heywood	6*x*	subalpine (1900-2600 m)
subsp. *tomentosa* (Loisel.) Heywood	2*x*	alpine
Leucanthemopsis flaveola (Hoffmanns. & Link) Heywood		submontane-subalpine
Leucanthemopsis longiectinata (Font Quer) Heywood	6*x*	subalpine
Leucanthemopsis pallida (Mill.) Heywood		
subsp. *pallida* var. *pallida*	4*x*	mid-montane
var. *alpina* (Boiss. & Reuter) Heywood	4*x*	subalpine
subsp. *spathulifolia* (J.Gay) Heywood	4*x*	mid-montane
subsp. *virescens* (Pau) Heywood var. *virescens*	2*x*	submontane /mid-montane
var. *bilbilitanum* (Pau) Heywood	2*x*	submontane (700-1300 m)
Leucanthemopsis pectinata (L.) G.López & C.E.Jarvis	2*x*	alpine
Leucanthemopsis pulverulenta (Lag.) Heywood		
subsp. *pulverulenta*	2*x*	submontane
subsp. *pseudopulverulenta* (Heywood) Heywood		submontane

monospecific *Castrilanthemum* Vogt & Oberpr., *Hymenostemma* Willk. and *Prolongoa* Boiss., and the larger perennial genus *Leucanthemopsis* (Giroux) Heywood. Excluding the two species *Prolongoa hispanica* G.López & C.E.Jarvis and *Hymenostemma pseudoanthemis* (Kunze) Willk., all the representatives of the subtribe are to a greater or lesser extent linked to mountain environments. All the species grow in least-developed, incoherent soils, most often represented by sands or debris on siliceous or calcareous rocks, rather close to the coast (e.g., *Hymenostemma pseudoanthemis*) or in open environments at high altitudes (e.g., various *Leucanthemopsis* taxa). All the species of the subtribe are confined to the Iberian Peninsula, except the Moroccan *Leucanthemopsis longipectinata* (FontQuer) Heywood and the widespread *Leucanthemopsis alpina* (L.) Heywood.

Leucanthemopsis (Giroux) Heywood is the largest genus of the subtribe, consisting – according to the present day taxonomy – of six species and numerous infraspecific taxa.

Leucanthemopsis alpina (with all its infraspecific taxa), *L. pectinata* (L.) G.López & C.E.Jarvis and *L. pallida* var. *alpina* (Boiss. & Reuter) Heywood are strictly alpine plants, whereas the rest of the genus consists of taxa being linked at various degrees to high elevations. Four of the six species are polyploid complexes, with ploidy levels ranging from $2n = 2x = 18$ to $2n = 6x = 54$. The most widespread species (*L. alpina*) is a polymorphic species distributed above 2000 m in all the major European mountain systems (Pyrenees, Alps, Apennines, mountains of Corsica, and Carpathians). All three ploidy levels are realized in the different populations of the species. In Table 1.1 a concise description for the different taxa included in the Leucanthemopsidinae is provided.

1.5 Thesis outline

The scope of the present thesis is to shed light on the processes producing diversification through polyploidy in plants, with particular attention to mountain/alpine species. In order to do this, we have investigated the evolution of the members of the subtribe Leucanthemopsidinae at three different hierarchical level.

The first chapter of the thesis is dedicated to the phylogeny of the entire subtribe, with particular emphasis on the position of the Baetic endemic *Castrilanthemum debeauxii* (Degen, Hervier & É.Rev.) Vogt & Oberp. *Castrilanthemum debeauxii* is one of the rarest Iberian plants (Vargas 2010), being found nowadays with only two populations in the "Sierra de Guillimona" (Jaen, Spain). Using coalescence-based methods for species tree reconstruction, we have intended to date the divergence of the narrow endemic *C. debeauxii* from the rest of Leucanthemopsidinae, and to test the monophyly of the subtribe as well as of the genera within it.

In the following two chapters we investigate the reticulate evolution of the genus *Leucanthemopsis*. First, we have tried to establish a suitable method for reconstructing phylogenetic networks in polyploid complexes while disentangling the effect of both stochastic processes intrinsic of (polyploidy) speciation [i.e.., incomplete lineage sorting (ILG)] and hybridization (i.e., allopolyploidization). In the following, we aim at reconstructing a complete phylogeny of the genus. Additionally, we conducted niche reconstruction analyses in order to provide a hypothesis for the origin of the polyploidy taxa of the genus

The last chapter is devoted to the phylogeography of the widespread and polymorphic species *L. alpina*. Here we aimed at evaluating the importance of both polyploidization and glacial history on the ongoing diversification processes in the species. *Leucanthemopsis alpina* is a polyploid complex, showing an extremely high degree of morphological variation throughout its distributional range.

Chapter 2

Chapter 2

Is the extremely rare Iberian monospecific genus *Castrilanthemum* (Compositae, Anthemideae) a "living fossil"? Evidence from a multi-locus species tree reconstruction

Published in: *Molecular Phylogenetics and Evolution* 82 (2015): 118-130.

Salvatore Tomasello[1], Inés Álvarez[2], Pablo Vargas[2], Christoph Oberprieler[1]

[1] Institute of Plant Sciences, University of Regensburg; [2] CSIC "Real Jardín Botánico", Madrid.

2.1 Introduction

The annual species *Castrilanthemum debeauxii* (Degen, Hervier & É.Rev.) Vogt & Oberp. (Compositae, Anthemideae) is one of the rarest flowering plant species of the Iberian Peninsula (Vargas 2010, Jiménez-Mejías et al. 2012). It is the sole member of the genus *Castrilanthemum* Vogt & Oberpr., which has been described based on the type species *Pyrethrum debeauxii* Degen, Hervier & É.Rev. in 1996 (Vogt & Oberprieler 1996) and for which, besides the type specimen collections of Élisée Reverchon dating to the year 1903, only a single further collection made by J. Leal Pérez-Chao in 1978 was available until most recently. Presently, only one restricted population in Sierra de Guillimona is known and has appeared with continuity during the last decade. Its remote and very local potential distribution in some Sierras (Sierra de Castril, Sierra de Cuarto, Sierra de la Cabrilla, Sierra de Guillimona) in the provinces of Jaen and Granada (SE Spain) and its ephemeral appearance as an annual plant led to the inclusion of the species in the Red List of the Spanish Vascular Flora as "critically endangered" (Moreno 2011).

The phylogenetic position of *Castrilanthemum* has been studied by Vogt & Oberprieler (1996) based on morphological characters and by Oberprieler & Vogt (2000), Oberprieler (2005), and Oberprieler et al. (2007a) using molecular phylogenetic methods based on nrDNA ITS and cpDNA trnL/trnF intergenic spacer (IGS) sequences. While cladistic analyses of morphological data (Vogt & Oberprieler 1996) turned out to be equivocal in respects to the phylogenetic position of *Castrilanthemum* in the subtribe Leucantheminae

sensu Bremer & Humphries (1993), the subsequent molecular studies focussing on the Mediterranean representatives of the tribe Anthemideae (Oberprieler & Vogt 2000, Oberprieler 2005) and on the whole tribe (Oberprieler et al. 2007a, 2009) elaborated the consistent placement of the genus in a small and well-supported monophyletic group of genera with a western Mediterranean core distribution. This generic group was raised to subtribal rank as Leucanthemopsidinae Oberpr. & Vogt by Oberprieler et al. (2007a) and, besides *Castrilanthemum,* comprises the larger (6 species) perennial genus *Leucanthemopsis* (Giroux) Heywood and the two annual unispecific genera *Hymenostemma* Willk. and *Prolongoa* Boiss. Within that group, *Castrilanthemum* was found to be the sister-group to the other three genera with a 6-7 Ma long period of independent evolutionary history (Oberprieler 2005). This phylogenetic isolation, together with its geographical restrictedness and its rarity, makes *C. debeauxii* a potential candidate for its designation as "living fossil", a term with some potential for grabbing attention but with an equally divergent history of semantic connotations in evolutionary biology (Darwin 1859; Stanley 1979; Eldredge & Stanley 1984; Fisher 1990; Vrba 1984; Gould 2002).

The molecular phylogenetic reconstructions mentioned suffer from two main shortcomings that hamper a more substantiated discussion of the "living fossil" topic for *Castrilanthemum:* (1) all previous studies were based on a restricted sampling of the members of subtribe Leucanthemopsidinae*,* with the name-giving genus *Leucanthemopsis* only represented by the single species *L. alpina* (L.) Heywood and all other taxa included only sampled from single accessions; (2) the previous studies were based on either the nrDNA ITS region alone or on a combined analysis of this standard region with the cpDNA *trnL*/*trnF* IGS region. Since especially the multi-copy nuclear region nrDNA ITS is quite problematic due to phenomena like concerted evolution and high levels of homoplasy (Álvarez & Wendel 2003), the usage of low- and single-copy nuclear regions have gained further attraction for phylogenetic studies. Candidate single-copy regions for application in the sunflower family (Compositae) were proposed by Chapman et al. (2007) and have been successfully applied since then in a number of studies (Smissen et al. 2011; Brennan et al. 2012; Guo et al. 2012; Gruenstaeudl et al. 2013). With this new array of phylogenetic regions available, however, problems come into focus that are connected to the fact that stochastic mechanisms may produce discordance among the individual gene trees and that those gene trees may not correspond to the underlying species tree (e.g., Brower et al. 1996, Maddison 1997; Avise & Wollemberg 1997; Kingman 1982, 2000; Degnan & Rosenberg 2009; Edwards 2009).

The challenge for the systematists who want to undertake a phylogenetic study based on data from multiple loci is that usually widespread incongruence among gene trees is found as the number of regions taken into account increases. In the past, the standard and universally accepted way to deal with multi-locus data was the concatenation of the sequences from the different regions and the analysis of the obtained "supergene" with the traditional methods used in molecular phylogeny, despite the awareness of the processes leading to different evolution between unlinked genes. Weisrock et al. (2012) have shown that, when processing regions with high levels of discordance, concatenated analyses may produce robust, well-supported, but inaccurate phylogenetic reconstructions. As a consequence, an increasing number of methods have been proposed to estimate the correct species tree without concatenation of sequence data, especially for those cases when incomplete lineage sorting (ILS) is the reason for incongruence among gene trees (Liu 2008; Than & Nakhleh 2009; Liu et al. 2009; Heled & Drummond 2010; Knowles & Kubatko 2010; Fan & Kubatko 2011).

With the present study we aim therefore to (i) reconstruct a well resolved phylogeny of the Leucanthemopsidinae, (ii) to verify the monophyly of the subtribe as well as the monophyly of the genera included in it, sheding light also on the relationships among the different taxa of the subtribe, and (iii) to apply a molecular clock approach to find out the absolute time of the divergence of *Castrilanthemum debeauxii* from the lineage of its closest relatives. In order to achieve these goals we used two plastid regions (cpDNA), the ribosomal internal transcribed spacer (nrDNA ITS), and two single-copy nuclear regions, for a representative number of accessions for each taxon of the subtribe. We used three different approaches to reconcile the results from the different regions, including (i) an analysis based on concatenated sequences, (ii) a tree reconciliation approach by minimizing the number of deep coalescences (Maddison 1997), and (iii) a coalescent-based species-tree method in a Bayesian framework (Heled & Drummond, 2010).

2.2 Material and methods

2.2.1 Plant material. – During 2010 and 2011, individuals belonging to all the taxa of the subtribe Leucanthemopsidinae plus the outgroup taxon *Phalacrocarpum oppositifolium* were collected in the Iberian Peninsula, Corsica, and the Alps. With regards to the Leucanthemopsidinae, three specimens were used for *Castrilanthemum debeauxii*, two for

Hymenostemma pseudoanthemis, and *Prolongoa hispanica,* and 12 for the different *Leucanthemopsis* species with at least one accession per taxon. Since the infrageneric phylogeny of *Leucanthemopsis* was beyond the scope of the present analysis and inclusion of polyploid taxa from that genus reaching tetra- and hexaploid levels would have complicated sequencing and analysis, mainly diploid representatives of this genus were included.

In order to test for the monophyly of the subtribe, further 14 accessions for the analysis came from species belonging to several subtribes of Anthemideae besides the Leucanthemopsidinae. Among those accessions, two individuals belonging to *Phalacrocarpum oppositifolium*, a species which is still unassigned to any subtribe of the Anthemideae (Oberprieler et al. 2009) but considered to be presumably related to the Leucanthemopsidinae, were analysed. A total amount of 31 accessions were included in the present study.

Almost all of the specimens of Leucanthemopsidinae used in the study were collected in the field and instantly dried in silica gel. *Leucanthemopsis pallida* subsp. *virescens* var. *virescens* (sample number LPS185) and *L. pallida* (LPS186) were sampled from specimens kept at MA herbarium. The accessions for *Leucanthemopsis alpina* subsp. *tatrae* (LPS037) and *Phalacrocarpum oppositifolium* subsp. *oppositifolium* (LPS147) were sampled from specimens kept at M herbarium and from the private herbarium of the first author (S.T.), respectively. A complete list of the accessions used in the present study is given in Table 2.1.

2.2.2 DNA extraction, amplification and sequencing. – For the outgroup samples included in the present analysis, we employed DNA extracts stored at the Institute of Plant Sciences of Regensburg University and used in former studies (Oberprieler & Vogt 2000; Oberprieler 2004a, 2004b; Himmelreich et al. 2008). All silica-gel samples belonging to subtribe Leucanthemopsidinae and collected in the Iberian Peninsula during 2011 were extracted using the DNeasy Plant Mini Kit (Qiagen, Venlo, Netherlands). *Leucanthemopsis pallida* (LPS186), *L. pallida* subsp. *virescens* var. *virescens* (LPS185), *L. alpina* subsp. *alpina* (LPS074-1), *L. alpina* subsp. *tatrae* (LPS037), *L. alpina* subsp. *tomentosa* (LPS181-3), and *L. pallida* var. *alpina* (LPS157-3) were extracted using a modified protocol based on the CTAB method by Doyle & Doyle (1987). The quality of the extracted DNA was checked on 1.5% TBE-agarose gels.

Table 2.1: List of the samples used in the study. Asterisks (*) beside accession numbers indicate samples cloned for some of the marker used. Numbers in brackets behind GenBank codes indicate sequences from former studies: (1) Himmelreich et al. (2008), (2) Oberprieler (2004a), (3) Oberprieler (2004b), (4) Oberprieler & Vogt (2000), (5) Lo Presti et al. (2010), and (6) Sonboli et al. (2012).

Taxon	Sample no.	Voucher Information	ITS1	ITS2	*psbA-trnH*	*trnC-petN*	*C16*	*D35*
Achillea tenuifolia Lam.	A205	Armenia, 18.06.2002, Oberprieler 10094 (Herb. Oberprieler).	KM589804	KM589830	FR689911(5)	FR690061(5)	KM589665	KM589719
Artemisia vulgaris L.	A838*	Germany, Regensburg, 16.09.2010, Konowalik s.n. (Herb. Konowalik).	KM589806-KM589809	KM589836	KM589761	KM589799	KM589674	KM589718
Heliocauta atlantica (Litard. & Maire) Humphries	A176	Marocco, Toubkal, 3850 m, 23.08.1992, Kreisch 92/0589 (Herb. Kreisch).	AJ748782(2)	AJ748782(2)	FR689913(5)	FR690063(5)	KM589666	KM589720
Ismelia carinata (Schousb.) Sch.Bip.	A007*	Morocco, Agadir, 26.04.1994, Kilian 3384 (B).	KM589810	KM589832	KM589759	KM589797	KM589675 KM589676	KM589730
Leucanthemum vulgare. subsp. *pujulae* Semmen	A045	France, Pyrenees orientales, Prats de Molo la Preste, 850m, 24.08.1986, Vogt 5053 & C. Prem (Herb. Vogt).	AJ329639(4)	AJ329643(4)	FR689914(5)	FR690064(5)	KM589667	KM589721
Matricaria discoidea DC.	A069	Germany, Jena, Botanischer Garten, Oberprieler 9762 (Herb. Oberprieler, B).	AJ329641(4)	AJ329644(4)	FR689917(5)	FR690067(5)	KM589668	KM589722 KM589723
Nananthea perpusilla DC.	A170*	Italy, Sardinia, Sulcis, NW Portoscuso, 0-20 m, 9.-20.04.1966, Merxmüller 21023 & Oberwinkler (M).	AJ864579(3)	AJ864579(3)	AB683361 (6)	KM589796	KM589672 KM589673	KM589748-KM589750
Plagius flosculosus (L.) Alavi & Heyw.	A793	Italy, Sardinia, Sassari, Ittiri, Bacino Cuga, 19.08.1996, Zedda s.n. (Herb. Vogt).	AJ329640(4)	AJ329640(4)	FR689918(5)	FR690068(5)	KM589669	KM589724
Santolina rosmarinifolia L.	A077*	Morocco, Er-Rachidia, Tounfite - Boumia, 1810-1850 m, 01.07.1989, Oberprieler 1950 (cult. in HB Berol. 07-1-52-91-10).	AJ329638(4)	AJ329642(4)	KM589760	KM589798	KM589677 KM589678	KM589728 KM589729
Tanacetum coccineum (Willd.) Grierson	A197	Armenia, 12.06.2002, Oberprieler 10045 (Herb. Oberprieler).	KM589805	KM589831	FR689920(5)	FR690070(5)	KM589670	KM589725
Tripleurospermum caucasicum (Willd.) Hayek	A192	Armenia, 30.06.2002, Oberprieler 10192 (Herb. Oberprieler).	AJ864590(3)	AJ864590(3)	FR689921(5)	FR690071(5)	KM589717	KM589726 KM589727
Ursinia anthemoides subsp. *versicolor* (DC.) Prassler	A436*	South Africa, Cape Province, Kamiesbergpas, ENE Kamieskroon, 800-1000 m, 12.09.1993, Strid & Strid 37382 (S)	AM774473(1)	AM774473(1)	HE818814(5)	HE818929(5)	KM589671	KM589751-KM589755
Phalacrocarpum oppositifolium (Brot.) Willk. subsp. *oppositifolium*	LPS147	Portugal, Serra de Estrela, Manteigas - La Torre, 1000 m, 10.05.2011, Tomaselli 281 (MA).	KM589820	KM589843	KM589770	KM589790	KM589710	KM589744
Phalacrocarpum oppositifolium subsp. *anomalum* (Lag.) Vogt & Greuter	LPS162-1	Spain, Venta Pepin, Puerto de las Piedra luengas, 1200 m, 16.06.2011, Tomaselli 360 (MA).	KM589822	KM589845	KM589771	KM589803	KM589712	KM589745
Hymenostemma pseudoanthemis (Kunze) Willk.	LPS130-7	Spain, Pinar del Hierro, Chiclana de la Frontera, 30 m, 16.04.2011, Tomaselli 195 (MA).	KM589815	KM589838	KM589765	KM589784	KM589700	KM589740
Hymenostemma pseudoanthemis (Kunze) Willk.	LPS131-9	Spain, Arcos de la Frontera, 260 m, 17.04.2011, Tomaselli 197 (MA).	KM589828	KM589839	KM589766	KM589785	KM589701	KM589741
Prolongoa hispanica G.López & C.E.J.Jarvis	LPS133-6*	Spain, Las Nieves (Nambroca), 650 m, Tomaselli 212 (MA).	KM589816	KM589840	KM589767	KM589786	KM589700-KM589706	KM589742

Table 2.1: Continued.

Taxon	Sample no.	Voucher Information	ITS1	ITS2	*psbA-trnH*	*trnC-petN*	*C16*	*D35*
Prolongoa hispanica G.López & C.E.Jarvis	LPS135-10	Spain, Puente Duero, 695 m, 23.04.2011, Tomasello 221 (MA).	KM589818	KM589842	KM589768	KM589788	KM589708	KM589743
Castrilanthemum debeauxii (Degen & al.) Vogt & Oberpr.	IA2169-20 *	Spain, Sierra Guillimona, 10.06.2011, Alvarez 2169 & Tomasello (MA).	KM589811	KM589833	KM589762	KM589781	KM589668-KM589686	KM589738
Castrilanthemum debeauxii (Degen & al.) Vogt & Oberpr.	IA2170-4 *	Spain, Sierra Guillimona, 10.06.2011, Alvarez 2170 & Tomasello (Herb. Tomasello, MA).	KM589812	KM589834	KM589763	KM589782	KM589668-KM589693	KM589739
Castrilanthemum debeauxii (Degen & al.) Vogt & Oberpr.	IA2171-28 *	Spain, Sierra Guillimona, 10.06.2011, Alvarez 2171 & Tomasello (MA).	KM589813	KM589835	KM589764	KM589783	KM58969-KM589697	KM589746
Leucanthemopsis pulverulenta (Lag.) Heywood	LPS134-1	Spain, Puente Duero, 695 m. 23.04.2011, Tomasello 217 (MA).	KM589817	KM589841	KM589769	KM589787	KM589707	KM589734
Leucanthemopsis pallida var. *alpina* (Boiss. & Reuter) Heywood	LPS157-3	Spain, La Mira (Sierra de Gredos), 2300 m, 12.06.2011, Tomasello 332 (MA).	KM589821	KM589844	KM589774	KM589801	KM589711	KM589755 KM589756
Leucanthemopsis pallida (Mill.) Heywood	LPS186	Spain, Pico Revolcadores (Murcia), 1970 m, 20.04.2006, Aedo 11398 (MA)	KM589827	KM589850	KM589777	KM589794	KM589716	KM589737
Leucanthemopsis pallida subsp. *virescens* var. *bilbilitanum* (Pau) Heywood	LPS138-1 *	Spain, Puerto de Aguaron (Sierra del Vicort), 1000 m, 1.05.2011, Tomasello 247 & Hilpold (MA).	KM589819	KM589851 KM589852	KM589772	KM589789	KM589709	KM589733
Leucanthemopsis pallida subsp. *virescens* (Pau) Heywood var. *virescens*	LPS163-2	Spain, Sierra del Brezo (Montaña Palentina), 1670 m, 17.06.2011, Tomasello 361 (MA).	KM589823	KM589846	KM589773	KM589791	KM589713	KM589732
Leucanthemopsis pallida subsp. *virescens* (Pau) Heywood var. *virescens*	LPS185*	Spain, Valle de Losa, Monte Peñalta, 1000-1095 m, Uribe-Echebarria 77690 (MA)	KM589826	KM589849	KM589780	KM589802	KM589667-KM589681	KM589757 KM589758
Leucanthemopsis pectinata (L.) G.López & C.E.Jarvis	LPS166-11	Spain, Veleta (Sierra Nevada), 13.07.2011, Vargas, Cano & Tomasello 372 (MA).	KM589824	KM589847	KM589775	KM589792	KM589714	KM589735
Leucanthemopsis alpina subsp. *tomentosa* (Loisel.) Heywood	LPS181-3	France, Corsica, Monte Renoso, 2300 m, 08.08.2011, Tomasello 409 (Herb. Tomasello).	KM589825	KM589848	KM589776	KM589793	KM589715	KM589736
Leucanthemopsis alpina (L.) Heywood sub sp. *alpina*	LPS074-1	France, Vallouise, Glacier Blanc, 2380 m, 18.07.2010, Tomasello 40 (Herb. Tomasello).	KM589814	KM589837	KM589778	KM589795	KM589698	KM589747
Leucanthemopsis alpina subsp. *tatrae* (Vierh.) Holub	LPS037	Romania, Gilort, Papusa – Lespezi, c. 2100 m, 29.06.1963, Buia, Paum, Casanova, Fulga & Olaru s.n. (M)	KM589829	KM589853	KM589779	KM589800	KM589699	KM589731

For the phylogenetic analyses, we used two intergenic spacer regions on the plastid genome (*psbA-trnH* and *trnC-petN*), the nuclear ribosomal internal trascribed spacer region (nrDNA ITS), and two single-copy nuclear regions (*C16, D35*) characterised by Chapman et al. (2007). The plastid spacer *psbA-trnH* was amplified using the primers psbAf and trnHr (Sang et al. 1997), whereas for *trnC-petN* we used the primers trnC (Demesure et al. 1995) and petN1r (Lee & Wen, 2004). PCR amplification was performed using the Taq DNA Polymerase Master-mix Red (Ampliqon, Odense, Denmark) in a final volume of 12.5 µl, using the protocol suggested of the company. The following temperature profile was employed: 2 min at 95°C, then 36 cycles of 30 s at 95°C, 60 s at 62°C, 60 s at 72°C, with a final extension of 5 min at 72°C.

Concerning the nrDNA ITS region, ITS1 and ITS2 were amplified separately using the primers 18SF (Rydin et al. 2004) and P2B (White et al. 1990) for ITS1 and P3 (White et al. 1990) and SR (Blattner et al. 2001) for ITS2. The temperature profile used for nrDNA ITS was the same as for the plastid regions, with the only difference that the annealing temperatures of 50°C and 60°C were used for ITS1 and ITS2, respectively. The two single-copy nuclear regions (*C16, D35*) were amplified using either a touch-down PCR program as recommended by Chapman et al. (2007) or the same program used for the ITS and plastid regions with an annealing temperature of 58°C.

The PCR products were purified using Agencourt AMPure magnetic beads (Agencourt Bioscience Corporation, Beverly, Massachusetts, USA). Cycle sequencing was performed using the DTCS Sequencing Kit (Beckman Coulter, Fullerton, California, USA), following the protocol suggested of the manufacturer. Sequences were analysed on a CEQ 8000 sequencer (Beckman Coulter, Fullerton, California, USA) and the obtained electropherograms were carefully checked for ambiguities using Chromas Lite 2.10 (Technelysium Pty Ltd., Tewantin, Australia; http://technelysium.com.au/chromas.html). We used the IUPAC ambiguity code to indicate single nucleotide polymorphisms. In the electropherograms, a site was considered polymorphic when more than one peak was present and the weakest one reached at least the 25% of intensity of the strongest one (Fuertes Aguilar et al. 1999; Mansion et al. 2005). We considered reliable those sequences where the percentage of polymorphisms was not higher than approximately 2% of the total sequence (Lo Presti et al. 2010). Eleven accessions needed to be cloned either for nrDNA ITS or for one of the low-copies nuclear regions (see Table 2.1 for details). Cloning was done using the CloneJET PCR cloning kit (Fisher Scientific, Waltham, Massachusetts, USA) according to the manufacturer's recommendations. Eight colonies were picked for each accession cloned

in order to sample the two possible alleles of a heterozygous individual with a probability of 0.99 (formula from Joly et al. 2006).

2.2.3 Data processing and phylogenetic analyses. – Alignments were done using the Clustal W progressive method for multiple sequences alignment (Thompson et al. 1994) as implemented in BioEdit, version 7.0.5.3 (Hall 1999; http://www.mbio.ncsu.edu/bioedit/bioedit.html) and improved in MAFFT (Katoh et al. 2002; http://mafft.cbrc.jp/alignment/software/), which uses a two-cycle progressive method called FFT-NS-2 (Katoh & Toh 2008). Alignments were finally checked and edited manually. In the *trnC-petN1* alignment, the region between alignment positions 392 and 422 was deleted due to a poly-A microsatellite motive that produced non-informative, presumably highly homoplastic differences among sequences. Gaps were coded as binary characters using the simple gap coding method of Simmons & Ochoterena (2000) as implemented in the software programme GapCoder (Young & Healy 2003).

A maximum parsimony analysis (MP) was done for the plastid regions (*psbA-trnH* and *trnC-petN* concatenated into a single alignment), nrDNA ITS, *C16,* and *D35* separately using PAUP* 4.0 version beta 10 (Swofford 2002). For the plastid alignment, nrDNA ITS, and *D35* the heuristic search was performed with TBR branch swapping in action, for 1,000 random addition replicates. Support for clades was evaluated using bootstrap analyses (Felsenstein 1985). These were performed using 1,000 bootstrap replicates, 100 random addition sequence replicates per bootstrap replicate, with a time limit of 10 seconds per random addition sequence replicate, and ACCTRAN, TBR, and MULPARS in action. For *C16*, the same settings as above were used with the only difference that a time limit of 60 seconds per replicate was used in the heuristic search.

As in the MP analyses, Bayesian inference (BI) phylogenetic analyses were performed with MrBayes, version 3.2.1 (Ronquist et al. 2012) for the plastid regions, nrDNA ITS, *C16*, and *D35* separately. BI is dependent on assumptions about the process of DNA substitution (a model of DNA evolution). Therefore, the models that best fit the sequence information for each of the different regions were selected based on the Akaike Information Criterion (AIC) in MODELTEST, version 3.7 (Posada & Crandall 1998). Information concerning the evolution model and the parameter values accepted for each region is provided in Appendix 1.

The BI analyses were conducted using seven heated chains and one cold one, with a chain heating parameter of 0.2 in the individual runs. The Metropolis-coupled Markov chain

Monte Carlo (MC^3) chains were run for 10^8 generations, with trees sampled every 1,000th generation. Reaching of convergence among searches was checked by examining the average standard deviation of split frequencies and by comparing likelihood values and parameter estimates in Tracer, version 1.5 (Rambaut & Drummond 2007). A burn-in equal to 25% of the run-length was applied as by default (Ronquist et al. 2011). The remaining trees were used to estimate topology and posterior probability (PP) using the "halfcompat" setting for the consensus tree.

2.2.4 Total-evidence tree inference and dating. – The first approach to infer a total-evidence tree from the four gene trees was done producing a supermatrix data set from the five different regions and running a concatenated analysis. One major problem for the implementation of concatenated analyses is the selection of alleles when the accessions (OTUs) are heterozygous at multiple loci. Weisrock et al. (2012) showed that phylogenetic results are influenced by the selection of alleles in the concatenation process and that it is preferable to produce multiple analyses pruning randomly different allele copies across regions each time than choosing arbitrarily only one of the alleles or producing accession-wise consensus sequences of alleles. In contrast to these suggestions, however, we decided to produce allelic consensus sequences for those accessions which had more than one allele per region. This was done because of the observation that in all heterozygous cases in our data set, the different allelic forms of an accession (OTU) formed monophyletic groups in the gene trees. A MP analysis was performed for the concatenated data set for 1,000 random addition replicates, with a time limit of 60 seconds for each replicate. A bootstrap analysis was run using 100 bootstrap replicates, 1,000 random addition sequence replicates per bootstrap replicate and a time limit of 60 seconds per random addition sequence replicate. For the Bayesian analysis, we used a partitioned approach with the model parameters for each locus as in the single region analyses (see above). Two runs, each of eight MC^3 chains (seven heated and one cold one, chain heating parameter of 0.2) were run for 10^7 generations, with trees sampled every 1,000th generation. A "halfcompat" consensus tree was estimated after applying a burn-in equal to the 25% of the total number of sampled trees.

For the coalescent-based, multi-locus tree inference using the minimizing deep coalescences (MDC) criterion, we followed three different procedures: (i) we used the four gene trees obtained from the Bayesian analyses to produce a MDC species tree using the computer package PhyloNet (Than et al. 2008). (ii) We employed the method in an exploratory way, so that we obtained not only the optimal clique (i.e., the MDC tree(s) with

the minimum number of extra lineages), but also the sub-optimal cliques with higher numbers of assumed extra lineages (Than & Nakhleh 2009). In analogy to maximum-parsimony (MP) analyses in gene tree studies, we summarised those sub-optimal clique species-trees by computing a strict consensus tree. In order to express the robustness of clades in the optimal species tree, we calculated equivalents to "Bremer support" or decay index (Bremer 1988) values known from MP analyses by successively computing strict consensus trees with one, two, or more steps (i.e., number of extra lineages) longer than the most parsimonious species trees and inferring whether a certain clade was still present in those sub-optimal solutions. This was done for a total of 40 suboptimal trees with the number of extra lineages up to six steps longer than the number in the optimal reconstruction. (iii) Since the described procedures assume that the gene trees are correct and that their incongruence is a consequence of incomplete lineage sorting alone, we proceeded to infer the species tree under the MDC method to account also for topological uncertainty in the gene tree reconstructions as follows: we used Phylm (Guindon et al. 2010) to produce 100 bootstrap replicate ML gene trees for each of the four independent region sets (cpDNA, nrDNA ITS, *C16, D35*) using the same evolutionary models as for the Bayesian analyses (see above). We then estimated 100 MDC trees in PhyloNet based on the replicate ML gene trees obtained from the Phyml analyses and finally computed a 50%-majority-rule consensus tree from these MDC trees using PAUP* 4.0.

In a third approach to infer a total-evidence tree based on all regions and accessions, we submitted the complete data set to the species tree reconstruction and divergence time estimation procedure in the program *BEAST (Heled & Drummod 2010). The BEAST.xml input files were produced using BEAUti, version 1.8 (Drummond et al. 2012) and comprised 10 different partitions (the sequence information plus the binary coded gap sequences for each of the 5 regions). During the tree search, monophyly was enforced for the Eurasian taxa (all except *Ursinia anthemoides* subsp. *vesicolor* from S Africa). Nucleotide substitution models were chosen as in the Bayesian analyses (see above), but allowed to vary in parameter space around a mean value corresponding to the one given by ModelTest in a normal distribution manner, whereas for the five indel partitions the stochastic Dollo model was employed following Alekseyenko et al. (2008), who argued that this model does not allow back-mutation, being therefore more appropriate to treat indel mutations. A Yule speciation process was chosen as species tree prior, along as the "piece-wise linear and constant root" model for population size. In order to test whether sequences evolved in a clock-like manner, we ran two independent analyses with BEAST version 1.8 (Drummond

et al. 2012) for 5×10^8 generations, sampling every 50,000th generations, and applying in the first analysis a strict-clock model and an uncorrelated log normal relaxed-clock model (Drummond et al. 2006) in the second one. We performed marginal likelihood estimation (MLE) using stepping-stone sampling (SS; Xie et al. 2011; chain length for the MLE = 10^6, number of steps = 100 and alpha = 0.3), for allowing comparison between the two models. Since the uncorrelated log normal relaxed-clock performed better than the strict-clock model (log marginal likelihood: -11721.13 and -11896.88, respectively) an additional analysis was run using the relaxed-clock and the rest of settings as described above. After checking convergence and determining burn-in values in Tracer v1.6, the two independent *BEAST runs were merged using LogCombiner v1.8 (Drummond et al. 2012) and applying a burn-in period of 10% of the total amount of trees sampled. Finally, the remaining 18,000 trees were used to construct a maximum-clade-credibility tree with a posterior probability limit set to 0.5 using TreeAnnotator v1.8 (Drummond et al. 2012).

Two calibration points were used in order to obtain absolute divergence times: The first one was the crown age of the tribe Anthemideae (i.e., the age of the node at the split between *Ursinia* and the Euro-Mediterranean clade of the tribe). It was estimated following Oberprieler (2005), using *ndhF* data for the whole family of Compositae (Kim & Jansen 1995) but adding to the data set the *ndhF* sequence of *Artemisia absintium* L. Re-calibration of these analyses was also necessary because of the fact that a new "oldest" fossil of the family Compositae from North-Western Patagonia suggests an origin of the family in the Early Eocene (50 Ma; Barreda et al. 2010). As a consequence, the age of the tribe Anthemideae was estimated to range between 28 Ma and 38 Ma (for more details about the analysis see Appendix 2). Owing to these age estimates for the tribe, a normally distributed prior for the time to the most recent common ancestor (*tmrca*) was used for the root age (mean: 33.8 Ma, SD: 3 Ma). The second calibration point was the age of *Artemisia* L.*:* The earliest records of *Artemisia* type pollen fossils are from the Lower and Upper Oligocene, in the provinces of Xinjiang and Qinghai, in North-Eastern China (Wang 2004). This allowed us to set a *tmrca* prior for a subset of taxa including the whole Eurasian grade and Euro-Mediterranean clade of Anthemideae, to calibrate the split between the Artemisiinae (the subtribe of Anthemideae exhibiting the *Artemisia* pollen type) and the accessions belonging to the rest of the subtribes of the Euro-Mediterranean clade included in our analysis. Therefore, we applied a log normal prior for this calibration point with an offset of 23.05 Ma (mean: 2.7, SD: 0.5).

2.3 Results

Detailed information on the different regions used in the present study is given in Table 2.2. The nuclear regions are fairly more variable than the two plastid intergenic spacer regions. The most variable region is the low-copy nuclear gene *D35*, which exhibits 159 variable sites (134 of which being parsimony-informative) along its total length of 318 bp. Although being the shorter of the plastid regions, *psbA-trnH* provides a higher number of variable sites and indels.

Table2.2: Characteristics, substitution models, and number of parsimony-informative characters (PI) for each of the molecular markers used.

Marker	Length	Model	Variable sites	PI variable sites	Indels	PI indels
psbA-trnH	493	TVM+G	138	77	49	19
trnC-petN	617	TVM+G	134	69	26	10
nr DNA ITS	495	SYM+G	226	152	40	18
C16	349	HKY+G	139	75	29	11
D35	318	K81uf+I	156	134	31	21

2.3.1 Gene trees. – The four gene trees with support values obtained both from the BI and the MP analyses are shown in Figure 2.1. They are characterised by different degrees of resolution and a considerable amount of topological incongruence among each other. In general, the results of the MP analyses were consistent with those obtained from the BI analyses in all four region sets.

The accessions belonging to subtribe Leucanthemopsidinae form a monophyletic group with strong support (PP and BS values) in both the cpDNA and the nrDNA ITS analyses (Figure 2.1a,b) where *C. debeauxii* is always found holding the basal position. Conversely, the monophyly of the subtribe is not supported in the trees obtained from the two low copies nuclear regions: In region *D35* (Figure 2.1d), the genus *Leucanthemopsis* forms a monophyletic and well-supported group, while the other three annual genera of the subtribe are found as a further monophyletic group with no supported sister-group relationship. In region *C16* (Figure 2.1c), Leucanthemopsidinae are split into two clades, the first being formed by all cloned sequences from *Castrilanthemum,* while the second comprises *Leucanthemopsis*, *Hymenostemma* and *Prolongoa* accessions. The gene tree based on *C16* is highly unresolved when further relationships among genera are considered, presumably a

consequence of the high degree of variation exhibited by this region causing higher levels of homoplasy in the data set (CI = 0.7993, RI = 0.9085).

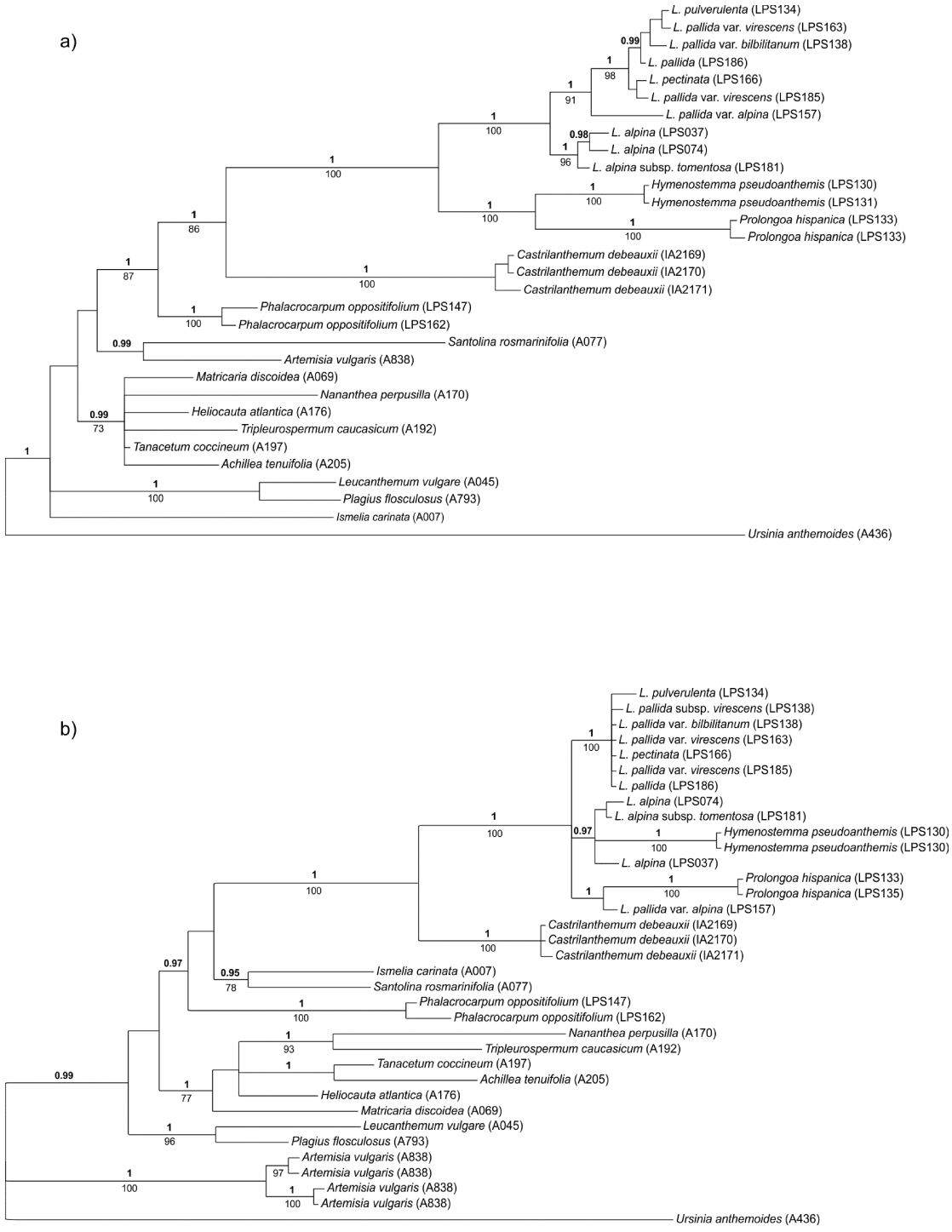

Figure 2.1: Half-compat consensus gene trees obtained from the Bayesian analyses (BI) of (a) the concatenated data set of the two plastid intergenic spacer regions *psbA-trnH and trnC-petN*, (b) the nrDNA ITS region, (c) the single/low-copy region *C16* (Chapman et al. 2007), and (d) the single/low-copy region *D35* (Chapman et al. 2007). Numbers above branches indicate Bayesian posterior probabilities, while those below the branches refer to the bootstrap support values from the Maximum Parsimony (MP) analyses. Accession codes (see Table 2.1) are given in brackets in the leaf labels.

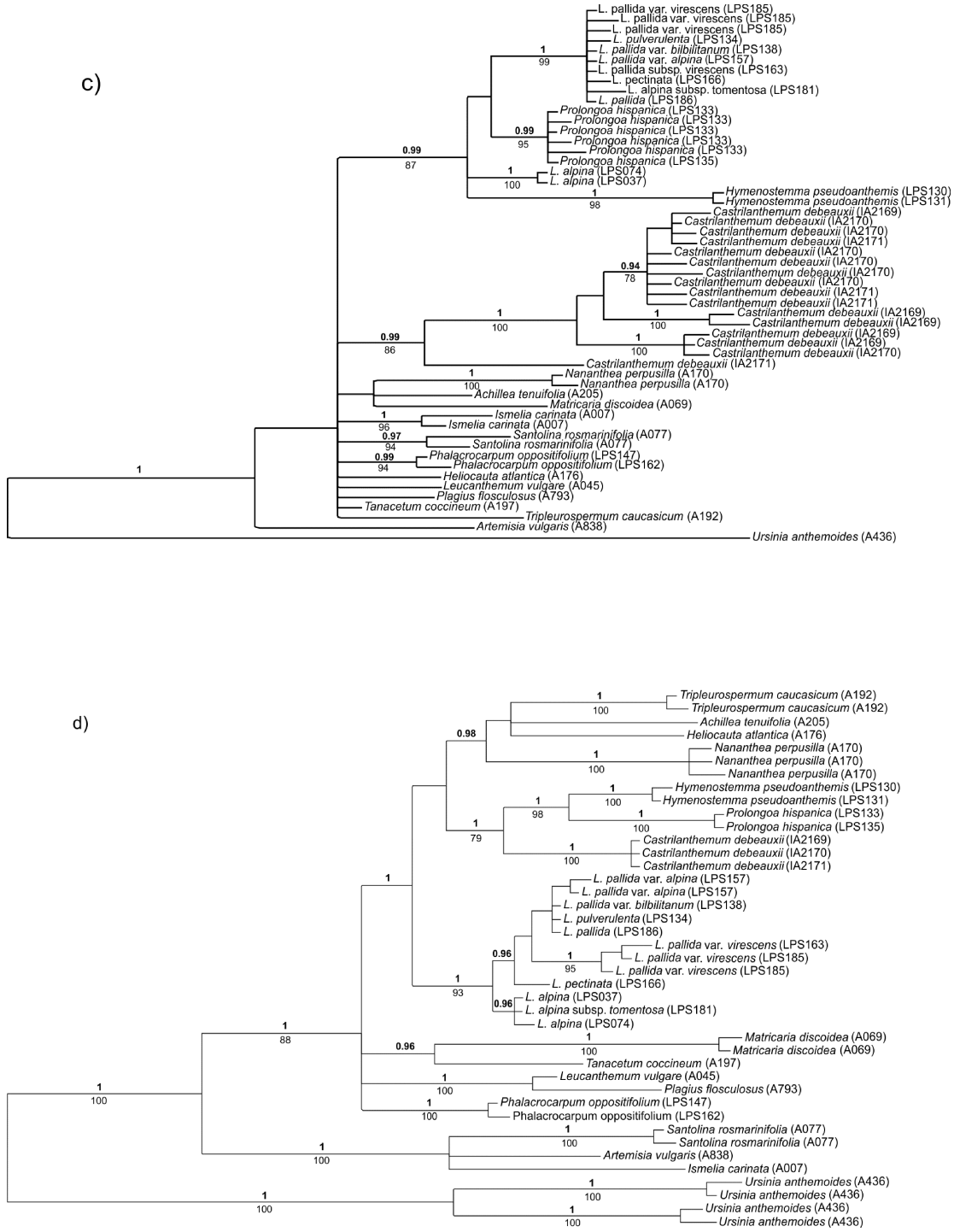

Figure 2.1: Continued.

While in the cpDNA data set, the Iberian genus *Phalacrocarpum* is strongly supported as the sister-group of Leucanthemopsidinae, unresolved relationships in the remaining gene trees based on nrDNA ITS, *C16,* and *D35* render this association equivocal. Besides the above mentioned remoteness of *Castrilanthemum* from the other three genera of the subtribe seen in the cpDNA, nrDNA ITS, and *C16* trees, relationships within the subtribe consistently point towards a bipartition within the genus *Leucanthemopsis* with accessions LPS037 and

LPS074 of the Central European *L. alpina* on the one and the Iberian species *(L. pallida, L .pectinata, L. pulverulenta)* on the other hand, while the position of *L. alpina* subsp. *tomentosa* (LPS181) from Corsica remains equivocal.

2.3.2 Total-evidence tree based on concatenated sequences. – The analyses based on concatenated sequences resulted in well-resolved trees with strong support from posterior probability and bootstrap values (Figure 2.2). The MP analysis yielded six equally-parsimonious trees with a length of 1,482 steps and a topology corresponding to the tree found in the BI analysis. The monophyly of the subtribe Leucanthemopsidinae is strongly supported, along with *Castrilanthemum* being the basal taxon of the clade. The sister-group relationship of *Phalacrocarpum* with the subtribe is also found with considerable support (PP: 1.0, BS: 89%). Within subtribe Leucanthemopsidinae, the monophyly of each of the four genera is well-supported. As in the individual gene trees, the taxa of *Leucanthemopsis* are again grouped into two distinct, well-supported clades, with only *L. alpina* subsp. *tomentosa* (LPS181) remaining unassigned as a consequence of its ambiguous position in the gene trees (cpDNA, nrDNA ITS, and *D35* vs. *C16*).

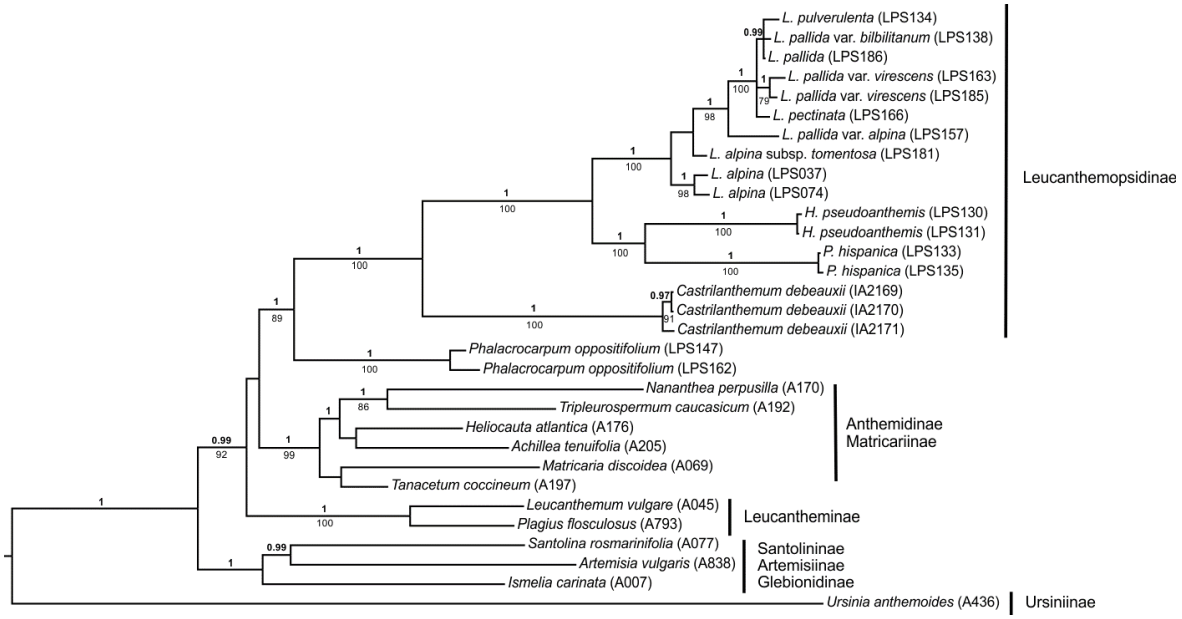

Figure 2.2: Total-evidence tree obtained from the Bayesian analysis of the data set with concatenated sequences from all five regions (*psbA-trnH*, *trnC-petN*, nrDNA ITS, *C16*, *D35*). Numbers above branches indicate Bayesian posterior probabilities, while those below the branches refer to the bootstrap support values from the Maximum Parsimony (MP) analysis.

2.3.3 Coalescent-based multi-locus tree inference with MDC. – The MDC analysis based on four gene trees from three nuclear and two plastid regions produced five equally parsimonious trees. All of them required 54 extra lineages to reconcile the four gene trees used. The strict consensus tree based on the equally parsimonious trees obtained from the MDC analysis is shown in Figure 2.3. Incongruence among these equally parsimonious species/accession trees were only found concerning the relative position among the outgroup taxa from subtribes Matricariinae and Anthemidinae but not in the ingroup of subtribe Leucanthemopsidinae. The bootstrapped analysis produced as expected less resolved results. This is especially pronounced within the genus *Leucanthemopsis,* where the topology of the clade of Iberian representatives is completely unsupported. On the other hand, the monophyly of subtribe Leucanthemopsidinae*,* the basal position of *Castrilanthemum* within the subtribe, the bipartition of *Leucanthemopsis* species into accessions of *L. alpina* on the one side and the Iberian species on the other receive support from bootstrap and decay index values. The sister-group relationship of *Phalacrocarpum* and Leucanthemopsidinae is supported by the bootstrap although it shows a low decay index value.

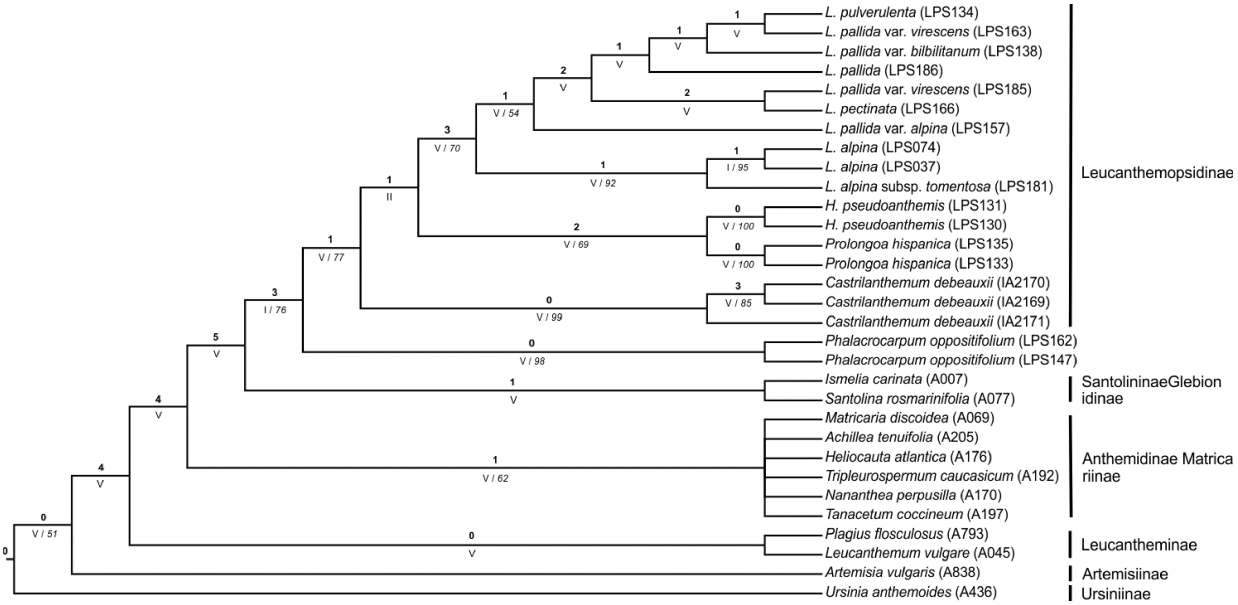

Figure 2.3: Strict consensus tree summarizing the five MDC species tree inferred using the four gene trees (cpDNA, nrDNA ITS, *C16*, and *D35*). The number of extra lineages is given in bold above each branch. Below the branches, the support values obtained from the bootstrap analysis (in italics) and those from the decay index analysis (in roman numbers) are shown. The lowest value for the decay index found (I) is given to clades which are found only in one of the five sub-optimal cliques obtained when running the analyses in an exploratory manner, while the highest values for this index (V) indicates that a clade is found in all the five sub-optimal cliques considered in the exploratory analysis.

*2.3.4 Coalescent-based multi-locus tree and chronogram inference with *BEAST.* – The maximum clade credibility (MCC) tree obtained from the *BEAST analysis is shown in Figure 2.4. Besides its topology, which is corresponding in all major aspects to the species tree reconstruction via the MDC method (see above), it provides time estimates for many important nodes in the evolution of the subtribe Leucanthemopsidinae (Table 2.3). Following these reconstructions, *Phalacrocarpum* forms the sister-group of the subtribe and diverged from the common ancestor of Leucanthemopsidinae around 20 Ma (16.6-24.1 Ma) ago. The divergence of *Castrilanthemum* is dated to the Early Miocene (13.2-20.8 Ma) while the split between the annuals *Hymenostemma* and *Prolongoa* and the perennial genus *Leucanthemopsis* is dated to around 10 Ma ago. Finally, the speciation processes within *Leucanthemopsis* seem to be all influenced by the glaciation cycles during the Pleistocene, with the crown age of the genus (split between *L. alpina* and the Iberian taxa *L. pallida, L. pectinata,* and *L. pulverulenta*) dated to 4.4 Ma (2.6-6.4 Ma) and the further speciation processes within these two sub-groups to more recent times.

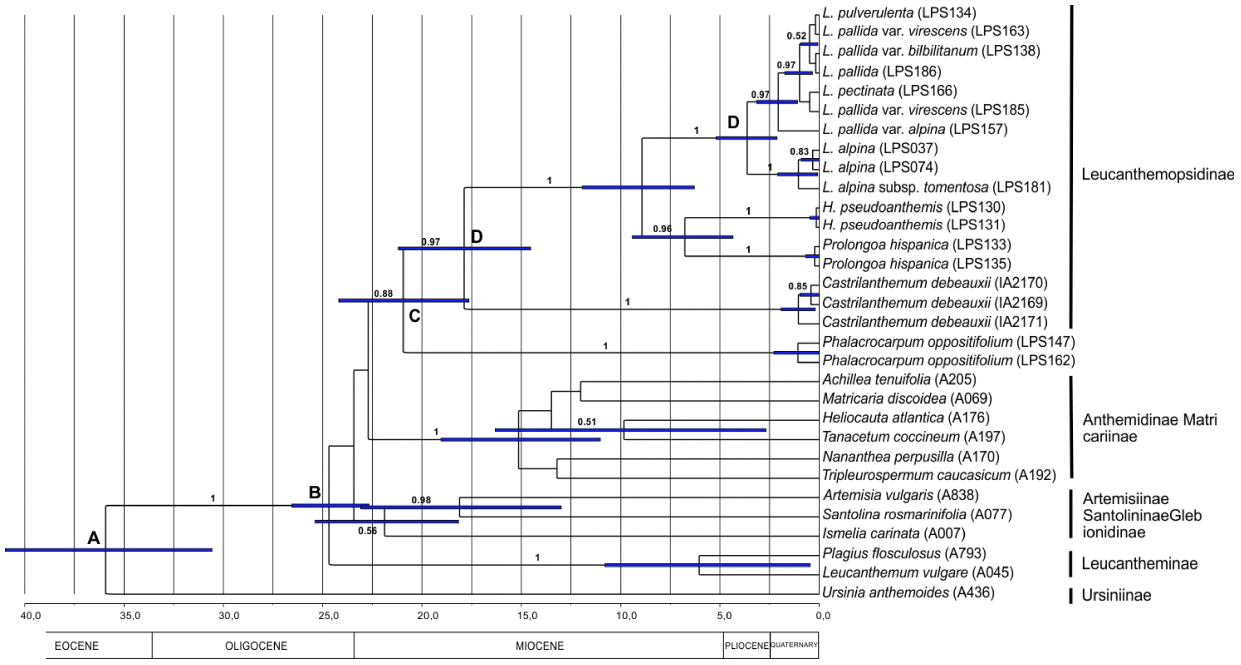

Figure 2.4: Dated multi-locus species tree for the subtribe Leucanthemopsidinae estimated using *BEAST. The chronogram was inferred using sequence data from the five regions (*psbA-trnH*, *trnC-petN*, nrDNA ITS, *C16*, *D35*). The error bars indicate the 95% highest posterior density (HPD) intervals for the divergence times estimates. Numbers above branches indicate Bayesian posterior probabilities. Age estimates for the nodes used for calibration (A and B) as well as age estimates for other important branching events in the subtribe Leucanthemopsidinae (C–E) are detailed in Table 2.3.

Table 2.3: Prior and posterior distribution of age estimates for the calibration points (A and B) and for important nodes (C, D, and E) of the *BEAST chronogram (see Figure 2.4).

node	Description	Prior distribution		Posterior distribution	
		Median	95% HPD interval	Mean age	95% HPD interval
A	Root age	33.78	28.85-38.72	35.46	30.34-40.45
B	Euro-Asian grade crown age	25.43 (Offs.= 23.05)	24.1-28.47	25.16	23.69-27.10
C	*Phalacrocarpum* stem age			20.47	16.64-24.07
D	Leucanthemopsidinae crown age			16.95	13.17-20.78
E	*Leucanthemopsis* crown age			4.39	2.61-6.37

2.4 Discussion

The phylogenetic relationships among members of the subtribe Leucanthemopsidinae of Compositae-Anthemideae presented in this study are based on DNA sequence information from three nuclear and two plastid regions analysed in both a traditional manner after concatenation of sequences and using multi-species coalescent species tree methods. The latter interpret incongruence among gene trees as the result of incomplete lineage sorting (ILS) which is known to negatively influence the soundness of phylogenetic inference especially in the most recent branches of an organism group (Knowles & Kubatko 2010). Despite some incongruence among the four underlying gene trees (three for the nuclear regions, one for the jointly analysed plastid regions), however, we observe a (nearly) complete correspondence between the phylogenetic reconstruction based on a sequence concatenation on the one hand and the two methods of coalescent-based species tree reconstruction (minimizing deep coalescences, MDC; Bayesian species tree reconstruction, *BEAST) on the other hand. We think that this result indicates that the often-disturbing effects of incomplete lineage sorting observed in comparable studies (e.g., Sanchez-Garcia & Castresana 2012) are minimal in the present study group and/or region set. Possible explanations for this lack of dramatic consequences of incomplete lineage sorting in the study group may be due to the small effective population sizes of the mostly narrowly distributed species of Leucanthemopsidinae in conjunction with long branches of species reaching back from between 15 and 25 Ma in the cases of *Castrilanthemum* and *Phalacrocarpum,* and the prevailing of short generation times in the subtribe, with only *Leucanthemopsis* exhibiting perennial life-forms. As a consequence, the most distinctive differences between the concatenated and the coalescent-based analyses are found

concerning the relationships among the taxa of *Leucanthemopsis* (e.g., the position of *L. alpina* subsp. *tomentosa*), where species are more widespread, the generation times of all species are longer, and their radiation into the present diploid taxa was presumably caused by allopatric differentiation processes not earlier than during the Pleistocene.

In this respect, the concatenated analysis exhibits the higher degree of resolution and shows highly supported groups even in the clade of the Iberian representatives of *Leucanthemopsis,* while in the results obtained from the two species-tree reconstruction approaches this is not the case. We consider this observation being a further example for the general trend described by Weisrock et al. (2012) that in the presence of incomplete lineage sorting concatenated analyses could produce well-resolved and highly supported, but untrustworthy clades. Concerning the relationships among taxa within *Leucanthemopsis*, it seems clear that incomplete lineage sorting has played a major role and that more comprehensive studies are needed to shed light on the reticulate evolution of the genus, surely influenced further by polyploidy and (possibly) homoploid hybridisation.

Irrespective of the two reconstruction strategies (concatenated sequences vs. species tree reconstruction methods) or sub-strategies [species tree reconstruction based on a fast maximum parsimony method (MDC) vs. a more time-consuming model-based Bayesian inference method (*BEAST)] the subtribe Leucanthemopsidinae is found to form a monophyletic group with high statistical support. While this is in accordance with previous studies solely based on nrDNA ITS and cpDNA *trnL*/*trnF* intergenic spacer sequences (Oberprieler & Vogt 2000, Oberprieler 2005, Oberprieler et al. 2007a), the phylogenetic relationships among the four genera of the subtribe found in the present, more comprehensive analysis are deviating from these older reconstructions: the two unispecific genera *Hymenostemma* and *Prolongoa* form a well-supported monophyletic group being itself sister to *Leucanthemopsis* in the present reconstructions while the previous ones pointed towards a sister-group relationship between *Prolongoa* and *Leucanthemopsis.* However, since our present analyses are based on more regions, a more representative sampling of taxa (all diploid species of *Leucanthemopsis,* more accessions of the three monotypic genera), and more sophisticated reconstruction methods, we consider the relationships among the four genera of Leucanthemopsidinae as depicted in Figures 2.2, 2.3, and 2.4 more trustworthy. Despite its strongly supported monophyly in the molecular phylogenetic analyses, the subtribe is less well-defined in morphological and anatomical respects: while the three core-genera *Leucanthemopsis, Hymenostemma,* and *Prolongoa* according to a cladistic analysis by Bremer & Humphries (1993) share the presumed

synapomorphies of a reduced number of achene ribs and the joint possession of a scarious adaxial achene corona, the fruits of *Castrilanthemum* with its ten ribs and its lack of an apical corona (Vogt & Oberprieler 1996) changed the circumscription of the subtribe considerably. Because the closely related genera *Hymenostemma* and *Prolongoa* are also quite different in fruit morphological and anatomical respect (with 5-7 equally sized ribs in *Hymenostemma* and two large and three small ribs in *Prolongoa,* Oberprieler et al. 2007b), it is only the annual life-form that is shared between these two genera, which contrasts with the perennial life-form realised in *Leucanthemopsis,* and that may be considered as a synapomorphy of the two (but see discussion of life-form evolution below).

In contrast to previous nrDNA-based phylogenetic studies of the Compositae-Anthemideae (Oberprieler 2005; Oberprieler et al. 2007a) our present results point towards a sister-group relationship between subtribe Leucanthemopsidinae and the hitherto unclassified genus *Phalacrocarpum,* represented here by one of its two species endemic to the Iberian Peninsula. While some morphological features support this interpretation (*Phalacrocarpum* achenes are 7-9-ribbed as in *Hymenostemma* and *Leucanthemopsis* and apically rounded as in *Castrilanthemum*), others like the opposite leaf arrangement and the lack of myxogenic cells on the fruit walls (Oberprieler et al. 2007b) set *Phalacrocarpum* aside from the Leucanthemopsidinae. However, the strong support from the plastid sequence data (Figure 2.1a) together with the lack of hard incongruence between the cpDNA topology and each of the gene trees based on the three nuclear regions and along with the observation that the basal-most leaves of *Castrilanthemum* are also arranged in opposite pairs (Oberprieler et. al. 2007b) corroborate this formerly discussed (Vogt & Oberprieler 1996) but never re-evaluated hypothesis of a closer phylogenetic relationship between *Phalacrocarpum* and the Leucanthemopsidinae.

A further discrepancy between our present analyses and those previous ones based on nrDNA ITS sequences (Oberprieler 2005; Oberprieler et al. 2007a) concerns the temporal diversification of the Leucanthemopsidinae. While the split between *Castrilanthemum* and the other three genera was dated to the Late Miocene (6-7 Ma) in Oberprieler (2005), this split was shifted towards the Early Miocene (13.2-20.8 Ma) in our present multi-locus *BEAST reconstruction (Figure 2.4) and renders *Castrilanthemum* to be an extremely old unispecific lineage. This temporal discrepancy is considerable, but we think that our present reconstructions are more trustworthy because the former estimate has been based on a single region (nrDNA ITS), which is considered quite problematic for phylogenetic reconstructions due to its nature of being a multi-copy region, potentially comprising multiple paralogous

copies that show signs of concerted evolution (Álvarez & Wendel 2003). Additionally, the former reconstruction (Oberprieler 2005) used a less sophisticated molecular dating method (non-parametric rate smoothing, NPRS, Sanderson 1997) with only a single calibration point at the base of the tree (the crown age of the tribe Anthemideae as being 21 Ma) and no internal ones. Finally, our present dating was now based on a newly determined and higher crown age of Anthemideae (27-42 Ma; see Appendix 2) as a consequence of a recently discovered fossil of Compositae from NW Patagonia, which suggests the origin of the family to date back to the Early Eocene (50 Ma; Barreda et al. 2010) as compared to the hitherto alleged maximum age of 35-42 Ma of the family (Graham 1996) used in Oberprieler (2005).

While the Mediterranean region has experienced a trend towards aridification in the Late Miocene between 12 and 7 Ma (Ivanov et al. 2002, Fortelius et al. 2006, Van Dam 2006), the stabilization of a truly Mediterranean climate with summer droughts that may have triggered the switch towards annuality as an efficient adaptation was observed not earlier than in the Pliocene at 5 to 3 Ma (Suc 1984; Bertoldi et al. 1989; Thompson 2005). It is therefore evident that the divergence of *Castrilanthemum* from the closest lineages predates significantly the establishment of the Mediterranean climate in Europe as well as the salinity crisis occurred during the Messinian (5.96-5.33 Ma; Fauquette et al. 2006, Krijgsman et al. 1999). Instead it coincides nicely with the uplift of the Prebaetic System, comprising today's Sierra de Guillimona and Sierra de Castril, occurred during the Middle Miocene, approximately 16 Ma (Sanz de Galeano 1990; Braga et al. 2003). Since the Prebaetic chain emerged as a island system between the water bodies formed by the Guadalquivir depression on the one side and the "Infra Mountains basins" on the other (Vera 2000), the split between the *Castrilanthemum* lineage and its sister-lineage giving rise to the three other genera of the Leucanthemopsidinae could have been the consequence of an allopatric or peripatric speciation process.

When *Phalacrocarpum* is considered to be the sister-group to Leucanthemopsidinae, two equally parsimonious scenarios emerge concerning the evolution of life form in the study group: either we have to assume that a primarily perennial life form evolved into annuality in the most recent common ancestor of the tribe (17-20.5 Ma) and reversed to perennial in the stem species leading to *Leucanthemopsis* (4.5-10.5 Ma), or that an annual life form evolved independently in *Castrilanthemum* (1-17 Ma) and in the ancestor of *Hymenostemma* and *Prolongoa* (7-10.5 Ma). While it has been demonstrated in other plant groups (e.g., Orobanchaceae subtribe Castillejinae; Tank & Olmstead 2008) that a perennial life-form may evolve form an annual one, the palaeoclimatological evidences on the settlement of a

Mediterranean climate in Southern Europe discussed above, are considered to add more weight to the latter scenario (parallel gain of annuality during the Late Miocene and/or Pliocene) than to the former one (evolution of an annual life form in the Early Miocene) and support an interpretation of Leucanthemopsidinae evolution with a permanently perennial stock of mountain-dwelling (*Leucanthemopsis*-like) species as a backbone that shifted towards annuality in at least two independent lineages (*Castrilanthemum, Hymenostemma/Prologoa*).

Following Gould (2002), living fossils are species "belonging to ancient lineages from which most species are now extinct, and which have undergone relatively little evolutionary change" (Wright et al. 2012). While our present analyses demonstrate that the criterion of taxonomical independence or low taxonomic diversity along with a great antiquity of the lineage is certainly true for *Castrilanthemum debeauxii,* the proof of a long-lasting morphological and eco-physiological conservatism is hard to show when fossil evidences are missing, as it is the case in this small and herbaceous representative of Compositae-Anthemideae. As reasoned above, however, it appears reproducible to assume that the shift from an originally perennial to the annual life form of *Castrilanthemum* might have been happened along the long branch leading to its present-day representative *C. debeauxii,* presumably not longer than 3 Ma ago. As a consequence, in respect of this important life-history trait, the modern representative of this lineage might be deviating from the stem species of this branch and, therefore, may not be in accordance with morphological conservatism required for its perception as being a "living fossil". Nevertheless, the evolutionary distinctiveness and the scarcity of this rare species definitively prioritise it and its habitat for conservation efforts (Rosauer et al. 2009; Cadotte & Davies 2010).

Chapter 3

Inferring species networks from gene trees in polyploid complexes by minimizing deep coalescences: an example using the genus *Leucanthemopsis* (Compositae, Anthemideae)

3.1 Introduction

In the last decades, since the development of genome wide techniques of sequencing, molecular phylogenetic studies based on multiple genes have become more and more frequent. As a consequence it has become clearer how important and widespread are discordances across genes, and since Maddison (1997), increasing attention has been paid to the different phenomena producing incongruence. The processes leading to discordant gene trees are diverse and can be grouped in three categories: i) *Stochastic factors* such as incomplete sampling, wrong assumptions, and wrong taxonomical treatment; ii) *Intra-specific stochastic factors* like gene loss/duplication and incomplete lineage sorting (ILS); iii) *Inter-specific factors* as gene flow, horizontal gene transfer (quite common in prokaryotes) and hybridization. Although systematic errors as those mentioned in the first group can be avoided with a good sampling and experimental design, processes as ILS must always be taken in account, as they are intrinsic of the speciation event (Edwards 2009).

Many methods are nowadays available for inferring correct species trees from a sample of gene trees or gene sequences under ILS. Some of these methods use fast algorithms to determine the right species tree topology under the coalescent by Minimizing Deep Coalescences (MDC) (Maddison, 1997), by using average coalescent times (STEAC; Liu et al. 2009) and average ranks of coalescent time [STAR (Liu et al. 2009) and AGID (and Liu & Yu 2011)], or by estimating the species tree using minimum coalescence times across genes (GLASS; Mossel & Roch, 2010). These methods have the advantage of being relatively fast in inferring the species tree but usually the performance is strongly affected as the number of gene used decreases. The alternative would be to use a maximum likelihood (ML) estimation of the species tree (e.g., STEM; Kubatko et al. 2009) and maximum pseudo-

likelihood (MP-EST; Liu et al. 2010), or a Bayesian approach as implemented in software programs like BEST (Liu, 2008) or *BEAST (Heled & Drummond 2010). All these methods assume that ILS is the only cause of incongruence among gene trees and/or between gene trees and the species tree. When other processes are involved in generating discordance, these methods lose accuracy and could even produce misleading results. Leaché et al. (2013) have shown how gene flow can affect the efficiency of Bayesian phylogenetic methods as well as phylogenomic approaches (like in MP-EST) when inferring the underlying species tree. Ignoring gene flow would affect not only the topology of the resulting species tree, but also dating of species divergence and population size in what is known respectively as "species tree compression" and "species tree dilatation". Chung and Ané (2011) came to similar results when using Bayesian approaches to infer the species tree in presence of horizontal gene transfer (HGT).

When hybrid speciation is involved, the idea itself of using a bifurcating tree to represent phylogenies is wrong, as in this case they would be better represented by networks. "Hybrid speciation" implies that hybridization between two species has had a principal role in the origin of a third new species (Mallet 2007). At least 25% of plant species and 10% of animal species are involved in hybridization with other species, especially in recently radiating groups (Mallet 2005). Since Doolittle (1999), who stated that history of life cannot be properly represented by trees, phylogenetic networks have received increasing attention (Linder et al. 2003; Nakhleh et al. 2005b; Gusfield et al. 2007; Jin et al. 2006; Cardona et al. 2008; Nakhleh et al. 2009). Despite that, not many software programs aiming to reconstruct phylogenetic networks are available. The majority of those are mostly useful for single locus analyses from sequence data [e.g., Splitree (Huson & Bryant 2006)]; for infering HGT events by comparing species tree and gene trees [e.g., T-REX (Makarenkov 2001) and RIATA-HGT (Nakhleh et al. 2005a)]; or represent methods for inferring species networks by joining leaves in multi-labeled species tree [e.g., PADRE (Lott et al. 2009) and Dendroscope (Huson & Scornavacca 2012)]. Although the latter would be useful for reconstructing reticulate phylogenies, they assume that the only cause of incongruence in the data set is hybridization (or more in general HGT), ignoring incomplete lineage sorting (ILS). Yu et al. (2013) and Yu et al. (2013) proposed respectively ML and parsimony methods to calculate species networks in presence of ILS, although in these methods the number of reticulations has to be assumed a priori.

Polyploidy (the presence of three or more chromosome sets in an organism) is common in plants, being one of the most important speciation processes in plant evolution. According

to recent estimates, the 15% of all speciation events in flowering plants and the 31% in ferns are represented by polyploid speciation (Wood et al. 2009). Indeed, polyploidization is associated to some of the most important features required by a new formed species, such as reproductive isolation from the parental lineage(s), ecological and/or morphological differentiation. Polyploid speciation can occur via autopolyploidy (when the different sets of chromosome are contributed by a single species) or allopolyploidy (when chromosome are provided by individual of different species and therefore hybridization is associated to it), although the boundary between those two phenomena can be vague. Between the two processes the latter is considered to be more common in plants (Coyne & Orr 2004), representing therefore one of the easiest way in which hybridization can occur. In fact, the reproductive isolation and ecological differentiation features accompanying polyploidization help to avoid most of the problems that a new formed hybrid has to deal with for the establishment of a new hybrid population (e.g., breeding with the parental species, minority cytotype exclusion, competition with individuals of the parental species). It seems obvious then, that a phylogenetic network represent a more proper way to describe the reticulate evolution of polyploid complexes. So far, attempts of reconstructing phylogenies in polyploid groups have been done mostly comparing different gene trees (Popp & Oxelman, 2001; Popp et al. 2005; Ghiselli et al. 2007; Krak et al. 2013), using the network reconstruction methods mentioned above (Lo et al. 2008; Brysting et al. 2011; Marcussen et al. 2012), or comparing morphological and molecular data (Cires & Prieto 2012). However, a proper method to infer phylogenetic networks in polyploid complexes and in presence of ILS has been missing. Jones et al. (2013) proposed novel models (AlloppNET and AlloppMUL) for inferring species networks and MUL-species trees in polyploid complexes, using a Bayesian approach and implemented in the BEAST software.

We are here presenting a simple approach to infer species networks using gene trees in polyploid complexes when both ILS and hybridization are involved. In this approach, the assignment of alleles to parental genome is done by minimizing the number of deep coalescences, as the only process producing incongruence in this case is ILS. Therefore, the network is reconstructed by joining leaves having the same name in the MUL species tree, that is, leaves belonging to the *n* parental genomes constituting the polyploid. We are going to test the efficiency of this method using simulated gene trees, and provide an example on a real data set, using gene trees from the dasy plant genus *Leucanthemopsis* (Giroux) Heywood (Compositae, Anthemideae). *Leucanthemopsis* is a small genus including six species and three different ploidy levels. Its monophyly has been corroborated (see Chapter

2), although no attempt of reconstructing the reticulate phylogeny of the genus including polyploids have been done yet.

3.2 Materials and Methods

3.2.1 Plant material. – A list of the accessions used in the present study, complete of collection information is provided in Table 3.1. Three accessions belonging to the three monospecific genera (*Castrilanthemum* Vogt & Oberpr., *Prolongoa* Boiss. and *Hymenostemma* Willk.), that together with *Leucanthemopsis* constitute of the subtribe Leucanthemopsidinae, were included in the study and used as outgroup. A total amount of 13 accessions from diploid taxa of the genus *Leucanthemopsis* were used in the analyses, possibly with more than one accession per taxon (only *L. pallida* subsp. *virescens* var. *bilbilitanum* (Pau) Heywood was present with one accession). Four polyploids were used to test our method. Two of them were tetraploid accessions belonging to the taxa *L. pallida* subsp. *spathulifolia* (J.Gay) Heywood and *L. alpina* (L.) Heywood. The remaining two were samples belonging to the hexaploid taxa *L. alpina* subsp. *cuneata* (Pau) Heywood from Northern Spain and *L. longipectinata* (FontQuer) Heywood from Morocco. All the accession were collected in the field during the summers of 2010 and 2011 and instantly dried in silica-gel. *Leucanthemopsis. pallida* subsp. *virescens* var. *virescens* (Pau) Heywood (sample number LPS185) was a herbarium specimen from the herbarium of the "Real Jardin Botanico" in Madrid (MA). *Leucanthemopsis longipectinata* (LPS189) consisted of leaf material from a herbarium specimen collected in Morocco in the summer 1992 by C. Oberprieler and R. Vogt (Vogt 9580 & Oberprieler 4016, B).

3.2.2 DNA extraction, DNA amplification, and sequencing. – DNA extracts were mainly obtained using the DNeasy Plant Mini Kit (Qiagen, Venlo, Netherland) in the laboratory of the CSIC "Real Jardin Botanico" in Madrid during summer 2011. Samples LPS185 (*L. pallida* subsp. *virescens*), *L. alpina* subsp. *alpina* (LPS074-1, LPS064-1, and LPS119-7), *L. alpina* subsp. *tomentosa* (Loisel.) Heywood (LPS181-3 and LPS182-1), and *L. longipectinata* (LPS189) were extracted using a modified protocol based on the CTAB method by Doyle & Doyle (1987).

Table 3.1: Comprehensive list of the samples used in the present study including voucher information and GenBank accession numbers. Asterisks (*) beside accession numbers indicate accessions cloned for some of the marker used.

Taxon	Sample no.	2*n*	Voucher Information	*psbA-trnH*	*trnC-petN*	*B12*	*B20*	*C12*	*C16*
Hymenostemma pseudoanthemis (Kunze) Willk.	LPS131-9	2*x*	Spain, Arcos de la Frontera, 260 m, 17.04.2011, Tomasello 197 (MA).	KM589766	KM589785				KM589701
Prolongoa hispanica G.López & C.E.Jarvis	LPS135-10	2*x*	Spain, Puente Duero, 695 m, 23.04.2011, Tomasello 221 (MA).	KM589768	KM589788				KM589708
Castrilanthemum debeauxii (Degen & al.) Vogt & Oberpr.	IA2170-4*	2*x*	Spain, Sierra Guillimona, 10.06.2011, Álvarez 2170 & Tomasello (Herb. Tomasello, MA).	KM589763	KM589782				KM589687-KM589693
Leucanthemopsis pulverulenta (Lag.) Heywood	LPS134-1	2*x*	Spain, Puente Duero, 695 m. 23.04.2011, Tomasello 217 (MA).	KM589769	KM589787				KM589707
Leucanthemopsis pulverulenta (Lag.) Heywood	LPS137-1	2*x*	Spain, Rascafria, 28.04.2011, A. Hilpold & S. Tomasello 235 (MA)						
Leucanthemopsis pulverulenta (Lag.) Heywood	LPS142-2	2*x*	Spain, Puerto de Villatoro, 08.05.2011, Tomasello 270 (MA)						
Leucanthemopsis pulverulenta (Lag.) Heywood	LPS159-1	2*x*	Spain, between Bouza and Pixeiros. 15.06.2011, Tomasello 336 (MA)						
Leucanthemopsis pallida subsp. *virescens* var. *bilbilitanum* (Pau) Heywood	LPS138-1 *	2*x*	Spain, Puerto de Aguaron (Sierra del Vicort), 1000 m, 01.05.2011, Tomasello 247 & Hilpold (MA).	KM589772	KM589789				KM589709
Leucanthemopsis pallida subsp. *virescens* (Pau) Heywood var *virescens*	LPS163-2	2*x*	Spain, Sierra del Brezo (Montaña Palentina), 1670 m, 17.06.2011, Tomasello 361 (MA).	KM589773	KM589791				KM589713
Leucanthemopsis pallida subsp. *virescens* (Pau) Heywood var *virescens*	LPS185*	2*x*	Spain, Valle de Losa, Monte Peñalta, 1000-1095 m, Uribe-Echebarria 77690 (MA)	KM589780	KM589802				KM589679-KM589681
Leucanthemopsis pectinata (L.) G.López & C.E Jarvis	LPS166-11	2*x*	Spain, Veleta (Sierra Nevada), 13.07.2011, Vargas, Cano & Tomasello 372 (MA).	KM589775	KM589792				KM589714
Leucanthemopsis pectinata (L.) G.López & C.E.Jarvis	LPS167-1	2*x*	Spain, Sierra Nevada, Sierro del Caballo, 14.07.2011, P. Vargas, E. Cano & S. Tomasello 364 (MA)						
Leucanthemopsis alpina subsp. *tatrae* (Vierh.) Holub	LPS064-1	2*x*	Slovakia, Visokè Tatry. 2050 m, 03.07.2010, Tomasello 1 (Herb. Tomasello)						
Leucanthemopsis alpina (L.) Heywood subsp. *alpina*	LPS074-1	2*x*	France, Vallouise, Glacier Blanc, 2380 m, 18.07.2010, Tomasello 40 (Herb. Tomasello).	KM589778	KM589795				KM589698
Leucanthemopsis alpina subsp. *tomentosa* (Loisel.) Heywood	LPS181-3	2*x*	France, Corsica, Monte Renoso, 2300 m, 08.08.2011, Tomasello 409 (Herb. Tomasello).	KM589776	KM589793				KM589715
Leucanthemopsis alpina subsp. *tomentosa* (Loisel.) Heywood	LPS182-1	2*x*	France, Vorsica, Col di Rinosu, 10.08.2011, Tomasello 413 (Herb. Tomasello)						
Leucanthemopsis alpina (L.) Heywood	LPS119-7	4*x*	Austria, Pfatcherkofer, 06.08.2010, Tomasello 137 (Herb Tomasello)						
Leucantemopsis pallida subsp. *spathulifolia* (J.Gay) Heywood	LPS150-1	4*x*	Spain, Sierra de Cazorla, 20.05.2011, Y. Sylvester & S. Tomasello 301 (MA)						
Leucanthemopsis alpina subsp. *cuneata* (Pau) Heywood	LPS168-9	6*x*	Spain, Pico de Urbión, 23.07.2011, Himmelreich & Tomasello 376 (Herb. Tomasello)						
Leucanthemopsis longipectinata (FontQuer) Heywood	LPS189	6*x*	Marocco, Djehel Tidirhine, 20.06.1992, R. Vogt & C. Oberprieler. Vogt9580 /Oberprieler4016						

Two chloroplast markers were employed, the intergenic spacer regions *psbA-trnH* and *trnC-petN*). Concerning the nuclear genome, we used four single-/low-copy nuclear markers (*C16*, *B20*, *B12*, *C12*) characterised by Chapman et al. (2007). The chloroplast spacer *psbA-trnH* was amplified using the primers psbAf and trnHr (Sang 1997), whereas for *trnC-petN* we used the primers trnC (Demesure et al. 1995) and petN1r (Lee & Wen 2004). PCR amplification was performed using the Taq DNA Polymerase Master-mix Red (Ampliqon/Biomol, Odense, Denmark) in a final volume of 12.5 µl, and using the protocol suggestions of the company. Except for some cases, the following temperature profile was employed: 2 min at 95°C, then 36 cycles of 30 s at 95°C, 60 s at 62°C, 60 s at 72°C, with a final extension of 5 min at 72°C. The single-copy nuclear markers *C16* were amplified using either a touch-down PCR program as recommended by Chapman et al. (2007) or the same program described for the chloroplast markers, with the only difference that the annealing temperature was set to 58°C. The PCR products were purified using Agencourt AMPure magnetic beads (Agencourt Bioscience Corporation, Beverly, Massachusetts, USA). Cycle sequencing was performed using the DTCS Sequencing Kit (Beckman Coulter, Fullerton, California, USA), following the protocol suggested of the manufacturer. Sequences were analysed on a CEQ 8000 sequencer (Beckman Coulter, Fullerton, California, USA) and the obtained electropherograms were carefully checked for ambiguities using Chromas Lite 2.10 (Technelysium Pty Ltd., Tewantin, Australia o http://technelysium.com.au/chromas.html).

Concerning the nuclear marker *C16*, almost all of the diploid accessions were directly sequenced, having no allelic variation or only single nucleotide polymorphisms. Only the diploid accessions IA2170-4 (from the outgroup taxon *Castrilanthemum debeauxii* (Degen et al.) Vogt & Oberpr.), LPS142 (*Leucanthemopsis pulverulenta* (Lag.) Heywood), and LPS185 (*L. pallida* subsp. *virescens* var. *virescens*) were cloned. All polyploids were cloned except sample LPS150-1 (*L. pallida* subsp. *spathulifolia*), for which direct sequencing electropherograms were readable and no allelic variation was detected. Cloning was done using the CloneJET PCR cloning kit (Fermentas, Waltham, Massachusetts, USA) according to the manufacturer's recommendations. Six, 16 and 27 Clones were picked for diploids, tetraploids, and hexaploids, respectively, in order to have a probability of 0.95 to get sequence information for all the alleles present in each sample (following the formula from Joly et al. 2006). When necessary, we used the IUPAC codes to indicate single nucleotide polymorphisms. In the electropherograms, a site was considered polymorphic when more than one peak was present and the weakest peak reached at least the 25% of intensity of the strongest (Fuertes Aguilar et al. 1999, Mansion et al. 2005).

Table 3.2: Primer information for the molecular markers employed in the study.

Region	Forward primer	Revers primer
psbA-trnH	GTTATGCATGAACGTAATGCTC	CGCGCATGGTGGATTCACAAATC
trnC-petN	CCAGTTCAAATCTGGGTGTC	CCCAAGCAAGACTTACTATATCC
B12	CAAGTGGCTGCAGCCATGGG	ACGTAGTAGTTGATCAACTG
B20	AGTGGWATYAGTGGKGCTAGTTACT	CCACCACGHACAAGMAGCCAAAG
C12	TCTTGCACCACCAACTGYTTGGC	GGGACAATGTTCAATGCTG
C16	ACAAGGCTTTTGGAATTGYCC	TTKCCAGCRAAATCATTWTCAGGRGT
M13	CACGACGTTGTAAAACGAC	
TitA	CGTATCGCCTCCCTCGCGCCATCAG	
TitB	CTATGCGCCTTGCCAGCCCGCTCAG	

Allelic variation for the remaining three low-/single-copy was inferred via Roche 454 next generation sequencing in order to avoid the cloning step. Amplicons to be used in the 454 sequencing procedure were produced using two rounds of PCRs. In the first round, Peqlab KAPAHiFi polymerase (Peqlab Biotechnologie GmbH, Erlangen, Germany) was employed in order to reduce as much as possible PCR errors. The PCR was performed in a final volume of 15 µl, following the manufacturer suggestions and using the following program: 95°C for 5 min; 20 sec at 98°C, 30 sec at 65°C to 61°C, 30 sec at 72°C for 5 cycles; finally 35 cycles of 98°C for 20 sec, 60°C for 30 sec, 72°C for 30 sec, with a final extension step of 72°C for 5 min. The forward primers used for the amplifications were especially designed from Chapman et al. (2007) by the addition of a 29 bp long M13 forward tail. A GS FLX Titanium Primer B was added to the original reverse primers. Reverse *B12* and *C12* primers were also modified in order to obtain amplicons that not exceed the length of approximately 350 base pairs. For complete information on the primers used in this study see Table 3.2. After purifying the PCR products as described above, the second PCR round was performed in order to add a 4 bp Multiplex Identifiers (MIDs) to the amplicons. The MIDs are the sequence tags that allow individual identification (a specific MID was assigned to each individual). The forward primer used for the second PCR round consisted therefore of the following sequence combination: GS FLX Titanium Primer A – MID – M13-tail, while the reverse primer was always the GS FLX Titanium Primer B. A two-steps-PCR program was employed: 3 min at 95°C; 20 cycles of 20 sec at 95°C and 1 min at 68°C; with a final extension of 5 min at 72°C. Subsequently, the PCR products were purified and the concentration measured by fluorometric quantification using the Qubit® 2.0 Fluorometer (Invitrogen, Carlsbad, California, USA). Additionally, the length of each amplicon was

assessed from an agarose gel picture using the software GelAnalizer2010a (available from www.gelanalyzer.com). Lengths and concentrations of products were then used to reach equimolarity among samples with equal ploidy. This was done in order to obtain numbers of reads per sample in the NGS process that would guarantee us a 0.95 probability of sampling all the alleles of an accession represented by at least 10 reads. It was considered important to have at least 10 reads of every allele in order to better distinguish between real alleles and eventual recombinants or PCR artifacts. The probability of obtaining a certain number of reads for an allele when having an *n* number of total reads for a sample (and for one marker) is actually following the binomial distribution:

$$P(k,n) = \left(\frac{n!}{k!(n-k)!} \right) \cdot p^k \cdot q^{n-k}$$

where *k* is the number of successes (e.g., the number of reads for a certain allele), *n* is the total number of reads, *p* the probability that the event occurs and *q* is the probability that it doesn't occur (i.e., $q = 1- p$). Since the sum of the probabilities of the binomial distribution is 1, the probability of obtaining at least 10 reads for one allele is:

$$1 - \sum_{k=0}^{10} P(k,n)$$

Finally the probability of having at least 10 reads for all the allele forms is the product of the probabilities for each allele:

$$\prod_{a=2}^{m} \left(1 - \sum_{k=0}^{10} P_a(k,n) \right)$$

a being the number of alleles and *m* the maximum value expected for this variable (i.e., four in tetraploids, six in hexaploids). According to the formulas above given, and assuming no PCR bias between alleles (but see Wagner et al. 1994), the number of reads we needed to have the 0.99 probability of obtaining at least 10 reads for each allele was 33 for a diploid, 102 for a tetraploid, and 155 for a hexaploid. These reads proportions were taken into account when preparing the final library and mixing samples of different ploidy. For example, if the PCR products of a diploid and a tetraploid were equimolar, an amount of the tetraploid's PCR product 3.09-fold the diploid's product amount (i.e., 102/33) was placed into the mix, in order to obtain the right number of reads for both samples after the sequencing process. The final library was processed and sequenced by Microsynth AG (Balgach, Switzerland).

3.2.3 Deciphering of alleles. – After retrieving of the reads, they were assigned to the species and marker using R (R Development Core Team 2008) and the Galaxy webportal (Giardine et al. 2005, Goecks et al. 2010) as described by Griffin et al. (2011). The MIDs, M13-tails, and the forward and reverse primer sequences were removed using the tools available in the Galaxy webportal (Blankenberg et al. 2010). Subsequently, the quality of reads was assessed and reads with phred values of 20 or below for more than 20% of the sequence positions were discarded (Blankenberg et al. 2010). After quality filtering, each accession was analyzed separately for each marker in the following way: to detect allelic variation, reads were aligned using mafft 6.833b (Katoh et al. 2002; Katoh & Toh 2008) and then subjected to a Bayesian cluster algorithm implemented in BAPS 5.2, using the "clustering with linked loci" option (Corander et al. 2006; Corander et al. 2008; Cheng et al. 2011). The clusters found by the program were considered being either alleles or recombinants.

According to the results of clustering, reads were grouped allele-wise for each accession and marker separately in BioEdit (Hall 1999). The alignments were inspected visually. When a read variant – cluster found in BAPS– was too rare (e.g., it was registered with a number of reads lower than axpected accourding to the probability function mentioned above) was considered a PCR artifact or a recombinant and excluded from further analyses. Read variants that exceded slightly the minimum number or reads expected, but were clearly composed by parts of other alleles (e.g., beginning of an allele and end of another) were considered recombinants and discarged. Recombinants were also discovered with BAPS, using admixture based on mixture clustering (Corander & Marttinen 2006). Therefore, in order to get rid of singleton PCR errors, the reads of those clusters that were considered to be alleles were collapsed to 80% majority rule consensus sequences, and those were finally kept for further analyses.

3.2.4 Gene tree estimations. – Bayesian Inference (BI) phylogenetic analyses were performed with MrBayes v.3.2.1 (Ronquist & Huelsenbeck 2003) for the chloroplast markers combined in a single alignment, and for the four low-/single-copy markers separately. Two sets of analyses were executed, one using only diploid accessions, the other including also all alleles from polyploids. Model selection for each analysis was done in jModelTest version 2 (Darriba et al. 2012) and using the Akaike information criterion (AIC) to choose the best fitting model. Comprehensive information on the alignments and selected models are given in Table 3.3.

Table 3.3: Molecular region characteristics. Variability is calculated as number of variable sites/alignment length.

Marker	Region type	OTUs	Length	Model	(a) Variable sites	(b) Indels	Variability (a)	Variability (a+b)
psbA-trnH	Chl. intergenic spacer	20	425	TPM1uf+I	59	10	0.139	0.162
trnC-petN	Chl. intergenic spacer	20	564	TPM1uf+I	91	11	0.112	0.128
B12	Coding	44	400	TIM1+G	81	10	0.203	0.238
B20	Coding	42	322	TIM3+G	66	8	0.205	0.23
C12	Coding	46	323	TPM2uf+G	78	12	0.241	0.279
C16	Coding	33	186	HKY+G	73	8	0.392	0.435

The analyses were run using seven heated chains and one cold one, with a chain heating parameter of 0.2 in the individual runs. The Metropolis-coupled Markov chain Monte Carlo (MC^3) chains were executed for 10,000,000 generations, with trees sampled every 1,000th generation. In order to check for reaching of convergence, the average standard deviation of split frequencies was considered (acceptable when < 0.01) and likelihood values and parameter estimates were compared in Tracer v.1.5 (Rambaut & Drummond 2007). A burn-in equal to the 25% of the total run length was applied as by default (Ronquist et al. 2011). The remaining 7,501 trees were used to estimate topology and posterior probability (PP) using the halfcompat settings for the consensus tree.

3.2.5 Species network inference. – The most crucial step in the reconstruction of the species network formed by diploids and their auto- or allopolyploid derivates was considered to be the reconstruction of the so-called multi-labelled tree (MUL-tree), in which terminal leaves represent either (i) diploid taxa/accessions or (ii) diploid genomes contributing to the formation of polyploids either in a reticulate (allopolyploids) or a non-reticulate (autopolyploids) manner. The inference of the MUL-tree for the present data set was carried out following the parsimony-based Minimizing Deep Coalescences (MDC) principle (Maddison 1997, Than & Nakhleh 2009) implemented in PhyloNet (Than et al. 2008). The inference of a species network was then easily accomplished by joining leaves representing "parental gemomes" of the polyploids into reticulation nodes using the software program PADRE (Lott et al. 2009).

Since the parental relationships of polyploids with the diploid ancestors are unknown, two main problems arise when more than two alleles per gene are present in a polyploid. (a) We do not know how the "parental genomes" contribute alleles to the polyploid for a given locus. When the maximum expected number of alleles in a polyploid is observed, the number

of possible combination of alleles contributed by parental genomes is 2^n-1 (n being the number of parental genomes). We addressed the problem of allele assignment by running for each polyploid accession several MDC species tree analyses (e.g., one for each possible allele combination in a gene) including the polyploid together with all diploid taxa. We kept then the allele combination leading to the best species tree result (i.e., the species tree with the lowest number of deep coalescences). After finding all the allele pairs per locus (and those for all polyploid accessions) another problem arises when working at multiple loci. (b) We do not know how the different allele pairs are combined one another across genes. The number of possible combinations in this case grows exponentially with the number of genes included in the study. For a tetraploid we will have 2^n possible combinations, 3^n for a hexaploid etc..., n being the number of genes used. We addressed this problem by running for each polyploid separately several further MDC species tree analyses based on all gene trees and including all diploid accessions together with the polyploid, in which all different combinations of allele pairs across loci were tried. As in the previous step, for each polyploid accession we kept finally the allele pair combination producing the most parsimonious species tree.

Once this procedure is repeated for all the polyploid accessions separately, we could produce an allele map, in which all alleles are associated to the different diploid taxa and "diploid parental genomes" of the polyploids. We proceeded therefore with the inference of the MUL-species tree and subsequently with the species network reconstruction as specified above. Compiling the input PhyloNet files during steps (a) and (b), as well as for scoring the results of the species tree analyses and inferring the MUL-species tree, was done automatically, using the script provided by Wagner (2013) and implemented in the software package MATLAB (MATLAB R2012b, MathWorks Inc., Natick, MA).

3.2.6 Coalescent simulations. – In order to infer whether and under which circumstances our here presented method for species network inference in polyploid complexes produces trustworthy results, we performed MUL-tree reconstructions (as a prerequisite of species networks) based on gene trees from coalescent simulations. The predefined hypothetical species networks (Figure 3.1) used for simulating the gene trees included three diploids and one tetraploid and the following parameters were allowed to vary: (1) topology of the species network (i.e., formation of the allotetraploid by (a) hybridization between two sister taxa, (b) hybridization between two non-sister taxa or (c) polyploidization involving the ancestor of two extant taxa); (2) the relative time intervals for the formation of the allotetraploid and

the age of the split between the two parental lineages; (3) the effective populations size N_e used in the coalescent simulations. The effect of the number of gene trees underlying the MUL-species tree reconstruction was also tested by using 2, 6 or 10 simulated gene trees in different analyses.

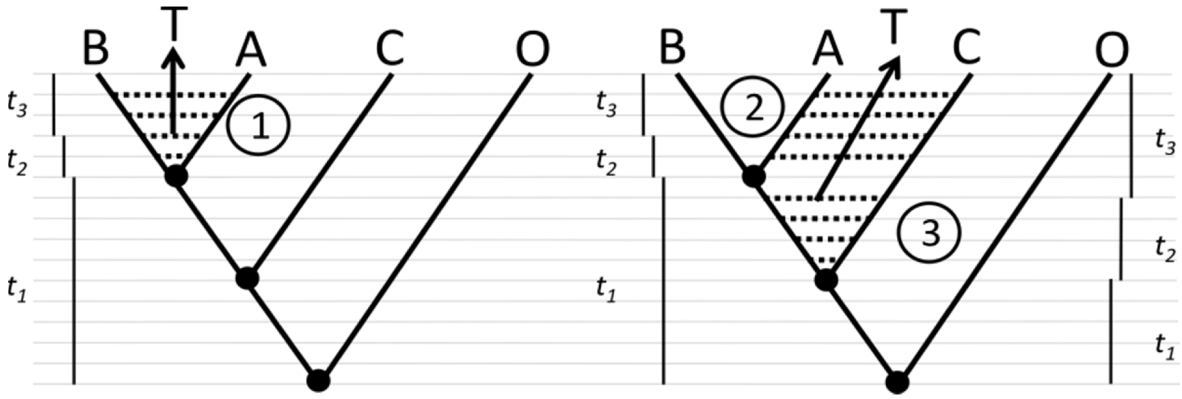

Figure 3.1: The 12 different combinations of topological and temporal scenarios. In scenario number 1, the allotetraploid (T) is formed by hybridization between the sister taxa A and B; in scenario 2 by hybridization between two non-sister taxa (A and C); finally in scenario 3 the polyploidization involves the ancestor of two extant taxa (A and B) and the non-sister taxon C. Time intervals t_3 and t_2 represent respectively the age of the formation of the allotetraploid and the temporal gap between the spit of the two parental species and the formation of the allotetraploids. t_1 is the time elapsed from the root of the MUL-tree to the split between the species forming the allotetraploid.

Based on the above described parameters (1) and (2), 12 MUL-tree chronograms were constructed for the combination of the three topological scenarios with the different, incrementally varying, temporal scenarios [the temporal gap between the split of the two parental species and the formation of the tetraploid (t_2 in Figure 3.1) = 2×10^4, 4×10^4, 6×10^4, and 8×10^4 generations, being the age of the split between the parental species ($t_2 + t_3$) = 1.0×10^5 and 2.0×10^5 generations in the topological scenarios (a) and (b) and scenario (c), respectively]. These chronograms were subjected to gene tree simulations in Mesquite (Maddison & Maddison 2011) using three different values for effective population size N_e (parameter 3; N_e = 10,000, 100,000, 1,000,000) and allowing for sampling two alleles per terminal taxon of the MUL tree (i.e., two alleles for diploids and four alleles for the allotetraploid). In order to allow the assessment of accuracy of our species network reconstruction method, gene tree simulations for each of the described parameter constellations were repeated 100 times. The results of the species network reconstruction following the algorithm described in the previous paragraph were finally scored for either correct or incorrect inference of the topology of the MUL-tree used for the simulations.

The effects of taking into account branch lengths of gene trees onto the accuracy of the species network reconstruction were studied by repeating the analyses on the above mentioned simulated data sets using the option “Infer_ST_MDC_Time” in PhyloNet.

3.3 Results

3.3.1 Coalescent simulations. – Results of the simulation studies based on the topologies of gene trees are depicted in Figure 3.2. As a first general trend concerning the accuracy of reconstructing the right MUL-tree is (a) the rise of score values with the increasing number of underlying gene trees. Further trends are the gain in accuracy of the reconstruction process with (b) decreasing effective population sizes N_e and (c) with allopolyploid formation taking place relatively recently (at higher values for t_2) with respect to the divergence age of the parental diploid lineages (i.e., values for $t_2 + t_3$). Finally (d), while accuracy values are only marginally different when allopolyploid formation results from combination of sister taxa (scenario 1) vs. non-sister taxa (scenario 2), with slightly higher values in the latter case, formation of allopolyploids in more internal (and less recent) regions of the tree (scenario 3) is observed to lead to a relative reduction of accuracy values, at least when effective population sizes exhibit medium or large values (N_e = 100,000, 1,000,000). Additionally, in this scenario the relative ratio between the divergence age of the parental diploid lineages ($t_2 + t_3$) and the age of the allopolyploid formation t_3 seems to be less influential than in the other two scenarios. Results are slightly improved when including gene tree branch lengths for the inference of the MUL species tree, especially under the parameter combinations that produce low accuracy. Detailed information on the results are given in Table 3.4 (with the branch length option off) and Table 3.5 (branch length option on).

3.3.2 Sequencing and gene tree estimation. – Concerning next generation sequencing results, the numbers of sequences obtained per individual per marker were higher or close to those we expected. Only for *L. pallida* subsp. *virescens* var. *virescens* (LPS185) in *B20* we obtained only 19 reads, while the preset number of reads was 33 in order to have 0.99 probability of owning at least 10 reads of each allele. The number of reads obtained for *Castrilanthemum debeauxii* (one of the outgroups) in *B20* and *B12*, for *L. pallida* subsp. *virescens* var. *bilbilitanum* (LPS138-1) and *L. pulverulenta* (LPS142) in *B20* was also slightly lower than expected. The number of alleles obtained for the nuclear markers did not

exceed the number expected, except for *L. pallida* subsp. *virescens* var. *bilbilitanum* (LPS138-1) and *L. alpina* subsp. *tomentosa* (LPS182-1), with three and four alleles respectively in *C12*, and for *C. debeauxii*, for which three alleles were found in *B20* and even seven in *C16*. Although, in the latter marker, many "pseudoalleles" may be the product of

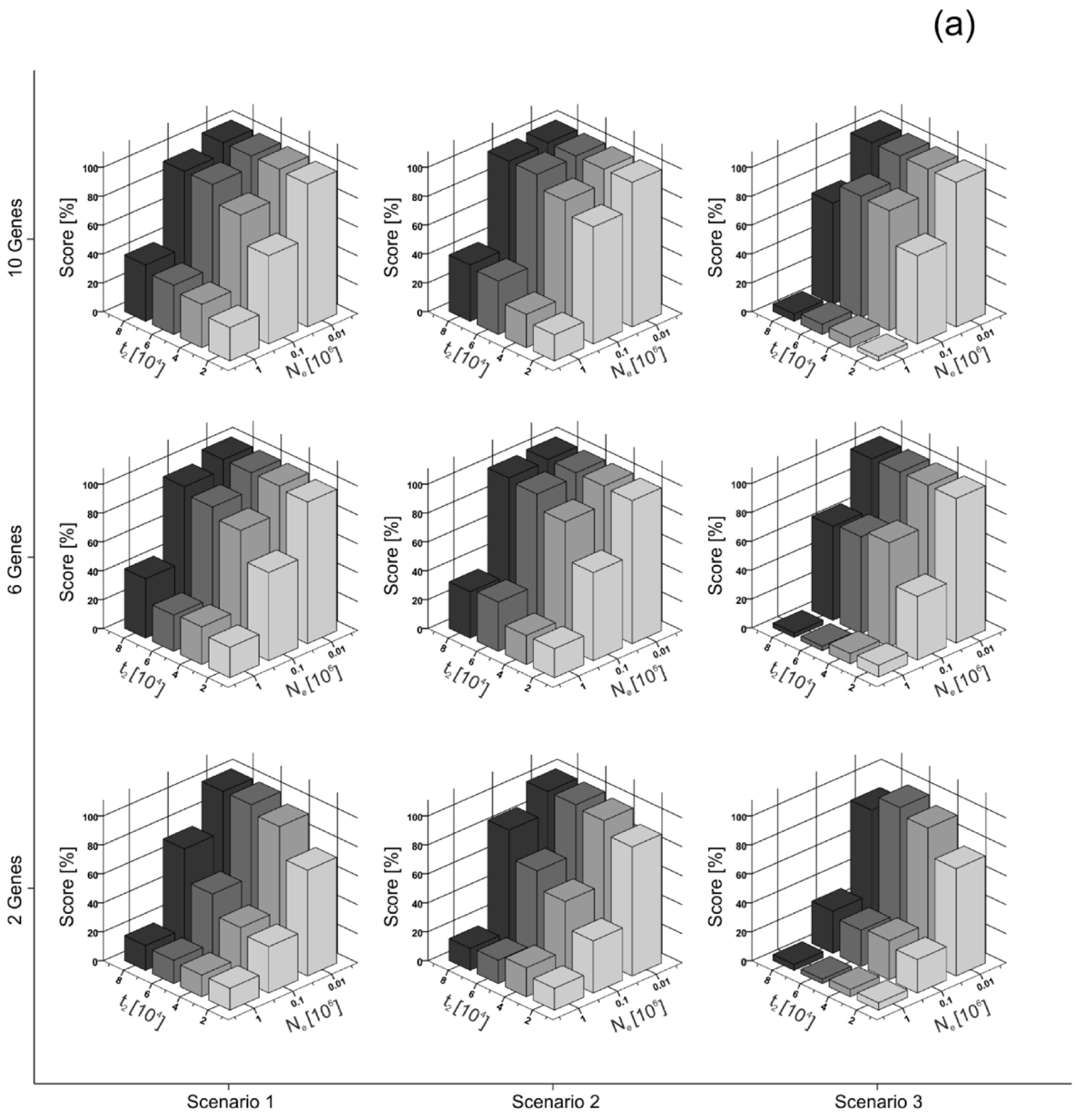

Figure 3.2: Results for the performance of the species network reconstructions using simulated gene trees without considering (panel a) or considering (panel b) gene tree branch lengths. *Y* axis in the diagrams represents the number of gene trees used for the reconstruction, while the *x* axis the three different topological scenarios. In each sub-diagram are shown the different values of effective populations size (N_e) and age of formation of the allotetraploid (t_2) used for the simulations. The scores of success during the species network reconstruction are assessed in axis *z* of each sub-diagram (modified from Wagner 2013).

PCR artefacts and cloning, showing as only difference a singleton substitution, the possibility of dealing with duplicated loci can not be excluded. However, we considered it not relevant for the scope of the present study, as *Castrilanthemum* is only part of the outgroup, and in the other two cases the different alleles formed mainly monophyletic groups in the gene tree reconstructions.

The gene trees obtained from the Bayesian analyses show different degree of resolution being in many cases discordant with one another. The complete set of gene trees with posterior probability values are given in Appendix 3.

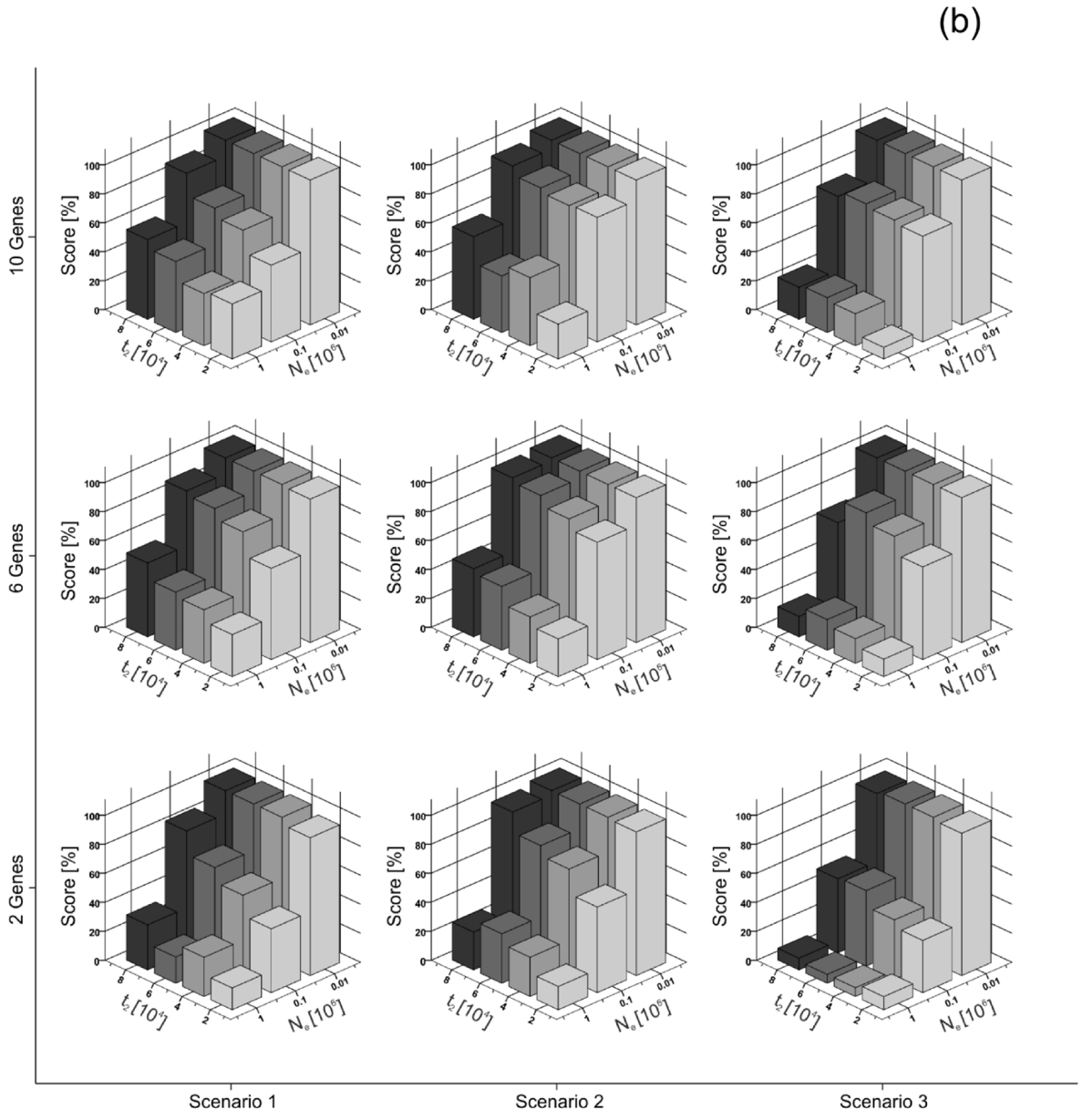

Figure 3.2: Continued.

Table 3.4: Information on the frequency of correct species network reconstruction using the approach described in the Material and Method section, and with the branch length option in PhyloNet not activated (modified from Wagner 2013).

t_2	N_e	2 gene trees	6 gene trees	10 gene trees
		Scenario 1		
t_2 = 20,000				
	N_e = 10,000	0.7300	0.9800	0.9900
	N_e = 100,000	0.3200	0.6100	0.6100
	N_e = 1,000,000	0.1500	0.2100	0.2300
t_2 = 40,000				
	N_e = 10,000	0.9400	1	1
	N_e = 100,000	0.3600	0.8100	0.8000
	N_e = 1,000,000	0.1500	0.2600	0.3000
t_2 = 60,000				
	N_e = 10,000	1	1	1
	N_e = 100,000	0.5000	0.8800	0.9200
	N_e = 1,000,000	0.1600	0.2500	0.3400
t_2 = 80,000				
	N_e = 10,000	1	1	1
	N_e = 100,000	0.7200	0.9300	0.9200
	N_e = 1,000,000	0.1700	0.4100	0.3900
		Scenario 2		
t_2 = 20,000				
	N_e = 10,000	0.8900	0.9900	1
	N_e = 100,000	0.3600	0.6100	0.8100
	N_e = 1,000,000	0.1500	0.2000	0.1800
t_2 = 40,000				
	N_e = 10,000	0.9800	1	1
	N_e = 100,000	0.5400	0.8700	0.9000
	N_e = 1,000,000	0.2000	0.2000	0.2300
t_2 = 60,000				
	N_e = 10,000	1	1	1
	N_e = 100,000	0.6600	0.9700	0.9900
	N_e = 1,000,000	0.1600	0.3400	0.3700
t_2 = 80,000				
	N_e = 10,000	1	1	1
	N_e = 100,000	0.8500	0.9900	0.9900
	N_e = 1,000,000	0.1500	0.3200	0.3900
		Scenario 3		
t_2 = 20,000				
	N_e = 10,000	0.7400	1	1
	N_e = 100,000	0.2300	0.4400	0.6100
	N_e = 1,000,000	0.0500	0.0800	0.0300
t_2 = 40,000				
	N_e = 10,000	0.9300	1	1
	N_e = 100,000	0.2700	0.7200	0.8300
	N_e = 1,000,000	0.0500	0.0700	0.0700
t_2 = 60,000				
	N_e = 10,000	0.9800	1	1
	N_e = 100,000	0.2500	0.6700	0.8400
	N_e = 1,000,000	0.0300	0.0300	0.0700
t_2 = 80,000				
	N_e = 10,000	0.8700	1	1
	N_e = 100,000	0.2900	0.6500	0.7000
	N_e = 1,000,000	0.0400	0.0300	0.0500

Table 3.5: Information on the frequency of correct species network reconstruction using the approach described in the Material and Method section, and considering information about gene trees branch lengths in PhyloNet (modified from Wagner 2013).

t_2	N_e	2 gene trees	6 gene trees	10 gene trees
		Scenario 1		
t_2 = 20,000				
	N_e = 10,000	0.9500	0.9900	1
	N_e = 100,000	0.4400	0.6300	0.5300
	N_e = 1,000,000	0.1500	0.2900	0.3800
t_2 = 40,000				
	N_e = 10,000	1	1	1
	N_e = 100,000	0.5800	0.7900	0.6800
	N_e = 1,000,000	0.2700	0.3700	0.3600
t_2 = 60,000				
	N_e = 10,000	1	1	1
	N_e = 100,000	0.6800	0.8600	0.7400
	N_e = 1,000,000	0.1800	0.4000	0.4900
t_2 = 80,000				
	N_e = 10,000	1	1	1
	N_e = 100,000	0.8400	0.8900	0.8900
	N_e = 1,000,000	0.3100	0.5100	0.5500
		Scenario 2		
t_2 = 20,000				
	N_e = 10,000	0.9900	1	1
	N_e = 100,000	0.5900	0.8100	0.8600
	N_e = 1,000,000	0.1600	0.2600	0.2400
t_2 = 40,000				
	N_e = 10,000	1	1	1
	N_e = 100,000	0.7600	0.8800	0.8500
	N_e = 1,000,000	0.2700	0.3200	0.4700
t_2 = 60,000				
	N_e = 10,000	1	1	1
	N_e = 100,000	0.8300	0.9500	0.8800
	N_e = 1,000,000	0.3400	0.4400	0.3900
t_2 = 80,000				
	N_e = 10,000	1	1	1
	N_e = 100,000	0.9700	0.9800	0.9400
	N_e = 1,000,000	0.2600	0.4700	0.5700
		Scenario 3		
t_2 = 20,000				
	N_e = 10,000	0.9800	1	1
	N_e = 100,000	0.3600	0.6400	0.7300
	N_e = 1,000,000	0.0900	0.1200	0.0800
t_2 = 40,000				
	N_e = 10,000	1	1	1
	N_e = 100,000	0.4100	0.7600	0.7500
	N_e = 1,000,000	0.0600	0.1700	0.2200
t_2 = 60,000				
	N_e = 10,000	1	1	1
	N_e = 100,000	0.5200	0.8300	0.7700
	N_e = 1,000,000	0.0600	0.2100	0.2400
t_2 = 80,000				
	N_e = 10,000	0.9800	1	1
	N_e = 100,000	0.5100	0.6700	0.7300
	N_e = 1,000,000	0.0800	0.1400	0.2200

3.3.3 MUL-tree and species network estimation in Leucanthemopsis. – The MUL-species tree and the species network are shown in Figure 3.3. The tetraploid accessions were found to be autopolyploids; *L. alpina* (LPS119) nested in the clade hosting the diploids accessions of the species, while *L. pallida* subsp. *spathulifolia* (LPS150) sister to the clade including *L. pulverulenta* and *L. pallida* subsp. *virescens* var. *bilbilitanum*. The hexaploid *L. longipectinata* is also reconstructed as having an autopolyploid origin and occupies a basal position in the *Leucanthemopsis* clade. *Leucanthemopsis. alpina* subsp. *cuneata* is found to be allo-hexaploid, formed with the contribution of the other hexaploid (*L. longipectinata*) and of the ancestor lineage giving rise to the clade including the diploids *L. pulverulenta* and *L. pallida* subsp. *virescens* var. *bilbilitanum*.

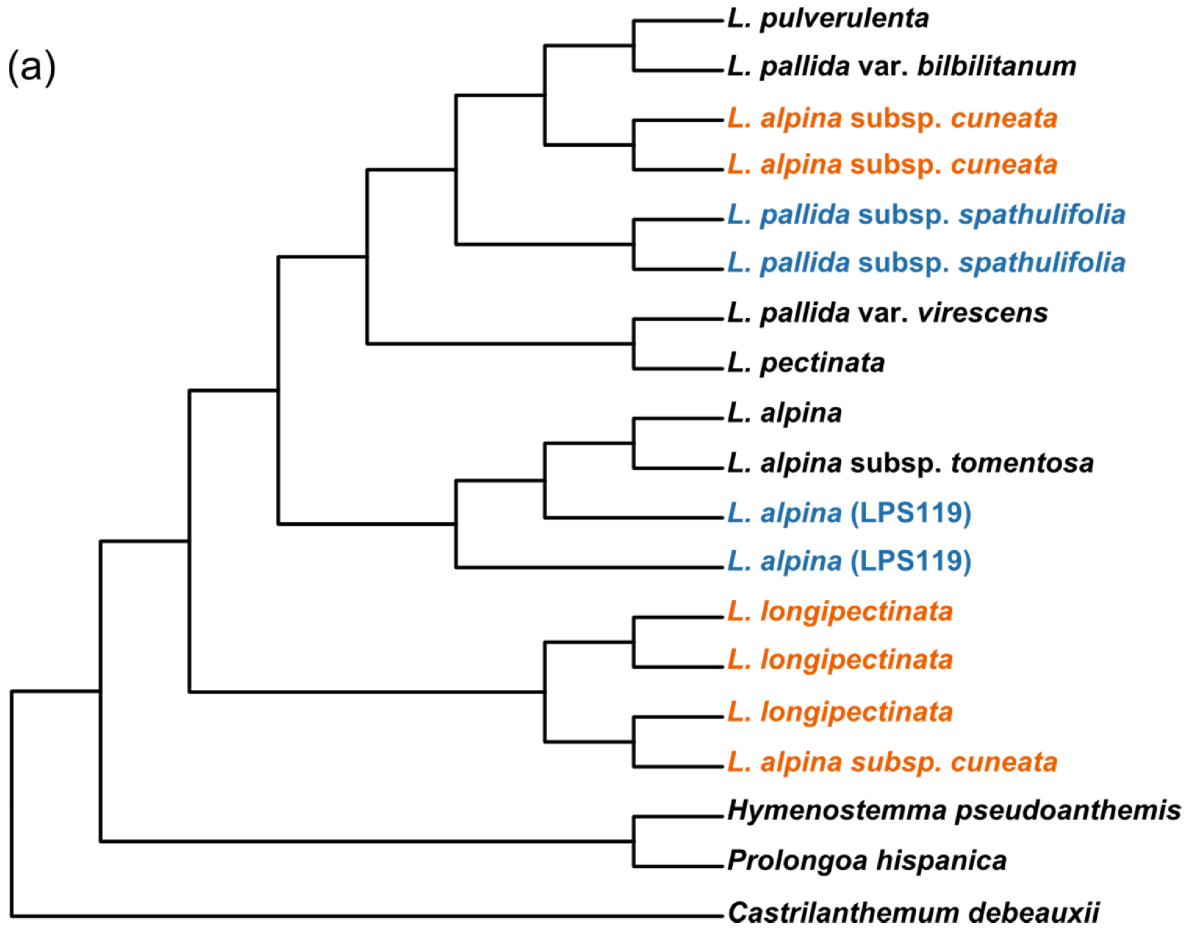

Figure 3.3: Results of the MUL-species tree (panel a) and of the species-network (panel b) reconstructions. Tetraploid accessions are in blue, hexaploid ones in orange. *Hymenostemma pseudoanthemis*, *Prolongoa hispanica* and *Castrilantemum debeauxii* are the outgroup accessions included in the study.

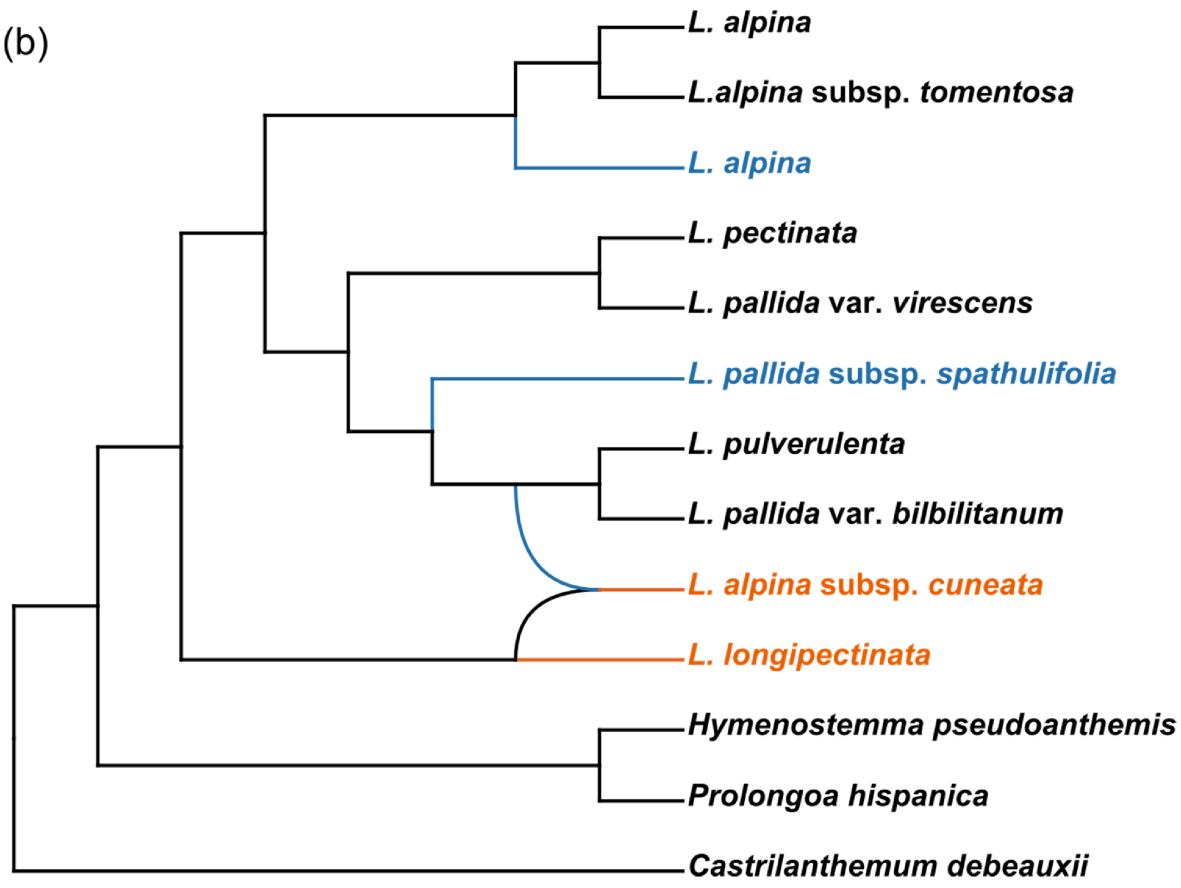

Figure 3.3: Continued.

3.4 Discussion

3.4.1 Network reconstruction method and performance. –The test on simulated data reveals that the performance of the method remains good until population size (considering the age of the speciation events) does not become unrealistically large. In the scenario with the largest population size the total height of the MUL-tree used for simulations was 0.15 coalescent units. Such value is surely more proper for describing the split among populations of the same species, rather than well-differentiated species that possibly hybridise after speciation is complete. If we consider for example that modern humans (indeed one of the most abundant species on earth) inhabit this planet since less than 200,000 Ma, and that human N_e is estimated to be not bigger than 4,000 (Melé et al. 2011), the tree describing the differentiation among human populations (assuming a generation time of 25 years) would have a total height of 1 N_e, one orders of magnitude higher than the values we used to simulate the scenarios with the largest effective population size. Estimates of N_e in plant

plant species reveal relatively modest population sizes, usually ranging from tens of thousands to just more than 100,000 (Grossmann et al. 2010), with the highest estimates in the genus *Helianthus* L. [*H. annuus* L.: ~675,000 (Strasburg et al. 2011) or 830,000 (Grossmann et al. 2010); *H petiolaris* Nutt.: ~845,000 (Strasburg et al. 2011)].

We tested the method with an amount of genes ranging from two to ten, considering this number still realistic for phylogenetic studies involving non-model species. Many species tree reconstruction methods as well as the network reconstruction method described by Yu et al. (2013a, 2013b) perform better as the number of loci considered increases. In Yu et al. (2013a), 50 loci seemed to be enough for the method in order to have 100% of successful reconstructions for deeper species network, whereas even more loci were required for shallower species network (i.e., in a network with longer branches the effect of ILS is lower than in network with shorter branches). To reach this amount of data represent still a challenge for many systematic biology groups working on non-model species. The opposite problem could be encountered when using a Bayesian approaches to infer phylogenetic networks, as they are mathematically robust but computationally intensive and time consuming. Jones et al. (2013) tried the Bayesian method AlloppMUL in empirical data with eight species, one individual per species and five genes, having problems to reach the convergence after 100 million generations. Considering more loci and/or more accessions, along with accessions with higher ploidy level than $2n = 4x$ could be challenging.

The analysis we have done with the here presented approach on the *Leucanthemopsis* data set, with 12 taxa, six markers, and more than one accession per diploid taxon (as well as more alleles per accession) lasted no more than one minute. To use higher numbers of loci at some point would make the analyses unsustainable, since the number of combination of allele pairs across genes (step (b), see material and methods) increases exponentially with the number of genes considered. For a tetraploid accession having the maximum number of expected alleles per gene (i.e., four), there would be over one billion possible combinations of allele pairs across genes, when using 30 loci. To include very high polyploids would represent an additional problem, as the number of "parental genomes" involved in the formation of the polyploid increases and therefore, keeping constant the number of loci in the analysis, the number of allele pairs combinations across genes would be much higher in an high polyploid than in a tetraploid. If for example we are using 10 genes, we will have to evaluate approximately one thousand allele pairs combinations across genes for a tetraploid, whereas already over 60 million combinations must be tried for a dodecaploid. The approach we are presenting here has the advantage to be suitable for relatively large data sets, with

undetermined number of polyploid accessions and polyploidization events (in contrast with the methods described by Yu et al. 2013a; and 2013b), and for a number of loci presumably not higher than 15-20. These numbers are consistent with a great amount of multilocus phylogenies produced nowadays.

3.4.2 The Leucanthemopsis data set. – The age of the split between *Castrilanthemum* and the rest of Leucanthemopsidinae was dated to 16.9 Ma ± 3.8 Ma (see Chapter 2). Following the method of Blanco-Pastor et al. (2012) to calculate the effective population size N_e from mutation rates found in chloroplast markers of *Leucanthemopsis alpina,* we found the effective population size for this species to be around 408,000 individuals using eight accessions of this species and the chloroplast markers *psbA-trnH*. Assuming a generation time of 3 years for this short- to long-lived perennial plant, the lower limit of 95% highest posterior density (HPD) of divergent time of 13.2 Ma translates into an age of the split between *Castrilanthemum* and the rest of Leucanthemopsidinae of 4,400,000 generations, and this turns to 5.39 coalescent units (being the age expressed in $2N_e$ generations).

When we look at the different N_e scenarios used for the simulations in coalescent units, we see that the *Leucanthemopsis* data set is comparable to the simulated ones with the lowest and the middle values of N_e, being therefore placed in a parameter zone where the method performs well, with success percents ranging from 60% to 100%. Any phylogenetic consideration regarding the network obtained should anyway be done cautiously, since only one accession per polyploid taxon and not all the polyploid taxa were included in the analyses.

3.4.3 Conclusions and prospects. – We aimed in this paper to present a simple approach for producing phylogenies in polyploid groups where reticulation is involved. In particular, while reconstructing the MUL-species tree, we tried to solve the problems related to allele assignment to parental genomes in a combinatory manner.

In the analyses on the *Leucanthemopsis* data set, gene trees were used as they were produced in the Bayesian analyses (i.e., branches with posterior probability values lower than 0.95 where kept). It was done because the method works better when the gene trees are better resolved. That is, it is more likely that two or more allele pairs during step (a) and/or two or more allele pairs combinations during step (b) are equally scored (i.e., the derived species tree reconstructions hold the same number of extra lineages), if the gene trees are not fully resolved. However, since gene trees are estimated from sequence data, there is often

uncertainty about them, and a proper way is needed, how to deal with this uncertainty during the species network reconstruction on real data. The use of a set of trees for each locus derived from bootstrap techniques (Soltis & Soltis 2003; Liu & Yu 2011) or a set of tree topologies sampled from the 95% HPD of a Bayesian analyses, along with their associated posterior probabilities (Yu et al. 2012) would represent surely a better way of taking in account gene trees uncertainty.

Concerning the problems related to the excessive number of combinations that must be tried when including high polyploids or numerous loci, some solution is available. High polyploids could be treated as derived from two (as for the tetraploid accessions) and not from *n* genomes. It makes sense even biologically if we consider that a high polyploid can only be the product of the hybridization of two other taxa. If these other taxa were already of hybrid origin can be tested, and eventually these can be included in a further analysis as product of the merging of two additional paternal genomes (and so on until the diploid progenitors are found). Although this approach may be intricate, it could overcome computational problems caused by excessive number of combinations. For large amount of genes, the development of heuristic tools for the search of the optimal allele pair combinations across genes is needed, since an exhaustive search would be computationally too intensive and time consuming.

Chapter 4

Chapter 4

Polyploidy and reticulate evolution in the genus *Leucanthemopsis* (Giroux) Heywood

4.1 Introduction

Polyploidy – or whole Genome Duplication (WGL) – is the presence of three or more complete chromosome sets in an organism. The frequency of polyploidy changes consistently throughout the tree of live, being particularly important in plants. Since its discovery on *Oenothera lamarckiana* mut. *Gigas* made by Lutz (1907) in the early 20th century, several estimates of the frequency of polyploidy in plants have been given, ranging from 30-35% (Stebbins 1950), 50% (Müntzing, 1936; Darlinton, 1937), up to 70-80% (Goldblatt 1980; Lewis 1980). According to a more recent evaluation, approximately 35% of the extant flowering plant species are polyploids (Wood et al. 2009). Despite its prominent presence in flowering plants, the importance of polyploidy as an evolutionary driving force has been undervalued in the past, being polyploids rather considered "dead-ends" in the evolutionary path of taxonomic groups (as reviewed in Fawcett et al. 2013 and in Soltis et al. 2014). In the last decade and thanks to the advent of genome sequencing techniques, it has become clear that polyploidy has played a principal role in the evolution of plants. Already at the first attempt of entire genome sequencing, the *Arabidopsis thaliana* genome, it turned out that even though diploid and with a small genome size, this species had experienced multiple rounds of WGD in its evolutionary history. Nowadays we know that all the eudicots likely derived from a common hexaploid ancestor (Jaillon et al. 2007; Tang et al. 2008) and that many of the economically relevant flowering plants have experienced additional WGD events after the initial "hexaploidization" (see Fawcett et al. 2013).

Polyploidization has been proposed as one of the most common speciation mechanisms in plants, and recent estimates indicate that the 15% of the amount of speciation events in angiosperms involves an increase in the number of complete chromosome sets (Wood et al.

2009). The understanding of how new polyploid species are formed and become established is therefore fundamental to our appreciation of plant biodiversity, and studies devoted to a better comprehension of the phylogenetic patterns associated with polyploidy are needed. However, some issues have to be taken into account when reconstructing molecular phylogenies in polyploid complexes. The higher number of chromosome sets exacerbates problems connected to gene duplication/pseudogenes, and the effect of stochastic factors such as Incomplete Lineage Sorting (ILS) become more dramatic as a consequence of the increased effective population size. Moreover, it must be considered that polyploidization is often accompanied by hybridisation, in what is known as allopolyloidization. Allopolyploidization occurs when individuals of different species (or diverging population of the same species) contribute to the genome of the newly formed polyploid, as opposed to autopolyploidization, where the polyploid arise from a single individual through genome duplication. Of the two processes, the first one has been always consideres more common. The idea of autopolyploids being rarer than allopolyploids was based on concerns about chromosome pairing and segregation during meiosis. In fact, being present in an autopolyploid every homeolog chromosome four or more times, the formation of multivalents during meiosis would have led to reduced fertility (Stebbins 1950; see also Soltis et al. 2014). Although in the last years the importance of autopolyploidy has been reconsidered, the idea that allopolyploids are more abundant in nature is still the common thinking, as confirmed by recent reviews (e.g., Coyne & Orr 2004). For all these reasons, and in addition to the issues previously mentioned, hybridization has to be considered when inferring phylogenies in polyploid complexes.

Disentangling between hybridization and ILS is not a simple task, as several authors have highlighted (e.g., Avise 1994; Rosewich & Kistler 2000; Linder et al. 2003). Nevertheless, the number of phylogenetic studies aiming at reconstructing reticulate evolution in polyploids complexes increased in the last decade. Pioneer examples are given for well-studied plant groups like potatoes (*Solanum tuberosum* L.*;* Martinez-Zapater & Oliver 1984; Rodriguez & Spooner 2009; Cai et al. 2012) or soy bean (*Glycine max* (L.) Merr.*;* Doyle et al. 2004; Egan & Doyle 2010; Bombarely et al. 2014). Recently, numerous other studies have been published, in which reticulate evolution has been inferred mostly by comparing different gene trees and interpreting discordance as a signal of hybridization (Popp & Oxelman, 2001; Popp et al. 2005; Krak et al. 2013; Mason-Gamer, 2013). Triplett al. (2014) brilliantly reconstructed the phylogeny of the woody bamboos and inferred the origin of its allopolyploid representatives, using three nuclear genes and comparing the position held in

these trees by the homeologs of the polyploid taxa. However, the usage of incongruence or homeolog positions in gene trees alone might in some cases lead to erroneous conclusions due to the fact that not only hybridization but also other factors can be the cause of incongruence among gene trees (e.g., ILS or gene loss/duplication), especially in organisms that experienced fast radiation or in which speciation processes are still active. Numerous have been also studies that employed methods inferring phylogenetic networks using either sequence data or gene trees as input (among others Brysting et al. 2011; Marcussen et al. 2012; Garcia et al. 2014; Scheunert & Heubl 2014). Jones et al. (2013) tested the novel methods AlloppNET and AlloppMUL (that produce phylogenetic networks and multi-labeled (MUL-)species trees in the presence of both ILS and hybridization) on real data from the polyploid complexes *Pachycladon* Hook (Brassicaceae; data from Joly et al. 2009) and *Silene* L. (Caryophyllaceae). The results were very promising, although both phylogenies consisted of a single reticulation event, and the efficiency of these methods needs to be tested with more complex data sets. In a recent work, Marcussen et al. (2014) investigated the relationship between the three different subgenomes contributing to the formation of the bread wheat (*Triticum aestivum* L.) genome, using the parsimony method described by Yu et al. (2013) and implemented in PhyloNet (Than et al. 2008). This method infers phylogenetic networks from gene trees, but the number of reticulations has to be known in advance.

Leucanthemopsis (Giroux) Heywood is a small genus of the daisy family (Compositae, subtribe Anthemideae), described by Heywood in 1975. Being over time considered part of *Chrysanthemum* L., *Pyrethrum* Zinn, *Leucanthemum* Mill. and *Tanacetum* L., the new genus was finally described based on morphological differences and on the distinctiveness of *Leucanthemopsis* achenes. While homomorphic achenes and the presence of mucilaginous cells in the epicarp placed *Leucanthemopsis* closer to *Leucanthemum*, the absence of vallecular secretory canals recall more *Tanacetum* achenes. Furthermore, the number of ribs and the behaviour on hydration of the mucilaginous cells represent exclusive characters of *Leucanthemopsis* achenes compared to those of the previously mentioned genera. The distinctiveness of *Leucanthemopsis* and the affinity of the genus with three other unispecific genera (*Castrilanthemum* Vogt & Oberpr., *Prolongoa* Boiss., and *Hymenostemma* Willk.) was corroborated by molecular phylogenetic studies (Oberprieler & Vogt 2000; Oberprieler 2005), and consequently the new subtribe *Leucanthemopsidinae* was described (Oberprieler et al. 2007a). According to the presently accepted taxonomy of the subtribe, the genus consists of six species, all of them linked to a greater or lesser extent to mountain/alpine

environments. Four of the six species constitute polyploidy complexes, with ploidy levels ranging from $2n = 2x$ to $2n = 6x$. The most widespread species, *L. alpina* (L.) Heywood, is a polymorphic complex distributed in all the circum-mediterranean alpine ranges (from the Pyrenees to the Carpathians), and in which all the three ploidy levels are realized in different populations. All the other taxa are confined to the Iberian Peninsula, and only the hexaploid species *L. longipectinata* (FontQuer) Heywood is growing in the Rif Mountains (N Morocco). Most of the species, especially the polyploid complexes, show a high degree of morphological polymorphism and several infraspecific taxa have been described and treated at different taxonomical ranks by the botanists who have dealt with this plant group taxonomically. A scheme listing all the subspecies and varieties presently accepted for the genus *Leucanthemopsis* is given in Table 4.1, and a distribution map is provided in Figure 4.1. Although the monophyly of the genus has been corroborated in a previous phylogenetic analyses (see Chapter 2), the phylogenetic relationships among the different taxa of the genus are still unclear. Moreover in the above-mentioned study, mainly diploid taxa were included, leaving therefore questions on the reticulate evolution of the whole genus and on the origin of polyploidy still unanswered.

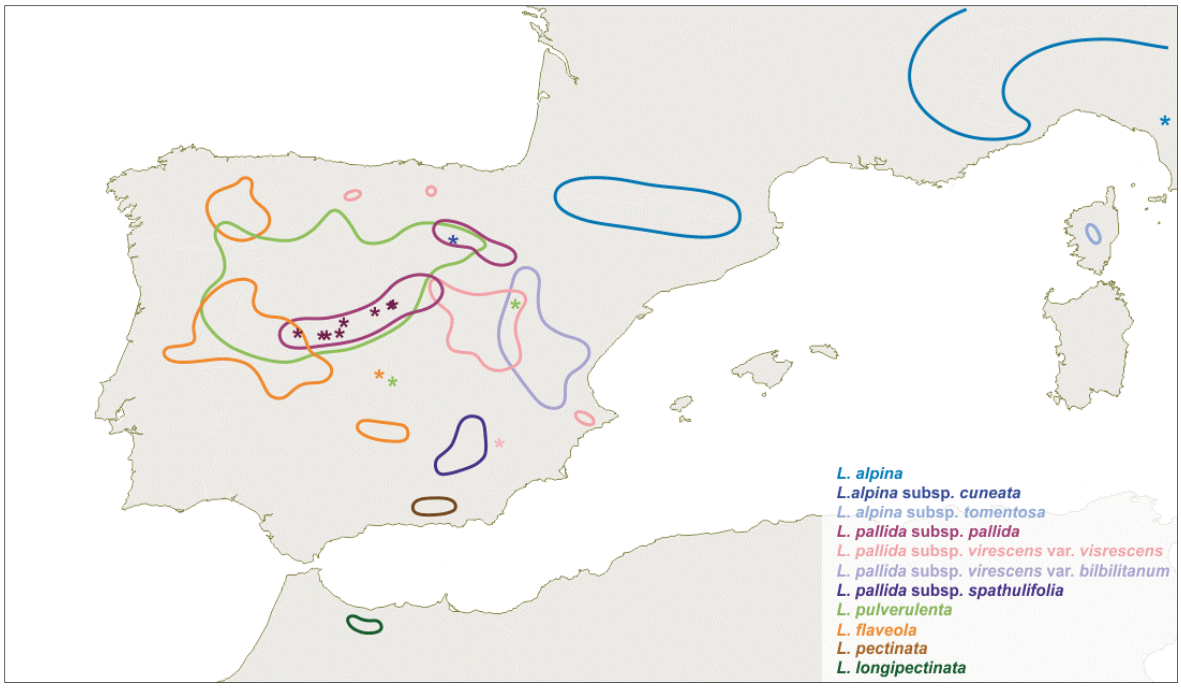

Figure 4.1: Distribution in the Iberian Peninsula of all the different taxa of *Leucanthemopsis* considered in the study, following Heywood (1975) and Gonzáles & Jarvis (1984).

Table 4.1: List of *Leucanthemopsis* taxa considered in the study, with the major ecological and morphological distinctive traits.

	Ploidy	Ecology		Morphology	
		Altitudinal zone	Substrate	Ligules colour	Leaf shape
Leucanthemopsis alpina (L.) Heywood					
subsp. *alpina*	2*x* 4*x* 6*x*	alpine (2600-3800 m)	Silicates	white	Ovate 5 to 9 -fid
subsp. *cuneata* (Pau) Heywood	6*x*	subalpine (1900-2600 m)	Silicates/Limestone	white	Cuneate
subsp. *tomentosa* (Loisel.) Heywood	2*x*	alpine	Silicates	white	Ovate 5 to 9 -lobed
Leucanthemopsis flaveola (Hoffmanns. & Link) Heywood		submontane-subalpine	Silicates	yellow	Linear-oblong 9-11-partite
Leucanthemopsis longiectinata (FontQuer) Heywood	6*x*	subalpine	Silicates	white	Linear-oblong 7-15-partite
Leucanthemopsis pallida (Mill.) Heywood					
subsp. *pallida* var. *pallida*	4*x*	mid-montane (1300-1900 m)	Silicates	pale yellow	Linear-spatulate 3 to 5-fid
var. *alpina* (Boiss. & Reuter) Heywood	4*x*	subalpine	Silicates	white	Linear-spatulate 3 to 5-fid
subsp. *spathulifolia* (J.Gay) Heywood	4*x*	mid-montane	Limestone	pale yellow	Spatulate
subsp. *virescens* (Pau) Heywood var. *virescens*	2*x*	submontane /mid-montane	Limestone	yellow	Spatulate/linear
var. *bilbilitanum* (Pau) Heywood	2*x*	submontane (700-1300 m)	Silicates	white	Linear
Leucanthemopsis pectinata (L.) G.López & C.E.Jarvis	2*x*	alpine	Silicates	yellow	Linear-oblong 7-9-partite
Leucanthemopsis pulverulenta (Lag.) Heywood					
subsp. *pulverulenta*	2*x*	submontane	Silicates	white	Linear-oblong 8 to 14 -partite
subsp. *pseudopulverulenta* (Heywood) Heywood		submontane	Limestone	white	

The crown age of the genus was estimated to be ~4.39 Ma (see Chapter 2), and the differentiation among the different Iberian taxa may have taken place most likely within the last 2 Ma. The young age of the genus and the short time in which most of the taxa diverged

make problems related to ILS to be particularly influential in this plant group. Moreover, it is inescapable to take into consideration ongoing hybridization and/or allopolyploid origin of the polyploid representatives of *Leucanthemopsis*. The existence of intermediate forms and the possibility of hybridization among different "races" of the Iberian *Leucanthemopsis* taxa was in fact already postulated by Heywood (1955). The hybrid origin of the polyploid members of the genus was speculated upon also by Antunez (1981), in a karyological and palynological study on species belonging to *Leucanthemopsis* and closely related genera.

All these reasons make it particularly challenging to reconstruct the reticulate evolution of this genus. The fact that we do not know how many reticulations have taken place in the evolutionary history of *Leucanthemopsis*, makes it difficult to use the method described by Yu et al. (2013). In addition, the complexity of the data set (e.g., number of polyploidy taxa included, number of sample per taxon, etc.) is already above the actual scalability of both the previously mentioned method and the method proposed by Jones et al. (2013). In the Chapter 3, we presented a simple approach to infer phylogenetic networks in polyploidy complexes in the presence of both ILS and hybridization (e.g., polyploid and homoploid hybridization). In the present study, we aim to reconstruct the reticulate evolution of the genus *Leucanthemopsis*, using sequence data from the chloroplast and from single/low copy nuclear genes. To the authors' knowledge, it would be the first time that the evolution of a polyploidy complex of this dimension is inferred using network reconstruction methods and trying to disentangle the effects of hybridization from those (stochastic) factors intrinsic of speciation processes (e.g., ILS). To evaluate the plausibility of those allopolyploidization events pointed out in the phylogenetic analyses, we use finally niche/range reconstruction analyses in order to verify potential past contact zones between the diploid taxa involved in the formation of the polyploids in the past.

4.2 Materials and Methods

4.2.1 Plant material. – Accessions belonging to the three monospecific genera (*Castrilanthemum*, *Prolongoa,* and *Hymenostemma*) that together with *Leucanthemopsis* constitute the subtribe Leucanthemopsidinae, and of the closely related genus *Phalacrocarpum* (DC.) Willk. were included in the study and used as outgroup. Accessions from 15 different taxa, belonging to the six accepted species of *Leucanthemopsis* were included in order to reconstruct the complete phylogeny of the genus. The taxonomic

treatment follows Heywood (1975) with minor adjustments concerning the nomenclature of the species *L. pectinata* following Gonzáles & Jarvis (1984). A total amount of 44 ingroup accessions were included, two to seven per taxon, according as well to the size of the distribution range of each taxon. For the hexaploid species *L. longipectinata* only a single accession was available, being a herbarium specimen collected in 1992 by Vogt & Oberprieler. The herbarium specimen determined as *L. pallida* (sample number LPS186), was included in the study as *Leucanthemopsis spec.*, being difficult to classify precisely into one of the infraspecific taxa because of its intermediate morphology and atypical collection locality.

The majority of the samples were collected in the field in the summers of 2010 and 2011 and instantly dried in silica-gel. Around ten individuals per population were collected in each locality. *Leucanthemopsis pallida* subsp. *virescens* var. *virescens* (LPS185), and the above mentioned LPS186 were herbarium specimens from the herbarium of the "Real Jardín Botánico" in Madrid (MA). The *L. pallida* subsp. *virescens* var. *bilbilitanum* (LPS052) and the *L. flaveola* accessions (LPS038; LPS039) were herbarium specimens from the herbarium of the Botanical Museum Berlin-Dahlem (B). All the herbarium specimens were carefully revised before being included in the study. A complete list of the accessions used in the present study is provided in Table 4.2.

4.2.2 DNA extraction, DNA amplification, and amplicon sequencing. – DNA extracts were obtained either using the DNeasy Plant Mini Kit (Qiagen, Venlo, Netherland) in the laboratory of the CSIC "Real Jardín Botánico" in Madrid or using a modified protocol based on the CTAB method by Doyle & Doyle (1987) at the Institute of Plant Sciences of Regensburg University.

For the phylogenetic reconstructions, two chloroplast markers were employed, the intergenic spacer regions *psbA-trnH* and *trnC-petN*. Concerning the nuclear genome, we used four single-/low-copy nuclear markers (*C16*, *B20*, *D35*, *C12*) as characterised by Chapman et al. (2007). The chloroplast spacer region *psbA-trnH* was amplified using the primers psbAf and trnHr (Sang 1997), whereas for the *trnC-petN* spacer region we used the primers trnC (Demesure et al. 1995) and petN1r (Lee & Wen 2004). PCR amplification was performed using the *Taq* DNA Polymerase Master-mix Red (Ampliqon/Biomol, Odense, Denmark) in a final volume of 12.5 µl, according to the protocol suggestions of the company. Except for some cases, the following temperature profile was employed: 2 min at 95°C, then 36 cycles of 30 s at 95°C, 60 s at 62°C, 60 s at 72°C, with a final extension of 5 min at 72°C.

Table 4.2: Comprehensive list of the samples used for the phylogenetic analyses in the present chapter including voucher information and GenBank accession numbers for the already published sequences.

Taxon	Sample no.	Voucher no.	Collection site	State	Latitude	Longitude	Ploidy	*psbA-trnH*	*trnC-petN*	*C16*	*B20*	*D35*	*C12*
Phalacrocarpum oppositifolium (Brot.) Willk. subsp. *oppositifolium*	LPS147	TS281	Serra d'Estrela	P	40°22'22"	7°32'58"	2x	KM589770	KM589790			KM589744	
Castrilanthemum debeauxii (Degen & al.) Vogt & Oberpr.	IA2170-4		Sierra de Guillimona	E	N 38°1'50"	W 2°32'1"	2x	KM589763	KM589782			KM589739	
Hymenostemma pseudoanthemis (Kunze) Willk.	LPS131-9	TS197	Arcos de la Frontera	E	36°44'54"	5°43'26"	2x	KM589766	KM589785			KM589741	
Prolongoa hispanica G.López & C.E.Jarvis	LPS135-10	TS221	Puente Duero	E	41°34'17"	4°46'50"	2x	KM589768	KM589788			KM589743	
Leucanthemopsis pulverulenta (Lag.) Heywood	LPS134-1	TS217	Puente Duero	E	41°34'17"	4°46'50"	2x	KM589769	KM589787			KM589734	
Leucanthemopsis pulverulenta (Lag.) Heywood	LPS137-1	TS235	Rascafría	E	40°53'22"	3°51'13"	2x						
Leucanthemopsis pulverulenta (Lag.) Heywood	LPS141-1	TS268	Puerto de Parameda	E	40°31'03"	4°39'26"	2x						
Leucanthemopsis pulverulenta (Lag.) Heywood	LPS142-2	TS270	Puerto de Villatoro	E	40°32'15"	5°9'38"	2x						
Leucanthemopsis pulverulenta (Lag.) Heywood	LPS145-1	TS(01)277	Payo	E	40°19'24,1"	06°43'57,8"	2x						
Leucanthemopsis pulverulenta (Lag.) Heywood	LPS149-3	TS297	Vitigudino	E	40°00'17"	6°23'33"	2x						
Leucanthemopsis pulverulenta (Lag.) Heywood	LPS159-1	TS336	Pixeiros	E	42°06'43"	7°5'55"	2x						
Leucanthemopsis pallida (Miller) Heywood var. *pallida*	LPS139-1	TS264	Puerto de Parameda	E	40°31'03"	4°39'26"	4x						
Leucanthemopsis pallida (Miller) Heywood var. *pallida*	LPS143-7	TS273	Puerto de Tornavacas	E	40°16'21"	5°30'45"	4x						
Leucanthemopsis pallida (Miller) Heywood var. *pallida*	LPS158-1	TS333	Los Galayos	E	40°15'26" / 40°14'53"	5°10'26" / 5°10'6'	4x						
Leucanthemopsis pallida (Miller) Heywood var. *pallida*	LPS164-1	TS364	Sierra de la Demanda	E	N 42°11'1"	W 3°4'0"	4x						
Leucanthemopsis pallida (Miller) Heywood var. *pallida*	LPS165-1	TS367	Sierra de Toranzo	E	N 41°43'06"	W 1°55'57"	4x						
Leucanthemopsis pallida (Miller) Heywood var. *pallida*	LPS184	HP20111227	Puerto de Mijares	E	N 40°18'58"	W 4°49'56"	4x						
Leucanthemopsis pallida var. *alpina* (Boiss. & Reuter) Heywood	LPS136-6	TS223	Navacerrada	E	N 40°46'55"	W 3°59'51"	4x						
Leucanthemopsis pallida var. *alpina* (Boiss. & Reuter) Heywood	LPS157-3	TS332	La Mira	E	N 40°15'35"	W 5°10'57"	4x	KM589774	KM589801			KM589755 KM589756	
Leucanthemopsis pallida subsp. *virescens* var. *bilbilitanum* (Pau) Heywood	LPS138-1	TS247	Puerto de Aguarón	E	N 41°19'12"	W 1°20'27"	2x	KM589772	KM589789			KM589733	
Leucanthemopsis pallida subsp. *virescens* var. *bilbilitanum* (Pau) Heywood	LPS052	B10 0846945	Sierra de Piña	E	N 40° 01' 26"	W 0° 37' 33"							
Leucanthemopsis pallida subsp. *virescens* (Pau) Heywood var. *virescens*	LPS163-2	TS361	Sierra del Brezo	E	N 42°50'28"	W 4°4'5'	2x	KM589773	KM589791			KM589732	

Table 4.2: Continued.

Taxon	Sample no.	Voucher no.	Collection site	State	Latitude	Longitude	Ploidy	*psbA-trnH*	*trnC-petN*	*C16*	*B20*	*D35*	*C12*
Leucanthemopsis pallida subsp. *virescens* (Pau) Heywood var. *virescens*	LPS185	MA786958	Monte Peñalta	E	N 42°56'5"	W 3°14'45'		KM589780	KM589802			KM589757 KM589758	
Leucantemopsis pallida subsp. *spathulifolia* (J.Gay) Heywood	LPS150-1	TS301	Sierra de Cazorla	E	N 37°54'24"	W 2°56'36"	4*x*						
Leucantemopsis pallida subsp. *spathulifolia* (J.Gay) Heywood	LPS151-4	TS316	Pueto del Arenal	E	N 38°28'05"	W 2°27'21"	4*x*						
Leucantemopsis pallida subsp. *spathulifolia* (J.Gay) Heywood	LPS152-1	TS318	Puerto de Crucetillas	E	N 38°31'38"	W 2°25'31"	4*x*						
Leucantemopsis pallida subsp. *spathulifolia* (J.Gay) Heywood	LPS153-1	TS324	Sierra de Guillimona	E	N 38°1'50"	W 2°32'1"	4*x*						
Leucantemopsis pallida subsp. *spathulifolia* (J.Gay) Heywood	LPS154-1	TS326	Puerto de la Losa	E	N 38°0'48"	W 2°3'50"	4*x*						
Leucanthemopsis flaveola (Hoffmanns. & Link) Heywood	LPS144-11	TS(01)270	Puerto de Paroles	E	N 40°1'45"	W 6°41'12"	4*x*						
Leucanthemopsis flaveola (Hoffmanns. & Link) Heywood	LPS146-7	TS279	Sortelha	P	N 40°20'6'	W 7°12'57"	4*x*						
Leucanthemopsis flaveola (Hoffmanns. & Link) Heywood	LPS148-1	TS285	Serra d'estrela	P	N 40°22'22"	W 7°32'58"	4*x*						
Leucanthemopsis flaveola (Hoffmanns. & Link) Heywood	LPS160-4	TS350	Sierra do Eixe	E	N 42°18'45"	W 6°43'16"	4*x*						
Leucanthemopsis flaveola (Hoffmanns. & Link) Heywood	LPS161-1	TS352	Alto de la Portilla	E	N 42°23'19"	W 6°29'59"	4*x*						
Leucanthemopsis flaveola (Hoffmanns. & Link) Heywood	LPS038	B10 0846952	Viniegra de Arriba	E	N 42°05'44"	W 02°50'04"							
Leucanthemopsis flaveola (Hoffmanns. & Link) Heywood	LPS039	B10 0846953	Pico del Judio (Almodovar del Campo)	E									
Leucanthemopsis pectinata (L.) G.López & C.E.Jarvis	LPS166-11	TS372	Veleta (Sierra Nevada)	E	N 3°37'45"	W 3°22'20"	2*x*	KM589775	KM589792			KM589735	
Leucanthemopsis pectinata (L.) G.López & C.E.Jarvis	LPS167-1	TS374	Cerro del Caballo (Sierra Nevada)	E	N 37°0'55"	W 3°27'16"	2*x*						
Leucanthemopsis alpina subsp. *tomentosa* (Loisel.) Heywood	LPS181-3	TS409	Monte Renoso	F	N 42°03'51"	E 9°7'48"	2*x*	KM589776	KM589793			KM589736	
Leucanthemopsis alpina subsp. *tomentosa* (Loisel.) Heywood	LPS182-1	TS413	Col di Rinosu	F	N 42°12'26"	E 9°2'12"	2*x*						
Leucanthemopsis alpina (L.) Heywood	LPS064-1	TS1	Visokè Tatry	SK	49°11'28"	E 20°11'40"	2*x*						
Leucanthemopsis alpina (L.) Heywood	LPS074-1	TS409	Glacier Blanc	F	N 44°55'59"	E 06°24'36"	2*x*	KM589778	KM589795			KM589747	
Leucanthemopsis alpina (L.) Heywood	LPS119-7	TS137	Pfatcherkofer	A	N 47°12'43"	E 11°2'29"	4*x*						
Leucanthemopsis alpina (L.) Heywood	LPS180-1	TS407	Puigmail	E	N 42°22'53"	E 2°07'10"	4*x*						

Table 4.2: Continued.

Taxon	Sample no.	Voacher no.	Collection site	State	Latitude	Longitude	Ploidy	*psbA-trnH*	*trnC-petN*	*C16*	*B20*	*D35*	*C12*
Leucanthemopsis alpina (L.) Heywood	LPS173-6	TS398	Ibon de la Anclusa (la Maladeta)	E	N 42°40'07"	E 0°38'48"	6x						
Leucanthemopsis alpina (L.) Heywood	LPS174-5	TS399	Portillón Inferior (la Maladeta)	E	N 42°39'28"	E 0°39'00.8"	6x						
Leucanthemopsis alpina subsp. *cuneata* (Pau) Heywood	LPS168-9	TS376	Laguna Negra (Sierra de Urbión)	E	N 42°00'40"	W 2°52'36"	6x						
Leucanthemopsis alpina subsp. *cuneata* (Pau) Heywood	LPS168-1	TS376	Laguna Negra (Sierra de Urbión)	E	N 42°00'40"	W 2°52'36"	6x						
Leucanthemopsis longipectinata (FontQuer) Heywood	LPS189	Vogt9580/Oberprieler4016	Djehel Tidirhine	M	N 34°52'	W 4°31'							
Leucanthemopsis spec.	LPS186	MA726728	Pico Revolcadores	E	N 38°3'52"	W 2°15'50"		KM589777	KM589794			KM589737	

The PCR products were purified using Agencourt AMPure magnetic beads (Agencourt Bioscience Corporation, Beverly, Massachusetts, USA). Cycle sequencing was performed using the DTCS Sequencing Kit (Beckman Coulter, Fullerton, California, USA), following the protocol suggested of the manufacturer. Sequences were analysed on a CEQ 8000 sequencer (Beckman Coulter, Fullerton, California, USA) and the obtained electropherograms were carefully checked for ambiguities using Chromas Lite 2.10 (Technelysium Pty Ltd., Tewantin, Australia http://technelysium.com.au/chromas.html). When necessary, we used the IUPAC codes to indicate single nucleotides polymorphism. In the electropherograms, a site was considered polymorphic when more than one peak was present and the weakest reached at least the 25% of intensity of the strongest (Fuertes Aguilar et al. 1999, Mansion et al. 2005).

Allelic variation for three of the four low-/single-copy nuclear markers (except *D35*) was inferred via Roche 454 next generation pyrosequencing. Amplicons to be used in the 454 sequencing were produced using two rounds of PCRs. In the first round, Peqlab KAPAHiFi polymerase (Peqlab Biotechnologie GmbH, Erlangen, Germany) was employed in order to reduce PCR errors as much as possible. The PCR was performed in a final volume of 15 µl, with concentration of reagents as indicated by the manufacturer and using the following "touch-down" program: 95°C for 5 min; 20 s at 98°C, 30" at 65°C to 61°C, 30" at 72°C for 5 cycles; finally 35 cycles of 98°C for 20", 60°C for 30", 72°C for 30", with a final extension step of 72°C for 5 min. The forward primers used for the amplifications were especially designed from those specified by Chapman et al. (2007) by the addition of a 29 bp long M13-forward tail. A GS FLX Titanium Primer B sequence was added to the original reverse primers. The reverse *C12* primer was also modified in order to obtain amplicons shorter than obtained with the normal reverse primer, not exceeding the length of approximately 350 bp. For complete information on the primers used in this study see Table 4.3. After purification of the PCR products, the second PCR round was performed in order to add 4 bp or 5 bp long barcodes [else said Multiplex identifiers (MIDs)] to the amplicons. The MIDs are the sequence tags that allow individual identification (a specific MID was assigned to each individual). The forward primer used for the second PCR round consisted therefore of the following sequence combination: GS FLX Titanium Primer A – MID – M13-tail, while the reverse primer was always the GS FLX Titanium Primer B. A two-steps PCR program was employed: 3 min at 95°C; 20 cycles of 20" at 95°C and 1' at 68°C; with a final extension of 5 min at 72°C. After purification of PCR products, concentration and length measurements,

Table 4.3: Primer information for the marker regions employed in the study.

Region	Forward primer	Revers primer
psbA-trnH	GTTATGCATGAACGTAATGCTC	CGCGCATGGTGGATTCACAAATC
trnC-petN	CCAGTTCAAATCTGGGTGTC	CCCAAGCAAGACTTACTATATCC
C16	ACAAGGCTTTTGGAATTGYCC	TTKCCAGCRAAATCATTWTCAGGRGT
D35	AAGGAGGMTTCATGGADTTYGACAA	CCWGTTTTGTCTGCTCTGAATTC
B20	AGTGGWATYAGTGGKGCTAGTTACT	CCACCACGHACAAGMAGCCAAAG
C12	TCTTGCACCACCAACTGYTTGGC	GGGACAATGTTCAATGCTG
M13	CACGACGTTGTAAAACGAC	
TitA	CGTATCGCCTCCCTCGCGCCATCAG	
TitB	CTATGCGCCTTGCCAGCCCGCTCAG	

library preparation, sequencing, and allele deciphering were done as described in the Chapter 3.

The forth single-copy nuclear marker *D35* included *Simple Sequence Repeat* microsatellite (SSR). Because of this, even diploid accessions often shown alleles that differed in length. That allowed us to decrypt the different alleles by using forward and reverse sequence information as described by Flot et al. (2006), and avoiding therefore next generation sequencing or cloning. For the diploids, the software CHAMPURU 1.0 (Flot et al. 2007) was employed, while tetraploids were edited by hand. Since this method is not applicable when more than four sequences of different length overlap in the electropherogram, we cloned the hexaploid accessions (two *L. alpina* subsp. *alpina*, two *L. alpina* subsp. *cuneata,* and one *L. longipectinata* accessions). For this purpose, we used the CloneJET PCR cloning kit (Fermentas, Waltham, Massachusetts, USA) according to the manufacturer's recommendations. Twenty-seven clones were picked for each accession, in order to have a probability of 0.95 to get sequence information for all theoretically possible six alleles (formula from Joly et al. 2006).

4.2.3 Gene tree estimation. – The alleles obtained for each region were aligned in BioEdit (version 7.0.5.3; Hall 1999; http://www.mbio.ncsu.edu/bioedit/bioedit.html) using the Clustal W method for multiple sequences alignment (Thompson et al. 1994). When necessary, alignments were improved in MAFFT (Katoh et al. 2002; http://mafft.cbrc.jp/alignment/software/), which uses a two-cycle progressive method called FFT-NS-2 (Katoh & Toh 2008), and finally checked manually. In *D35*, the region between alignment positions 250 and 294, characterizes by the microsatellite motive (see above) was

Table 4.4: Molecular region characteristics. Variability is calculated as number of variable sites/alignment length.

Marker	Gene type	OTUs	Length	Model	(a) Variable sites	(b) Indels	Variability (a)	Variability (a+b)
psbA-trnH	Chl. intergenic spacer	49	461	TVM+G	71	19	0.154	0.195
trnC-petN	Chl. intergenic spacer	49	639	K81uf+I	91	11	0.142	0.160
C16	Coding	113	202	HKY	97	9	0.480	0.624
D35	Coding	124	305	HKY+G	116	10	0.380	0.413
B20	Coding	111	329	TrN+G	130	18	0.395	0.450
C12	Coding	138	632	TVM+I+G	131	20	0.207	0.239

excluded from further analyses. Gaps were coded as binary characters using the simple gap coding method of Simmons & Ochoterena (2000) as implemented in the software programme GapCoder (Young & Healy 2003).

Bayesian Inference (BI) phylogenetic analyses were performed with MrBayes v.3.2.1 (Ronquist et al. 2012) for the chloroplast markers concatenated in a single alignment, and for each of the four low-/single-copy markers separately. Model selection for each analysis was done in MODELTEST version 3.7 (Posada & Crandall 1998) using the Akaike information criterion (AIC) to choose the best fitting model. Comprehensive information on the alignments and selected models are given in Table 4.4.

The analyses were run using seven heated and one cold chain, with a chain heating parameter of 0.2 in the individual runs. The Metropolis-coupled Markov chain Monte Carlo (MC^3) chains were executed for 10,000,000 generations, with trees sampled every 1,000th generation. In order to check for the reaching of convergence of the runs, the average standard deviation of split frequencies was considered (acceptable when < 0.01) and likelihood values and parameter estimates were compared in Tracer v.1.5 (Rambaut & Drummond 2007). A burn-in equal to 25% of the length of the complete run was applied as by default (Ronquist et al. 2011). The remaining 7,501 trees were used to estimate topology and posterior probability (PP) using the allcompat settings for the consensus tree.

In addition, the chloroplast regions were used to reconstruct a haplotype network using the software TCS version 1.13 (Clement et al. 2000), according to the statistical parsimony algorithm described by Templeton et al. (1992).

4.2.4 Test for hybridization at the diploid level. – Before reconstructing the network including all the accessions, we wanted to detect potential hybrids among the diploid taxa. For this, the method described by Konowalik et al. (submitted) was used including two

accession per diploid taxon and *Hymenostemma pseudoanthemis* as outgroup. The method is based on the estimation of the probability of gene tree topologies for a given phylogenetic network/tree as described in Yu et al. (2012) and implemented in PhyloNet (Than et al. 2008). In this approach, a "hybrid index" is calculated for each taxon, based on the fact that for a given taxon either a hybridization network or a tree is found to be the most likely scenario to describe the parental relationships among the given taxon and two other randomly taken taxa. Taxa for which more often the most likely scenario is a hybridization network therefore receive higher hybrid indices than taxa for which often a tree was the most likely explanation [see Konowalik et al. (submitted) for detailed information]. We used the MATLAB (MATLAB R2013b, MathWorks Inc., Natick, Massachusetts, USA) script provided in the above-mentioned work to score hybrid indexes and detect potential hybrid taxa.

Since for the calculation of gene tree probabilities it is important that branch lengths in the species networks/tree are expressed in coalescent units (i.e., in $2N_e$ generations, where N_e is the effective population size), values for the split between outgroup and ingroup and for N_e were needed. The split between *Hymenostemma* and *Leucanthemopsis* (10.35 Ma) was taken from the dated phylogeny in Chapter 2, and a generation time of three years was considered to be realistic for the short-lived perennial herbs like the *Leucanthemopsis* taxa. Effective population size was calculated as described in Blanco Pastor et al. (2012) for both the widespread species *L. alpina* and the narrowly distributed species *L. pulverulenta*. Population genetic parameters (mutation rate μ; and interpopulation pairwise nucleotide differences D_{xy}) were calculated with the software DnaSP 5.10 (Librado & Rozas 2009), using eight individuals per species. N_e values of ~334,615 and ~30,620 were found for *L. alpina* and *L. pulverulenta,* respectively. We used the mean between those two values (i.e., ~182,620) to set the age in coalescent units of the split *Hymenostemma-Leucanthemopsis*, being:

$$\frac{t_g}{2 \cdot N_e} \cong 5.75$$

where t_g is time in generations.

As in Konowalik et al. (submitted), the above-explained procedure was repeated using simulated gene trees in order to test whether the value of the hybrid index could be explained with Incomplete Lineage Sorting (ILS) alone (as for the simulated gene trees) or whether the contribution of hybridization processes had to be also assumed (i.e., when the value for the

hybrid index was found to be significantly higher than those found using simulated trees). Gene trees were simulated in Mesquite 2.75 (Maddison & Maddison 2011), using the plastid gene tree as a species tree, and the N_e value as specified above.

4.2.5 Species network inference. – We inferred species networks by (i) first reconstructing a multi-labelled trees (MUL-tree), in which terminal leaves represent either diploid taxa or diploid genomes contributing to the formation of polyploids, and then (ii) joining leafs belonging to the same taxon. Allele mapping (i.e., assignment of alleles to putative parental species) was done in a combinatory manner, following the procedure described in Chapter 3. For the scope, we used the gene trees obtained from the Bayesian analyses and the MATLAB script provided by Wagner (2013). Since more than one accession per polyploid taxon was included in the study, a further combinatory step was needed in order to find out how the best allele pairs found for each sample were combined across the different accessions of a given taxon. It was done following the same principle (see Chapter 3), but all the procedure was done by hand, since modifying the MATLAB script would have likely needed more time. The gene tree pruning was done therefore in R (R Development Core Team, 2008) using the package phytools (Revell 2012). Scoring of the best allele combination was done by running several independent Minimizing Deep Coalescences (MDC; Maddison 1997, Than & Nakhleh 2009) species tree analyses in PhyloNet (Than et al. 2008) and choosing the combination leading to the species tree with the lowest number of extra lineages (as described in more detail in Chapter 3). Once that the most suitable allele mapping was found for all the polyploid taxa, the MUL-species tree reconstruction was performed using *BEAST (Heled & Drummod 2010), for two main reasons: (i) to incorporate uncertainly in the gene trees/species tree estimation, and (ii) to obtain dated trees to be used afterwards to calculate gene tree probabilities and choose the best taxa scenario (see below). The MUL-species trees were analysed in Dendroscope (Huson & Scornavacca 2012) to produce species networks using the cluster-based algorithm.

Concerning the taxonomic treatment, we followed two approaches when reconstructing the species network. In the first one, we addressed accessions to taxa, according to the taxonomic revision of the genus provided by Heywood (1975). *BEAST analyses were run for $2.5*10^8$ generations in BEAST 1.8. The BEAST.xml input files were produced using BEAUti, version 1.8 (Drummond et al. 2012) and comprised ten different partitions (the sequence information plus the binary coded gap sequences for each of the 5 markers). Nucleotide substitution models were accepted as specified in ModelTest, but allowed to vary

in parameter space in a normal distribution manner. The Yule speciation process was chosen as species tree prior, along with the "piece-wise linear and constant root" model for population size. Since we did not know whether sequences evolved in a clock-like manner, we performed different analyses both with a strict clock and with a lognormal relaxed clock (Drummon et al. 2006). Model selection was therefore assessed estimating marginal likelihoods using the Stepping Stone (SS) sampling method (Xie et al. 2011). It has been demonstrated that this method outperforms other ones [e.g., the harmonic mean (HME) or the Akaikes's information criterion through MCMC (AICM)] when computing Bayesian factors to compare model fit (Xie et al. 2011; Baele et al. 2012). Since the lognormal relaxed clock gave better results than the strict clock (Log Marginal Likelihood: -12,568.334 vs. -12,576.759), another independent *BEAST run was performed as above, using the relaxed clock. After checking convergence and determining burn-in values in Tracer v1.6, the two independent *BEAST runs were merged using LogCombiner v1.8 (Drummond et al. 2012) applying a burn-in period of 10%. Finally, the remaining trees were used to construct a maximum-clade-credibility tree with a posterior probability limit set to 0.5 in TreeAnnotator 1.8 (Drummond et al. 2012).

Since taxa delimitation/determination can be quite problematic in the genus – especially when looking at the tetraploid taxa growing in the Iberian Peninsula – and since we did not know how many times (allo)polyploidization took place independently (how many reticulation events), we followed a second approach for the reconstruction of the species network. We performed separate network reconstructions applying different delimitations of the tetraploid taxa (i.e., all tetraploids together assuming only one event of tetraploid formation, all taxa separately assuming that all tetraploid taxa were formed independently, etc.). The obtained MUL-species trees were used to calculate gene trees probability for all the different scenarios using the software STELLS 1.6.1 (Wu 2012). Twenty gene trees taken randomly from the Bayesian search for the chloroplast data set were used for the scope, and the scenario leading to the best likelihood score was considered to be the most reliable one, describing the evolutionary history of the genus. A scheme showing the taxa delimitations used in the different scenarios is given in Table 4.5. Once the best scenario was found, definitive *BEAST analyses and network reconstructions were performed as above explained for the first approach.

Table 4.5: Scheme of the taxa delimitations for the Iberian tetraploids used to calculate the most likely network scenario. The abbreviation Lpal refers to the taxon *Leucanthemopsis pallida* var. *alpina*; Lppa to *L. pallida* var. *pallida*; Lspa: to *L. pallida* subsp. *spathulifolia*; and Lfla: to *L. flaveola*. *k* indicate the number of taxa partitions. To take into account model parameterization in the likelihood computation, we used the akaike information criterion (AIC = -2 lnL + 2k).

	Tetraploid taxa partition	k	Log likelihood	AIC
Scenario 1	[Lpal+Lppa+Lspa+Lfla] [LPS186]	16	-3481.74	6995.48
Scenario 2	[Lpal+Lppa+Lspa+LPS186] [Lfla]	16	-4099.17	8230.34
Scenario 3	[Lpal+Lppa+Lspa] [LPS186] [Lfla]	17	-3746.55	7527.1
Scenario 4	[Lpal+Lppa] [Lspa+LPS186] [Lfla]	17	-3944.42	7922.84
Scenario 5	[Lpal] [Lppa] [Lspa+LPS186] [Lfla]	18	-5862.32	11760.64
Scenario 6	[Lpal+Lppa] [Lspa] [LPS186] [Lfla]	18	-3547.18	7130.36
Scenario 7	[Lpal] [Lppa] [Lspa] [LPS186] [Lfla]	19	-4071.48	8180.96
Scenario 8	[Lpal+Lppa+Lspa+LPS186] [LflaN] [LflaS+LPS038]	17	-4272.63	8579.26
Scenario 9	[Lpal+Lppa+Lspa] [LPS186] [LflaN] [LflaS+LPS038]	18	-4208.67	8453.34
Scenario 10	[Lpal+Lppa+Lspa+LflaS+LPS038] [LPS186] [LflaN]	17	-2996.31	6026.62
Scenario 11	[Lpal+Lppa] [Lspa+LPS186] [LflaN] [LflaS+LPS038]	18	-4036.54	8109.08
Scenario 12	[Lpal] [Lppa] [Lspa+LPS186] [LflaN] [LflaS+LPS038]	19	-3883.58	7805.16
Scenario 13	[Lpal+Lppa] [Lspa] [LPS186] [LflaN] [LflaS+LPS038]	19	-3882.17	7802.34
Scenario 14	[Lpal] [Lppa] [Lspa] [LPS186] [LflaN] [LflaS+LPS038]	20	-4116.67	8273.34
Scenario 15	[Lpal+Lppa+Lspa+LPS186] [LflaN+LPS038] [LflaS]	17	-3725.91	7485.82
Scenario 16	[Lpal+Lppa+Lspa] [LPS186] [LflaN+LPS038] [LflaS]	18	-3426.01	6888.02
Scenario 17	[Lpal+Lppa] [Lspa+LPS186] [LflaN+LPS038] [LflaS]	18	-3952.23	7940.46
Scenario 18	[Lpal] [Lppa] [Lspa+LPS186] [LflaN+LPS038] [LflaS]	19	-3589.33	7216.66
Scenario 19	[Lpal+Lppa] [Lspa] [LPS186] [LflaN+LPS038] [LflaS]	19	-3487.43	7012.86
Scenario 20	[Lpal] [Lppa] [Lspa] [LPS186] [LflaN+LPS038] [LflaS]	20	-3856.16	7752.32

4.2.6 Flow cytometry. – Ploidy was usually determined for five accessions per population based on silica-gel dried material. For the populations collected in "Puerto de Parameda" (LPS139-LPS141), where the diploid species *L. pulverulenta* grows sympatrically with the tetraploid *L. pallida* subsp. *pallida*, all the collected individuals were measured. Approximately 10% of the samples were independently remeasured and used as replicates

in order to test how trustworthy the measurements were. Ploidy was determined through flow cytometry using *Petunia hybrida* E.Vilm. cv. PxPc6 as an internal standard (2C = 2.85 pg; Marie & Brown, 1993). Approximately 0.5-1cm^2 leaf tissue of the standard and 2- to 3-fold tissue of the dehydrated samples material was employed. Nuclei were isolated grinding the leaf material in Otto I buffer (Otto 1992; Doležel & Göhde 1995), and subsequently stained with 4',6-diamidino-2-phenylindole (DAPI) in a LB01 buffer (Doležel et al. 1989) modified with the supplement of β-Mercaptoethanol (0.015 mM). The preparation was measured on a PARTEC CyFlow® Space instrument (Partec GmbH, Münster, Germany). For each sample, over 8500 nuclei were counted. The results were processed using the FloMax® (Partec) software. The relative fluorescence intensity of DAPI-stained nuclei was registered and the ratio between the relative fluorescence of the sample and the relative florescence of the standard was used as indicator of DNA content and ploidy.

4.2.7 Eco-climatological niche reconstruction. – In order to corroborate the results produced by the phylogenetic analyses and to look for past contact zones among putative diploid parental taxa of the polyploids, we estimated the ranges for all the *Leucanthemopsis* taxa in the present and in the past. We inferred eco-climatological niches using present day occurrence for all taxa applying the maximum-entropy method implemented in the software programme Maxent, version 3.3.3 (Phillips et al. 2004; Phillips et al. 2006; Elith et al. 2011). Present day occurrences were recorded using collections from the herbarium of the "Real Jardín Botánico" in Madrid (MA), from the Botanische Staatssammlung in Munich (M), and from the herbarium of the Botanical Museum in Berlin-Dahlem (B), along with personal collection data of the author. Herbarium specimens were carefully revised before including label information into the analyses. Only vouchers for which coordinates were available or label descriptions allowed for a precise geo-referencing of the collection point (within a diameter of approximately 5 km) were further included in the niche reconstruction analyses. We used over 650 records for all taxa of *Leucanthemopsis*. A complete list of the presence data used in the study is given in Appendix 4. In addition, for the tetraploid species *L. flaveola* – having a disjunct distribution range – niches were inferred for both the populations occurring in the northern part of the distribution range and for those occurring in the southern part separately.

For each species, we performed 100 bootstrap replicates using random test, training and background points in each run (option "Random seed"). As test data set, we used 25% of our presence data points. Maximum iterations were set to 10,000 and output was set to logistic.

All other options were left as default. As climatic input data for the present conditions, we used 19 eco-climatological variables at a spatial resolution of 30 arc-seconds (~1 km), developed by Hijmans et al. (2005) and available from the WorldClim data set (http://www.worldclim.org). We subsequently projected our models into past conditions using: (i) data from the Model for Interdisciplinary Research on Climate, version 3.2 (MIROC; Hasumi & Emori 2004; Braconnot et al. 2007) for the Last Glacial Maximum (LGM, c. 21,000 years BP); and (ii) data from Otto-Bliesner et al. (2008) for the Last Inter-Glacial (LIG; ~120,000-140,000 years BP). Climatic data were trimmed down in order to include the area between the coordinates 15°W-30°E and 30°N-60°N (i.e., the complete Euro-Mediterranean region).

Finally, we calculated range overlaps for the all species pairs using ENMTools v1.3 (Warren et al. 2008, 2010), assuming the broadest possible range. When calculating range overlaps for the LGM, the area north of 50°N was excluded in order to avoid misleading results due to the artificial presence prediction in the artic area for some taxa.

4.3 Results

The nuclear markers were found fairly more variable than the two plastid intergenic spacer regions. Among the nuclear regions, the most variable marker is the low-copy nuclear gene *C16*, which exhibits 97 variable sites and 9 indels along its 202 bp long alignment. Of the two plastid regions, *psbA-trnH* is the more informative one compared to *trnC-petN* [variability (variable sites/alignment length): 0.19 and 0.16 respectively]. For more information, see Table 4.4.

4.3.1 Roche 454 next generation sequencing. – Library preparation and equimolar mixing worked well and we did not have missing data for any sample, although the number of reads varied considerably across markers and accessions. In total 19,565 reads were obtained. When looking at the differences in number of reads among nuclear regions, *C16* was the least represented, and the samples for which we obtained lower than expected numbers of reads were usually diploid accessions. The quality of the reads – with some variation among samples – was relatively good, leading to approximately 90% of the total number of reads kept after barcode assignment and quality control (17,605 reads).

The number of alleles retained per individual was usually not higher than the one expected based on ploidy level of the sample and under the assumption of each region being a single-copy marker. Only in few cases, and mostly for the outgroup accessions, we registered more alleles than expected. A complete list with detailed information on number of reads and alleles for each sample and marker is given in Appendix 5.

4.3.2 Gene trees. – Apart for the plastid DNA tree with its highly resolved topology and well-supported monophyletic groups, the gene trees obtained from the Bayesian analyses show low degree of resolution and high topological discordance. Concerning the nuclear genes, *Leucanthemopsis* is found to be monophyletic only based on *D35* sequence variation, while in the other nuclear regions alleles from the closely-related genera are nested within it. In general, the most informative regions seem to be *C16* and *D35*, for which it is possible to track down some general patterns. In these gene trees, accessions from *L. alpina* and from the Iberian diploid taxa form two different well-supported groups, in which are nested alleles from the polyploid taxa. Alleles from the hexaploid subspecies *L. alpina* subsp. *cuneata* are always found together with the Iberian taxa. In some cases, *L. alpina* polyploids from the Pyrenees presented alleles clustering together with the Iberian taxa, being a possible indication of gene flow among these well-differentiated entities in the Iberian Peninsula. Very interestingly, in *C16* and *B20* alleles from the tetraploid subspecies *L pallida* subsp. *spathulifolia* are found together with *Castrilanthemum debeauxii*, two taxa separated from each other by approximately 17 Ma of divergent evolution (see Chapter 2), but growing sympatrically in some mountain peaks of the Baetic System (SE Spain). The complete set of gene trees are given in Appendix 6.

The haplotype network (Figure 4.2) shows four well-defined haplotype groups for *Leucanthemopsis*. The first one (blue in Figure 4.2), is represented by accessions belonging to the species *L. alpina*. The second group includes the hexaploid Moroccan species *L. longipectinata*. Interestingly, the Iberian taxa are divided into two main haplotype groups, which are not corresponding to the present taxonomy but to ploidy levels: the first of these haplotype groups is formed by only tetraploid accessions, while the second includes mainly diploids. The hexaploid *L. alpina* subsp. *cuneata* (from Sierra de Urbión, NE Spain) clusters together with the Iberian diploid representatives of the genus, being a further evidence that this taxon should be treated as an independent entity and that *L. alpina* in Spain does not extend further south than the Pyrenees. One of the accessions of *L. flaveola* from the northern

the northern part of its disjunct range shares the haplotype with *L. pulverulenta*, a fact that will be further discussed in this paper.

4.3.3 Test for homoploid hybridization. – The result for the hybridization test for the diploid taxa is shown in Figure 4.3. Only for the dwarf Corsican *L. alpina* subsp. *tomentosa*, the hybrid index using the real gene trees was found being significantly higher than those obtained using the simulated trees, pinpointing this taxon as a potential hybrid.

4.3.4 Species network. – Phylogenetic networks obtained using the first approach (using taxa delimitation according to Heywood, 1975) and in the second (using the best-scored taxa delimitation for the tetraploid representatives of the Iberian Peninsula) are presented in Figures 4.4a and 4.4b, respectively. Scenario 10, in which all tetraploid *L. pallida* accessions were treated together with *L. flaveola* from the southern part of the species' range while *L. flaveola* populations from the north were kept separated, was found to be the best-fitting one (Log likelihood: -2,996.31; AIC: 6,026.62; Table 4.5). Although the results of the two approaches show similarities, some incongruence is observed together with low support values, especially in the terminal parts of the networks.

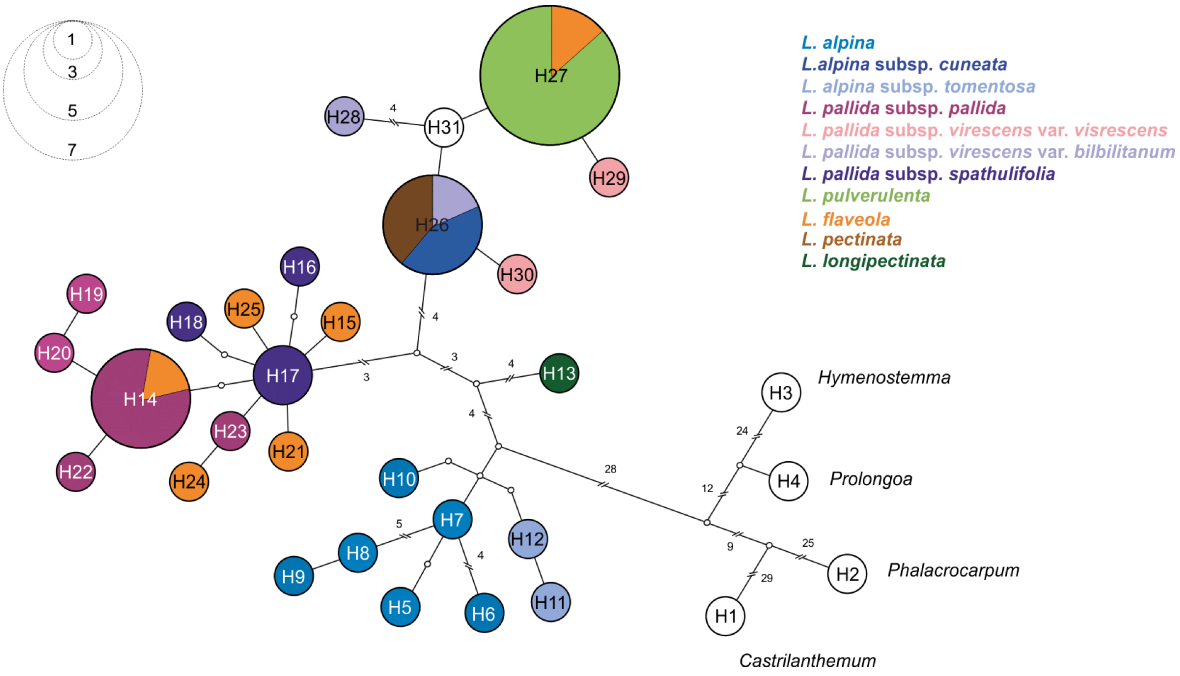

Figure 4.2: cpDNA haplotype network obtained sequencing the intergenic spacer regions *psbA-trnH* and *trnC-petN*. Circle dimension are proportional to the haplotype occurrence, whereas small white circles represent non-detected intermediate haplotypes. When more than two non-detected haplotypes, numbers are given along edges.

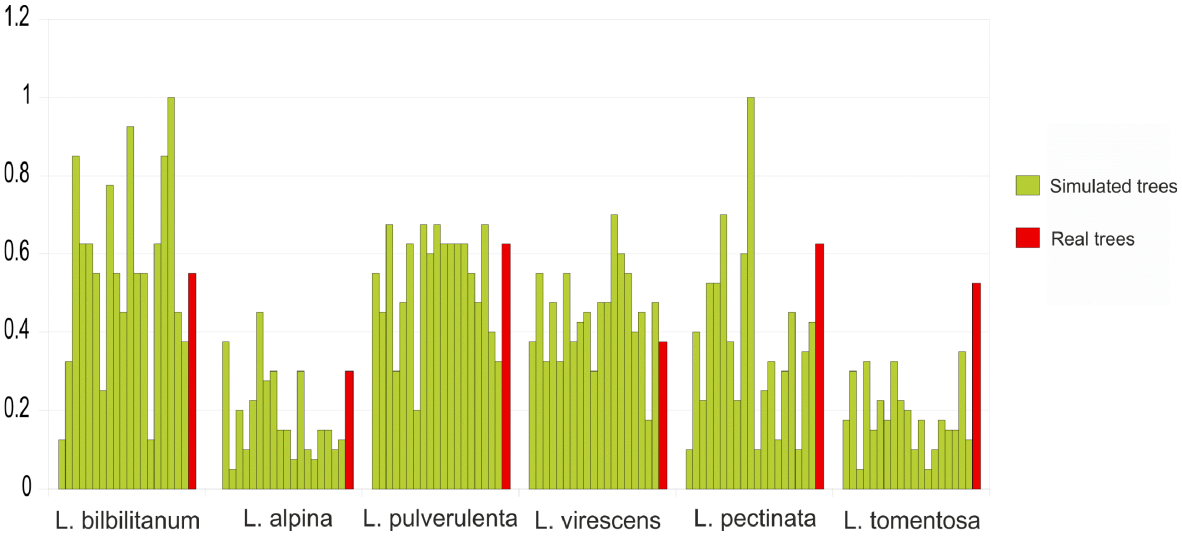

Figure 4.3: Results of the hybridization test for the diploid taxa. Green bars are for the hybrid index values obtained using simulated gene trees; red bars are for the values obtained with the gene trees from the Bayesian analyses.

In both cases, the diploid taxon *L. alpina* subsp. *tomentosa* is not found being of hybrid origin, which is in contrast with the results of the test for hybridization (see above; Figure 4.3). Concerning the origin of the polyploids (those that are present in both reconstructions), there is in large part correspondence between the two results. *Leucanthemopsis longipectinata* and the hexaploid *L. alpina* resulted autopolyploid, while the tetraploids of *L. alpina* seem to be of allopolyploid origin and being formed with the contribution of the hexaploids and the diploids of the same species. As for the latter, the hexaploid *L. alpina* subsp. *cuneata* is also found to be allopolyploid.

4.2.5 Flow cytometry. – The quality of the measurements in most of the cases was high, with an average of the Coefficient of Variation (CV) equal to 3.128 (± 0.706) and 3.958 (± 0.954) for the *Petunia* and the sample peaks, respectively. The average of standard deviation within repeated measurements was 0.038, while among different samples of a same population it was in average 0.140.

For all the examined taxa, the ploidy level observed was corresponding to the one expected based on former counts. DNA content seems to vary slightly among taxa having the same ploidy. While diploids of *L. alpina* show a *Leucanthemopsis/Petunia* ratio around 3.3, Iberian diploid taxa exhibit higher values (3.722 and 3.866 in *L. pectinata* and *L. pulverulenta,* respectively). Different tetraploid taxa from the Iberian Peninsula show either ratios around 6.2 (e.g., *L. pallida* subsp. *spathulifolia*) or 5.7 (as in *L. flaveola* and *L. pallida*

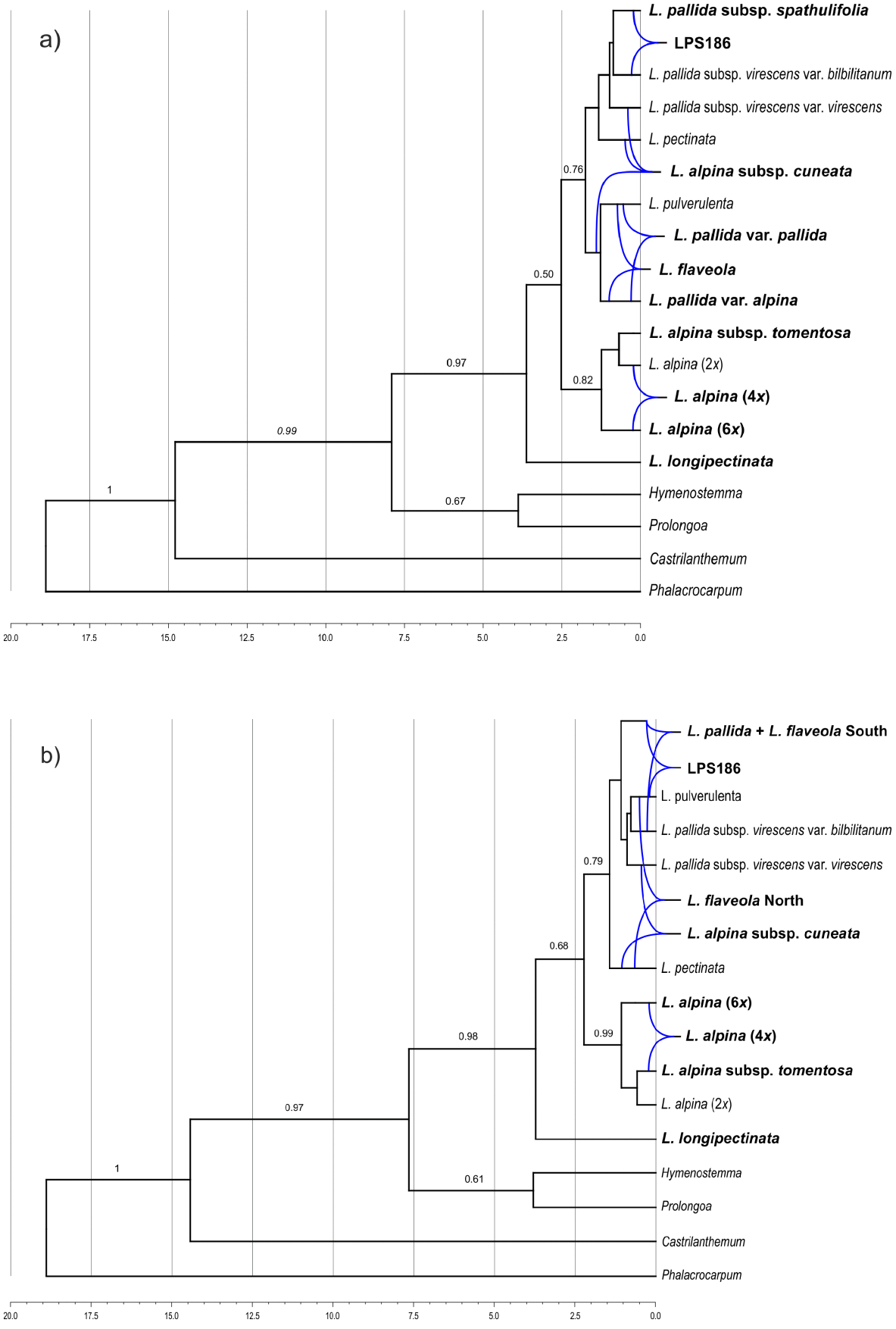

Figure 4.4: Network reconstructions using: a) the first approach [applying the taxa classification as in Heywood (1975)]; and b) using the best-scored taxa delimitation for the tetraploid taxa of the Iberian Peninsula. Taxa in bold are those included in the analyses as putative hybrids. Blue edges represent reticulation events.

var. *alpina*). Detailed results for all the taxa are given in Table 4.6. No intermediate values (as expected for putative triploid or pentaploid individuals) were found, even not in the mixed population of "Puerto de Parameda". Interestingly, the resulting histograms for three individuals from three different populations of *L. pallida* subsp. *spathulifolia* presented an additional fluorescence peak, for which its ratio with the Petunia peak (c. 4.0) corresponded approximately to the same value obtained for an Iberian diploid (e.g., 3.866 in average for *L. pulverulenta*).

Table 4.6: Average fluorescence ratio and ploidy for all the taxa investigated.

Taxon	*Leucanthemopsis/Petunia* Ratio		Ploidy	counts	populations
	μ	SD			
L. alpina 2*x*	3.334	0.188	2*x*	11	2
L. alpina 4*x*	5.804	0.384	4*x*	10	2
L. alpina 6*x*	7.861	0.190	6*x*	10	2
L. alpina subsp. *cuneata*	7.431	0.079	6*x*	5	1
L. alpina subsp. *tomentosa*	3.216	0.049	2*x*	10	2
L. flaveola	5.795	0.113	4*x*	23	5
L. pallida var. *alpina*	5.759	0.213	4*x*	10	2
L. pallida var. *pallida*	6.227	0.265	4*x*	28	5
L. pallida subsp. *spathulifolia*	6.118	0.173	4*x*	25	5
L. pallida subsp. v*irescens* var. *virescens*	3.420	0.106	2*x*	5	1
L. pallida subsp. v*irescens* var. *bilbilitanum*	3.672	0.089	2*x*	5	1
L. pectinata	3.722	0.215	2*x*	10	2
L. pulverulenta	3.866	0.143	2*x*	42	7

4.3.6 Eco-climatological niche reconstruction. – The results of the eco-climatological modelling of potential distribution areas in the present, Pleistocene (LGM), and Last inter-glacial (LIG) for diploids and polyploids representatives of *Leucanthemopsis* are shown in Figure 4.5. The potential distribution in the present corresponds generally to the realized distribution for all the taxa. However, for some of the Iberian representatives of the genus, the potential niche extends outside the Iberian Peninsula, especially into the Maghreb area and into the further eastern areas of the Mediterranean basin (e.g., in *L. flaveola* and *L. pallida* subsp. *virescens*). When looking at modelled distributions in the past, taxa linked to high mountain environments in the temperate region (*L. alpina*, *L. alpina* subsp. *cuneata,* and *L. flaveola* growing in NW Iberian Peninsula) show potential range expansion during the LGM and a drastic reduction during the drier conditions of the LIG. On the other hand, oro-mediterranean taxa (e.g., *L. pectinata*, *L. pallida* var. *alpina*) show a broader expansion

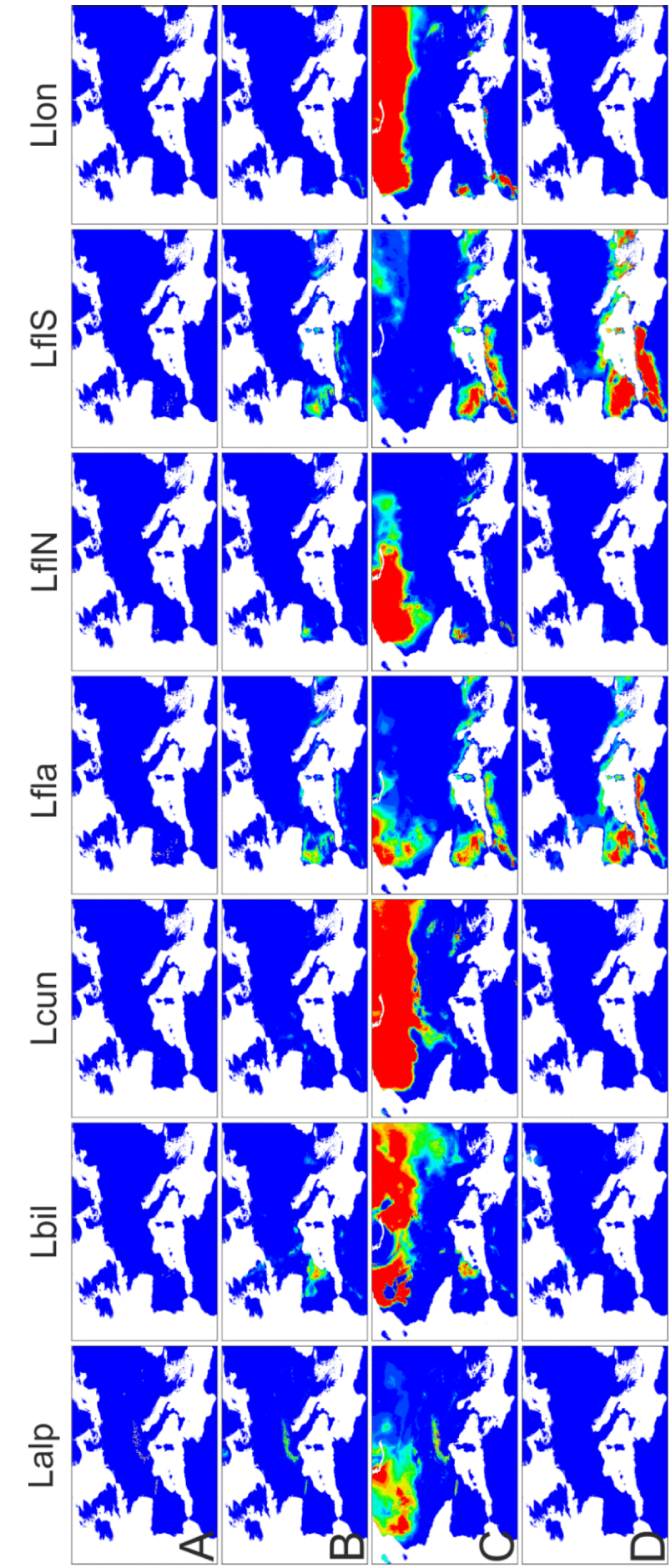

Figure 4.5: Realized and potential distribution of the different *Leucanthemopsis* taxa. Line A: realized actual distribution; line B: potencial actual distribution; line C: potential distribution during the last glacial maximum (LGM); line D: potential distribution during the last inter-glacial (LIG). Taxa abbreviations stand for: **Lalp** = *Leucanthemopsis alpina*; **Lbil** = *L. pallida* subsp. *virescens* var. *bilbilitanum*; **Lcun** = *L. alpina* subsp. *cuneata*; **Lfla** = *L. flaveola* (all); **LflN** = *L. flaveola* (northern part of the disjunct range); **LflS** = *L. flaveola* (southern part of the disjunct range); **Llon** = *L. longipectinata*; **Lpal** = *L. pallida* var. *alpina*; **Lpec** = *L. pectinata*; **Lppa** = *L. pallida* var. *pallida*; **Lpul** = *L. pulverulenta*; **Lspa** = *L. pallida* subsp. *spathulifolia*; **Lvir** = *L. pallida* subsp. *virescens* var. *virescens*.

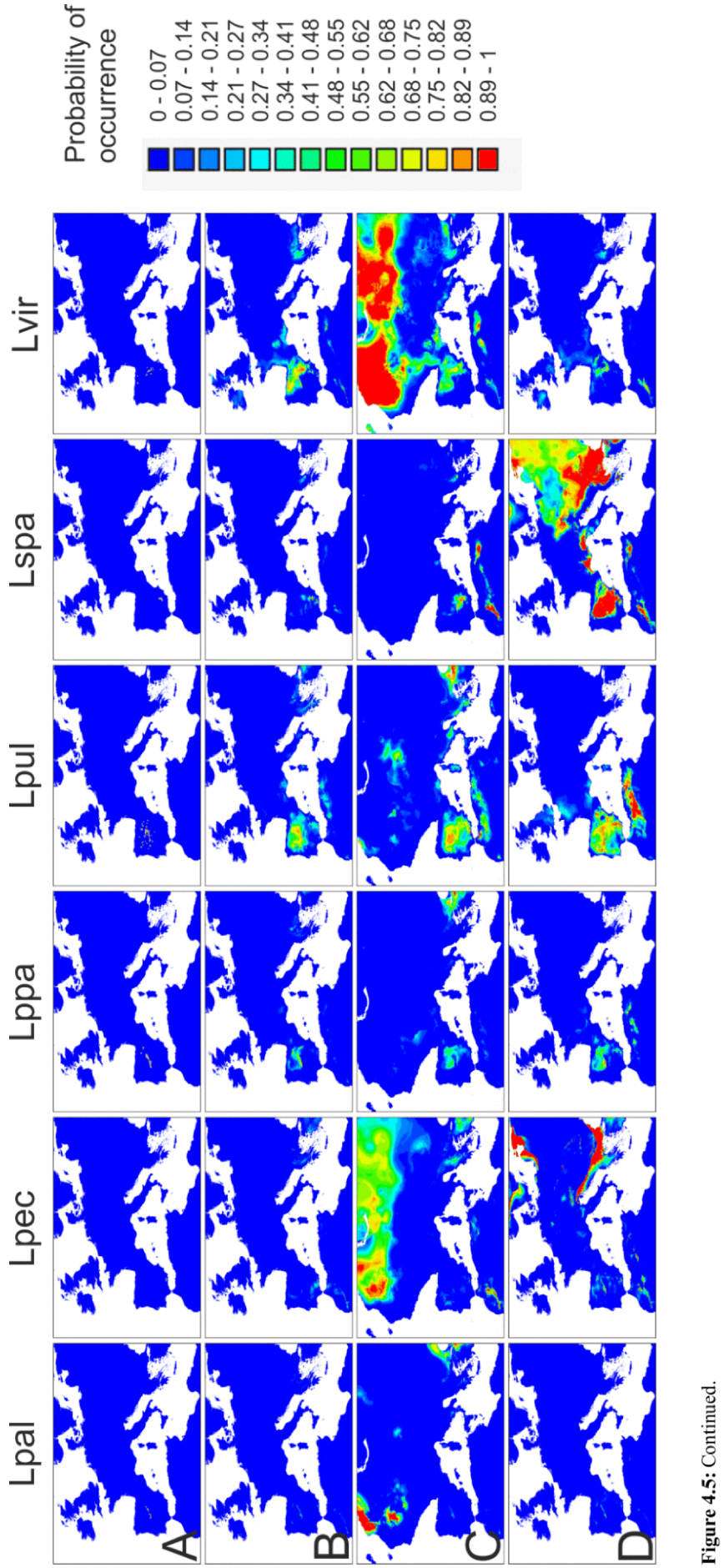

Figure 4.5: Continued.

during the LIG. The same trend can be observed for the taxa linked to lower altitude habitats (*L. pulverulenta*, *L. pallida* subsp. s*pathulifolia,* and *L. flaveola* in the southern part of its disjunct range). *Leucanthemopsis flaveola* (especially when considering the southern representatives alone) is the taxon that shows the largest difference between potential and realized distribution range and a larger expansion both during the LGM and the LIG. Percentages of predicted distribution overlaps between different taxa of *Leucanthemopsis* are given in Table 4.7.

4.4 Discussion

4.4.1 Phylogeny of the genus Leucanthemopsis. – In the present study, we have aimed at reconstructing the evolution of the genus *Leucanthemopsis* trying to perceive the signal of hybrid speciation while taking into account the stochastic processes producing incongruence among gene trees and lack of monophyly for alleles belonging to the same taxon within the gene trees. In order to do this, we have used plastid regions and single-/low-copy nuclear markers. In contrast with the tree obtained for the concatenated chloroplast regions, the nuclear markers resulted in weakly resolved gene trees, polyphyly of taxa and incongruence among gene trees. We have tried to solve these issues using coalescent-based species tree reconstruction methods, and applied the procedure described in Chapter 3 to shed light on the reticulate evolution of the polyploid representatives of the genus.

We have used two approaches concerning the assignment of alleles to taxa: in the first one, we followed the taxonomic treatment proposed by Heywood (1975); in the second, we used the best (most likely) taxa delimitation scenario for the Iberian polyploids. In both cases, results corroborated the monophyly and the previous age estimate for *Leucanthemopsis* with an age around 4 Ma, being in accordance with a previous study (see Chapter 2). The hexaploid *L. longipectinata*, an endemic species of the Rif Mountains in N Morocco, occupies an early diverging position in the genus. Excluding this taxon, the genus appears clearly divided in two taxon aggregates. The first one comprises all representatives of *L. alpina* except for the N Spanish subspecies *L. alpina* subsp. *cuneata*, while the second one is a clade that includes all the Iberian *Leucanthemopsis* taxa. In both network reconstructions, no reticulation events involving member of the one and of the other group are reported. However, in some of the nuclear gene trees, alleles from the Pyrenean *L. alpina* are found closely-related to those from the Iberian taxa (expecially *L. alpina* subsp. *cuneata*),

Table 4.7: Overlap between potential distribution areas of pairs of *Leucanthemopsis* taxa resulting from the eco-climatological modelling. Numbers on the upper part of the table refer to present day overlaps. On the bottom, numbers before slashes refer to last glacial maximum (LGM) range overlaps, whereas numbers after slashes are for potential range overlaps during the last interglacial (LIG).

Taxon	Lalp	Lbil	Lcun	Lfla	LflN	LflS	Llon	Lpal	Lpec	Lppa	Lpul	Lspa	Lvir
Lalp		0.001	0.107	0.006	0.008	0.008	0.021	0.013	0.012	0.003	0.009	0.000	0.022
Lbil	0.029/0.000		0.299	0.130	0.031	0.128	0.042	0.359	0.018	0.571	0.419	0.329	0.665
Lcun	0.223/0.000	0.237/0.000		0.332	0.101	0.429	0.152	0.259	0.160	0.420	0.348	0.042	0.652
Lfla	0.004/0.000	0.067/0.031	0.059/0.890		0.970	0.830	0.569	0.827	0.682	0.500	0.596	0.736	0.299
LflN	0.007/0.000	0.012/0.000	0.009/0.051	0.975/0.999		0.712	0.229	0.453	0.213	0.181	0.639	0.040	0.484
LflS	0.005/0.000	0.069/0.076	0.013/1.000	0.866/0.922	0.535/0.836		0.673	0.949	0.743	0.528	0.579	0.775	0.268
Llon	0.038/0.000	0.256/0.000	0.114/0.170	0.511/0.921	0.326/0.106	0.529/0.985		0.298	0.389	0.028	0.286	0.065	0.229
Lpal	0.001/0.000	0.136/0.010	0.026/0.212	0.462/0.998	0.184/0.138	0.560/1.000	0.110/0.105		0.551	0.588	0.609	0.251	0.866
Lpec	0.052/0.142	0.449/0.601	0.193/1.000	0.390/0.321	0.326/0.270	0.411/0.432	0.521/0.325	0.223/0.824		0.134	0.373	0.121	0.287
Lppa	0.001/0.000	0.136/0.012	0.116/0.003	0.736/0.950	0.101/0.083	0.730/0.953	0.042/0.004	0.520/0.777	0.162/0.309		0.897	0.203	0.904
Lpul	0.001/0.000	0.135/0.136	0.060/0.008	0.791/0.810	0.416/0.820	0.792/0.842	0.322/0.742	0.548/0.825	0.233/0.129	0.804/0.942		0.667	0.468
Lspa	0.000/0.000	0.067/0.670	0.000/0.838	0.078/0.442	0.054/0.089	0.084/0.426	0.068/0.068	0.000/0.814	0.070/0.699	0.000/0.778	0.002/0.404		0.632
Lvir	0.032/0.000	0.447/0.072	0.404/1.000	0.417/0.660	0.487/0.367	0.302/0.659	0.132/0.126	0.402/0.746	0.320/0.229	0.639/0.324	0.381/0.545	0.076/0.435	

even in those gene trees where sequences belonging to different species are better sorted (e.g., *D35*). In our view, this could be an indication of gene flow between members of *L. alpina* in the Pyrenees and some of the Iberian taxa, most probably *L. alpina* subsp. *cuneata*. The latter species is presently growing in the "Pico the Urbión", a mountain peak 200 km south-east from the E Pyrenees. Although nowadays those taxa do not grow sympatrically, results from the niche reconstruction analyses indicate the E Pyrenees (the area were the hexaploid *L. alpina* are found) as a suitable habitat for *L. alpina* subsp. *cuneata*. Results from the LGM projections point to a broader expansion towards the Eastern Pyrenees of this taxon during the last glaciation. It is therefore likely that in the past, contact zones were formed in the E Pyrenees, allowing gene flow between these two taxa.

Nevertheless, it is evident that *L. alpina* subsp. *cuneata* should not be considered part of the species *L. alpina* for several other reasons. The chloroplast network (Figure 4.2) shows that this taxon shares the chloroplast type rather with diploid taxa from the Iberian Peninsula (more specifically *L. pectinata* and *L. pallida* subsp. *virescens* var. *bilbilitanum*) and in both species network reconstructions, none of the other representatives of *L. alpina* are related to it or contribute to its formation. It was Heywood (1975) who placed this taxon under the actual taxonomic position based on its dwarf habit, white ligules, and some characters of the leaf shape that somehow recalled *L. alpina*. However, other authors considered it as an independent species (Holub 1977; Valdez-Bermejo in Antunez 1981) and the Spanish botanist Carlos Pau, who first described this taxon, regarded it as a variety of *L. pallida* (Pau, 1906). The results of the phylogenetic analyses we are presenting here, corroborate the hypothesis of *L. alpina* subsp. *cuneata* being an independent entity (likely at the species level), included in the Iberian species aggregate rather than belonging to *L. alpina*.

The diploid subspecies *L. alpina* subsp. *tomentosa* from Corsica was indicated as a potential hybrid by the test for homoploid hybridization (Figure 4.3). It was likely the effect of the fact that in some of the nuclear gene trees, alleles from the samples belonging to this taxon cluster together with lineages from the Iberian aggregate rather than with *L. alpina*. It was therefore included in the species network analysis in the same way as for the polyploid taxa, being allowed to have a hybrid origin. Despite that, in both network reconstructions it turned out to be non-hybrid and nicely nested within the *L. alpina*-aggregate.

The situation becomes more blurred when looking inside the Iberian clade, and posterior probability values in both network analyses get considerably low (only posterior probabilities higher that 0.5 are reported in the networks; Figures 4.4a,b). The lack of support and the incongruence between the two reconstructions might be a consequence of a weak

phylogenetic signal in the data set as also observed in comparable studies (Cranston et al. 2009; Amaral et al. 2012; Sistrom et al. 2014). However, in species tree/network analyses posterior probabilities must not be considered as in usual gene tree Bayesian analyses, and values higher than 0.8 tend already to describe highly accurate clades following Leaché & Rannala (2011). In addition, as we used the MUL-species tree obtained in *BEAST to build the species network with Dendroscope, some branch lengths were transformed and clades were lost, so that support values and age estimate should be taken with caution. When we look at the position of the diploid taxa of the Iberian aggregate, the main difference concerns the placement of the species *L. pulverulenta* and *L. pectinata*. While in the first network reconstruction (the one in which all the taxa recognised by Heywood (1975) are included separately), *L. pulverulanta* is sister to the other three diploid taxa of the Iberian clade, with the second approach (in which we used the taxa delimitation for the tetraploid Iberian taxa resulting in the highest probability of the gene trees) the situation is inverted. The remaining two diploid taxa in the Iberian aggregate are the two varieties of the subspecies *L. pallida* subsp. *virescens*. The results of the network reconstruction (Figure 4.4a), the fact that they share a great part of their distribution range, together with some morphological patterns of the leaf shape, point towards a strict relationship of these two taxa. They differ mainly in the colour of the ligules (variety *virescens* having yellow ligules, variety *bilbilitanum* entirely white ones), and in their edaphic requirements, the former being principally a calcicole and the latter being a calcifuge. On the other hand, the close relationship of those two varieties with the polyploid taxa of the species *L. pallida* seems totally invalidated by the results of the present study. While the member of the subspecies *virescens* are diploids with a chloroplast type similar to the other diploid taxa of the Iberian Peninsula, the rest of the *L. pallida* is constituted by tetraploids having a completely different chloroplast type (Figure 4.2). The taxonomic distance between diploid and tetraploid members of *L. pallida* has been pointed out in the past by Spanish botanists, who aimed to rise subspecies *L. pallida* subsp. *virescens* to the species rank (Valdez-Bermejo in Antunez, 1981; Pérez-Romero et al. 2005). Anyway, those proposals remained forgotten and generally not applied, maybe due to the lack of strong evidences provided by the authors for such a taxonomical change.

The taxa scenario that gives the MUL-tree leading to the best likelihood score (Figure 4.4b), was indeed the one in which all the samples belonging to *L. pallida* (all except sample LPS186, a controversial herbarium specimen from the province of Murcia) were placed together with those of *L. flaveola* from the southern part of the range, and samples from the northern ranges of *L. flaveola* were treated separately. This argues for two different origins

of the tetrapoid representatives of *Leucanthemopsis* in the Iberian Peninsula: the first giving rise to all the tetraploid infraspecific entities of *L. pallida* and the *L. flaveola* found in the eastern "Sistema Central", "Montes de Toledo", and "Sierra Morena", and the second independently leading to *L. flaveola* growing between Galicia and León (NE Spain). Taking for granted that this scenario reflects the real evolutionary history of the genus *Leucanthemopsis*, the network reconstruction in Figure 4.4a [obtained treating all the infraspecific taxa described by Heywood (1975) separately] can give however useful information on how the infraspecific taxa in *L. pallida* diverged from one another after the single collective polyploidization event.

4.4.2 Origin of polyploids. – Two of the hexaploid taxa of *Leucanthemopsis* have clearly an autopolyploid origin. *Leucanthemopsis longipectinata* is the only representative of the genus is North Africa. It early differentiated from the other *Leucanthemopsis* already 4 Ma ago, although – as mentioned before – date estimates given here have to be taken with caution. It is likely the descendant of a Tertiary *Leucanthemopsis* diploid, confined to the North African mountain ranges, which gave rise to the actual hexaploid as unique extant species. Although it may have come into contact with other *Leucanthemopsis* taxa in the past (projections for the last interglacial show potentially suitable areas for this species in the Iberian Peninsula; Figure 4.5), it does not seem to be the case according to the results of the phylogeny.

We preferred to treat the samples from the three ploidy levels found in *L. alpina* separately, although it is very unlikely that they constitute entities completely isolated reproductively from one another. In any case, no other species participate in the formation of both the tetraploids and the hexaploids in *L. alpina*. The hexaploids, which are found only in the "La Maladeta" massif (Central Pyrenees), constitute a unit well-separated from the diploid accessions from the Alps and from those belonging to the Corsican subspecies *L. alpina* subsp. *tomentosa*. The tetraploids strangely result as the product of the hybridization between the hexaploid and either the diploids from the typical or from the Corsican subspecies. In the present study, two tetraploid accessions of *L. alpina* were included, one from the Pyrenees and the other from the E Alps. The results need therefore to be taken with precaution, and might be just the effect of geographic patterns in the genetic diversity within the species *L. alpina*. *Leucanthemopsis alpina* is the widest distributed species in *Leucanthemopsis*, with diploids and tetraploids spread almost evenly throughout the species range and without clear morphological and ecological differences among the

levels. Further studies with a more intensive sampling and with more powerful molecular methods at the infraspecific level would be useful to clarify the relationship among the different ploidies and the origin (single or multiple) of the polyploids.

The thirth hexaploid taxon, *L. alpina* subsp. *cuneata*, seems to have a hybrid origin to which the two diploid taxa *L. pallida* subsp. *virescens* and *L. pectinata* may have contributed. Although the latter is nowadays only present in the Sierra Nevada (S Spain), far from the current range of *L. alpina* subsp. *cuneata*, it could have undergone further expansion towards the north in the past (and especially during the last interglacial; Figure 4.5). Oro-mediterranian taxa like *L. pectinata* have very likely experienced migrations towards the north in the past, following the way formed in the E Iberian Peninsula by the mountains of the Baetic system, the "Serrania de Cuenca", the Iberian System, until Urbión and the Pyrenees (Rivaz-Martinez 1969, 1973). When we look at the results of the range overlap analyses, we can see that the two taxa showing the highest range overlap with *L. alpina* subsp. *cuneata* during the last inter-glacial are indeed *L. pectinata* and *L. pallida* subsp. *virescens* var. *virescens* (Table 4.7).

Concerning the tetraploid taxa in the Iberian Peninsula, we need firstly to assert that they cannot be exclusively the product of polyploid hybridization between extant diploid taxa, and the contribution of a diploid and nowadays extinct lineage has to be assumed. All tetraploids share in fact haplotypes from the same unique group, greatly different from those found in the Iberian diploids. Therefore, they could either be autotetraploid, formed from the previous mentioned extinct diploid, or allotetraploid, in which case the maternal genome was contributed by the extinct diploid lineage. Results from the phylogenetic species network analyses suggest two different origins for the tetraploids as the most plausible scenario.

The first origin, which involved the two diploid species *L. pulverulenta* and *L. pectinata*, produced the populations of *L. faveola* found nowadays in the mountain range between Galicia and León (NW Spain), and corresponding approximately to the form *L. flaveola* f. *alpestre* firstly described by Mariz (1891). As already mentioned, *L. flaveola* is a widely distributed species in the Western Iberian Peninsula with a high phenotypic plasticity, presenting disjointedly some populations in the "Montes de León" (NW Spain) and others more south, from the easternmost part of the Central System until the "Sierra Morena". It entails that populations from different parts of the range are subjected to very diverse ecological conditions. The *L. flaveola* from the NW in fact grows in the highest peaks of the "Montes Aquilianos", "Sierra del Teleno" and "Sierra de la Cabrera" (Montes de León), at

altitudes between 1700-2000 m, under temperate sub-alpine conditions, whereas on the other extreme the "Sierra Morena" reaches approximately 1000 m, hosting a strict Mediterranean climate. It has to be noticed that Heywood (1954, 1975) considered under this taxon only the populations growing in the NW Iberian Peninsula, regarding the southernmost populations rather belonging to *L. pallida* subsp. *pallida*. Ladero & Velasco (1978) ascribed *Leucanthemopsis* from the "Sierra Morena" and eastern Central System to *L. flaveola* (considered in their study as being a subspecies of *L. pallida*), due to the leaf morphology, that verily recall the traits of this species rather than *L. pallida* subsp. *pallida*. It was in the view of all this, and of the fact that one of the two populations of NW *L. flaveola* included in the study presents chloroplast type as in the diploids, that we tested as well scenarios in which the *L. flaveola* from the North and those from the South were treated separately. The results of our study support this possible situation, and the fact that we found in the ancestors of *L. pulverulenta* and *L. pectinata* the parental diploid taxa of the NW *L. flaveola*, fits nicely with the ideas of previous botanists, who considered this taxon linked to both the previously mentioned diploids (Mariz 1891) or to the only *L. pectinata* (Heywood 1955; Antunez 1981).

However, it is unavoidable to consider the possibility of a decisive influence of the chloroplast regions on these results. The plastid heterogeneity found in the two populations from the NW Iberian Peninsula, might either be the effect of a multiple origin of the tetraploids in this area or the effect of chloroplast capture as already pointed out for other polyploid complexes (Ito et al. 2013). In the latter case, two possible scenarios need to be considered: chloroplast captures through hybridization between the southern *L. flaveola* as maternal contributor and the north-western representatives of the species (and subsequent backcross of the hybrids with the only paternal contributors) or chloroplast capture through hybridization (posterior to the initial allopolyploidization) of the north-western *L. flaveola* with *L. pulverulenta* as maternal contributor (and subsequent backcross of the hybrids with the only *L. flaveola*). Sequencing of more individuals from those populations as well as a more intensive sampling in this area would definitively help to discriminate between all those possible explanations.

The second origin gave rise to all the infraspecific taxa of *L. pallida* and to the *L. flaveola* from the south. To this contribute, besides the unknown diploid maternal ancestor, *L. pallida* subsp. *virescens* var. *bilbilitanum*. Recognizing a unique origin of all these taxa, it becomes hard to explain the high morphological and ecological diversity found nowadays in *L. flaveola* and in the different subspecies of *L pallida*. The results of the network reconstruction done using the first approach [species delimitation following the treatment of

Heywood (1975)] shown in Figure 4.4a, together with biogeographical and ecological considerations, might give useful hints towards further interpretations of the actual situation. In our view, the newly formed tetraploid would have been able to radiate into a large part of the Iberian Peninsula, getting in contact with other taxa of *Leucanthemopsis*, and eventually giving rise to diverse hybridization processes in different areas. The purest remnant of the ancestral *L. pallida* could be the variety *alpina*, found above 2000 m in the highest peaks of the Central System. This could have generated the variety *L. pallida* var. *pallida*, by coming into contact with the diploid *L. pulverulenta*, which grows at lower altitudes in the same mountain range. In the westernmost part of the Central System, and further towards the north, the putative tetraploid ancestor could have been strongly influenced by the NW *L. flaveola*, explaining in this way the *flaveola*-like leaf traits of the populations growing there. In the southeasternmost part of the range, in the Baetic System, hybridization with the diploid *L. pallida* subsp. *virescens* – and likely with the typical form of this taxon – could have produced *L. pallida* subsp. *spathulifolia*, as suggested by other authors in the past (e.g., Antunez 1981). That would provide a good explanation to the similarities concerning the morphology and regarding ecological and especially edaphic requirements (these two taxa are the only calcifuges in the genus *Leucanthemopsis*).

4.4.3 Species dubiae. – The sample LPS186 constitutes in our opinion a problematic case in the present study. It consists of a herbarium specimen collected in 2005 in "Pico Revolcadores" (Province of Murcia). It was collected at an altitude of almost 2000 m on limestone, and has been determined as *L. pallida* without further specifying its infraspecific classification. Concerning the geographical situation, it could be somehow included in the range of *L. pallida* subsp. *spathulifolia*, although already at its easternmost extreme. The leaves are much smaller than those of the latter taxon and their morphology could rather recall to some extent *L. pallida* subsp. *virescens*. This sample shows a chloroplast type similar to the Iberian diploid taxa, but results from the network reconstruction are quite contradicting. It could be a diploid, although in the marker *C12*, three alleles were recorded. It would be crucial to know the ploidy of this *Leucanthemopsis* population growing in "Pico Revolcadores". If diploid, they might be a deviating relict population of *L. pallida* subsp. *virescens* (the variety *virescens* most probably, although with white ligules), growing in some mountain peaks much further South than the actual range of the taxon.

Heywood (1954, 1975) described a subspecies of *L. pulverulenta*, growing in the eastern Iberian Peninsula on limestone. This taxon, named by the author *L. pulverulenta* subsp.

pseudopulverolenta (Heywood) Heywood, differs from the typical subspecies in substrate requirement, being indeed calcicolous, and in geographical distribution, representing the vicariant form in the east of *L. pulverulenta* subsp. *pulverulenta*. Heywood based his decision on four herbarium specimens, three of which being from S Aragón (Javalambre, Reverchon nr. 785, in herb. M; Sierra de Noguera, Reverchon nr. 785, in herb. M; Sierra de Albarracín, Cerro de San Jinés, MA128808), and the fourth being from the "Sierra de Cazorla" (Reverchon n 785, in herb. M). Other taxa of *Leucanthemopsis* are presently growing in both areas (*L. pallida* subsp. *virescens* and *L. pallida* subsp. *spathulifolia,* respectively). We have seen those vouchers in the herbaria of München (M) and Madrid (MA), and it must be said that they cannot be ascribed to any of those co-occurring taxa. The entirely divided leaves and the conspicuous number of segments recall indeed *L. pulverulenta*, although other features and general habit are quite peculiar. The taxon seems to be rare, and to our knowledge, it was collected (beside the four specimens already cited) only an additional time in 1976 by Leal, Pajarón and Rodríguez Pascual (MA512875). We have been personally in the "Sierra de Javalambre", the "locus classicus" of the taxon described by Heywood, but we were not able to find the taxon. It was therefore not included in the present study.

There is in our opinion another interesting taxon of *Leucanthemopsis* growing in S Aragón, definitively different from the previous one. It consists of very tomentose specimens with cuneate and almost undivided leaves, white ligules, growing on silicates at relatively high altitudes. The most representative sample for this taxon is a plant collected in 1962 in the "Sierra Alta, Bronchales" (Mexmüller nr. 17125, in herb. M) and determined as *L. alpina* subsp. *cuneata*. Similar plants were collected in the "Eremita del Tremedal" by Koch in 1972 (M), in Javalambre (MA442950) and in "Puerto de Orihuela" (MA421802). Apart for the specimen from Javalambre, all the other plants are from an area within a radius of 10 km around the "locus classicus" of the controversial species *Chrysanthemum alpinum* Asso described by Asso in the 1779. This name is invalid because of a name previously given by Linneus to the current *Leucanthemopsis alpina*, and when Heywood (1955) examined a herbarium voucher collected by Pau in the same place (MA128778), he considered this plant rather to be part of *L. pallida* subsp. *virescens* var. *bilbilitanum*. Again, we have been in the precise localities cited in those herbarium vouchers, but we were not able find any representative of the taxon. We included in our present study material from the first herbarium voucher mentioned, but because of problems during amplification and sequencing, we decided to exclude it from the analyses.

4.4.4 Conclusion and perspectives. – We treated here the phylogeny of *Leucanthemopsis* using over 50 accessions from different taxa, two chloroplast intergenic spacer and four single-/low-copy nuclear markers. In Chapter 3, while describing a novel approach to reconstruct reticulate evolution in polyploidy complexes, we provided as example a phylogeny based on a reduced *Leucanthemopsis* data set. In those analyses, only four polypoid taxa were included, with a single accession per taxon. Also concerning the diploid taxa, a reduced number of accessions was included. Reconstructing a complete phylogeny of the genus was beyond the scopes of the study in Chapter 3, and incongruence between their analyses and the here presented one (only concerning the only *L. alpina* subsp. c*uneata*) can be therefore ascribed to the lack of a comprehensive sampling.

One of the main issues of the present study was the low support obtained in the species networks for the terminal clades of the Iberian aggregate (but see discussion above). A higher number of genome regions as well as the use of more powerful molecular methods at this fine scale could help to improve the situation. RADseq, for example, proved to be very useful especially in presence of hybridization and introgression (Eaton & Ree 2013).

In a second approach for inferring the species network, we tried different scenarios of taxa delimitation (for the Iberian tetraploids only), scoring then the most likely as the one describing trustworthy the real evolutionary history of the genus. We considered it a good approach when few is known about the number or polyploidization (and/or reticulation) events, especially if working with taxonomically problematic groups.

As a general trend, the results from the niche reconstruction analyses point towards a range expansion of oro-mediterranean *Leucanthemopsis* taxa (e.g., *L. pectinata*, *L. pallida* var. *alpina*) further north and at lower altitudes during warmer interglacial periods. It could have allowed the contact of these taxa with meso-mediterranian *Leucanthemopsis*, and consequent new polyploid hybrids formations (as also corroborated by the phylogenetic analyses), being therefore one of the most relevant driving force in the diversification of the genus.

Chapter 5

The role of polyploidy and past glacial history for the diversification processes in the alpine species *L. alpina* (L.) Heywood

5.1 Introdution

Speciation events involving an increase of the complete chromosome set (polyploid speciation) are considered very common in flowering plants. Wood et al. (2009) estimated that the 15 % of all speciation events occurring in plants involve polyploidization. Polyploidy has often been considered a particularly important feature in alpine and arctic floras. Higher frequencies of polyploids are found at higher altitudes and latitudes (see Stebbins 1950, 1984; Dodson & Dodson 1976; Ehrendorfer 1980; Thompson & Lumaret 1992; Brochmann et al. 2004 for reviews). This pattern was generally linked to a supposed higher capacity of polyploids to tolerate environmental stress and extreme habitats (Hagerup 1931; Cain 1944), or to selective advantages that polyploids own compared to the diploids (due to greater genetic variability) in areas that experienced repeated catastrophic climatic fluctuations (Manton 1950; Löve & Löve 1957). However, Favarger (1957) did not find any difference between the frequency of polyploids in areas above the snow line and the surrounding lowlands in Swiss Alps. In experimental studies, artificial polyploids were not found to be more resistant to environmental stresses than the diploid progenitors (Stebbins 1985; Tal 1980). An alternative explanation for the observed higher rate of polyploids in arctic and alpine environments recall the presumed predisposition of polyploids to colonize newly deglaciated areas because of their greater ecological adaptability (Stebbins 1950; Hodgson 1987).

It is common knowledge that Alps have experienced during the Pleistocene multiple glaciation cycles, during which thick ice sheets covered a great parts of the mountain range (Wilson et al. 2000). During the Last Glacial Maximum only few parts of the Southwestern and Eastern Alps were uncovered by glaciers, and the ice sheet in the central region of the

Alps could reach 2300- 2700 m of thickness (Voges 1995; van Husen 1997). Marginal areas of the alpine range as well as few delimited mountain ridges in the inner part [Nunataks; see Schneeweiss & Schönswetter (2011) for a recent reconsideration of the concept] remained uncovered by the ice and continued to constitute a suitable habitat for alpine species through the glaciations. Those areas (refugia) are nowadays well know both for calcicolous and calcifuge species, being inferred in the past by analysing pattern of endemism in the alpine flora (Pawłowski 1970; Tribsch & Schönswetter 2003) or by looking at geographical patterns in the intraspecific genetic variation of alpine species (Schönswetter et al. 2005 for a review).

The quaternary climatic oscillations have been most probably one of the principle driving force for speciation in the alpine flora. Kadereit et al. (2004) interpreted the negative correlation found between temperature and rate of diversification in *Primula* sect. *Auriculata* as an indication that speciation processes in the group occurred principally during glacial periods in geographically isolated refugial areas. For arctic-alpine species, polyploidization has been an important mechanism for "stabilizing" new evolutionary lineages in areas that have been covered by ice during the Pleistocene glaciations, as pointed out in different studies for the Alps (Marhold & Lihovà 2006; Albach 2007; Hörandl et al. 2005; Burnier et al. 2008; Casazza et al. 2012) and for the arctic region (see Abbott & Brochmann 2003; Brochmann et al. 2004 for reviews). The importance of polyploidization for species diversification in areas heavily affected by glaciation might be explained by the "secondary contact model" (Stebbins 1984, 1985). Accordingly, the advancement of the ice sheet during cold period confined alpine species in marginal areas uncovered by ice. Isolated populations would have had enough time to differentiate from one another, and the retreat of ice following the climate warming of interglacial periods (with subsequent range expansion of those populations), would have produced contact zones between diverging lineages and -occasionally- "intra-specific" hybridization stabilized by polyploidization. Beside the presumed among cytotypes reproductive isolation automatically acquired with the polyploidization, additional mechanisms such as fitness advantages (Sonnleitner et al. 2013) or niche differentiation (Mráz et al. 2008; Raabová et al. 2009; Sonnleitner et al. 2010; García-Fernández et al. 2012) could have finally helped to establish coexistence of lineages with different ploidy.

Leucanthemopsis alpina (L.) Giroux is a little caespitose, scapose perennial herbs, growing in high alpine environments at altitudes between 2000 and 3600 m (Pignatti 1982). The species grows essentially on siliceous rocks, in shallow clastic alpine soils, screes and

ridges. It is widely distributed in all the main European alpine ranges, from the Pyrenees to the Carpathians, and three ploidy levels are realized within the species. Diploids are distributed mainly in Western Alps, Corsica, and Carpathians, while tetraploids in the Pyrenees, in Eastern Alps and irregularly also in the Cottian and Pennine Alps (Contandriopoulos & Favarger 1959; Skalinska et al. 1959; Heywood 1975). Hexaploids are only found in a restricted area of the Central Pyrenees (Küpfer & Favarger 1967). Favarger & Küpfer (1968) reported the presence of a single diploid plant in "Pas de la Casa" (Andorra, Eastern Pyrenees). Diploids have been surprisingly found by Küpfer (1974) in the Dolomites, although the rest of the Eastern Alps is inhabited by tetraploid populations. The species does not extend extensively in the main Mediterranean peninsulas, being represented by a single population in the Apennines (Mt. Prado, Tuscan-Emilian Apennines), and its presence in the Balkan must be considered rather rare or uncertain. Beck et al. (1984) indicate the presence of *L. alpina* in Mt. Vranica and Mt. Maglić (Bosnia-Herzegovina), although those are calcareous mountains (not a suitable bedrock for the species) and in the red list of the Bosnian flora (EU Greenway Sarajevo 2013) the status of the species is uncertain due to lack of information. Recently, in a study on the genome size of over 300 taxa of the Balkan flora, Siljak-Yakovlev et al. (2010) collected the species in Mt. Jahorina (Bosnia-Herzegovina). The hexaploid population from "Sierra de Úrbion", belonging to the subspecies *L. alpina* subsp. *cuneata* (Northern Spain), cannot be considered part of the species, as it has been pointed out in Chapter 4.

Leucanthemopsis alpina constitutes a polymorphic complex as well from a morphological point of view, and several intraspecific taxa at different level have been described in the past. Apart from the well-differentiated Corsican subspecies *L. alpina* subsp. *tomentosa*, Vierhapper (1914) distinguished six forms in the species: *L. alpina* f. *hutchinsiifolia*, *L. alpina* f. *pseudotomentosa*, *L. alpina* f. *minima*, *L. alpina* f. *pyrenaica*, *L. alpina* f. *cuneifolia*, and *L. alpina* f. *tatrae*. Those forms differed from one another principally by the dimension of leaves and capitula, for the extent of leaf incisions, spacing of the leaflets, and for the abundance of indumentum. Over the years, as more and more karyological studies became available, different authors changed the taxonomic rank or considered invalid some of those taxa, depending as well on the importance given by these botanists to the above mentioned morphological characters (e.g., Heywood 1955, 1975; Marchi & Illuminati 1974; Holub 1977). In the Flora d'Italia, Pignatti (1982) even treated the populations from the Alps as two different species (i.e., *L. alpina* and *L. minima*, the diploids and the tetraploids, respectively), each of which comprising additional infraspecific taxa. However, the whole

complex is monophyletic, and constitutes the Euro-Siberian lineage of the strictly Mediterranean genus *Leucanthemopsis* (Giroux) Heywood, diverged around 2.5 Ma ago from the other representatives of the genus (see Chapter 4). Hexaploids are autopolyploid, while strangely enough the tetraploids were reconstructed as being the product of hybridization processes between the hexaploids and the diploids. In the mentioned study, only two tetraploids were included for *L. alpina* (one from Pyrenees, where the hexaploids are found, and one from the Alps, where one of the diploids came from), and that result might be simply the effect of geographical patterns of genetic variation and incomplete sampling for *L. alpina*, as pointed out in Chapter 4.

In the present study we aim to investigate the ongoing diversification processes in the high alpine species *L. alpina*. More specifically, we want to answer the following questions: i) Is polyploidy playing a primary role in the diversification of lineages within the polymorphic complex *L. alpina*? In other words, has polyploidization arisen rarely producing isolation between diploids and polyploid lineages, or is it rather a common feature in the species, reflected in an intensive gene flow between cytotypes? ii) Has the Pleistocene glaciation cycles played a role in the diversification (eventually due to secondary contact stabilized by polyploidization), as already highlighted for other alpine species (see above)? iii) Is there any connection between genetic differentiation patterns and the morphological polymorphism observed in the species? In order to answer those questions, we delineated the geographic distribution of cytotypes, using a dense enough populations sampling throughout the vast majority of the species distribution range. We assessed genetic variation through plastid DNA sequencing and scoring of AFLP fingerprinting markers. A morphometric study then evaluated morphological polymorphism among different populations of *L. alpina*.

5.2 Materials and Methods

5.2.1 Plant material. – 82 populations of *Leucanthemopsis alpina* were collected during summers of 2010 and 2011, covering the whole distribution range of the species. We included in the study all the intraspecific taxa of *L. alpina*, except for the Iberian subspecies *L. alpina* subsp. *cuneata*, which clearly represents a separate entity, well distinct from the rest of the species (see Chapter 4). However, for the purpose of the present study, all populations were treated indiscriminately as *L. alpina*, without further investigate the

intraspecific taxon belonging. Leafs from up to ten individuals per population were collected and instantaneously dried in silica-gel, in order to be used for flow-cytometric purposes and for the molecular analyses. Additional individuals were herborized, used for the morphometric analyses and as reference for the populations collected. A complete list of the populations collected is given in Table 5.1.

5.2.2 DNA extraction, DNA amplification, and marker sequencing. – DNA was extracted using a modified protocol based on the CTAB method (Doyle & Doyle 1987) and the quality was checked on 1.5% TBE-agarose gels. The two chloroplast intergenic spacers *psbA-trnH* and *trnC-petN* were used for reconstructing the phylogeography of *L. alpina*. For this purpose, we employed three individuals per population together with two accessions from *L. alpina* subsp. *cuneata* (Pau) Heywood and one from *L. pectinata* (L.) G.López & C.E.Jarvis used as outgroup, for a total amount of 241 OTUs. Polymerase chain reaction (PCR) was performed with primers psbAf and trnHr (Sang 1997) for the first region, and trnC (Demesure et al. 1995) and petN1r (Lee & Wen 2004) for the second. We used the *Taq* DNA Polymerase Master-mix Red (Ampliqon/Biomol, Odense, Denmark) in a final volume of 12.5 µl, using the reagents' concentrations suggested by the company. The following temperature profile was employed: 2 min at 95°C; 36 cycles of 30 sec at 95°C, 60 sec at 62°C, 60 sec at 72°C; final extension of 5 min at 72°C. The PCR products were purified using Agencourt AMPure magnetic beads (Agencourt Bioscience Corporation, Beverly, Massachusetts, USA) and sequenced using the DTCS Sequencing Kit (Beckman Coulter, Fullerton, California, USA), following the protocol suggested by the manufacturer. Sequences were analysed on a CEQ 8000 sequencer (Beckman Coulter, Fullerton, California, USA). The electropherograms were carefully checked for ambiguities using Chromas Lite 2.10. (Technelysium Pty Ltd., Tewantin, Australia; http://technelysium.com.au/chromas.html), and – when necessary – IUPAC codes were used to indicate single nucleotides polymorphism. In the electropherograms, a site was considered polymorphic when more than one peak was present and the weakest reached at least the 25% of intensity of the strongest (Fuertes Aguilar et al. 1999, Mansion et al. 2005). Alignments for each plastid region was done using the software BioEdit (Hall 1999; http://www.mbio.ncsu.edu/bioedit/bioedit.html) and improved by hand and with the help of MAFFT (Katoh et al. 2002; http://mafft.cbrc.jp/alignment/software/), a computer program that uses a two-cycle progressive method called FFT-NS-2 (Katoh & Toh 2008). In *trnC-petN* a region of 30 bp length was deleted due to a poly-A microsatellite motive that produced

Table 5.1: List of populations included in the study. All of them are populations belong to *Leucanthemopsis alpina* except for the last two. Nei's refers to the Nei's diversity index, whereas DW to the frequency down-weighted marker values based on AFLP data. Asterisks beside the ploidy indicate populations in which intermediate cytotypes were found, circles indicate mixed populations.

Code	Collection site	State	Latitude	Longitude	Ploidy	Nei's GD	DW
LPS064	Visokè Tatry	SK	N 49°11'28.2"	E 20°11'40.6"	2*x*	0.118	12.732
LPS065	Sestriere	I	N 44°59'8.4"	E 6°52'13.8"	4*x*	0.076	6.545
LPS066	Colle dell'Agnello	I-F	N 44°41'5.5"	E 6°58'43.1"	4*x*	0.195	14.243
LPS067	Col De Fenestre	F	N 44°6'59.9"	E 7°21'39.3"	2*x*	0.162	25.259
LPS068	Col du Lombard	I-F	N 44°12'09"	E 07°09'02"	2*x*	0.135	11.121
LPS069	Baisse de Druos	F	N 44°11'28"	E 07°11'31"	2*x**	0.113	8.063
LPS070	Col de la Bonette	F	N 44°19'13.2"	E 6°48'25.2"	2*x*	0.093	7.915
LPS071	Pas du Lausson	F	N 44°14'30.1"	E 6°43'44.8"	4*x*	0.127	10.826
LPS072	Col D'Allos	F	N 44°18'25.9"	E 6°35'14.3"	4*x*	0.160	13.328
LPS073	Tre Vescovi	I	N 44°21'30.7"	E 06°54'03.1"	4*x*	0.052	4.396
LPS074	Glacier Blanc	F	N 44°55'58.7"	E 06°24'36.2"	2*x*	0.147	15.636
LPS075	Col du Galibert	F	N 45°3'38.8"	E 6°24'39.4"	2*x*	0.127	8.571
LPS076	Les Amoreux	F	N 45°7'34.5"	E 5°54'20.3"	2*x*	0.095	4.176
LPS077	Lac Perrin Superieur	F	N 45°12'9.9"	E 6°52'58.4"	2*x*	0.111	6.203
LPS078	Col de L'Iseran	F	N 45°25'7.4"	E 7°1'52.9"	2*x*	0.093	7.426
LPS079	Piccolo San Bernardo	F	N 45°40'45.8"	E 6°52'59.8"	2*x*	0.125	10.137
LPS080	Courchevel	F	N 45°23'19.4"	E 6°36'58.7"	2*x*	0.096	6.145
LPS081	Plan de l'Aiguille, Mont Blanc	F	N 45°54'02"	E 06°53'07"	2*x*	0.148	12.938
LPS082	Ponton	I	N 45°35'59.1"	E 7°27'4.8"	4*x*	0.124	5.981
LPS083	Bionaz	I	N 45°54'30.9"	E 7°29'21.9"	4*x*	0.180	12.007
LPS084	Gran San Bernardo	I	N 45°52'08"	E 07°10'16"	2*x*	0.088	7.619
LPS085	Staffal	I	N 45°51'22.9"	E 07°50'44.5"	4*x*	0.122	4.587
LPS086	San Bernardino	CH	N 46°29'45"	E 09°10'14"	4*x*	0.140	7.978
LPS087	Mt. Collon	CH	N 45°59'57.5"	E 7°29'40.4"	2*x*°	0.122	6.841
LPS088	Mt. Noble	CH	N 46°12'44.4"	E 7°29'1.2"	2*x*	0.127	8.059
LPS089	Schwarzsee	CH	N 45°59'24.1"	E 7°42'18.4"	2*x*	0.116	7.059
LPS090	Riffelberg	CH	N 45°59'20.5"	E 7°45'7.9"	4*x*	0.131	11.293
LPS091	Gornergrat	CH	N 45°59'5.6"	E 7°46'18.5"	4*x*	0.142	7.521
LPS092	Saas Almagell	CH	N 46°2'13"	E 7°56'39.8"	2*x*	0.100	7.119
LPS093	Simplonpass	CH	N 46°15'6.1"	E 8°0'57.5"	2*x*	0.116	7.382
LPS094	Passo della Novena	CH	N 46°28'37"	E 08°23'15"	2*x*	0.163	9.323
LPS095	Furkapass	CH	N 46°34'21"	E 08°24'55"	2*x*	0.116	5.200
LPS096	Grimselpass	CH	N 46°33'43"	E 08°20'44"	2*x*	0.078	5.605
LPS097	Kleine Scheidegg	CH	N 46°34'41"	E 07°58'12"	4*x*	0.148	8.892
LPS098	Sustenpass	CH	N 46°43'49"	E 08°26'58"	2*x*	0.111	7.594
LPS099	Julierpass	CH	N 46°28'13"	E 09°43'33"	4*x*	0.171	11.144
LPS100	Passo Bernina	CH	N 46°24'38"	E 10°01'31"	4*x*	0.141	11.596
LPS101	Gerola Alta	I	N 46°01'13.7"	E 09°34'22.7"	4*x*	0.145	8.788
LPS102	Passo dello Stelvio	I	N 46°31'57"	E 10°26'50"	4*x*	0.111	4.837
LPS103	Val Martello	I	N 46°28'46.8"	E 10°41'4.1"	4*x*	0.157	9.136
LPS104	Mt. Colombine	I	N 45°50'35.6"	E 10°22'3.7"	4*x*	0.123	6.831

Table 5.1: Continued.

Code	Collection Place	State	Latitude	Longitude	Ploidy	Nei's GD	DW
LPS105	Passo Maghen	I	N 46°10'12.3"	E 11°26'55.3"	4*x*	0.111	14.854
LPS106	Passo Rolle	I	N 46°16'55.6"	E 11°47'2.3"	2*x*	0.117	10.079
LPS107	Rittner Horn	I	N 46°36'52.5"	E 11°27'41.4"	2*x*	0.099	5.119
LPS108	Passo Stalle	I-A	N 46°53'15.4"	E 12°11'56.6"	2*x*	0.125	9.047
LPS109	Passo di Vizze	I-A	N 46°59'29.8"	E 11°39'30.4"	4*x*	0.162	11.276
LPS110	Passo di Rombo	I-A	N 46°54'18"	E 11°05'47"	4*x*	0.125	6.758
LPS111	Maso Corto	I	N 46°46'2.3"	E 10°46'39.2"	4*x*	0.152	11.251
LPS112	Flüelapass	CH	N 46°44'57"	E 09°56'54"	4*x*	0.133	10.974
LPS113	Arosa	CH	N 46°46'5.1"	E 9°37'15.4"	4*x*	0.175	10.551
LPS114	Flims	CH	N 46°5'2 44.6"	E 9°15'55.2"	4*x*	0.098	6.254
LPS115	Fellhorn	D	N 47°20'55"	E 10°12'58"	4*x*	0.129	7.523
LPS116	Sannigrat	A	N 47°4'3.1"	E 9°58'23.4"	4*x*	0.130	8.742
LPS117	Bielerhöhe	A	N 46°55'5.8"	E 10°5'24.3"	4*x*	0.149	13.211
LPS118	Küthai	A	N 47°12'49"	E 11°1'51.2"	4*x*	0.129	7.935
LPS119	Patscherkofel	A	N 47°12'43"	E 11°27'28.9"	4*x*	0.202	13.535
LPS120	Wildkogel	A	N 47°16'51"	E 12°17'01"	4*x*	0.116	7.975
LPS121	Sesto	I	N 46°42'45"	E 12°23'01"	2*x*	0.091	6.655
LPS122	Rauchkofel	A	N 46°36'59.5"	E 12°52'48.3"	4*x*	0.105	6.722
LPS123	Großglockner	A	N 47°05'08"	E 12°50'25"	4*x*	0.106	3.962
LPS124	Bad Gastein	A	N 47°06'20"	E 13°05'44"	4*x*	0.140	10.223
LPS125	Radstädter Tauerpass	A	N 47°16'12"	E 13°34'17"	4*x*	0.199	18.435
LPS126	Kornhock	A	N 46°54'56"	E 13°51'23"	4*x*	0.085	5.516
LPS127	Sölkpass	A	N 47°16'17"	E 14°04'46"	4*x*	0.129	9.174
LPS128	Bösenstein	A	N 47°26'24"	E 14°24'50"	4*x*	0.118	9.540
LPS129	Frauenalp	D	N 47°24'51.7"	E 11°07'11.4"	4*x*	0.108	6.504
LPS169	Macizo de los Infiernos	E	N 42°47'20.1"	W 0°14'10"	4*x*	0.163	21.245
LPS170	Port de Boucharo	F	N 42°42'16.5"	W 0°3'48.8"	4*x*	0.186	15.458
LPS171	Pic du Midi Bigole	F	N 42°55'40"	E 0°8'17.3"	4*x*	0.131	17.235
LPS172	Posets	E	N 42°37'57.6"	E 0°27'10.9"	4*x*	0.132	10.778
LPS173	Ibón de la Renclusa	E	N 42°40'07"	E 0°38'48"	6*x*	0.160	14.863
LPS174	Portillon Inferior, La Maladeta	E	N 42°39'28"	E 0°39'00.8"	6*x*	0.143	13.307
LPS175	Colamoforno, Aigües Tortes	E	N 42°34'22.1"	E 0°49'14.9"	4*x*	0.135	9.830
LPS176	Estany D'Amitges	E	N 42°35'51.3"	E 0°59'0.7"	4*x*	0.125	10.905
LPS177	Port de Cabus	AND	N 42°32'28.4"	E 1°25'14"	4*x*	0.138	6.297
LPS178	Port del Rat	AND	N 42°37'43"	E 1°28'47"	4*x*	0.125	8.980
LPS179	Puerto de Envalira	AND	N 42°32'34.9"	E 1°43'15.7"	4*x*	0.121	18.694
LPS180	Puigmal	E	N 42°22'53.2"	E 2°07'10.4"	4*x*	0.165	9.670
LPS181	Mt. Renoso	F	N 42°03'51.5"	E 9°7'48.5"	2*x*	0.091	13.269
LPS182	Mt. Rotondo	F	N 42°12'26.4"	E 9°2'11.7"	2*x*	0.120	10.013
LPS183	Mt. Prado	I	N 44°14'58"	E 10°24'24.5"	4*x*	0.112	8.304
LPS190	Mt. Retezat	RO	N 45°23'18.4"	E 22°50'18.4"	2*x*	0.117	18.045
LPS168	Pico de Urbión	E	N 42°00'39.8"	W 2°52'36"	6*x*		
LPS167	Sierra Nevada	E	N 37°0'55.1"	W 3°27'16.2"	2*x*		

non-informative homoplastic differences among sequences. Gaps were coded as binary characters using the simple gap coding method of Simmons & Ochoterena (2000) as implemented in the software programme GapCoder (Young & Healy 2003). The two alignments were finally concatenated and used to reconstruct the haplotype network with the software TCS version 1.13 (Clement et al. 2000), according to the statistical parsimony algorithm described by Templeton et al. (1992).

5.2.3 AFLP fingerprinting. – The AFLP procedure followed a modified protocol based on Meister et al. (2006). As for the chloroplast phylogeography, three samples per population were included, 24 (approximately the 10%) were replicated in order to test for reproducibility. After an initial screening of selective primers, the following marker combinations were used: EcoRI (D2-Blue)-ACA/MseI-CTAG; EcoRI (D3-Green)-AGG/ MseI-CTAG; EcoRI (D4-Black)-ACC/ MseI-CTAG. Due to the relatively big genome size of *Leucanthemopsis*, we used MseI primers with four user-selected nucleotides (instead of the normally employed three user-selected nucleotides primers) in order to reduce the number of amplified fragments and increase the reliability of the analyses. Selective amplifications were performed in a total volume of 5µl and D2-dayed PCR products were diluted 1:5 in water, before being mixed with the two other products for the precipitation. The samples were finally diluted in the sample loading solution (SLS) with CEQ Size Standard 400 (both from Beckman Coulter, Fullerton, California, USA), and separated in a CEQ 8000 sequencer (Beckman Coulter). Fragment scoring was then archived automatically with the software GelCompare II v.5.0 (Applied Maths, Sint-Martens-Latem, Belgium). Different presence/absence matrices were produced varying the following scoring parameter settings: minimum profiling of bands during the auto-search (0.25%, 0.5%, 0.75%, 1%, 1.5%, 2%, and 3%; percent relative to the maximum value of the lane); minimum area of bands (0.1%, 0.2%, 0.3%, 0.4%, and 0.5%); matching tolerance for band position (0.02%, 0.06%, 0.1%, and 0.14%; 1 bp = ca. 0.08%); the extent of the increase change towards longer fragments of the matching tolerance (0%, 0.21%, and 0.5%). Additionally, we tried all the combinations of the above mentioned scoring parameters on both the total length of the AFLP output (from fragments of 60 bp to 420 bp long) and a reduced one (from 120 bp to 420 bp), in order to test the negative effect of the high number of homoplastic fragments found in the region between 60 and 120 bp. We scored finally the optimal parameter setting using the script provided by Holland et al. (2008). The best results were produced on the

total length of the AFLP output results, and using the following combination of parameter settings: minimum profiling = 3%; minimal area = 0.5%; matching tolerance = 0.14%; change towards longer fragments of the matching tolerance = 0.21%. The results of the scoring were finally exported in a presence/absence matrix.

Nei's gene diversity and frequency down-weighted marker values (DW; Schönswetter & Tribsch 2005), were calculated for each population using the script AFLPDAT (Ehrich 2006) in R (R Development Core Team, 2008). A principal coordinate analysis (PCoA) was performed, using the software FAMD 1.31 (Schlüter & Harris 2006), and applying chord distances from allele frequencies estimates with Bayesian non-uniform prior (Zhivotovsky 1999) to build the distance matrix. The same population distance matrix was used to infer genetic breaks in the distribution range of the species using the software BARRIER 2.2 (Manni et al. 2004), a program that uses Monmonier's maximum differences (Monmonier 1973) to find zones of largest genetic distance. To examine genetic structure in the data set we utilised STRUCTURE 2.3.4 (Pritchard et al. 2000), a Bayesian clustering approach for dominant marker (Falush et al. 2007), using an admixture model with correlated allele frequencies. We performed ten independent runs for each *k* (ranging from one to ten), and using 10^5 MCMC iterations after a burn-in period of 10^4 generations. We used the procedure described by Evanno et al. (2005) to estimate the most probable number of groups (the value for *k*). Once found the most appropriate *k*, the results from the 10 independent runs were merged using CLUMMP (Jakobsson & Rosenberg 2007), and a graphical representation was produced with DISTRUCT (Rosenberg 2004).

5.2.4 Flow Cytometry. – Ploidy level was determined through flow cytometry on five silica-dried samples per population. *Petunia hybrida* E.Vilm. cv. PxPc6 (2C = 2.85 pg; Marie & Brown, 1993) was used as internal standard. For each measurement, approximately 0.5-1 cm^2 leaf tissue of the standard and 2- to 3-fold amount of leaf tissue of the dehydrated samples material was employed. Nuclei were isolated in Otto I buffer (Otto 1992; Doležel & Göhde 1995), and subsequently stained with 4',6-diamidino-2-phenylindole (DAPI) in a LB01 buffer (Doležel et al. 1989) modified with the supplement of β-Mercaptoethanol (0.015 mM). Samples were measured on a PARTEC CyFlow® Space (Partec GmbH, Münster, Germany) and results were analysed using the software FloMax® (Partec). For each sample over 8500 nuclei were counted. The relative fluorescence intensity of DAPI-stained nuclei was registered and the ratio between sample's/standard's relative florescence (hereafter called fluorescence ratio) was used as indicator of DNA content and ploidy. More

than the 10% of the samples were remeasured and used to test the reliability of the measurements. A complete list of the measurements obtained is provided in Appendix 7.

Due to the observation that tetraploid samples from the Pyrenees showed lower fluorescence ratio compared to the representatives of the same ploidy found in the Alps, we decided to test it statistically. First of all we tested the significance of the difference in fluorescence ratio between ploidies performing a Kruskal-Wallis test. Since, as expected, this difference resulted to be significant, we portioned the data according to the ploidy (only diploids and tetraploids; hexaploid are just found in a restricted area of the Pyrenees), and after checking for normality, we tested with an analysis of variance (ANOVA) the significance in each ploidy of i) date of measurement and ii) geographical area of sample provenience on the fluorescence ratio. We tested the effect of the date in order to be sure that the results were not biased by factors others than the geographic area and depending on the day in which measurements were performed (e.g., freshness of buffers, age of the dried material employed, slight differences during preparation). Concerning the area of provenience, we defined six different geographical regions: Pyrenees, W Alps, E Alps, Apennines, Corsica, and Carpathians. Since both factors resulted significant in both ploidy levels (in diploids $F = 12.642$, $p < 0.001$ and $F = 10.308$, $p < 0.001$ for the date and the area, respectively; in tetraploids $F = 23.96$, $p < 0.001$ and $F = 76.661$, $p < 0.001$, respectively), we tested the significance of the difference between measurements obtained in a date with those from the others dates (*t*-test). In both ploidies, only the early done measurements (from the 2nd, 4th, and the 8th February of 2011) were significantly different from the other. The measurements obtained in those days seems to have slightly higher values of the sample/Petunia fluorescence ratio, most likely due to the freshness of the silica-dried material, which produced a higher sample fluorescence. Although in those dates one individual per population was measured (distributing therefore the error uniformly through populations and, as a consequence, areas of origin), we decided to exclude the measurements in order to test finally the significance of the geographic area of sample provenience on the fluorescence ratio (as an indicator of the genome size).

5.2.5 Morphological analyses. – Herbarium vouchers gained at each population site were used for the morphometric analysis. Due to the small dimension of the plants, usually a herbarium voucher consisted on several individuals. When possible, we measured five individuals randomly chosen for each population. For population LPS073, only two

individuals were measured, due to the reduced size of the population and the paucity of the herbarium voucher.

Sixteen continuous characters were measured, fifteen of which concerned the leaf shape (see Figure 5.1), and one being a peduncle character. Four additional categorical character were considered, three of which regarding the characteristics of the capitula, one the leaf indumentum. Due to their minute size, for the majority of the characters above listed, a Zeiss Stemi 2000 stereomicroscope (Zeiss, Göttingen, Germany) was employed. A list of all characters used, including the categories defined for the ordinal characters, is given in Table 2. Some of the continuous characters were used to produce average values and indexes, and at the end, 14 variables were employed for the statistical analyses. Average population values were produced out the five individuals measured per populations. We performed a Principal Coordinate Analyses (PCoA) with the software MVSP 3.12f (Kovach Computing Services, Pentraeth, UK). Since we were dealing with mixed data types, we employed the Gower's General Similarity Coefficient (Gower 1971) to build the matrix for the PCoA.

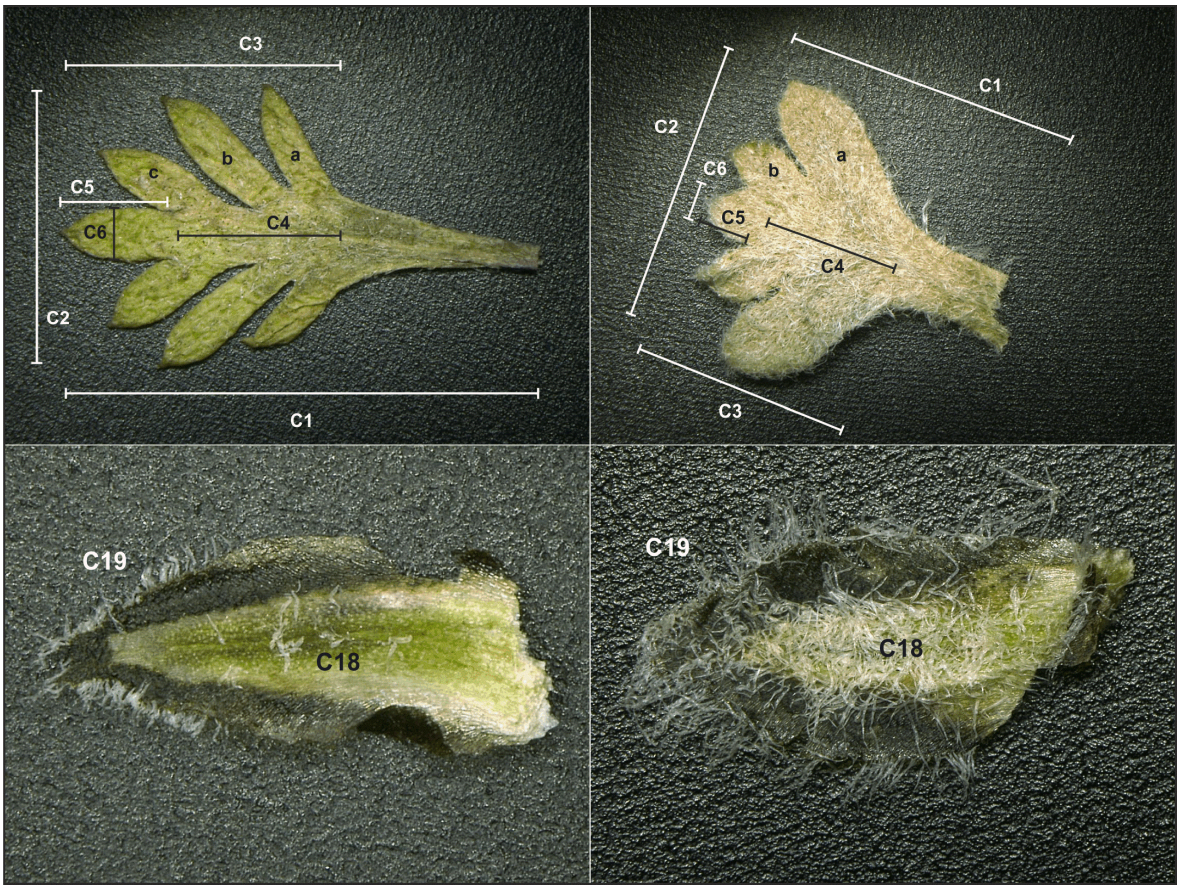

Figure 5.1: Leaf and involucral bract of a *L. alpina* collected in Simplonpass, Switzerland (LPS093; left side on the figure); and of *Leucanthemopsis. alpina* subsp. *tomentosa* collected in Monte Renoso, Corsica (LPS181; right side of the figure). Abbreviation codes for morphological characters correspond to those reported in Table 5.2.

Table 5.2: Morphological characters and indices used in the morphometrical study.

abb.	Character name	Character specification
C1	Leaf length	
C2	Leaf breadth	
C3	Blade length I	Blade length including terminal leaflet
C4	Blade length II	Blade length excluding terminal leaflet
C5	Tip-leaflet lenght	
C6	Tit-leaflet breadth	
C7	Number of lateral leaflets	
C8	Leaflet lenght a	length of the first lateral leaflet
C9	Leaflet lenght b	length of the second lateral leaflet
C10	Leaflet lenght c	length of the third lateral leaflet
C11	Leaflet breadth a	breadth of the first lateral leaflet
C12	Leaflet breadth b	breadth of the second lateral leaflet
C13	Leaflet breadth c	breadth of the third lateral leaflet
C14	Rachis breadth a	Rachis breadth at the blade beginning
C15	Rachis breadth b	Rachis breadth at the blade ending
C16	Ligules color	0 = ligules always white 1 = ligules redish at the end of anthesis
C17	Number of stem leafs	
C18	Leaf indumentum	0 = no hairs 1 = sparse hairs 2 = numerous hairs 3 = thick indumentum
C19	Involucral bract cilia	0 = rare cilia 1 = sparse cilia 2 = numerous cilia 3 = aboundant cilia
C20	Involucral bract indumentum	0 = no hairs 1 = sparse hairs 2 = numerous hairs 3 = thick indumentum

abb.	Index name	Index specification
F1	Leaf length	C1
F2	Leaf shape	C1/C2
F3	Blade relative length	C3/C1
F4	Relative End-leaflet length	C5/C3
F5	Tip-leaflet shape	C6/C5
F6	Number of lateral leaflets	C7
F7	Lateral leaflet shape	$\bar{x}$(C8,C9,C10)/ $\bar{x}$(C11,C12,C13)
F8	Incision index	$\bar{x}$(C8,C9,C10)/ $\bar{x}$(C14,C15)
F9	Leaflet spacing index	{C4-[C7*$\bar{x}$(C11,C12,C13)]}/C4
F10	Ligules color	C16
F11	Number of stem leafs	C17
F12	Leaf indumentum	C18
F13	Involucral bract cilia	C19
F14	Involucral bract indumentum	C20

5.3 Results

5.3.1 Plastid DNA sequence variation. – The alignment of two intergenic spacer regions *psbA-trnH* and *trnC-petN* were 540 bp and 590 bp long respectively, and showed in total 86 polymorphic sites (71 parsimony informative sites). Sequences LPS116-1 and LPS117-1 were excluded from the analyses because of a long deletion of 204 bp in *trnC-petN* that did not allow for a reliable placement of these accessions in the haplotype network. Samples LPS070-2 and LPS088-3 were also excluded due to bad sequence quality. The final concatenated alignment consisted of 240 sequences from 84 different populations (82 belonging to *L. alpina*, plus two additional outgroup samples) and it was 1130 bp long. When necessary, loops in the networks were solved using the criteria proposed by Pfenninger & Posada (2002). The statistical parsimony network (Figure 5.2) found 50 different haplotypes, 14 of which being singletons. Intrapopulational haplotype variation was detected in 36 of the 82 populations taken into account (see Appendix 7 for detailed information on haplotypes and sequence

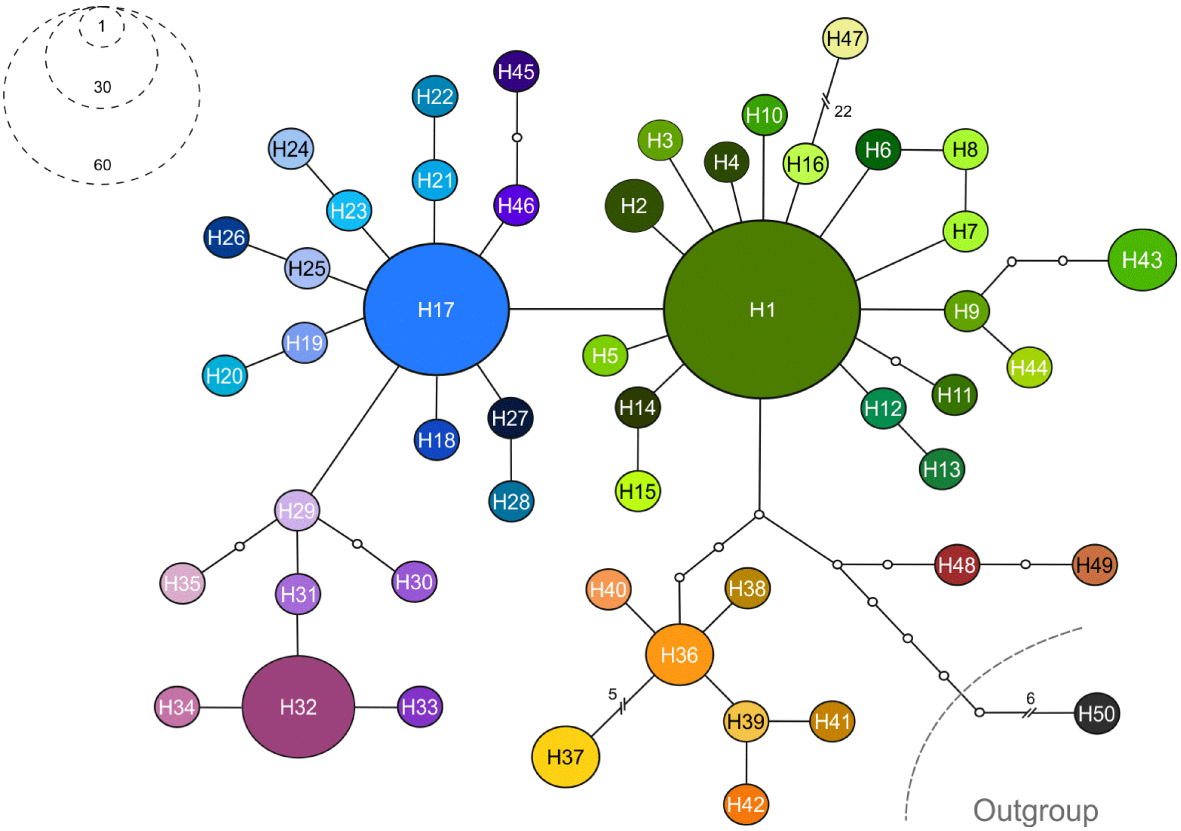

Figure 5.2: cpDNA haplotype network obtained sequencing the intergenic spacer regions *psbA-trnH* and *trnC-petN* for 240 individuals from 82 different populations of *Leucanthemopsis alpina*. Circle dimension are proportional to the haplotype occurrence, whereas small white circler represent non-detected intermediate haplotypes.

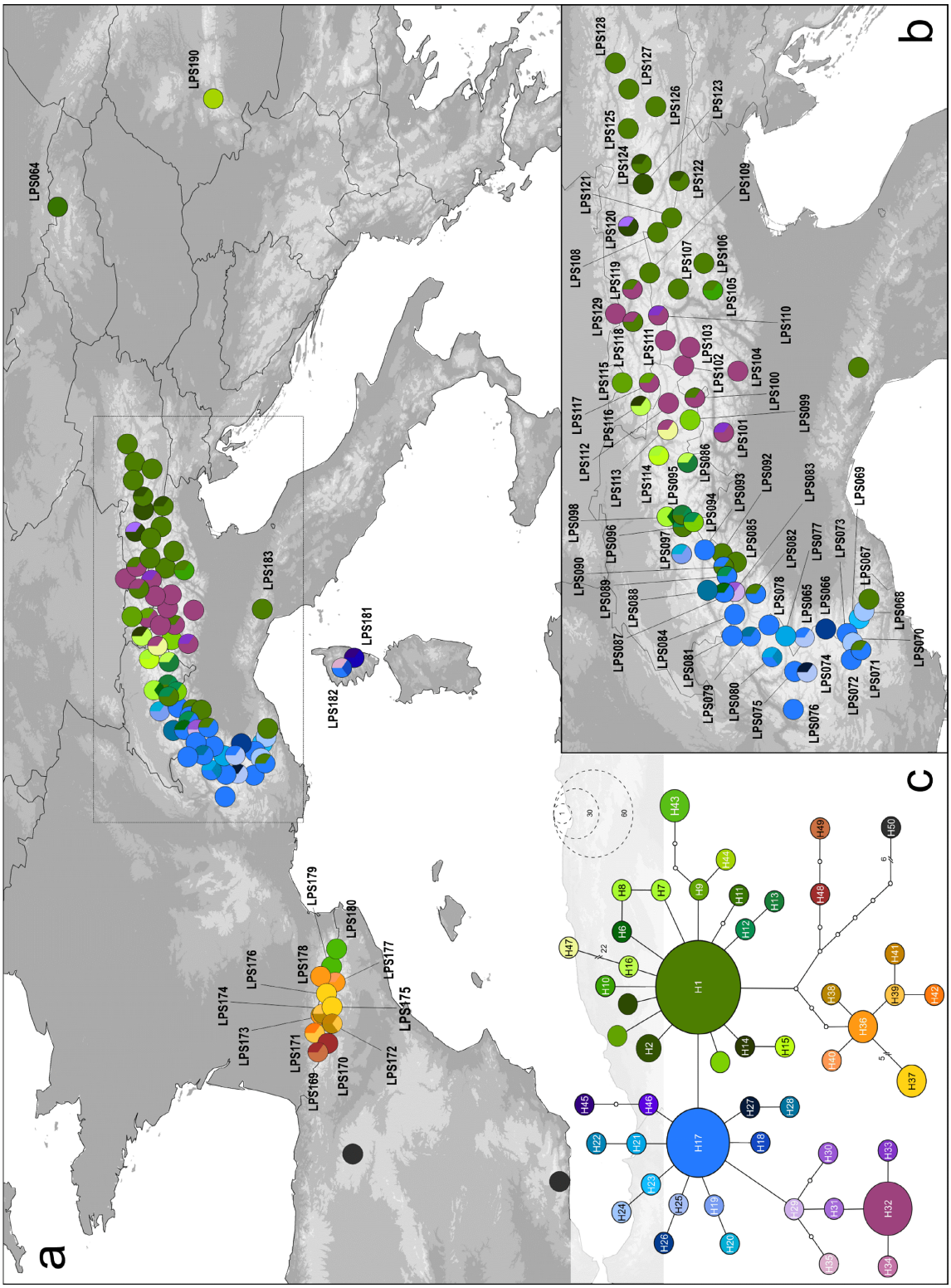

Figure 5.3: Haplotype distribution maps in Europe (a) and in the Alps (b) for the species *Leucanthemopsis alpina*. Colors correspond to those in the haplotype network (c).

GenBank codes for all the samples). In population LPS113, two sequences showed a very deviating 30 bp long region in *psbA-trnH* (haplotype H47). Five haplotype groups can be identified in the haplotype network, one of which (green in the picture) scattered distributed in the whole species range, two (bright and dark brown) from Western and Central Pyrenees, and two (blue and purple) typical of Western and Central Alps, respectively (Figure 5.3).

5.3.2 AFLP fingerprinting. – For all three primers combinations, a total amount of 657 fragments were scored, 609 of which found to be polymorphic. The error rate (according to Bonin et al. 2004) was 16.7%. Nei's genetic diversity ranged from 0.051 (LPS073, a small population in L'Enchastraye, Maritime Alps) to 0.201 (LPS119, Innsbruck), while DW index ranged from 3.96 (LPS123, close to the Großglockner, Austria) to 25.26 (LPS067 in the Maritime Alps). Mean values per mountain area of the two indices are given in Table 5.3.

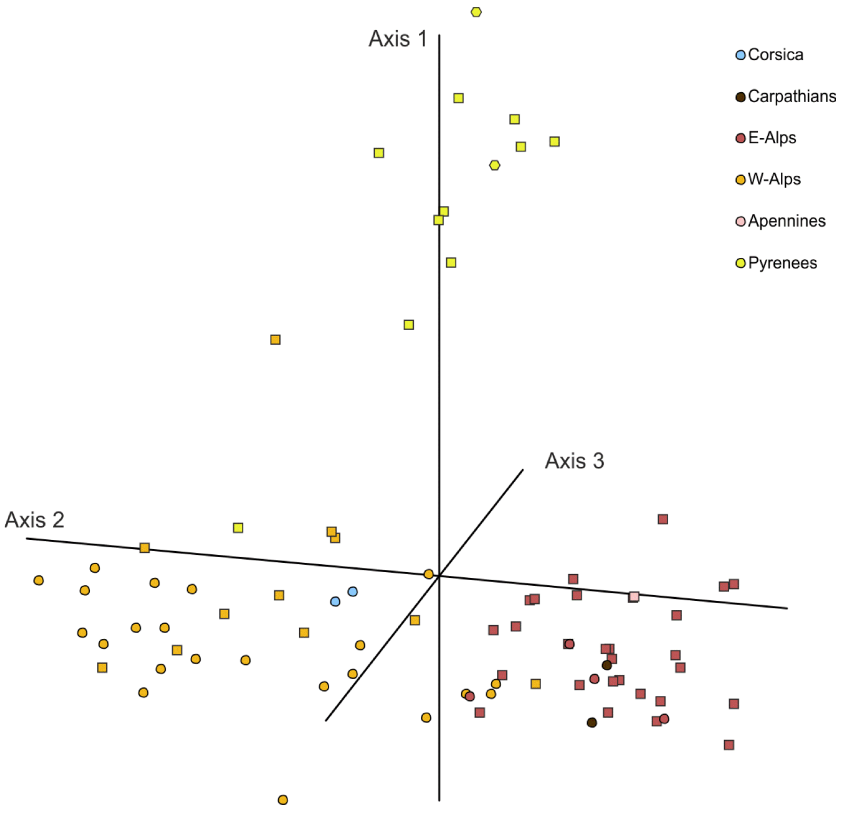

Figure 5.4: Scatterplot showing the first three axes of the PCoA analysis inferred from pairwise distances between AFLP profiles of *L. alpina*. Colors refer to geographic area, whereas shape indicates ploidy (circle: diploids; squares: tetraploids; hexagons: hexaploids).

Table 5.3: Average values for mountain area of the Nei's diversity index and the frequency down-weighted marker values (DW) based on AFLP data. Standard deviation is expressed within parenthesis.

Mountain ranges	Area	pop.	DW	Nei's
Apennines	Tuscan-Emilian Apennines	1	8.304	0.112
Carpathians	S Carpathians	1	18.045	0.117
Carpathians	Tatra Mt.	1	12.732	0.118
Corsica	Corsica	2	11.641 (2.303)	0.106 (0.020)
E Alps	Carnic Alps	2	6.689 (0.047)	0.098 (0.009)
E Alps	Dolomiti	3	10.017 (4.868)	0.109 (0.009)
E Alps	Glarus Alps	1	6.254	0.098
E Alps	Lombard Alps	2	7.809 (1.384)	0.134 (0.016)
E Alps	Noric Alps. Hohe Tauern	3	7.744 (3.327)	0.123 (0.017)
E Alps	Noric Alps. Kitzbühel	1	7.975	0.116
E Alps	Noric Alps. Niedere Tauern	3	12.383 (5.245)	0.148 (0.044)
E Alps	Noric Alps. Turracher	1	5.516	0.085
E Alps	Noric Alps Tuxer Gebirge	1	13.535	0.202
E Alps	Noric Alps. Zillertal	1	11.276	0.162
E Alps	Bavarian Prealps	2	7.013 (0.721)	0.118 (0.015)
E Alps	E Rhaetian Alps	3	8.648 (2.330)	0.135 (0.015)
E Alps	S Rhaetian Alps	1	9.136	0.157
E Alps	W Rhaetian Alps	7	10.151 (2.692)	0.144 (0.023)
Pyrenees	Aiguestortes	2	10.367 (0.760)	0.130 (0.007)
Pyrenees	Andorra	3	11.323 (6.522)	0.128 (0.009)
Pyrenees	Perdido Mt.	3	17.979 (2.964)	0.160 (0.028)
Pyrenees	Catalan Pyrenees	1	9.670	0.165
Pyrenees	Posets and La Maladeta	3	12.983 (2.062)	0.145 (0.014)
W Alps	Bernese Alps	2	8.243 (0.918)	0.129 (0.027)
W Alps	Provencal Alps	1	13.328	0.160
W Alps	Cottian Alps	3	8.997 (4.546)	0.127 (0.061)
W Alps	Dauphiné Alps	3	9.461 (5.782)	0.123 (0.026)
W Alps	Graian Alps	5	8.525 (2.976)	0.117 (0.023)
W Alps	Lepontine Apls	4	7.026 (1.961)	0.124 (0.036)
W Alps	Marittime Alps	6	11.263 (7.276)	0.114 (0.038)
W Alps	Pennine Alps	10	7.949 (2.168)	0.124 (0.025)

The three axes of the PCoA analysis (Figure 5.4) explain together the 24.03 % of the total variation (9.75%, 8.1% and 6.18% for the first, second and third axes, respectively). Populations from the Pyrenees appear well differentiated and separated from the others on the axis 1. Although without clear discontinuity, populations from W Alps and E Alps are mainly separated along axis 2. The easternmost Pyrenean population included in this study (LPS180) clusters together with populations from Western Alps. Populations from Apennines and Carpathian group with the Eastern Alpine populations.

The Evanno method indicated $k = 6$ as the most appropriate number of clusters. Populations show a high degree of admixture (Figure 5.5). However, five of the six clusters are easily attributable to precise geographic areas, being two clusters distinctive of Western

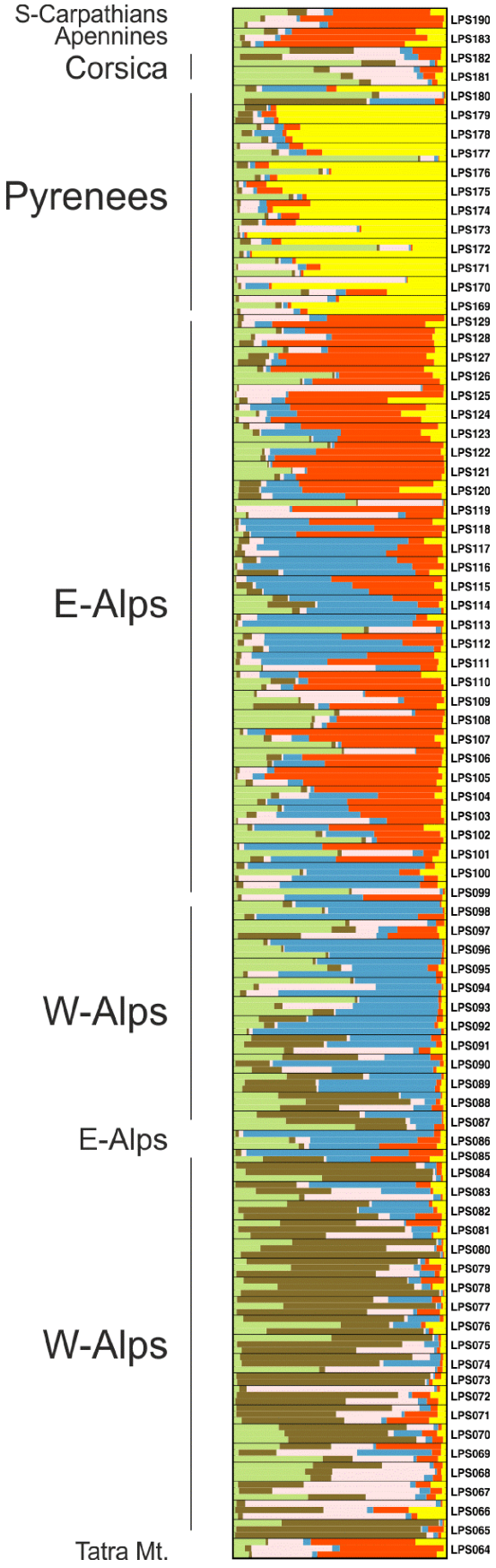

Figure 5.5: The membership coefficients for the 243 *L. alpina* individuals as obtained merging the 10 independent STUCTURE runs in CLUMPP. Each column corresponds to one individual, and populations are separated by black horizontal lines. Different colors represent the different groups (*k*)**.**

Alps, two of Eastern Alps, and one typical for the Pyrenees. As in the plastid analyses, populations from Carpathians and Apennines show high similarity with those from Eastern Alps. Population LPS180 differs from the other Pyrenean populations, having individuals exhibiting affinity with those from Western Alps.

When setting the number of barriers to five (the most appropriate clusters number identified in STRUCTURE was six), BARRIER recognises two genetic barriers in the Pyrenees (one separating the single population LPS170, the other Western and Eastern Pyrenees), and one secluding Maritime Alps from Corsica, Apennines and Central Alps. The other three barriers isolate single populations (LPS066, LPS119 and LPS125) in the Alps. When setting the number of barriers to 10 (the maximum allowed by the program), additional genetic barriers are identified between Carpathians and Eastern Alps, between population LPS180 and the rest of the Pyrenean populations, plus two further single population barriers in the Maritime Alps. Barriers in the Pyrenees fit nicely with the results from the haplotype network reconstruction, while less congruence is found in the Alps, where most likely the uniqueness of single deviating populations is overemphasized (Figure 5.5).

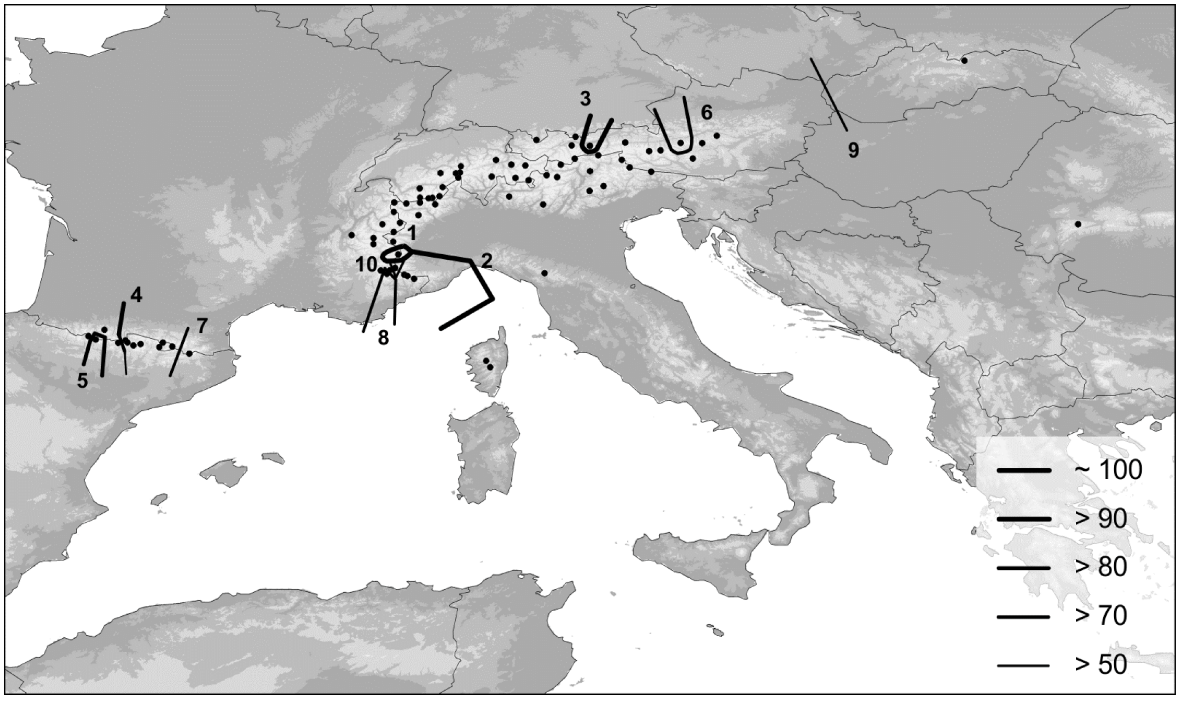

Figure 5.6: Barriers between geographically coherent areas as identified in BARRIER. Barriers are named with numbers following the order given by the program. Line thickness is proportional to the support obtained for each genetic barrier (100 bootstrap replicates).

5.3.3 Flow cytometry. – In total, over 400 measurements were done. The Coefficient of Variation (CV) was on average 3.23% (±1.17), 4.17% (±2.47) for the internal standard and the sample peaks, respectively. The difference in sample/standard fluorescence ratio between sample replicates was on average 0.076 (±0.06). A list with all measurements made is provided in Appendix 7. The sample/standard ratio was 3.34 (±0.15), 5.93 (±0.40), and 7.86 (±0.19) for the diploids, the tetraploids, and the hexaploids, respectively. Diploids are found in Western Alps, Corsica, Carpathians, and in the area surrounding the Dolomites. Tetraploids are distributed in the vast majority of the species distribution range, except for Corsica (where the subspecies *L. alpina* subsp. *tomentosa* is found) and Carpathians. Moreover, in Western Alps this cytotype is almost completely substituted by diploids, being solely present in the Pennine and Cottian Alps. Hexaploids are uniquely found in the "Maladeta" massif in Central Pyrenees, and are here represented by two populations only. A map of the distribution of the different cytotypes is shown in Figure 5.7.

A single population (LPS087; Wallis, Switzerland) was found to have individuals of different ploidy levels, comprising mostly diploids and a single tetraploid sample. Only one sample having indisputably an intermediate ploidy was found. It was a triploid collected in

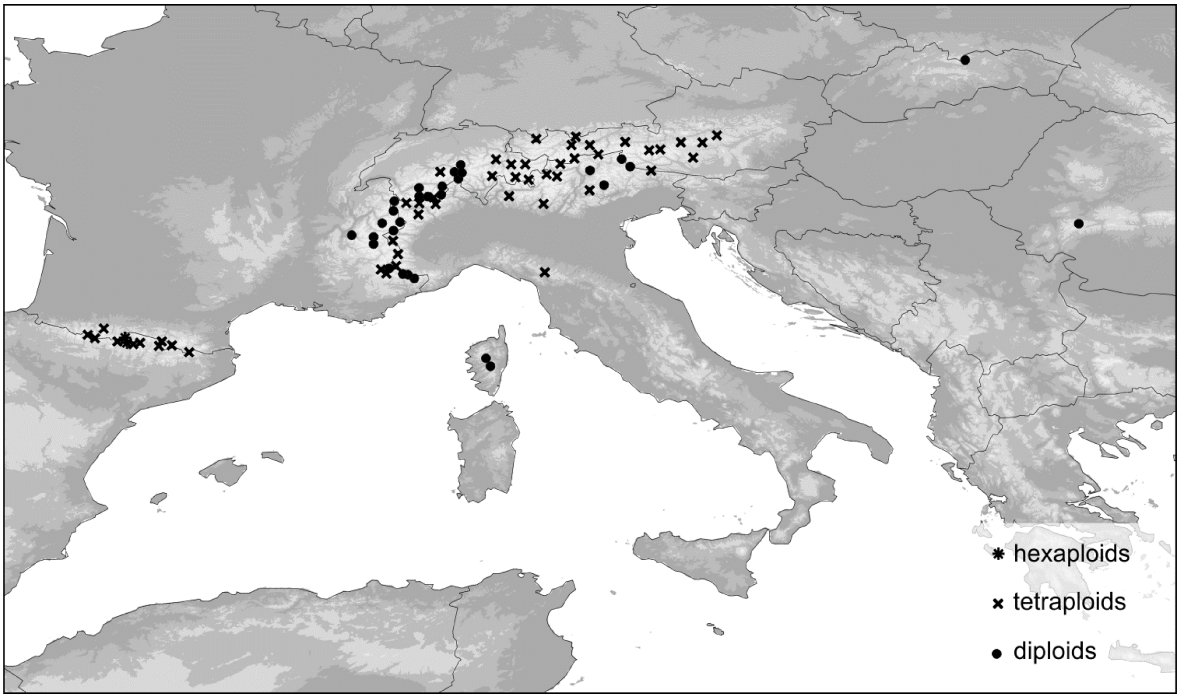

Figure 5.7: Cytotype distribution map for the species *Leucanthemopsis alpina*. Circles are for diploids, crosses for tetraploids, asterisks for hexaploids.

the "Baisse de Druos", Maritime Alps (LPS069-3; ratio: 4.65; CV: 5.36%). Other measurements showed considerable higher florescence ratio than normally expected for their supposed ploidy [e.g., the diploid LPS108-5 (ratio: 4.12; CV. 4.44%) and the tetraploid LPS129-1 (ratio: 7.06; CV: 6.13%). However, since these samples were part of those measured at the very beginning, in the dates in which measurements showed slightly higher fluorescence ratios (see Materials and Methods), we considered them rather deviating measurements than trustworthy triploids and pentaploids. Samples belonging to population LPS120 produced low quality measurements, maybe due to high levels of clayish debris on the dried plant material from this population that could have disturbed the measurements.

Diploids from the subspecies *L. alpina* subsp. *tomentosa* produced fluorescence ratios significantly lower than diploids from other parts of the species distribution range ($p < 0.05$, Student's t-test). Concerning tetraploids, those from Pyrenees and from Apennines were found to produce lower fluorescence ratios than those from the Western and Eastern Alps, while non-significant differences were found between the two different parts of the Alps or

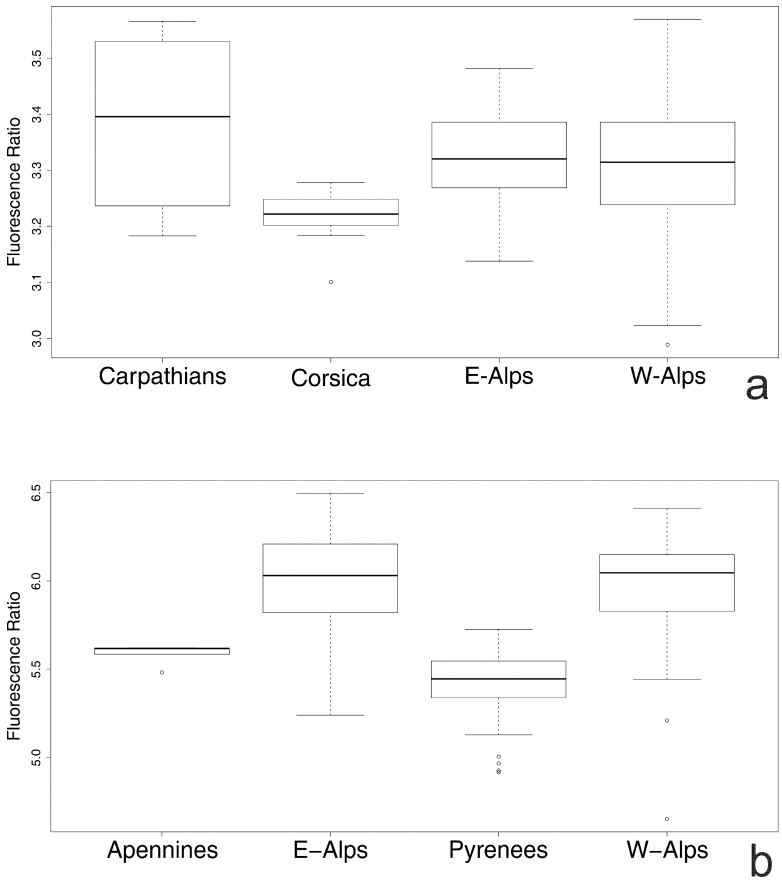

Figure 5.8: Boxplot of the fluorescence ratio from measurements of diploid (a) and tetraploid (b) samples of *L. alpina* from different geographic areas.

between Apennines and Pyrenees (Figure 5.8 a, b). Although we used the base-specific DAPI staining buffer, and the GC content in the genome of the sample influences the relative fluorescence peak measured (and therefore the sample/standard ratio), we believe that such divergences can be the effect of differences in genome size.

5.3.4 Morphology. – The results of the PCoA are shown in Figure 5.9. The analysis did not produce a clear separation of the populations in different clusters. Only the two populations belonging to the Corsican subspecies *L. alpina* subsp. *tomentosa* appears clearly distanced from the others. The rest of the populations are rather arranged without discontinuities along the axis 1, with the populations from Pyrenees and W Alps mostly represented in the left part of the diagram and those from E Alps and Carpathians in the right one. The two axes together explain 25.8% of the total variability (13.2% and 12.5% for the axes 1 and 2, respectively).

This W-E gradual morphological variability is reflected as well in the correlation shown by some of the morphological characters with the geographic longitude (Figure 10). In particular, when we move from west to east leaves become progressively less divided (Pearson correlation coefficient: -0.59), and tip and lateral leaflets become stockier (Pearson correlation coefficient for F5 and F7: -0.53 and -0.51, respectively). A weaker but still present geographical pattern is present as well in the spacing index of the leaflets (from west to east: -0.11).

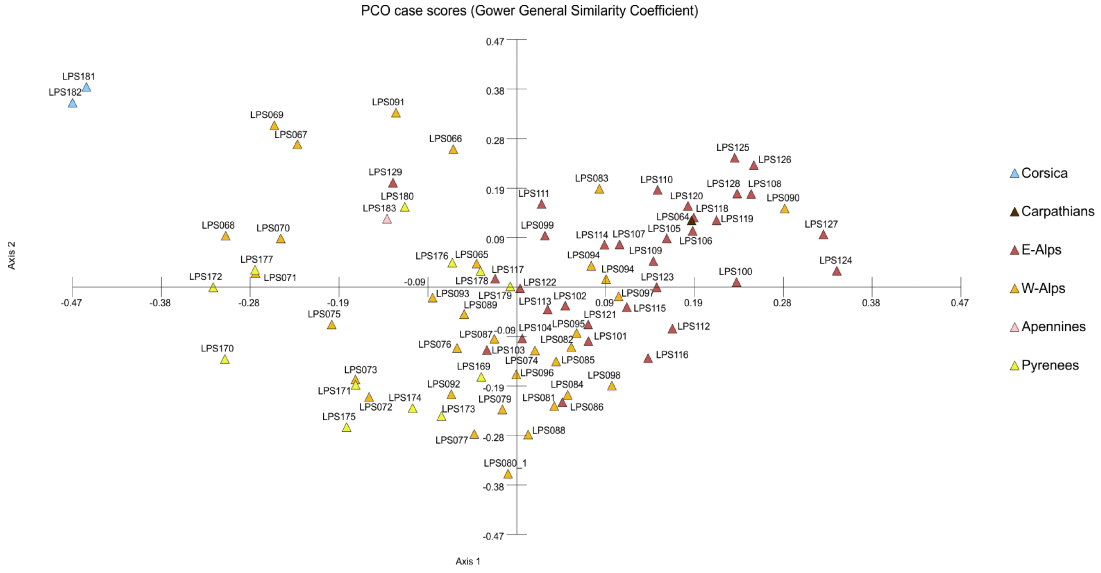

Figure 5.9: Scatterplot showing the first two axes of the PCoA analysis based on the morphological characters listed in Table 5.2, and inferred using Gower similarity coefficient for 82 populations of *L. alpina*. Colors refer to different geographic areas.

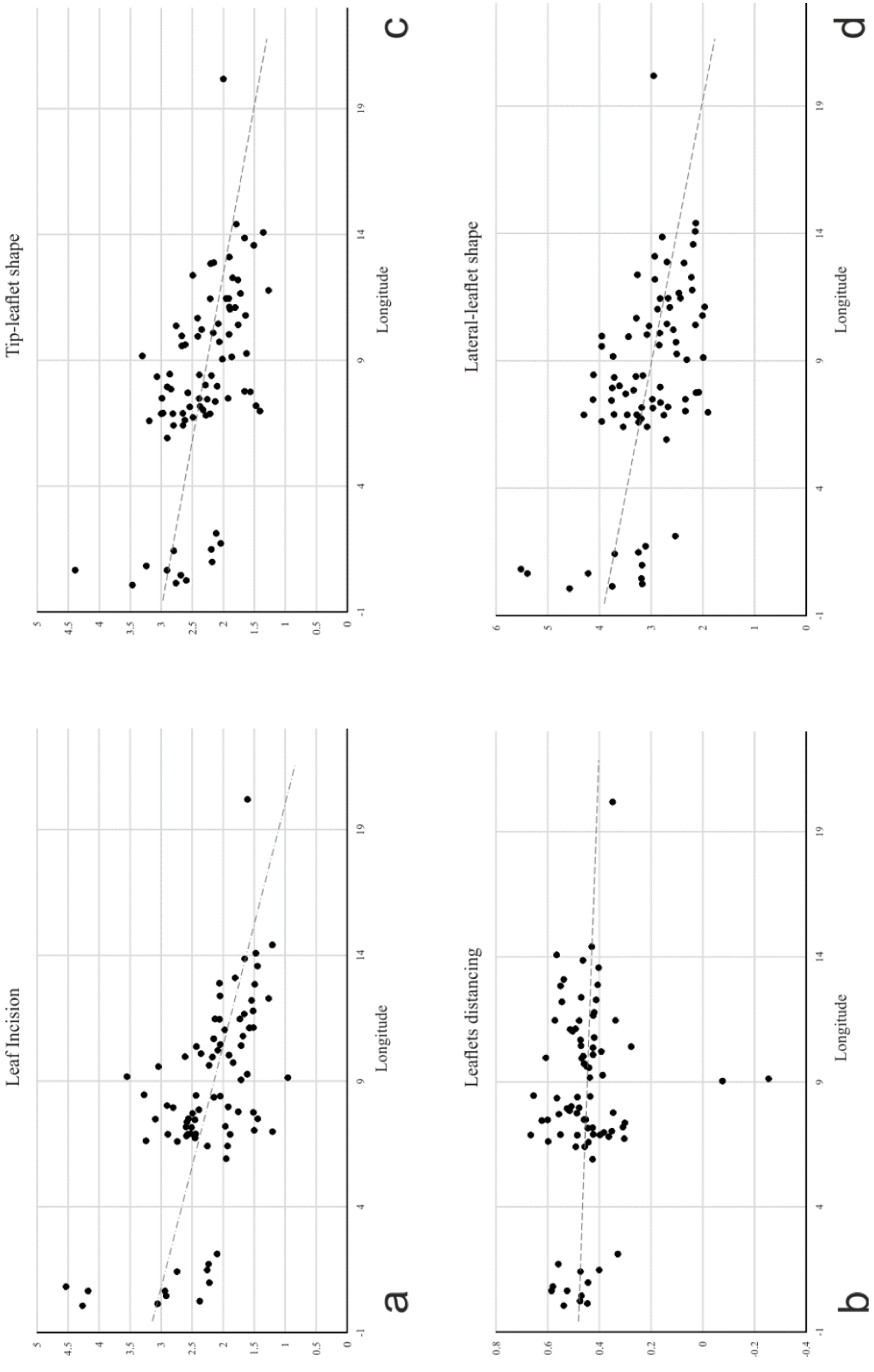

Figure 5.10: Gradual change of the most representative morphological characters according to the longitude. a) Leaf incision (F8 in Table 5.2); b) Leaflet spacing (F9); c) Tip-leaflet shape (F5); and d) lateral-leaflet shape (F7).

5.4 Discussion

5.4.1 Cytotype distribution and the role of polyploidization in L. alpina *evolution.* – With the present study we broaden the knowledge about the geographical distribution of the different cytotypes in *L. alpina*, both spatially (collecting at a finer geographical scale or in localities for which population cytotype was unknown), and by collecting more individual per population. Until now, cytological studies on the species were rather circumscribed to specific areas [the Alps and especially W Alps in Contandriopoulos & Favarger (1959); the Pyrenees (Küpfer 1974); Tatra (Skalinska et al. 1959); Corsica (Contandriopoulos 1962)], and no information for other parts of the species range (such us Apennines or Southern Carpathians) were until now available.

In general, our results reflect the situation depicted in the previous studies. However, in contrast with what reported by Favarger & Küpfer, (1968) and Heywood (1975), we did not find any diploid in the Pyrenees, even though we measured all the individuals collected in "Pas de la Casa" (Puerto de Envalira, LPS179; Appendix 7). The total absence of diploids in the Pyrenees opens interesting phylogeographical questions. Since the rest of the species belonging to *Leucanthemopsis* are distributed in the Iberian Peninsula and in North Africa, one would expect that the oldest lineages of the species are found in this mountain chain. Küpfer (1974) interpreted this absence as the result of extinction of the old Pyrenean lineages and subsequent recolonization by Alpine tetraploid races. However, the fact that the haplotypes found in the Pyrenees are the closest to the outgroup one (Figure 5.3), the high diversity found both in haplotypes and in the AFLP patterns (Nei's diversity and DW indexes in Table 5.1), and the difference in genome size between tetraploids in the Alps and in the Pyrenees (Figure 5.8b), contradict this hypothesis and point towards a long time establishment of Pyrenean populations.

We can confirm the existence of diploids in Eastern Alps, as already reported for a single individual by Küpfer (1974). Four diploid populations were found in Eastern Alps (Table 5.1 and Figure 5.7), all from marginal areas of the Dolomites with siliceous outcrop (Passo Rolle, Rittnerhorn, Passo Stalle, and Dolomiti di Sesto). These populations represent the only diploids characterized by the most widespread haplotype (H1 in Figure 5.2) together with a population in the southernmost collection locality in the Maritime Alps (LPS067), while in the Carpathians and in two populations of the Pennine Alps (LPS089, Schwarzsee; LPS087, Mt. Collon) singleton haplotypes derived from the widespread one are found. If we assume that diploid populations in the Dolomites reached Eastern Alps before than the

tetraploids, this area would represent most probably a Pleistocene refugium for *L. alpina* in the Eastern Alps. The alternative would be an improbable recent long distance dispersal from Maritime or Pennine Alps to Dolomites (considering that *Leucanthemopsis*' achenes are relatively sessile, being devoid of pappus or any other dispersal structure). Although the Dolomites are mainly calcareous, the southern part of this mountain range have been proposed as putative refugium for several calcifuge plant species (Schönswetter et al. 2002, 2003b; Tribsch et al. 2002; Winkler et al. 2010).

Siljak-Yakovlev et al. (2010) collected *L. alpina* in Mt. Jahorina (Bosnia-Herzegovina) and determined the genome size of five individuals through flow cytometry. The authors did not indicate chromosome number and ploidy of those samples, and reported a genome size of 2C = 25.13 pg (SD: 0.32). Unfortunately, we did not include any population from the Balkans in our study and we do not have original information on the *L. alpina* cytopytes occurring in this region. Moreover, we used the base specific DAPI fluorochrome for our flow cytometric measurements, and any consideration on genome size should be taken with caution. However, it is interesting to notice that the genome size value obtained by Siljak-Yakovlev et al. (2010) would translate in a sample/standard fluorescence ratio around 8.8 when using *Petunia hybrida* as internal standard. This value would fit with those we obtained for the Pyrenean hexaploid populations, and a CG content of about 0.3 have to be assumed in order to obtain fluorescence ratios more proper of a tetraploid sample (considering that the genome size of *P. hybrida* is 2.85 and its CG content 0.41). If confirmed, the presence of hexaploid populations in the Balkans would open new biogeographical scenarios, and further studies would be needed with an accurate sampling in the region.

A single odd-ploidy individual was found in over 400 measurements, being a triploid in the otherwise diploid population of "Baisse de Druos" (Maritime Alps). Triploid individuals in mixed populations or in areas where different cytotypes grow in proximity represent a preferential way for interploidal gene flow. If we considered that the vast majority of the counts were done in cytotypical homogeneous populations, the low frequency of odd-ploidy individuals observed for *L. alpina* is congruent with those found in other plant species (Suda & Herben 2013). Comparable odd-ploidy frequencies do not seem to constitute absolute mating barriers in the *Knautia arvensis* aggregate (Kolář et al. 2009) and are enough for increasing genetic variation by interploidal backcrossing in other plant species (Baack 2004; Stift et al. 2010).

Only one population was found to have individuals with different ploidy (Mt. Collon, Valais, Switzerland). A single tetraploid was measured in this otherwise diploid population.

Valais region – and especially the area surrounding Zermatt – was already known for hosting populations of different ploidy levels (Contandriopoulos & Favarger 1959). However, the case of the Mt. Collon population seems rather unique in our data set. We have extensively sampled in the area of Zermatt (one population in the western side of the valley: LPS089; and two populations at different altitudes in the eastern side: LPS090 and LPS091), and even measuring all the individuals collected (Appendix 7), populations resulted homogeneous concerning cytotypes, consisting of only diploids the one west of Zermatt, and tetraploids the ones on the eastern side. These patterns mismatch with those found in comparable plant species systems, where within population ploidy heterogeneity and ecological differentiation among cytotypes were observed (e.g., *Jacobea carniolica* (Willd.) Schrank; Sonnleitner et al. 2010, 2013), and fit rather with those of another alpine complex (Casazza et al. 2012). As in the latter study, not only we identify a vast within population cytotype homogeneity, but the lack of morphological distinctiveness among cytotypes (Figure 5.9), as well as the fact that the different ploidies occur evenly in all haplotype groups or clusters of the STRUCTURE analysis (i.e., cytotypes do not form monophyletic clades in both the cpDNA and the AFLP analyses), point toward a non-adaptative role of polyploidization in *L. alpina*. Polyploidization occurred most probably several times independently, and did not served to stabilize diverging lineages. Stochastic processes (e.g., the recolonization of new areas after the retreat of the ice sheet, frequency-dependent mechanisms producing cytotype exclusion) would have then gradually led to the actual distribution of cytotypes observed in the species.

5.4.2 Spatial genetic variation and the importance of Pleistocene glaciation cycles. – The area showing the highest genetic diversity in *L. alpina* are the Pyrenees. Haplotypes belonging to three diverse haplotype groups are present in this mountain range (Figure 5.3). The area that most heavily was affected by the glaciation ("La Maladeta" massif) represented probably an insurmountable barrier during cold periods between populations from Eastern and Western Pyrenees, as reflected by the nowadays observed plastidial (Figure 5.2) and nuclear (Figure 5.6) genetic distribution patterns. The high haplotype diversity together with the on average high AFLP markers diversity and rarity (Table 1 and 3) reported in those populations support the hypothesis of an old establishment and longtime persistence of *L. alpina* in the Pyrenees. The results from the STRUCTURE analysis show however higher uniformity among Pyrenean population (Figure 5.5), indicating that high admixture levels could have swamped old geographic patterns in the genetic variation or that Central Pyrenees could have represented in the past a big barrier for seed but not for pollen dispersal.

The easternmost Pyrenean populations are characterized by the haplotype H43, belonging to a different haplotype group (green in Figure 5.2) than those showed by the western and central populations of the Pyrenees. This haplotype group is the most widespread, being observed in populations from the Pyrenees, Western and Eastern Alps, Apennines and Carpathians. In our view, this haplotype groups, and more specifically the central (and vastly represented) haplotype H1, was in the past widely distributed in the Alps, being then able to reach the Carpathians and the Tatra. When we sum up a general trend in the colonization route followed by the species, it has clearly a west to east direction, similarly to other alpine plants having a Mediterranean origin (e.g., *Anthyllis montana* L.; Vargas 2003). Over the repeated cycles of species range contraction and expansion caused by the Pleistocene glaciations, this haplotype group was substituted by derived ones in Western and in Central Alps (the blue and the purple haplotype groups in Figure 5.3, respectively), being however able to persist in putative refugial area like the Maritime and Pennine Alps. The presence of a haplotype from the widespread green group (Figure 5.3) in populations from the Catalan Pyrenees, together with the fact that concerning AFLP results (Figure 5.4, and 5.5) the easternmost Pyrenean population clusters together with those of the Western Alps (even though showing high degree of admixture in the STRUCTURE analysis), represent a clear indication of backwards recolonization of the Eastern Pyrenees from Western Alps. Genetic similarity between W Alps and E Pyrenees was already observed in several alpine plants (e.g., *Pyteuma globularifolium* Sternb. & Hoppe, Schönswetter et al. 2002; *Soldanella alpina* L., Vargas 2003; *Saxifraga fragilis* Schrank, Reisch 2008; *Artemisia eriantha* Ten., Sanz 2014) and animals (*Erebia epiphron* Knoch, Schmitt et al. 2006).

When we look at the situation in the Alps, the geographic pattern found in the haplotype distribution might be explained by the repeated range contraction and expansion cycles experienced by the species during the Pleistocene glaciations. The western and the central haplotype groups (blue and purple in the Figure 5.2, and 5.3, respectively) may have formed in isolated populations able to overcome glacial cold periods in suitable refugial area uncovered by the ice sheet. Concerning the Western Alps haplotype group, putative area could be represented by the Maritime and Provencal Alps, as reflected as well in the on average high values obtained for the diversity and rarity indices of the AFLP results (Table 3). Those areas are well known as peripheral Pleistocene refugia for alpine plants (Schönswetter et al. 2002, 2003a, 2004, 2005; Garnier et al. 2004; Diadema et al. 2005; Grassi et al. 2006, 2009; Schmitt & Haubrich 2008; Dixon et al. 2009; Burnier et al. 2009). The high haplotype diversity found in Western Alps, with many derived haplotypes often

present in single populations suggest glacial survival of the species in several different unglaciated areas, rather than post-glacial expansion from one of few refugial populations. Less clear is the situation in the Central Alps haplotype group. Although the existence of peripheral refugia for species preferring siliceous outcrop in the southern side of the Central Alps (e.g., Bergamasque Alps, Mt. Adamello) has been demonstrated for several alpine species (Schönswetter et al. 2002, 2005; Stehlik 2003), the low values of DW and Nei's indices obtained for the populations characterized by the Central Alps haplotype group (purple in Figure 5.3) do not provide enough prompts to identify putative refugial areas. This haplotype group may have formed recently (it is the most derived group in the haplotype network; Figure 5.2), and may not have had enough time to develop high within-population genetic variation. Another explanation might be that this haplotype group overcame Pleistocene glaciations in few bottlenecked populations situate in the southern margin of Central Alps, as already postulated in comparable cases (e.g., *Androsace wulfeniana* W.D.J.Koch populations from the Dolomites; Schönswetter et al. 2003b).

Concerning the widespread haplotype group (green in Figure 5.2), two main aspects are worth of consideration. Although haplotypes from this group are non-continuously present throughout the whole species range, two are the regions were its presence is more accentuated: Central and Western Alps (Lepontine, Glarus and W Rhaetian Alps), and Eastern Alps. In the first region, the high number of singleton haplotypes observed, some of which very divergent from the central one (H47 in population LPS113; Arosa, Switzerland), supports *in situ* survival of isolated populations in interior Pleistocene refugia. For *Eritrichium nanum* (L.) Gaudin it has been demonstrated that Upper Engadin have hosted Nunatak refugia during Pleistocene glaciations (Stehlik 2003). On the other hand, the haplotype uniformity present in Eastern Alps, suggests recent recolonization from one/few refugial areas. In the case of *L. alpina* the most likely areas are represented by the easternmost part of the alpine arch (as suggested as well by the high DW and Nei's indices values obtained for some population of the Niedere Tauern; Table 3), or the Dolomites, where diploids are found (see discussion above). Niedere Tauern are known to be one of the principal peripheral refugial area for strictly alpine plants linked to siliceous outcrop, as highlighted by pattern of endemism (Tribsch & Schönswetter 2003) and molecular data (see Schönswetter et al. 2005 for a review).

Populations from Carpathians and Apennines results similar to those from Eastern Alps, as showed by plastid (Figure 5.3) and AFLP (Figure 5.5) data. Although in other species similarity between Eastern Alps and Apennines has been observed in the genetic patterns

(e.g., *Anthyllis montana* L., Vargas 2003; and *Pinus sylvestris* L., Labra et al. 2006), it is difficult to find an explanation for this occurrence in *L. alpina*. *Leucanthemopsis alpina* do not produce achenes furnished with a pappus, therefore long distance dispersal from Central and Eastern Alps to Apennines is not a good explanation. Moreover, the PoValley may have not provided a suitable environment for an alpine plant even during cold glaciation periods, as already stressed by other authors in the past (Ravazzi 2002; Schönswetter et al. 2005).

5.4.3 Morphology and intraspecific diversity. – The morphometrical analyses carried out in the present study did not report strong discontinuities in the morphological variation within *L. alpina* (Figure 5.9). The only group that appear clearly distinct from the other is the one formed by the two Corsican populations (belonging to *L. alpina* subsp. *tomentosa*). This subspecies looks in fact different from the other representatives of the species for several features (i.e., the very dwarf and tomentose habit, the reddish proximal part of the ligules, the leaves almost palmatifide with very short spacing between leaflets). However, concerning genetic variation this subspecies does not show the same distinctiveness shown for the morphology, being rather close to the *L. alpina* populations growing in southwestern Alps.

When leaving aside the Corsican populations, there is not parallelism between distribution of cytotypes and of morphological variability, which seems to follow rather a longitudinal gradient (Figure 5.9). The west to east gradual change in some of the leaf characters (e.g., the width of the rachis compared to the leaflets length, and the leaflet shape; see Figure 5.10), validate the intuition that botanists had in the past in identifying the important diagnostic characters unraveling the interspecific variability in the species. Anyway, this variation is not enough to form discrete groups recognizable in taxonomic entities at the subspecies or higher level. According to Stuessy (2008), the subspecies rank should be given to cohesive series of morphologically (and/or genetically) well-distinct populations, showing an allopatric or peripatric distribution. Following the same author, the variety rank should be used for morphologically homogenous populations, which do not form geographical cohesive series (i.e., series of populations overlapping largely in their distribution ranges).

Concerning the morphological variation observed in *L. alpina*, it is possible to distinguish two extreme situations: the *alpina*-like morphotype, characterized by more deeply divided leaves and overall larger plant size, and the *minima*-like morphotype, consisting of usually smaller plants with less deeply divided leaves. Individuals of *L. alpina* growing in the

Pyrenees, Alps, Apennines, and Carpathians form morphologically homogenous populations (personal observation). In addition, populations of the two types are differently represented in different areas, the former type being more frequently observed in the western part of the distribution range, while the latter is more common in the eastern part (as shown by the latitudinal gradient observed in important morphological characters; Figure 5.10). However, these types do not form geographically cohesive population series, and *minima*-like populations can be found in the E Pyrenees (e.g., LPS180) and in the W Alps (e.g., some populations growing in the Dauphiné and Provencal Alps). Indeed, [*L. minima*] was first described by Villars (1789) for the Dauphiné Alps, in the western part of the species range. Those patters are in our view more compatible with a classification at variety rank (sensu Stuessy 2008) rather than at the subspecies one.

Finally, the idea to subdivide *L. alpina* in the Alps according to the ploidy into two species does not find any justification for a couple of reasons. a) Polyploidy has arisen several time independently in different populations of the species, being – like for morphological characters with a simple genetic basis – not enough for allowing delimitation of species (Stuessy 2008). As humorously stated by Lewis (1969): "if an organism does not take its chromosome number seriously, there is no reason why the systematist should". b) If we want to use the biological concept of species (Mayr 1942), reproductive isolation among ploidies must be demonstrated, and the results of the present study (e.g., presence of odd-ploidy individuals, founding of mixed populations, and patterns of distribution of genetic variation among cytotyopes) are not enough to unequivocally exclude interploidal gene flow in *L. alpina*. c) The correspondence between ploidy and morphology (i.e., diploids => *L. alpina*; tetraploids => *L. minima*) proposed by some authors (Marchi & Illuminati 1974; Pignatti 1982) is invalidated, since *alpina*-like tetraploids are largely found in the Pyrenees (the forma *pyrenaica* sensu Vierhapper 1914), or *minima*-like diploids in the area surrounding the Dolomites (E Alps).

5.4.4 Conclusions. – Polyploidization does not seem to be a driving diversification force in in *L. alpina*. Polyploids arisen several times independently and might not have provided alone a source of mating isolation between diverging lineages. Polyploidization has often been proposed as one of the easiest way in which diverging lineages can establish, thanks to the possibility (especially in case of hybrid origin of the polyploids) to provide reproductive isolation between (diverging) citotypes (Coyne & Orr 2004). In contrast, the large admixture found in the genetic patterns between cytotypes of *L. alpina* could be an indication of

interploidal gene flow, although similar patterns could be the effect of recurrent origin of polyploids alone, and further studies should be carried out to test experimentally interploidal mating in the species.

Much stronger seems to be the geographical imprint in the genetic and morphological variation in *L. alpina*. The Pleistocene glaciation cycles may have played a major role in driving lineages divergence in the species, as highlighted by the molecular variation patterns.

Chapter 6

General discussion

The present thesis aims at investigating differentiation processes in the subtribe Leucanthemopsidinae (Compositae, Anthemideae). Speciation involves three processes: (1) the initial origin of genetic differentiation among populations within existing species; (2) the evolution of reproductive isolation, that is, the rise of prezygotic or postzygotic barriers to mating among populations; and (3) the evolution of ecological divergence (Givnish 2010). Barriers driving reproductive isolation are various and different in kind (see Mayr 1970; Turelli et al. 2001; Coyne & Orr 2004). For a long time, geographical isolation was recognized as the most important way leading to reproductive isolation (Mayr 1954) and until recently, totally sympatric speciation was considered almost impossible (Hendry 2009). This idea has been recently criticized by different authors (see Mallet 2001), and the importance of other mechanisms for reproductive isolation was stressed (Gavrilets & Vose 2000; Turelli et al. 2001; Via 2001; Mallet 2007; Givnish 2010). Whole genome duplication is commonly considered a way in which reproductive isolation can arise in sympatry, due to the high proportion of unviable or sterile offspring generated by crossing between newly formed polyploids and their diploid progenitors (Stebbins 1950; Linder & Rieseberg 2004; Mallet 2007). Polyploidy does not enhance speciation only by being means of reproductive isolation between different cytotypes, it is itself increasing diversification and therefore speciation. Indeed, higher rates of diversification have been observed in clades that experienced ancient polyploidy compared to sister-clades that did not (Soltis et al. 2009).

Allopatric differentiation processes might have been at the origin of the lineage nowadays represented by the only species *Castrilanthemum debeauxii*. In the first chapter, we produced a comprehensive phylogeny of Leucanthemopsidinae using two plastid regions (cpDNA), the ribosomal internal transcribed spacer (nrDNA ITS), and two single-copy nuclear markers. We employed three different approaches to reconcile the results from the different markers. Firstly, we performed a standard (gene tree) phylogenetic analysis using a

concatenated data set that included all the different regions. Secondly, we used a tree reconciliation approach by minimizing the number of deep coalescences (MDC; Maddison 1997). Finally, we performed a Bayesian species tree analyses using the software *BEAST (Heled & Drummond 2010). Irrespective of the reconstruction strategy (concatenated sequence; MDC, or *BEAST), the subtribe Leucanthemopsidinae formed a highly supported monophyletic group. *Castrilanthemum debeauxii* occupies an early-diverging position in the subtribe, the split between this taxon and the rest of the Leucanthemopsidinae being dated to the Early Miocene (13-21 Ma). This age estimate significantly predates the establishment of the Mediterranean climate in S Europe which occurred in the Pliocene (5 to 3 Ma). It rather coincides with the uplift of the Prebaetic System, which took place approximately 16 Ma ago (Sanz de Galeano 1990, Braga et al. 2003). The "Sierra de Guillimona", where the few known populations of the species are found nowadays, is part of the above-mentioned mountain system. This mountain range emerged from the Thetys as an island system embedded between the Guadalquivir depression on the one side and the "Inframountain basins" on the other (Vera 2000). Therefore, the lineage that has given rise to the current *C. debeauxii* could have diverged in the old Baetic range as product of allopatric isolation in this mountain/island system.

As far as polyploids are involved, the possibility of hybrid origin of the taxa involved has to be considered. Polyploidy is a common feature in flowering plants. 35% of angiosperms is represented by polyploids (Wood et al. 2009), and within them allopolyploids are considered to be more abundant (Stebbins 1950; Coyne & Orr 2004). All above said, together with the practical problems arising due to the increased genome size, makes phylogenetic reconstructions in taxonomic groups including polyploids particularly challenging, and a proper method to infer species tree/networks in polyploid complexes has been missing. Despite that, attempts of reconstructing phylogenies in polyploid complexes have been done in the last decades (e.g., Popp & Oxelman 2001; Popp et al. 2005; Ghiselli et al. 2007; Lo et al. 2008). Jones et al. (2013) proposed a Bayesian method for inferring species networks and multilabeled species trees from sequences in polyploid groups using the phylogenetic computer program *BEAST. However, the Bayesian nature of the method and the complex statistics behind it, makes its employment difficult when the number of polyploid taxa and/or accessions per taxon become high. In the second chapter, we presented a new and simple approach to infer species networks from gene trees in plant groups including polyploids, while trying to disentangle the effects of both ILS and allopolyploid hybridization. We have tested the efficiency of the method using simulated gene trees and a

reduced data set including the diploid taxa and a few polyploid accessions of the genus *Leucanthemopsis*. The approach produced reliable results on simulated data, unless population size did not become unrealistically large.

We used the described approach to reconstruct the reticulate evolution of the complete genus *Leucanthemopsis* in the third chapter. For this scope, we employed sequence data from two chloroplast marker regions (*psbA-trnC* and *trnC-petN*) and from four single/low copy nuclear genes (*B20*, *C16*, *C12*, *D35*). We aimed at reconstructing a reliable phylogeny of the genus and to shed light on the origin of the polyploid taxa. Polyploidy has been a primary force driving diversification and species formation in the genus, both by simple genome doubling within a single species (autopolyploidy), and by forming novel lineages as products of the merging of genomes from different taxa (allopolyploidy). As autopolyploids were suggested the Moroccan endemic *L. longipectinata* (which occupies an early-diverging position in the genus) and the polyploids found within the species *L. alpina*. A hybrid origin was reconstructed for the hexaploid *L. alpina* subsp. *cuneata*, which should be considered being an indepemndent entity from the rest of the species. Concerning the tetraploids found in the Iberian Peninsula, two independent allopolyploid events are plausibly the most likely scenario: The first (allo-)polyploidization produced the *L. pallida* complex, subsequently further differentiated into the infraspecific taxa we observe today, possibly by getting in contact with other *Leucanthemopsis* taxa in different areas. The second allotetraploidization gave rise to the *L. flaveola* lineage growing in the NW Iberian Peninsula, in the mountain ranges between Galicia and León. Niche reconstruction analyses indicated that the interglacial range expansion of the oro-Mediterranean taxa (i.e., *L. pectinata*, *L. pallida* var. *alpina*) toward the north and/or to lower altitudes may have established contact zones with meso-Mediterranean *Leucanthemopsis* representatives (e.g., *L. virescens* var. *virescens*, *L. pulverulenta*), allowing formation of allopolyploid taxa.

While the last two chapters were devoted on the understanding of how past whole genome duplication (WGD) events have produced new species in the genus *Leucanthemopsis*, the fourth chapter addressed questions concerning the influence of polyploidy in the ongoing diversification processes (and therefore incipient speciation) in the species *L. alpina*. *Leucanthemopsis alpina* constitutes a good study group within the genus because three ploidy levels are realized ($2n = 2x$, $4x$, and $6x$) throughout its wide distributional range, showing as well high degree of morphological variation. In order to achieve this goal, a fine scale sampling of the species throughout the whole distributional range and ploidy determination for a considerable number of populations (and individuals per population)

were carried out. To assess geographic patterns of molecular variation we used two chloroplast marker regions and scoring of AFLP fingerprinting markers. A triploid individual was found in one of the over 400 measurements. It was a triploid found in a diploid population in "Baisse de Druos" (Maritime Alps). Triploids represent the most common way in which autotetraploids can arise in diploid populations (Ramsey & Schemske 1998). Moreover, odd-ploidies represent the main way for interploidal gene flow in populations where different cytotypes grow sympatrically. Mixed-ploidy populations, however, are not common in *L. alpina*. A single one was found in the Valais region (Switzerland). The within-population cytotype homogeneity found in the species is more likely the product of stochastic processes (e.g., minority cytotype exclusion), and witness – together with the fact that no significant ecological differences are observed among areas hosting populations of different ploidy – for a non-adaptative role of polyploidy in *L. alpina*.

The morphological variation observed in the species is not explained by ploidy levels but rather follows a west to east geographical gradient. The only group constituting a morphologically distinct entity, well separated from the rest of the species, is the Corsican subspecies *L. alpina* subsp. *tomentosa*. The fact that polyploids are found in all haplotype groups of the cpDNA network or AFLP clusters, together with the already mentioned lack of morphological distinctiveness among ploidy levels and within-population cytotype homogeneity indicate (a) the multiple origin of the polyploids and (b) the possible non-adaptative role of polyploidization in the ongoing diversification processes in *L. alpina*. More important seems to be the role played by the past glacial history as a diversification process for the species. There is in fact considerable correspondence between the geographical distribution of haplotype groups, genetic diversity and rarity, and the placement of well-known refugial areas in the Alps and in the Pyrenees.

Chapter 7

Summary

Polyploidy is a common feature in plants with 35% of angiosperms being polyploid species. Polyploidization has been proposed as one of the most important speciation mechanism in plants, with 15% of all speciation events in flowering plants and 31% in ferns entailing an increase in the number of complete chromosome sets. The frequency of polyploid species formation under natural conditions is often found to be enhanced by environmental changes, such as the large-scale re-structuring of species' ranges during Pleistocene glaciation cycles. Because of the prominence of polyploidy in flowering plants, understanding how new polyploid species are formed and become established is fundamental to our appreciation of plant biodiversity.

In the present thesis we aim to investigate the processes producing diversification (and consequently speciation) in the subtribe Leucanthemopsidinae (Compositae, Anthemideae). We approach diversification in the Leucanthemopsidinae at three different hierarchical levels: i) at the genus level, providing a comprehensive phylogeny for the subtribe; ii) at the species level, with particular attention to the origin of polyploids in the genus *Leucanthemopsis*; iii) at the infraspecific level, investigating the role of polyploidy and past glacial history on the ongoing diversification processes in the species *L. alpina*.

The subtribe Leucanthemopsidinae constitutes a suitable study group, including four genera (three of which monospecific), one representing a polyploidy complex of mountain/alpine species. Using coalescent-based species tree reconstruction methods, we proved the monophyly of the Leucanthemopsidinae, as well as the monophyly of the genera included in it. The rare Iberian endemic species *Castrilanthemum debeauxii* occupies an early-diverging position in the subtribe and diverged from the lineage giving rise to the other genera already in the Early Miocene (13.2–20.8 Ma). The phylogenetic distinctiveness and geographical rarity impart evolutionary importance to this enigmatic species, although a

possible recent change in live-form from perennial to annual makes its classification as a "living fossil" problematic.

Polyploidy seems to be the primary evolutionary force for evolution and species formation in the genus *Leucanthemopsis*. Using a novel approach for reconstructing phylogenetic networks in polyploidy complexes, jointly taking into account both incomplete lineage sorting (ILS) and hybridization (allopolyploidy), we reconstruct the reticulate evolution of the genus. For the scope, we used sequence information from four single/low copy nuclear genes and two chloroplast regions (*psbA-trnH* and *trnC-petN*). Allelic variation was inferred for the nuclear genes through Roche 454 next generation pyrosequencing. Results from the phylogenetic reconstruction indicate that both auto- and allopolyploidy were involved in the formation of the different polyploid taxa of the genus and that two independent (allo)polyploidization events need to be assumed for the formation of the Iberian tetraploid taxa. It is hypothesized that species range expansions during the past glacial cycles established contact zones between oro-Mediterranean and meso-Mediterranean diploid *Leucanthemopsis* species, allowing for hybridization and formation of the allopolyploid taxa.

In contrast to these findings on the generic level, the role of polyploidy as an evolutionary process driving diversification in the alpine plant *L. alpina* is found to be of minor importance. Phylogeographical studies based on chloroplast sequence variation (*psbA-trnH* and *trnC-petN*) and AFLP fingerprinting indicate that polyploid lineages originated multiple times and do not show morphological or genetic distinctiveness compared to the diploids. The morphological variability observed nowadays in the species follows rather a west-east geographic pattern in the Alps. Finding a good correspondence of genetic groups within the species with well-known areas housing refugia in the Alps and in the Pyrenees during the past glaciation cycles, Pleistocene glacial history played most likely a stronger role in shaping the genetic variation than polyploidization.

References

Abbott RJ, Brochmann C. 2003. History and evolution of the arctic flora: in the footsteps of Eric Hultén. – *Molecular Ecology* 12: 299-313.

Agakhanjanz O, Breckle SW. 1995. Origin and evolution of the mountain flora in Middle Asia and the neighboring mountain regions. In: Stuart Chapin III F, Körner C (Eds.). A*rctic and alpine Biodiversity*. Ecological studies vol. 113. Springer-Verlag. Berlin.

Albach DC. 2007. Amplified fragments length polymorphisms and sequence data in the phylogenetic analysis of polyploids: multiple origins of *Veronica cymbalaria* (Plantaginaceae). – *New Phytologist* 176: 481-498.

Alekseyenko A, Lee C, Suchard M, 2008. Wagner and Dollo: a stochastic duet by composing two parsimonious solos. – *Systematic Biology* 57: 772-784.

Álvarez I, Wendel JF, 2003. Ribosomal ITS sequences and plant phylogenetic inference. – *Molecular Phylogenetics and Evolution* 29: 417-434.

Amaral AR, Jackson JA, Möller LM, Beheregaray LB, Coelho MM. 2012. Species tree of a recent radiation: the subfamily *Delphininae* (Cetacea, Mammalia). – *Molecular Phylogenetics and Evolution* 64: 243-253.

Antunez AM. 1981. Aportación al conocimiento taxonómico de las especies ibéricas de los géneros *Leucanthemopsis* (Giroux) Heywood, *Phalacrocarpum* Willk. y *Prolongoa* Boiss. Unpublished thesis. Universidad Complutense. Madrid.

Arvanitis L, Wiklund C, Ehrlén J. 2007. Butterfly seed predation: effects of landscape characteristics, plant ploidy level and population structure. – *Oecologia* 152: 275-285.

Avise JC. 1994. *Molecular Markers, Natural History and Evolution*. Chapman & Hall. New York.

Avise JC, Wollenberg K. 1997. Phylogenetics and the origin of species. – *Proceedings of the National Academy of Sciences USA* 94: 7748-7755.

Baack EJ, Stanton ML. 2005. Ecological factors influencing tetraploid speciation in snow buttercups (*Ranunculus adoneus*): niche differentiation and tetraploid establishment. – *Evolution* 59: 1936-1944.

Baack EJ. 2004. Cytotype segregation on regional and microgeographic scales in snow buttercups (*Ranunculus adoneus*: Ranunculaceae). – *American Journal of Botany* 91: 1783-1788.

Baele G, Lemey P, Bedford T, Rambaut A, Suchard MA, Alekseyenko AV. 2012. Improving accuracy of demographic and molecular clock model comparison while accommodating phylogenetic uncertainty. – *Molecular Biology and Evolution* 29: 2157-2167.

Barreda VD, Palazzesi L, Tellería MC, Katinas L, Crisci JV, Bremer K, Passalia MG, Corsolini R, Rodríguez Brizuela R, Bechis F. 2010. Eocene Patagonia fossils of the daisy family. – *Science* 329: 1661.

Bayer RJ, Purdy BG, Lebedyx DG. 1991. Niche differentiation among eight sexual species of *Antennaria* Gaertner (Asteraceae: Innuleae) and *A. rosea*, their allopolyploid derivative. – *Evololutionary Trends in Plants* 5: 109-123.

Beck G, Maly K, Bjelčić Ž. 1983. Flora Bosne i Hercegovine IV. Sympetalae. Svjetlost. Sarajevo.

Bertoldi R, Rio D, Thunell R. 1989. Pliocene/Pleistocene vegetational and climatic evolution of the South-Central Mediterranean. – *Palaeogeography Palaeoclimatology Palaeoecology* 72: 263-275.

Billings WD. 1974. Adaptation and origin of alpine plants. – *Arctic and Alpine Research* 6: 129-142.

Blanco-Pastor JL, Vargas P, Pfeil BE. 2012. Coalescent simulations reveal hybridization and incomplete lineage sorting in Mediterranean *Linaria*. – *PLOSone* 7: e39089. doi:10.1371/journal.pone.0039089.

Blankenberg D, Gordon A, Von Kuster G, Coraor N, Taylor J, Nekrutenko A, The Galaxy Team. 2010. Manipulation of FASTQ data with Galaxy. – *Bioinformatics*. 26: 1783-1785.

Blattner FR, Weising K, Bänfer G, Maschwitz U, Fiala B. 2001. Molecular analysis of phylogenetic relationships among myrmecophytic *Macaranga* species (Euphorbiaceae). – *Molecular Phylogenetics and Evolution* 19: 331-344.

Bombarely A, Coate JE, Doyle JJ. 2014. Mining transcriptomic data to study the origins and evolution of a plant allopolyploid complex. – *PeerJ PrePrint* 2: e391. http://dx.doi.org/10.7287/peerj.preprints.243v1.

Bonin A, Bellemain E, Bronken Eidesen P, Pompanon F, Brochmann C, Taberlet P. 2004. How to track and assess genotyping errors in population genetic studies. – *Molecular Ecology* 13: 3261-3273.

Bowers JE, Chapman BA, Rong J, Paterson AH. 2003. Unravelling angiosperm genome evolution by phylo-genetic analysis of chromosomal duplication events. – *Nature* 422: 433-438.

Braconnot P, Otto-Bliesner B, Harrison S, Joussaume S, Peterchmitt J-Y, Abe-Ouchi A, Crucifix M, Driesschaert E, Fichefet T, Hewitt CD, Kageyama M, Kitoh A, Laîné A, Loutre M-F, Marti O, Merkel U, Ramstein G, Valdes P, Weber SL, Yu Y, Zhao Y. 2007. Results of PMIP2 coupled simulations of the mid-holocene and last glacial maximum—Part 1: experiments and large-scale features. – *Climate of the Pas*t 3: 261-277.

Braga JC, Martín JM, Quesada C. 2003. Patterns and average rates of late Neogene–Recent uplift of the Betic Cordillera, SE Spain. – *Geomorphology* 50: 3-26.

Bremer K, 1988. The limits of amino acid sequence data in angiosperm phylogenetic reconstruction. – *Evolution* 42: 795-803.

Bremer K, Humphries CJ. 1993. Generic monograph of the Asteraceae-Anthemideae. – *Bulletin of the Natural History Museum London, Botany Series* 23: 71-177.

Brennan AC, Barker D, Hiscock SJ, Abbot RJ. 2012. Molecular genetic and quantitative trait divergence associated with recent homoploid hybrid speciation: a study of *Senecio squalidus* (Asteraceae). – *Heredity* 108: 87-95.

Brochmann C, Brysting AK, Alsos IG, Borgen L, Grundt HH, Scheen A-C, Elven R. 2004. Polyploidy in arctic plants. – *Biological Journal of the Linnean Society* 82: 521-536.

Brower AVZ, DeSalle R, Vogler A. 1996. Gene tree, species tree and systematics: a cladistic perspective. – *Annual Reviews of Ecology and Systematics* 27: 423-450.

Brysting AK, Mathiesen C, Marcussen T. 2011. Challenges in polyploid phylogenetic reconstruction: A case story from the arctic-alpine *Cerastium alpinum* complex. – *Taxon* 60: 333-347.

Burnier J, Buerki S, Arrigo N, Küpfer P, Alvarez N. 2009. Genetic structure and evolution of Alpine polyploid complexes: *Ranunculus kuepferi* (Ranunculaceae) as a case study. – *Molecular Ecology* 18: 3730-3744.

Cadotte MW, Davies TJ. 2010. Rarest of the rare: advances in combining evolutionary distinctiveness and scarcity to inform conservation at biogeographical scales. – *Diversity and Distributions* 16: 376-385.

Cai D, Rodríguez F, Teng Y, Ané C, Bonierbale M, Mueller LA, Spooner DM. 2012. Single copy nuclear gene analysis of polyploidy in wild potatoes (*Solanum* section *Petota*). – *Evolutionary Biology* 12: 70. doi:10.1186/1471-2148-12-70

Cain SA. 1944. *Foundations of plant geography*. Harper and Brothers. London.

Cardona G, Rosselló F, Valiente G. 2008. Tripartitions do not always discriminate phylogenetic networks – *Mathematical Biosciences* 211: 356-370.

Casazza G, Granato L, Minuto L, Conti E. 2012. Polyploid evolution and Pleistocene glacial cycle: A case study from the alpine primrose *Primula marginata* (Primulaceae). – *BMC Evolutionary Biology* 12: 56. doi:10.1186/1471-2148-12-56.

Chapman MA, Chang J, Weisman D, Kesseli RV, Burke JM. 2007. Universal markers for comparative mapping and phylogenetic analysis in the Asteraceae (Compositae). – *Theoretical and Applied Genetics* 115: 747-755.

Cheng L, Connor TR, Aanensen DM, Spratt BG, Corander J. 2011. Bayesian semi-supervised classification of bacterial samples using MLST databases. – *BMC Bioinformatics* 12: 302. doi:10.1186/1471-2105-12-302.

Chung Y, Ané C. 2011. Comparing two Bayesian methods for gene tree/species tree reconstruction: simulations with incomplete lineage sorting and horizontal gene transfer. – *Systematic Biology* 60: 261-275.

Cires E, Fernández Prieto JA. 2012. The Iberian endemic species *Ranunculus cabrerensis* Rothm.: an intricate history in the *Ranunculus parnassiifolius* L. polyploidy complex. – *Plant Systematic and Evololution.* 298: 121-138.

Clement M, Posada D, Crandall KA. 2000. TCS: a computer program to estimate gene genealogies. – *Molecular Ecology* 9: 1657-1659.

Contandriopoulos J. 1962. Recherches sur la flore endémique de la Corse et sur ses origines. – *Annales de la Faculté des Sciences de Marseille* 32: 1-354.

Contandriopoulos J, Favarger C. 1959. Existence de races chromosomiques chez *Chrysanthemum alpinum* L. Leurs repartition dans les Alpes. – *Revue Générale de Botanique* 66: 341-357.

Cook LM, Soltis PS. 2000. Mating systems of diploid and allotetraploid populations of *Tragopogon* (Asteraceae). II. Artificial populations. – *Heredity* 84: 410-415.

Corander J, Marttinen P. 2006. Bayesian identification of admixture events using multi-locus molecular markers. – *Molecular Ecology* 15: 2833-2843.

Corander J, Marttinen P, Mäntyniemi S. 2006. Bayesian identification of stock mixtures from molecular marker data. – *Fishery Bulletin* 104: 550-558.

Corander J, Marttinen P, Sirén J, Tang J. 2008. Enhanced Bayesian modelling in BAPS software for learning genetic structures of populations. – *BMC Bioinformatics* 9: 539.

Coyne JA, Orr HA. 2004. *Speciation*. Sinauer Associates. Sunderland.

Cranston KA, Hurwitz B, Stein L, Wing RA. 2009. Species tree from highly incongruent gene trees in rice. – *Systematic Biology* 58: 489-500.

Darlington CD. 1937. *Recent advances in cytology*. J. & A. Churchill. London.

Darriba D, Taboada GL, Doallo R, Posada D. 2012. jModelTest 2: more models, new heuristics and parallel computing. – *Nature Methods* 9: 772.

Darwin C. 1859. *On the Origin of Species by Means of Natural Selection, or the Preservation of Favoured Races in the Struggle for Life.* John Murray. London.

Degnan JH, Rosenberg NA. 2009. Gene tree discordance, phylogenetic inference and the multispecies coalescent. – *TRENDS in Ecology and Evolution* 6: 332-340.

Demesure B, Sodzi N, Petit RJ. 1995. A set of universal primers for amplification of polymorphic non-coding regions of mitochondrial and chloroplast DNA in plants. – *Molecular Ecology* 4: 129-134.

Diadema K, Bretagnolle F, Affre L, Yuan Y-M, Médail F. 2005. Geographic structure of molecular variation of *Gentiana ligustica* (Gentianaceae) in the Maritime and Ligurian Alps. – *Taxon* 54: 887-894.

Dixon CJ, Schönswetter P, Suda J, Wiedermann MM, Schneeweiss GM. 2009. Reciprocal Pleistocene origin and postglacial range formation of an allopolyploid and its sympatric ancestors (*Androsace adfinis* group, Primulaceae). – *Molecular Phylogenenetics ans Evololution* 50: 74-83.

Dodson EO, Dodson P. 1976. *Evolution: process and product*. D. Van Nostrand Company. New York.

Doležel J, Binarová P, Lucretti S. 1989. Analysis of nuclear DNA content in plant cells by flow cytometry. – *Biologia Plantarum* 31: 113-120.

Doležel J, Göhde W. 1995. Sex determination in dioecious plants Melandrium album and M. rubrum using high-resolution flow cytometry. – *Cytometry* 19: 103-106.

Doolittle WF. 1999. Lateral genomics. – *Trends in Biochemical Sciences* 24: M5-M8. doi:10.1016/S0962-8924(99)01664-5.

Doyle JJ, Doyle JS. 1987. A rapid DNA isolation procedure for small quantities of fresh leaf tissue. – *Phytochemical Bulletin* 19: 11-15.

Doyle JJ, Doyle JL, Rauscher J, Brown A. 2004. Diploid and polyploid reticulate evolution throughout the history of the perennial soybeans (*Glycine* Subgenus *Glycine*). – *New Phytologist* 161: 121-132.

Drummond, AJ, Ho SYW, Phillips MJ, Rambaut A. 2006. Relaxed phylogenetics and dating with confidence. – *PLoS Biology* 4: e88. doi:10.1371/journal.pbio.0040088.

Drummond AJ, Suchard MA, Xie D, Rambaut A. 2012. Bayesian phylogenetics with BEAUti and the BEAST 1.7. – *Molecular Biology and Evolution* 29: 1969-1973.

Eaton DAR, Ree RH. 2013. Inferring phylogeny and introgression using RADseq data: an example from flowering plants (*Pedicularis*: Orobanchaceae). – *Systematic Biology* 62: 689-706.

Edwards SV. 2009. Is a new and general theory of molecular systematics emerging? – *Evolution* 63: 1-19.

Egan AN, Doyle JJ. 2010. A comparison of global, gene-specific, and relaxed clock methods in a comparative genomics framework: dating the polyploid history of soybean (*Glycine max*). – *Systematic Biology* 59: 534-547

Ehrendorfer F. 1980. Polyploidy and distribution. In: Lewis WH (Eds.). *Polyploidy: biologica relevance*. Plenum Press. New York.

Ehrich D. 2006. AFLPdat: a collection of R functions for convenient handling of AFLP data. – *Molecular Ecolology Notes* 6: 603-604.

Eldredge N, Stanley SM. 1984. *Living fossils*. Springer-Verlag. Berlin.

Elith J, Phillips SJ, Hastie T, Dudík M, Chee YE, Yates CJ. 2011. A statistical explanation of MaxEnt for ecologists. – *Diversity and Distributions* 17: 43-57.

EU Greenway Sarajevo. 2013. *Crvena lista flore federacije Bosne i Hercegovine*. Federalno ministarstvo okoliša i turizma Sarajevo.

Evanno G, Regnaut S, Goudet J. 2005. Detecting the number of clusters of individuals using the software structure: a simulation study. – *Molecular Ecology* 14: 2611-2620.

Falush D, Stephens M, Pritchard JK. 2007. Inference of population structure using multilocus genotype data: dominant markers and null alleles. – *Molecular Ecolology Notes* 7: 574-578.

Fan HH, Kubatko LS. 2011. Estimating species trees using approximate Bayesian computation. – *Molecular Phylogenetics and Evolution* 59: 354-363.

Fauquette S, Suc JP, Bertini A, Popescu SM, Marny S, Taofiq NB, Perez MJ, Chikhi H, Feddi N, Subally D, Clauzon G, Ferreira J. 2006. How much did climate force the Messinian salinity crisis? Quantified climatic conditions from pollen records in the Mediterraenean region. – *Palaeogeography, Palaeoclimatology, Palaeoecology* 238: 281-301.

Favarger C. 1957. Sur le pourcentage des polyploides dans la flore de l'étage nival des Alpes Suisses. In: *CR VIII Congrès International de Botanique*. Paris.

Favarger C, Küpfer P. 1968. Contribution à la cytotaxinomie de la flore alpine des Pyrénées. – *Collectanea Botanica* 7: 325-356.

Fawcett J, Van de Peer Y, Maere S. 2013. Significance and biological consequences of polyploidization in land plant evolution. In: Greilhuber J, Dolezel J, Leitch I, Wendel JF. *Plant genome diversity, vol. 2*. Springer-Verlag. Vienna.

Felsenstein J. 1985. Confidence limit in phylogenies: an approach using the bootstrap. – *Evolution* 39: 783-791.

Fisher DC. 1990. Rates of evolution - Living fossils. In: Briggs DEG, Crowther PR (Eds.). *Paleobiology: A Synthesis*. Blackwell Science. Hoboken.

Flot JF, Tillier A, Samadi S, Tillier S. 2006. Phase determination from direct sequencing of length-variable DNA regions. – *Molecular Ecology Notes* 6: 627-630.

Flot JF. 2007. CHAMPURU 1.0: a computer software for unraveling mixtures of two DNA sequences of unequal lengths. – *Molecular Ecology Notes* 7: 974-977.

Fortelius M, Eronen J, Liu L, Pushkina D, Tesakov A, Vislobokova I, Zhang Z. 2006. Late Miocene and Pliocene large land mammals and climatic changes in Eurasia. –

Palaeogeography, Palaeoclimatology, Palaeoecology 238: 219-227.

Fuertes Aguilar J, Rosselló A, Nieto Feliner G. 1999. Nuclear ribosomal DNA (nrDNA) concerted evolution in natural and artificial hybrids of *Armeria* (Plumbaginaceae). – *Molecular Ecology* 8: 1341-1346.

García N, Meerow AW, Soltis DE, Soltis PS. 2014. Testing Deep Reticulate Evolution in Amaryllidaceae Tribe Hippeastreae (Asparagales) with ITS and Chloroplast Sequence Data. – *Systematic Botany* 39: 75-89.

García-Fernández A, Iriondo JM, Vallès J, Orellana J, Escudero A. 2012. Ploidy level and genome size of locally adapted populations of *Silene ciliata* across an altitudinal gradient. – *Plant Systematics and Evolution* 298: 139-146.

Garnier S, Alibert P, Audiot P, Prieur B, Rasplus JY. 2004. Isolation by distance and sharp discontinuities in gene frequencies: implications for the phylogeography of an alpine insect species, *Carabus solieri*. – *Molecular Ecology* 13: 1883-1897.

Gavrilets S, Li H, Vose MD. 2000. Patterns of parapatric speciation. – *Evolution* 54: 1126-1134.

Ghiselli F, Milani L, Scali V, Passamonti M. 2007. The *Leptynia hispanica* species complex (Insecta Phasmida): polyploidy, parthenogenesis, hybridization and more. – *Molecular Ecology* 16: 4256-4268.

Giardine B, Riemer C, Hardison RC, Burhans R, Elnitski L, Shah P, Zhang Y, Blankenberg D, Albert I, Taylor J, Miller W, Kent WJ, Nekrutenko A. 2005. Galaxy: a platform for interactive large-scale genome analysis. – *Genome Research* 15: 1451-1455.

Givnish TJ. 2010. Ecology of plant speciation. – *Taxon* 59: 1326-1366.

Goecks J, Nekrutenko A, Taylor J, The Galaxy Team. 2010. Galaxy: a comprehensive approach for supporting accessible, reproducible, and transparent computational research in the life sciences. – *Genome Biology* 11: R86. doi:10.1186/gb-2010-11-8-r86

Goldblatt P. 1980. Polyploidy in angiosperms: Monocotyledons. In: Lewis WH (Eds.). *Polyploidy: Biological relevance*. Plenum Press. New York.

Gonzáles GL & Jarvis CE. 1984. De Linnei plantis hispanicis novitates nonnullae. – *Anales del Institudo Botanico A.J. Cavanilles* 40: 341-344.

Gould SJ. 2002. *The Structure of Evolutionary Theory*. The Belknap Press of Harvard University Press. Cambridge.

Gower JC. 1971. A general coefficient of similarity and some of its properties. – *Biometrics* 27: 857-874.

Grabherr G, Reiter K, Willner W. 2003. Towards objectivity in vegetation classification: the example of the Austrian forests. – *Plant Ecology* 169: 21-34.

Graham A, 1996. A contribution to the geologic history of the Compositae. pp. 123-140, *In:* Hind DJN & Beentje HJ (Eds.). *Compositae: Systematics. Proceedings of the International Compositae Conference, Kew, 1994, vol. 1*. Royal Botanic Gardens. Kew.

Grant V. 1963. *The origin of adaptations*. Columbia University Press. New York.

Grant V. 1975. *Genetics of flowering plants*. Columbia University Press. New York.

Grant V. 1981. *Plant speciation*, *2nd ed*. University Press. New York.

Grassi F, Labra M, Minuto L, Casazza G, Sala F. 2006. Natural hybridization in *Saxifraga callosa* Sm. – *Plant Biology* 8: 243-252.

Grassi F, Minuto L, Casazza G, Labra M, Sala F. 2009. Haplotype richness in refugial areas: phylogeographical structure of *Saxifraga callosa*. – *Journal of Plant Reserch* 122: 377-387.

Greuter W. 2006–2009. Compositae (pro parte majore). In: Greuter W, Raab-Straube E, von (Eds). *Compositae, Euro+Med Plantbase: the information resource for Euro-Mediterranean plant diversity.* Accessible at: http://www.emplantbase.org/home.htm

Griffin P, Robin C, Hoffmann A. 2011. A next-generation sequencing method for overcoming the multiple gene copy problem in polyploid phylogenetics, applied to *Poa* grasses. – *BMC Biology* 9: 19.

Grossmann TI, Song B, Windsor AJ, Mitchells-Olds T, Dixon CJ, Kapralov MV, Filatov DA, Eyre-Walker A. 2010. Genome wide analyses reveal little evidence for adaptive evolution in many plant species. – *Molecular Biology and Evololution* 27: 1822-1832.

Gruenstaeudl M, Santos-Guerra A, Jansen RK. 2013. Phylogenetic analyses of *Tolpis* Adans. (Asteraceae) reveal patterns of adaptive radiation, multiple colonization and interspecific hybridization. – *Cladistics* 29: 416-434.

Guindon S, Dufayard JF, Lefort V, Anisimova M, Hordijk W, Gascuel O. 2010. New algorithms and methods to estimate Maximum-Likelihood-phylogenies: Assessing the performance of PhyML 3.0. – *Systematic Biology* 59: 307-321.

Guo YP, Wang SZ, Vogl C, Eherendorfer F. 2012. Nuclear and plastid haplotypes suggest rapid diploid and polyploid speciation in the N Hemisphere *Achillea millefolium* complex (Asteraceae). – *BMC Evolutionary Biology* 12: 2. doi:10.1186/1471-2148-12-2.

Gusfield D, Bansal V, Bafna V, Song YS. 2007. A decomposition theory for phylogenetic networks and incompatible characters. – *Journal of Computational Biology* 14: 1247-1272.

Hagerup O. 1931. Über Polyploidie in beziehung zu klima, Ökologie und Phylogenie. – *Hereditas* 16: 19-40.

Hall TA. 1999. BioEdit: a user-friendly biological sequence alignment editor and analysis program for Windows 95/98/NT. – *Nucleic Acids Symposium Series* 41: 95-98.

Hasumi H, Emori S (Eds.). 2004. *K-1 Coupled GCM (MIROC) Description. K-1 Technical Report No. 1*. Center for Climate System Research. University of Tokyo. Tokyo.

Heled J, Drummond AJ. 2010. Bayesian inference of species trees from multilocus data. – *Molecular Biology and Evolution* 27: 570-580.

Hendry AP. 2009. Speciation. – *Nature* 458: 162-164.

Hermes K. 1955. *Die Lage der obenen Waldgrenze in den Gebirgen der Erde und ihr Abstand zu Schneegrenze*. Kölner geographische Arbeiten (Heft. 5). Universität Köln. Köln.

Heywood VH. 1955. A revision of the Spanish species of *Tanacetum* L. Subsect. *Leucanthemopsis* Giroux. – *Anales del Institudo Botanico A.J. Cavanilles* 12: 313-377.

Heywood VH. 1975. Leucanthemopsis (Giroux) Heywood. – A new genus of the Compositae – Anthemideae. – *Anales del Institudo Botanico A.J. Cavanilles* 32: 175-187.

Heywood VH. 1995. *Global diversity assessment*. Cambridge University Press. Cambridge.

Hijmans RJ, Cameron SE, Parra JL, Jones PG, Jarvis A. 2005. Very high resolution interpolated climate surfaces for global land areas. – *International Journal of Climatology* 25: 1965-1978.

Himmelreich S, Källersjo M, Eldenäs P, Oberprieler C. 2008. Phylogeny of southern hemisphere Compositae-Anthemideae based on nrDNA ITS and cpDNA *ndhF* sequence information. – *Plant Systematics and Evolution* 272: 131-153.

Hodgson JC. 1987. Why do so few plant species exploit productive habitats? An

investigation into cytology, plant strategies and abundance within a local flora. – *Functional Ecology* 1: 243-250.

Holland BR, Clarke AC, Meudt HM. 2008. Optimizing automated AFLP scoring parameters to improve phylogenetic resolution. – *Systematic Biology* 57: 347-36.

Holub J. 1977. New names in *Phanerogamae* 5. – *Folia Geobotanica et Phytotaxomica.* 12: 293-311.

Hörandl E, Paun O, Johansson JT, Lehnebach C, Armstrong T, Chen L, Lockhart P. 2005. Phylogenetic relationships and evolutionary traits in *Ranunculus* s.l. (Ranunculaceae) inferred from ITS sequence analysis. – *Molecular Phylogenetics and Evolution* 36: 305-327.

Husband BC, Schemske DW. 1997. The effect of inbreeding in diploid and tetraploid *Epilobium angustifolium* (Onagraceae): implications of the genetic basis of inbreeding depression. – *Evolution* 51: 737-746.

Husband BC. 2004. The role of triploid hybrids in the evolutionary dynamics of mixed-ploidy populations. – *Biological Journal of the Linnean Society.* 82: 537-546.

Huson DH, Bryant D. 2006. Application of Phylogenetic Networks in Evolutionary Studies. – *Molecular Biology and Evolution* 23: 254-267.

Huson DH, Scornavacca C. 2012 Dendroscope 3- An interactive viewer for rooted phylogenetic trees and networks – *Systematic Biology* 61: 1061–1067.

Ito Y, Ohi-Toma T, Murata J. 2013. Comprehensive phylogenetic analyses of the *Ruppia maritima* complex focusing on taxa from the Mediterranean. – *Journal of Plant Research.* 126: 753-762.

Ivanov D, Ashraf AR, Mosbrugger V, Palamarev E. 2002. Palynological evidence for Miocene climate change in the Forecarpathian Basin (Central Paratethys, NW Bulgaria). – *Palaeogeography, Palaeoclimatology, Palaeoecology* 178: 19-37.

Jaillon O, Aury JM, Noel B, Policriti A, Clepet C, Casagrande A, Choisne N, Aubourg S, Vitulo N, Jubin C, Vezzi A, Legeai F, Hugueney P, Dasilva C, Horner D, Mica E, Jublot D, Poulain J, Bruyere C, Billault A, Segurens B, Gouyvenoux M, Ugarte E, Cattonaro F, Anthouard V, Vico V, Del Fabbro C, Alaux M, Di Gaspero G, Dumas V, Felice N, Paillard S, Juman I, Moroldo M, Scalabrin S, Canaguier A, Le Clainche I, Malacrida G, Durand E, Pesole G, Laucou V, Chatelet P, Merdinoglu D, Delledonne M, Pezzotti M,

Lecharny A, Scarpelli C, Artiguenave F, Pe ME, Valle G, Morgante M, Caboche M, Adam-Blondon AF, Weissenbach J, Quetier F, Wincker P. 2007. The grapevine genome sequence suggests ancestral hexaploidization in major angiosperm phyla. – *Nature* 449: 463-467.

Jakobsson M, Rosenberg NA. 2007. *CLUMPP*: a cluster matching and permutation program for dealing with label switching and multimodality in analysis of population structure. – *Bioinformatics* 23: 1801-1806.

Jiménez-Mejías P, Amat E, Álvárez I, Vargas P. 2012. Nuevos nacimientos dan esperanza a las plantas españolas más amenazadas. – *Lychnos* 9: 22-27.

Jin G, Nakhleh L, Snir S, Tuller T. 2006. Maximum likelihood of phylogenetic networks. – *Bioinformatics* 22: 2604-2611.

Joly S, Starr JR, Lewis WH, Bruneau A. 2006. Polyploid and hybrid evolution in roses east of the rocky mountains. – *American Journal of Botany* 93: 412-425.

Joly S, Heenan PB, Lockhart PJ. 2009. A Pleistocene inter-tribal allopolyploidization event precedes the species radiation of *Pachycladon* (Brassicaceae) in New Zealand. – *Molecular Phylogenetics and. Evololution* 51:365-372.

Jones G, Sagitov S, Oxelman B. 2013. Statistical inference of allopolyploid species networks in the presence of Incomplete Lineage Sorting. – *Systematic Biology* 62: 467-478.

Jørgensen MH, Ehrich D, Schmickl R, Koch M, Brysting AK. 2011. Interspecific and interploidal gene flow in Central European *Arabidopsis* (Brassicaceae). – *BMC Evolutionary Biology* 11: 346.

Kadereit JW, Griebeler EM, Comes HP. 2004. Quaternary diversification in European alpine plants: pattern and process. – *Philosophical Transactions B of the Royal Society* 359: 265-274.

Katoh K, Misawa K, Kuma K, Miyata T. 2002. MAFFT: a novel method for rapid multiple sequence alignment based on fast Fourier transform. – *Nucleic Acids Research* 30: 3059-3066.

Katoh K, Toh H. 2008. Recent developments in the MAFFT multiple sequence alignment program. – *Briefings in Bioinformatics* 9: 286-298.

Kim KJ, Jansen RK. 1995. *ndhF* sequnce evolution and the major clades in the sunflower family. – *Proceedings of the National Academy of Sciences USA* 92: 10379-10383.

Kingman JFC. 1982. The coalescent. – *Stochastic Processes and Their Applications* 13: 235-248.

Kingman JFC. 2000. Origins of the Coalescent: 1974-1982. – *Genetics* 156: 1461-1463.

Knowles LL, Kubatko LS (Eds.). 2010. *Estimating Species Trees – Practical and Theoretical Aspects.* John Wiley & Sons, Hoboken.

Kolář F, Štech M, Trávníček P, Rauchová J, Urfus T, Petr V, Kubešová M, Suda M. 2009. Towards resolving the *Knautia arvensis* agg. (Dipsacaceae) puzzle: primary and secondary contact zones and ploidy segregation at landscape and microgeographic scales. – *Annals of Botany* 103: 963-974.

Konowalik K, Wagner F, Tomasello S, Vogt R, Oberprieler C. Detecting reticulate relationships among diploid *Leucanthemum* Mill. (Compositae, Anthemideae) taxa using multilocus species tree reconstruction methods and AFLP fingerprinting. – *Systematic Biology* (under review).

Körner C. 1995. Alpine plant diversity: A Global Survey and Functional Interpretations. In: Stuart Chapin III F, Körner C (Eds.). *Arctic and alpine Biodiversity*. Ecological studies vol. 113. Springer-Verlag. Berlin.

Körner C. 2003. *Alpine plant life*, *2nd ed*. Springer. Heidelberg.

Krak K, Caklová P, Chrtek J, Fehrer J. 2013. Reconstruction of phylogenetic relationships in a highly reticulate group with deep coalescence and recent spetiation (*Hieracium*, Ateraceae). – *Heredity* 110: 138-151.

Krijgsman W, Hilgen FJ, Raffi I, Sierro FJ, Wilson DS. 1999. Chronology, causes and progression of the Messinian salinity crisis. – *Nature* 400: 652-655.

Kubatko LS, Carstens BC, Knowles LL. 2009. STEM: species tree estimation using maximum likelihood for gene trees under coalescence. – *Bioinformatics* 25: 971-973.

Küpfer P. 1974. Recherches sur les liens de parenté entre la flore orophile des Alpes et celle des Pyrénées. – *Boissiera* 23: 1-322.

Küpfer P, Favarger C. 1967. Premières prospections caryologiques dans la flore orophile des Pyrénées et de la Sierra Nevada. – *Comptes rendus hebdomadaires des seances de l'Academie des sciences* 264: 2463-2465.

Labra M, Grassi F, Sgorbati S, Ferrari C. 2006. Distribution of genetic variability in southern populations of Scots pine (*Pinus sylvestris* L.) from the Alps to the Apennines. – *Flora* 201: 468-476.

Ladero M, Velasco A. 1978. Adiciones a la flora de los Montes de Toledo. – *Anales del Institudo Botanico A.J. Cavanilles* 34: 497-519.

Lagercrantz. 1998. Comparative mapping between *Arabidopsis thaliana* and *Brassica nigra* indicates that brassica genomes have evolved through extensive genome replication accompanied by chromosome fusions and frequent rearrangements. – *Genetics* 150: 1217–1228.

Lang G. 1994. *Quartäre Vegetationsgeschichte Europas*. Fischer. Jena.

Leaché AD, Rannala B. 2011. The accuracy of species tree estimation under simulation: a comparison of methods. – *Systematic Biology* 60: 126-137.

Leaché AD, Harris RB, Rannale B, Yang Z. 2013. The influence of gene flow on species tree estimation: a simulation study. – *Systematic Biology* 63:17-30.

Lee C, Wen J. 2004. Phylogeny of *Panax* using chloroplast *trnC-trnD* intergenic region and the utility of *trnC-trnD* in interspecific studies of plant. – *Molecular Phylogenetics and Evolution* 31: 894-903.

Leitch IJ, Bennett MD. 1997. Polyploidy in angiosperms. – *Trends in Plant Science* 2: 470-476.

Levin D. 2002. *The Role of Chromosomal Change in Plant Evolution*. Oxford University Press: New York.

Lewis H. 1969. Comparative cytology in systematics. In: Sibley CG (Ed.). *Systematic Biology*. National Academy of Science. Washington.

Lewis WH. 1980. Polyploidy in angiosperms: Dicotyledons. In: Lewis W (Ed.). *Polyploidy*. Springer, New York.

Librado P, Rozas J. 2009. DnaSP v5: a software for comprehensive analysis of DNA polymorphism data. – *Bioinformatics* 25: 1451-1452.

Linder CR, Moret BME, Nekhleh L, Warnow T. 2003. Network (Reticulate) evolution: biology, models and algorithms. In: *The Ninth Pacific Symposium on Biocomputing (PSB)*. Haway.

Linder R, Rieseberg LH. 2004. Reconstructing patterns of reticulate evolution in plants. – *American Journal of Botany* 91: 1700-1708.

Liu L. 2008. BEST: Bayesian estimation of species trees under the coalescent model. – *Bioinformatics* 24: 2542-2543.

Liu B, Wendel JF. 2003. Epigenetic phenomena and the evolution of plant allopolyploids. – *Molecular Phylogenetics and. Evololution* 29: 365-379.

Liu L, Yu L, Pearl DK, Edwards SD. 2009. Estimating species phylogenies using coalescence times among sequences. – *Systematic Biology* 58: 468-477.

Liu L, Yu L, Edwards SV. 2010. A maximum pseudo-likelihood approach for estimating species trees under the coalescent model. – *BMC Evolutionary Biology* 10: 302.

Liu L, Yu L. 2011. Estimating species trees from unrooted gene trees. – *Systematic Biology* 60: 661–667.

Lo EYY, Stefanović S, Dickinson TA. 2010. Reconstructing reticulation history in a phylogenetic framework and the potential of allopatric speciation driven by polyploidy in an agamic complex in *Crataegus* (Rosaceae). – *Evolution* 64: 3593-3608.

Lo Presti RM, Oppolzer S, Oberprieler C. 2010. A molecular phylogeny and a revised classification of the Mediterranean genus *Anthemis* s.l. (Compositae, Anthemideae) based on three molecular markers and micromorphological characters. – *Taxon* 59: 1441-1456.

Lott M, Spillner A, Huber KT, Moulton V. 2009. PADRE: a package for analyzing and displaying reticulate evolution. – *Bioinformatics* 25: 1199-1200.

Loureiro J, Castro M, Cerca de Oliveira J, Mota L, Torices R. 2013. Genome size variation and polyploidy incidence in the alpine flora from Spain. – *Anales del Jardín Botánico de Madrid* 70: 39-47.

Löve A, Löve D. 1949. The geoglobal significance of polyploidy. I. Polyploidy and latitude. – *Portugaliae Acta Biologica.* Ser. A, 2: 273-352.

Löve A, Löve D. 1957. Arctic polyploidy. – *Proceedings of the Genetics Society of Canada* 2: 23–27.

Löve A, Löve D. 1967. Polyploidy and altitude: Mt. Washington. – *Biologisches Zentralblatt* Suppl. Vol.: 307-312.

Lutz AM. 1907. A preliminary note on the chromosomes of *Oenothera lamarckiana* and one of its mutants, *O. gigas*. – *Science* 26: 151-152.

Mable B. 2004. ´Why polyploidy is rarer in animals than in plants´: myths and mechanisms. – *Biological Journal of the Linnean Society* 82: 453-466.

Maddison WP. 1997. Gene trees in species trees. – *Systematic Biology* 46: 523-536.

Maddison WP, Maddison DR. 2011. Mesquite: a modular system for evolutionary analysis, version 2.75. http://mesquiteproject.org.

Makarenkov V. 2001. T-REX: reconstructing and visualizing phylogenetic trees and reticulation networks. – *Bioinformatics* 17: 664-668.

Mallet J. 2001. The speciation revolution. – *Journal of Evolutionary Biology* 14: 887-888.

Mallet J. 2005. Hybridization as an invasion of the genome. – *TRENDS in Ecology and Evolution* 20: 229-237.

Mallet J. 2007. Hybrid speciation. – *Nature* 446: 279-283.

Manni F, Guerard E, Heyer E. 2004. Geographic patterns of genetic, morphologic and linguistic variation: how barriers can be detected by using Monmonier's algorithm. – *Human Biology* 76: 173-190.

Mansion G, Zeltner L, Bretagnolle F. 2005. Phylogenetic patterns and polyploid evolution within the Mediterranean genus *Centaurium* (Gentianaceae-Chironieae). – *Taxon* 54: 931-950.

Manton I. 1950. *Problems of cytology and evolution in the Pteridophyta*. Cambridge University Press. Cambridge.

Marchi P, Illuminati O. 1974. Notizie e considerazioni su i *Leucanthemum* (Compositae) della Flora d'Italia. – *Annali di Botanica* 33: 167-187.

Marcussen T, Jakobsen KS, Danihelka J, Ballard HE, Blaxland K, Brysting AK, Oxelman B. 2012. Inferring species networks from gene trees in high-polyploid North American and Hawaiian violets (*Viola*, Violaceae). – *Systematic Biology* 61: 107-126.

Marcussen T, Sandve SR, Heier L, Spannagl M, Pfeifer M, The International Wheat Genome Sequencing Consortium, Jakobsen KS, Wulff BBH, Steuernagel B, Mayer KFX, Olsen O. 2014. Ancient hybridizations among the ancestral genomes of bread wheat. – *Science* 345: 1250092. doi:10.1126/science.1250092.

Marhold K, Lihovà J. 2006. Polyploidy, hybridization and reticulate evolution: lessons from the Brassicaceae. – *Plant Systematics and Evolution* 259: 143-176.

Marie D, Brown SC. 1993. A cytometric exercise in plant DNA histograms, with 2C values for 70 species. – *Biology of the Cell* 78: 41-51.

Mariz J. 1891. Subsídios para o estudo da flora Portuguesa-Compositae L. (continuação). – *Boletim da Sociedade Broteriana* 9: 144-242.

Martinez-Zapater JM, Oliver JL. 1984. Genetic analysis of isozyme loci in tetraploid potatoes (*Solanum tuberosum* L.). – *Genetics* 108: 669-679.

Mason-Gamer RJ. 2013. Phylogeny of a Genomically Diverse Group of *Elymus* (Poaceae) Allopolyploids Reveals Multiple Levels of Reticulation. *PLOS ONE* 8: e78449. doi:0.1371/journal.pone.0078449

Mayr E. 1942. Systematics and the Origin of Species, from the Viewpoint of a Zoologist. Harvard University Press. Cambridge.

Mayr E. 1954. Change of genetic environment and evolution. In: Huxley J, Hardy AC, Ford EB (Eds.). *Evolution as a Process*. Allen & Unwin. London.

Mayr E. 1970. *Populations, Species, and Evolution*. Harvard University Press. Cambridge

Mayrose I, Zhan SH, Rothfels CJ, Magnuson-Ford K, Barker MS, Rieseberg LH, Otto SP. 2011. Recently formed polyploid plants diversify at lower rates. – *Science* 333: 1257.

Meister J, Hubaishan M, Kilian N, Oberprieler C. 2006. Temporal and spatial diversification of the shrub *Justicia areysiana* Deflers (Acanthaceae) endemic to the monsoon affected coastal mountains of southern Arabian Peninsula. – *Plant Systematics and Evolution* 262: 153-171.

Melé M, Javed A, Pybus M, Zalloua P, Haber M, Comas D, Netea MG, Balanovsky O, Balanovska E, Jin L, Yang Y, Pitchappan RM, Arunkumar G, Parida L, Calaffel F, Bertranpetit J, the Genographic Consortium. 2012. Recombination gives a new insight in the effective population size and the history of the old world human populations. – *Molecular Biology and Evolution.* 29: 25-30.

Mexmüller H. 1954. *Untersuchungen zum Sippengliederung und Arealbildung in den Alpen*. Verein zum Schutz der Alpenpflanzen und -tiere 19. München.

Monmonier M. 1973. Maximum-difference barriers: an alternative numerical regionalization method. – *Geographical Analysis* 3: 245-261.

Moreno JC (Ed.). 2011. *Lista Roja de la Flora Vascular Española 2008. Actualización con los datos del Adenda 2010 al Atlas y Libro Rojo de la Flora Vascular Amenazada*. Dirección General de Conservación de la Naturaleza y Sociedad Española de Biología de la Conservación de Plantas. Madrid.

Morton JK. 1993. Chromosome numbers and polyploidy in the flora of Cameroons Mountain. – *Opera Botanica* 121: 159-172.

Mossel R, Roch S. 2010. Incomplete lineage sorting: consistent phylogeny estimation from multiple loci. – *IEEE/ACM Transactions on Computational Biology and Bioinformatics* 7: 166-171.

Mráz P, Šinglarová B, Urfus T, Krahulec F. 2008. Cytogeography of *Pilosella officinarum* (Compositae): Altitudinal and longitudinal differences in ploidy level distribution in the Czech Republic and Slovakia and the general pattern in Europe. – *Annals of Botany* 101: 59-71.

Müntzing A. 1936. The evolutionary signifi cance of autopolyploidy. – *Hereditas* 21: 363-378.

Nagy L, Grabherr G. 2009. *The Biology of Alpine Habitats*. Oxford University Press. Oxford.

Nakhleh L, Ruths D, Wang LS. 2005a. RIATA-HGT: a fast and accurate heuristic for reconstrucing horizontal gene transfer. In: Wang L (Ed.) *Proceedings of the 11th International Computing and Combinatorics Conference (COCOON 05)*. Available at: http://www.phylo.org/pdf_docs/41_%2882%29Wang_NRW.pdf

Nakhleh L, Warnow T, Linder CR, John KST. 2005b. Reconstructing reticulate evolution in species - theory and practice. – *Journal of Computational Biology* 12: 796-811.

Nakhleh L, Ruths D, Innan, H. 2009. Gene trees, species trees, and species networks? In: Guerra R, Goldstein D (Eds.). *Meta-analysis and Combining Information in Genetics and Genomics*. Chapman & Hall. London.

Nie ZL, Wen J, Gu ZJ, Boufford DE, Sun H. 2005. Polyploidy in the flora of the Hengduan Mountains hotspot, southwestern China. – *Annals of the Missouri Botanical Garden* 92: 275-306.

Oberprieler C, Vogt R. 2000. The position of *Castrilanthemum* Vogt & Oberprieler and the phylogeny of Mediterranean Anthemideae (Compositae) as inferred from nrDNA ITS

and cpDNA *trn*L/*trn*F IGS sequence variation. – *Plant Systematics and Evolution* 225: 145-170.

Oberprieler C. 2004a. On the taxonomic status and the phylogenetic relationships of some unispecific Mediterranean genera of *Compositae-Anthemideae.* I. *Brocchia*, *Endopappus,* and *Heliocauta*. – *Willdenowia* 34: 39-57.

Oberprieler C. 2004b. On the taxonomic status and the phylogenetic relationships of some unispecific Mediterranean genera of *Compositae-Anthemideae.* II. *Daveaua*, *Leucocyclus,* and *Nananthea*. – *Willdenowia* 34: 341-350.

Oberprieler C. 2005. Temporal and spatial diversification of Circum-Mediterranean Compositae-Anthemideae. – *Taxon* 54: 951-966.

Oberprieler C, Himmelreich S, Vogt R. 2007a. A new subtribal classification of the tribe Anthemideae (Compositae). – *Willdenowia* 37: 89-114.

Oberprieler C, Vogt R, Watson LE. 2007b. Tribe Anthemideae Cass. In: Kadereit JW, Jeffrey C (Eds.). *The Families and Genera of Vascular Plants, Vol. VIII: Flowering Plants, Eudicots, Asterales*. Springer-Verlag. Berlin.

Oberprieler C, Himmelreich S, Källersjö M, Vallès J, Watson LE, Vogt R. 2009. Anthemideae. pp. 631-666. In: Funk VA, Susanna A, Stuessy TF, Bayer RJ (Eds.). *Systematics, Evolution, and Biogeography of Compositae.* International Association for Plant Taxonomy. Vienna.

Osborn TC, Pires JC, Birchler JA, Auger DL, Chen ZJ, Lee HS, Comai L, Madlung A, Doerge RW, Colot V, Martienssen RA. 2003. Understanding mechanisms of novel gene expression in polyploids. – *Trends in Genetics* 19: 141-147.

Otto F. 1992. Preparation and staining of cells for high-resolution DNA analysis. In: Radbruch A (Ed.). *Flow cytometry and cell sorting*. Springer-Verlag. Berlin.

Otto SP, Whitton J. 2000. Polyploid incidence and evolution. – *Annual. Review of Genetics* 34: 401-437.

Otto-Bliesner BL, Marshall SJ, Overpeck JT, Miller GH, Hu A, CAPE Last Interglacial Project members. 2006. Simulating Arctic Climate Warmth and Icefield Retreat in the Last Interglaciation. – *Science* 311: 1751.

Ozenda P. 1988. Die Vegetation der Alpen im europäischen Gebirgsraum. Fischer. Stuttgart.

Ozenda P. 1993. Etage alpin et Toundra de montagne: parenté ou convergence? – *Fragmenta Floristica et Geobotanica* 2: 457-471.

Palme AE, Su Q, Palsson S, Lascoux M. 2004. Extensive sharing of chloroplast haplotypes among European birches indicates hybridization among *Betula pendula*, *B. pubescens* and *B. nana*. – *Molecular Ecology* 13: 167-178.

Pau C. 1906. Sobre el "Pyrethrum hispanicum" de Willkomm. – *Butlleti de la Institució Catalana d'Historia Natural.* 6: 88-93.

Pawłowski B. 1928. Die geographischen Elemente und die Herkunft der Flora der subnivalen Vegetationsstufe im Tatra-Gebirge. – *Bulletin de l'Académie Polonaise des Sciences et des Lettres.Classe des Sciences Mathématiques et Naturelles* Sér. B: 161-202.

Pawłowski B. 1970. Remarques sur l'endémisme dans la flore des Alpes et des Carpates. – *Vegetatio* 21: 181-243.

Pérez-Romero R, Pérez-Morales, Del Río S, Penas Á. 2005. *Leucanthemopsis virescens* (Pau) R.Pérez-Romero, C. Pérez-Morales, S. del Río & Penas. A new combination. – *Studia Botanica* 24: 67-69.

Pfenninger M, Posada D. 2002. Phylogeographic history of the land snail candidula unifasciata (Helicellinae, Stylommatophora): fragmentation, corridor migration, and secondary contact. – *Evolution* 56: 1776-1788.

Phillips SJ, Anderson R, Schapire RE. 2006. Maximum entropy modeling of species geographic distributions. – *Ecological Modelling* 190: 231-259.

Phillips SJ, Dudík M, Schapire RE. 2004. A maximum entropy approach to species distribution modeling. In: *ICML "04" Proceedings of the 21st International Conference on Machine Learning*. ACM. New York.

Pignatti S. 1983. *Flora d'Italia, III*. Ed. Agricole. Bologna.

Popp M, Oxelman B. 2001. Inferring the history of the polyploid *Silene aegaea* (Caryophyllaceae) using plastid and homoeologous nuclear DNA sequences. – *Molecular Phylogenetics and Evolution* 20: 474-481.

Popp M, Erixon P, Eggens F, Oxelman B. 2005. Origin and evolution of a circumpolar polyploid species complex in *Silene* (Caryophyllaceae) inferred from low copy nuclear RNA polymerase introns, rDNA, and chloroplast DNA. – *Systematic Botany* 30: 302-313.

Posada D, Crandall KA. 1998. Modeltest: testing the model of DNA substitution. – *Bioinformatics* 14: 817-818.

Pritchard JK, Stephens M, Donnelly P. 2000. Inference of population structure using multilocus genotype data. – *Genetics* 155: 945-959.

R Development Core Team. 2008. R: A language and environment for statistical computing. R Foundation for Statistical Computing. Available at: http://www.R-project.org.

Raabová J, Fischer M, Münzbergová Z. 2008. Niche differentiation between diploid and hexaploid *Aster amellus*. – *Oecologia* 158: 463-472.

Rambaut A, Drummond AJ. 2007. Tracer v1.4: MCMC trace analyses tool. – Available at: http://beast.bio.ed.ac.uk/Tracer.

Ramsey J, Schemske DW. 1998. Pathways, mechanisms, and rates of polyploid formation in flowering plants. – *Annual Review of Ecology Evolution and Systematics* 29: 467-501.

Ramsey J, Schemske DW. 2002. Neopolyploidy in flowering plants. – *Annuals Review of Ecology, Evolution and Systematics* 33: 589-639.

Ravazzi C. 2002. Late Quaternary history of spruce in southern Europe. Review of – *Palaeobotany and Palynology* 120: 131-177.

Reisch C. 2008. Glacial history of *Saxifraga paniculata* (Saxifragaceae): Molecular biogeography of a disjunct arctic-alpine species from Europe and North America. – *Biological Journal of the Linnean Society* 93:385-398.

Revell LJ. 2012. phytools: an R package for phylogenetic comparative biology (and other things). – *Methods in Ecology and Evolution* 3: 217-223.

Rivaz-Martinez S. 1969. La vegetación de alta montaña española. In: *V simposio de Flora Europea*. Univiversidad de Sevilla. Seville.

Rivaz-Martinez S. 1973. Avance sobre una sintesi corologica de la Peninsula Iberica, Baleares y Canarias. – *Anales del Institudo Botanico A.J. Cavanilles* 30: 69-87.

Rodriguez F, Spooner DM. 2009. Nitrate Reductase Phylogeny of Potato (*Solanum* sect. *Petota*) Genomes with Emphasis on the Origins of the Polyploid Species. – *Systematic Botany* 34: 207-219.

Ronquist F, Huelsenbeck JP. 2003. MRBAYES 3: Bayesian phylogenetic inference under mixed models. – *Bioinformatics* 19: 1572-1574.

Ronquist F, Huelsenbeck J, Teslenko M. 2011. Draft MrBayes version 3.2 Manual: Tutorials and Model Summaries. – Available at http://mrbayes.sourceforge.net/mb3.2_manual.pdf.

Ronquist F, Teslenko M, Van Der Mark P, Ayres DL, Darling A, Höhna S, Larget B, Liu L, Suchard MA, Huelsenbeck JP. 2012. MrBayes 3.2: Efficient Bayesian phylogenetic inference and model choice across a large model space. – *Systematic Biology* 61: 539-542.

Rosauer D, Laffan SW, Crisp MD, Donnellan SC, Cook LG. 2009. Phylogenetic endemism: a new approach for identifying geographical concentrations of evolutionary history. – *Molecular Ecology* 18: 4061-4072.

Rosenberg NA. 2004. *Distruct*: a program for the graphical display of population structure. – *Molecular Ecology Notes* 4: 137-138.

Rosewich UL, Kistler HC. 2000. Role of horizontal gene transfer in the evolution of fungi. – *Annual Review of Phytopathology*. 38: 325-365.

Rydin C, Pedersen KR, Friis EM. 2004. On the evolutionary history of *Ephedra:* Cretaceous fossils and extant molecules. – *Proceedings of the National Academy of Sciences USA* 101: 16571-16576.

Sanchez-Garcia A, Castresana J. 2012. Impact of deep coalescence on the reliability of species tree inference from different type of DNA markers in mammals. – *PLoS One* 7: e30239. doi:0.1371/journal.pone.0030239.

Sanderson MJ. 1997. A nonparametric approach to estimating divergence times in the absence of rate constancy. – *Molecular Biology and Evolution* 14: 1218-1231.

Sang T, Crawford DJ, Stuessy TF. 1997. Chloroplast DNA phylogeny, reticulate evolution, and biogeography of *Paeonia* (Paeoniaceae). – *American Journal of Botany* 84: 1120-1136.

Sanz de Galeano C. 1990. Geologic evolution of the Betic Cordilleras in the Western Mediterranean, Miocene to the present. – *Tectonophysics* 172: 107-119.

Sanz M, Schönswetter P, Vallés J, Scheeweiss GM, Vilartesana R. 2014. Southern isolation and northern long-distance dispersal shaped the phylogeography of the widespread, but highly disjunct, European high mountain plant *Artemisia eriantha* (Asteraceae). – *Botanical Journal of the Linnean Society* 174: 214-226.

Scheunert A, Heubl G. 2014. Diversification of *Scrophularia* (Scrophulariaceae) in the Western Mediterranean and Macaronesia – Phylogenetic relationships, reticulate evolution and biogeographic patterns. – *Molecular Phylogenetics and Evolution* 70: 296-313.

Schlüter PM, Harris SA. 2006. Analysis of multilocus fingerprinting data sets containing missing data. – *Molecular Ecology Notes* 6: 569-572.

Schmitt T, Haubrich K. 2008. The genetic structure of the mountain forest butterfly *Erebia euryale* unravels the late Pleistocene and Postglacial history of the mountain forest biome in Europe. – *Molecular Ecology* 17: 2194-2207.

Schmitt T, Hewitt GM, Müller P. 2006. Disjunct distributions during glacial and interglacial periods in mountain butterflies: *Erebia epiphron* as an example. – *Journal of Evolutionary Biology* 19:108-113.

Schneeweiss GM, Schönswetter P. 2011. A re-appraisal of nunatak survival in arctic-alpine phylogeography. – *Molecular Ecology* 20: 190-192.

Schönswetter P, Tribsch A, Barfuss M, Nikfeld H. 2002. Several Pleistocene refugia detected in the high alpine plant *Phyteuma globulariifolium* Sternb. & Hoppe (Campanulaceae) in the European Alps. – *Molecular Ecology* 11: 2637-2647.

Schönswetter P, Tribsch A, Niklfeld H. 2003a. Phylogeography of the high alpine cushion-plant *Androsace alpina* (Primulaceae) in the European Alps. – *Plant Biology* 5: 623-630.

Schönswetter P, Tribsch A, Schneeweis GM, Nikfeld H. 2003b. Disjunctions in relict alpine plants: phylogeography of *Androsace brevis* and *A. wulfeniana* (Primulaceae). – *Botanical Journal of the Linnean Society* 141: 437-446.

Schönswetter P, Tribsch A, Stehlik I, Niklfeld H. 2004. Glacial history of high alpine *Ranunculus glacialis* (Ranunculaceae) in the European Alps in a comparative phylogeographical context. – *Biological Journal of the Linnean Society* 81: 183-195.

Schönswetter P, Stehlik I, Holderegger R, Tribsch A. 2005. Molecular evidence for glacial refugia of mountain plants in the European Alps. – *Molecular Ecology* 14: 3547-3555.

Schönswetter P, Tribsch A. 2005. Vicariance and dispersal in the alpine perennial, *Bupleurum stellatum* L. (Apiaceae). – *Taxon* 54: 725-732.

Segraves KA, Thompson JN. 1999. Plant polyploidy and pollination: floral traits and insect visits to diploid and tetraploid Heuchera grossulariifolia. – *Evolution* 53: 1114-1127.

Siljak-Yakovlev S, Pustahija F, Šolić EM, Bogunić F, Muratović E, Bašić N, Catrice O, Brown SC. 2010. Towards a Genome Size and Chromosome Number Database of Balkan Flora: C-Values in 343 Taxa with Novel Values for 242. – *Advanced Science Letters* 3: 190-213.

Simmons MP, Ochoterena H. 2000. Gaps as characters in sequence-based phylogenetic analyses. – *Systematic Biology* 49: 369-381.

Sistrom M, Hutchinson M, Bertozzi T, Donnellan S. 2014. Evaluating evolutionary history in the face of high gene tree discordance in Australian *Gehyra* (Reptilia: Gekkonidae). – *Heredity* 113: 52-63.

Skalinska M, Czapik R, Piotrowicz M et al. 1959. Further studies in chromosome numbers of Polish angiosperms (Dicotyledons). – *Acta Societatis Botanicorum Poloniae* 28: 487-529.

Smissen RD, Galbany-Casals M, Breitwieser I. 2011. Ancient allopolyploidy in the everlasting daisies (Asteraceae: Gnaphalieae): Complex relationships among extant clades. – *Taxon* 60: 649-662.

Soltis DE, Albert VA, Leebens-Mack J, Bell CD, Paterson AH, Zheng C, Sankoff D, dePamphilis CW, Wall PK, Soltis PS. 2009. Polyploidy and angiosperm diversification. – *American Journal of Botany* 96: 336-348.

Soltis DE, Visger CJ, Soltis PS. 2014. The polyploidy revolution then...and now: Stebbins revisited. – *American Journal of Botany* 101: 1057-1078.

Soltis PS, Soltis DE. 2003. Applying the bootstrap in phylogeny reconstruction. – *Statistical Science.* 18: 256-267.

Soltis PS, Soltis DE. 2009. The role of hybridization in plant speciation. – *Annual Review of Plant Biology* 60: 561-588.

Sonboli A, Stroka K, Kazempour Osaloo S, Oberprieler C. 2012. Molecular phylogeny and taxonomy of *Tanacetum* L. (Compositae Anthemideae) inferred from nrDNA ITS and cpDNA trnH-psbA sequence variation. – *Plant Systematics and Evolution* 298: 431-444.

Sonnleitner M, Flatscher R, Escobar García P, Rauchová J, Suda J, Schneeweiss GM, Hülber K, Schönswetter P. 2010. Distribution and habitat segregation on different spatial scales among diploid, tetraploid and hexaploid cytotypes of *Senecio carniolicus* (Asteraceae) in the Eastern Alps. – *Annals of Botany* 106: 967-977.

Sonnleitner M, Weis B, Flatscher R, Escobar Garcia P, Suda J, Krejčíková J, Schneeweiss GM, Winkler M, Schönswetter P, Hülber K. 2013. Parental ploidy strongly affects offspring fitness in heteroploid crosses among three cytotypes of autopolyploid *Jacobaea carniolica* (Asteraceae). – *PLOSone* 8: 78959. doi:0.1371/journal.pone.0078959.

Stanley SM. 1979. *Macroevolution: Patterns and Processes.* The John Hopkins University Press. Baltimore.

Stebbins GL. 1947. Types of polyploids: their classification and significance. – *Advances in Genetics* 1: 403-429.

Stebbins GL. 1950. *Variation and evolution in plants*. Columbia University Press. New York.

Stebbins GL. 1971. *Chromosomal evolution in higher plants*. Edward Arnold. London.

Stebbins GL. 1984. Polyploidy and the distribution of the arctic-alpine flora: new evidence and a new approach. – *Botanica Helvetica* 94: 1-13.

Stebbins GL. 1985. Polyploidy, hybridization, and the invasion of new habitats. – *Annals of the Missouri Botanical Garden* 72: 824-832.

Stehlik I. 2003. Resistence or emigration? Response of alpine plants to the ice ages. – *Taxon* 52: 499-510.

Stift M, Bregman R, Oostermeijer GB, van Tienderen PH. 2010. Other tetraploid species and conspecific diploids as sources of genetic variation for an autotetraploid. – *American Journal of Botany* 97: 1858-1866.

Strasburg JL, Kane NC, Radusky AR, Bonin A, Michelmore R, Rieseberg LH. 2011. Effective population size is positively correlated with levels of adaptive divergence among annual sunflowers. – *Molecular Biology and Evolution* 28:1569-1580.

Stuessy TF. 2008. *Plant taxonomy*, *2nd ed*. Columbia University Press. New York.

Suc JP. 1984. Origin and evolution of the Mediterranean vegetation and climate in Europe. – *Nature* 307: 429-432.

Suda J, Herben T. 2013. Ploidy frequencies in plants with ploidy heterogeneity: fitting a general gametic model to empirical population data. – *Proceedings B of the Royal Society* 282: 20122387. doi:10.1098/rspb.2012.2387.

Swofford DL. 2002. PAUP*: *Phylogenetic analysis using parsimony (*and other methods),* version 4.0b10. Sinauer. Sunderland.

Tal M. 1980. *Physiology and polyploidy*. In Lewis WH: Polyploidy, biological relevance. Plenum. New York.

Tang H, Wang X, Bowers JE, Ming R, Alam M, Paterson AH. 2008. Unraveling ancient hexaploidy through multiply-aligned angiosperm gene maps. – *Genome Reserches* 18: 1944-1954.

Tank DC, Olmstead RG. 2008. From annuals to perennials: Phylogeny of stubtribe Castillejinae (Orobanchaceae). – *American Journal of Botany* 95: 608-625.

Templeton AR, Crandall KA, Sing CF. 1992. A cladistic analysis of phenotypic associations with haplotypes inferred from restriction endonuclease mapping and DNA sequence data. III. Cladogram estimation. – *Genetics* 132:619-633.

Than C, Ruths D, Nakhleh L. 2008. PhyloNet: a software package for analyzing and reconstructing reticulate evolutionary relationships. – *BMC Bioinformatics* 9: 322.

Than C, Nakhleh L. 2009. Species tree inference by minimizing deep coalescences. – *PLoS Computational Biology* 5: e1000501. doi:10.1371/journal.pcbi.1000501.

Thompson JD. 2005. *Plant Evolution in the Mediterranean.* Oxford University Press. Oxford.

Thompson JD, Lumaret R. 1992. The evolutionary dynamics of polyploidy plants: origins, establishment and persistence. – *TRENDS in Ecology and Evolution* 7: 302-307.

Thompson JD, Higgins DG, Gibson TJ. 1994. CLUSTAL W: improving the sensitivity of progressive multiple sequence alignment through sequence weighting, position-specific gap penalties and weight matrix choice. – *Nucleic Acids Research* 22: 4673-4680.

Thompson JN, Nuismer SL, Merg K. 2004. Plant polyploidy and the evolutionary ecology of plant/animal inter-actions. – *Biological Journal of the Linnean Society* 82: 511-519.

Tischler G. 1935. Die Bedeutung der Polyploidie für die Verbreitung der Angiospermen, erläutert an den Arten Schles-wig-Holsteins, mit Ausblicken auf andere Florengebiete. – *Botanische Jahrbücher für Systematik, Pflanzengeschichte und Pflanzengeographie* 67: 1-36.

Tribsch A, Schönswetter P, Stuessy TF. 2002. *Saponaria pumila* (Caryophyllaceae) and the ice-age in the Eastern Alps. – *American Journal of Botany* 89: 2024-2033.

Tribsch A, Schönswetter P. 2003. Patterns of endemism and comparative phylogeography confirm paleo-environmental evidence for Pleistocene refugia in the Eastern Alps. – *Taxon* 52: 477-497.

Triplett JK, Clark LG, Fisher AE, Wen J. 2014. Independent allopolyploidization events preceded speciation in the temperate and tropical woody bamboos. – *New Phytologist* 204: 66-73.

Turelli N, Barthion NH, Coyne JA. 2001. Theory and speciation. – *TRENDS in Ecology and Evolution* 16: 330-343.

Vamosi JC, McEwen J. 2012. Origin, elevation, and evolutionary success of hybrids and polyploids in British Columbia, Canada. – *Botany* 91: 182-188.

van Andel TH, Tzedakis PC. 1996. Palaeolithic landscapes of Europe and environs, 150 000-25 000 years ago: an overview. – *Quaternary Science Reviews* 15: 481-500.

Van Dam JA. 2006. Geographic and temporal patterns in the late Neogene (12-3 Ma) aridification of Europe: The use of small mammals as paleoprecipitation proxies. – *Palaeogeography, Palaeoclimatology, Palaeoecology* 238: 190-218.

van Husen D. 1997. LGM and late-glacial fluctuations in the Eastern Alps. – *Quaternary International* 38/39: 109-118.

Vargas P. 2003. Molecular evidence for multiple diversification patterns of alpine plants in Mediterranean Europe. – *Taxon* 52: 463-476.

Vargas P. 2010. Estudio de plantas amenazadas en España: ¿hay fósiles vivientes aún desconocidos? – *Lychnos* 3: 19-23.

Vera JA. 2000. El Terciario de la Cordillera Bética: estado actual de conocimientos. – *Revista de la Sociedad Geológica de España* 13: 345-373

Via S. 2001. Sympatric speciation in animals: the ugly duckling grows up. – *TRENDS in Ecology and Evolution*. 16: 381-390.

Vierhapper F. 1914. Chrisanthemum alpinum forma Tatrae. – *Magyar Botanikai Lapok* 13: 13-35.

Villars D. 1789. Histoire des plantes de Dauphiné. III. Grenoble.

Vision TJ, Brown DG, Tanksley SD. 2000. The origins of genome duplications in *Arabidopsis*. – *Science* 290: 2114-2117.

Voges A. 1995. *International Quaternary Map of Europe, B10 Bern*. Bundesanstalt für Geowissenschaften und Rohstoffe/UNESCO. Hannover.

Vogt R, Oberprieler C. 1996. *Castrilanthemum* Vogt & Oberprieler, a new genus of the Compositae-Anthemideae. – *Anales del Jardín Botánico de Madrid* 54: 336-346.

Vrba ES. 1984. Evolutionary pattern and process in the sister-group Alcelaphini-Aepycerotini (Mammalia: Bovidae), pp. 62-79. In: Stanley SM, Eldredge N (Eds.). *Living Fossils.* Springer-Verlag. Berlin.

Wagner A, Blackstone N, Cartwright P, Dick M, Misof, B, Snow P, Wagner GP, Bartels J, Murtha M, Pendleton J. 1994. Surveys of gene families using polymerase chain reaction: PCR selection and PCR drift. – *Systematic Biology* 43: 250-261.

Wagner F. 2013. Molekulargenetische Untersuchungen zur homoploiden und polyploiden hybridisierung in der Gattung *Leucanthemum* Mill. (Compositae, Anthemideae). Unpublished thesis. Universität Regensburg. Regensburg.

Wang W. 2004. On the origin and development of *Artemisia* (Asteraceaea) in the geological past. – *Botanical Journal of the Linnean Society* 145: 331-336.

Warren DL, Glor RE, Turelli M. 2010. ENMTools: a toolbox for comparative studies of environmental niche models. – *Ecography* 33: 607-611.

Weisrock DW, Smith SD, Chan LM, Biebouw K, Kappeler PM, Yoder AD. 2012. Concatenation and concordance in the reconstruction of mouse lemur phylogeny: An empirical demonstration of the effect of allele sampling in phylogenetics. – *Molecular Biology and Evolution* 29: 1615-1630.

White TJ, Bruns T, Lee S, Taylor J. 1990. Amplification and direct sequencing of fungal ribosomal RNA genes for phylogenetics. In: Innis M, Gelfund D, Sninsky J, White T (Eds.). *PCR protocols: A guide to methods and application.* Academic Press. New York,.

Wilson RCL, Drury SA, Chapman JL. 2000. *The Great Ice-Age.* Open University. London.

Winkler M, Tribsch A, Paun O, Englisch T, IntraBioDiv-Consortium, Schönswetter P. 2010. Pleistocene distribution range shifts were accompanied by breeding system divergence within *Hornungia alpina* (Brassicaceae) in the Alps. – *Molecular Phylogenetics and Evolution* 54: 571-582.

Wood TE, Takebayashi N, Barker MS, Mayrose I, Greenspoon PB, Rieseberg LH. 2009. The frequency of polyploid speciation in vascular plants. –*Proceedings of the National Academy of Sciences, USA* 106: 13875-13879.

Wright JJ, David SR, Near TJ. 2012. Gene trees, species trees, and morphology converge on a similar phylogeny of living gars (Actinopterygii: Holostei: Lepidosteidae), an ancient clade of ray-finned dishes. – *Molecular Phylogenetics and Evolution* 63: 848-856.

Wu Y. 2012. Coalescent-based species tree inference from gene tree topologies under incomplete lineage sorting by maximum likelihood – *Evolution* 66: 763-775.

Xie W, Lewis PO, Fan Y, Kou L, Chen M. 2011. Improving marginal likelihood estimation for Bayesian phylogenetic model selection. – *Systematic Biology* 60:150-160.

Young N, Healy J. 2003. GapCoder automates the use of indel characters in phylogenetic analysis. – *BMC Bioinformatics* 4: 6. doi:10.1186/1471-2105-4-6.

Yu Y, Degnan JH, Nakhleh L. 2012. The probability of a gene tree topology within a phylogenetic network with applications to hybridization detection. – *PLoS Genetic* 8: e1002660. doi:10.1371/journal.pgen.1002660.

Yu Y, Barnett RM, Nakhleh L. 2013a Parsimonious inference of hybridization in the presence of incomplete lineage sorting – *Systematic Biology* 62: 738-751.

Yu Y, Ristic N, Nakhleh L. 2013b. Fast algorithms for reconciliation under hybridization and incomplete lineage sorting. – *BMC Bioinformatics* 14: S6. doi:10.1186/1471-2105-14-S15-S6.

Zhivotovsky LA. 1999. Estimating population structure in diploids with multilocus dominant DNA markers. – *Molecular Ecology* 8: 907-913.

Acknowledgements

First of all, I would like to thank my supervisor Prof. Dr. Christoph Oberprieler for the time dedicated to me and to the present work, for the availability helping at any time and the willingness to answer questions. Hardly I can imagine a better supervisor!

I am also very grateful to the two mentors of my PhD study, Prof. Dr. Peter Schönswetter and PD Dr. Christoph Schubart. It is a great pleasure for me to have you also as examiners.

I wish to express sincere gratitude to the scientists with whom I spent some time while carrying out part of my PhD project in Spain, and with whom I had the pleasure to collaborate. Thanks to Dr. Inés Álvarez and Dr. Pablo Vargas, always helpful.

Many thanks as well to the people who provided me technical help. Thanks to Peter Hummel, technician of the molecular laboratory of Prof. Dr. Christoph Oberprieler at the University of Regensburg. Thanks to Petra Schitko and Güntern Kolb, from the Plant Ecology group at the University of Regensburg, who never denied helping me when I needed. The technical help of Emilio Cano Cabezas and of Charo Noya Santos, respectively in the molecular laboratory and in the herbarium of the "Real Jardin Botanico" is greatfully acknowledged.

Thanks to the people with whom I shared experiences and time during these years. Thanks to my colleagues Dr. Rosa Maria Lo Presti, Dr. Sven Himmelreich, Dr. Jörg Meister, Dr. Roland Greiner, Dr. Kamil Konowalik, Manuela Bog, Dr. Martina Talianova, Alicia Agudo and David Gutierrez Larruscain. Thanks as well to all the colleagues of the department of Botany at the University of Regensburg.

Thanks to the people who stood me during excursions! Particular thanks to (again) Dr. Sven Himmelreich, Francesco Guzzo, Dr. Andreas Hilpold, my wife Yu-Mi, Dr. Andrea Sanchez Meseguer, and to all those who provided logistic help: my brother Daniele, Veronika Tomasello Staronova and the whole family Staron; Stefano Bertolotti; Marianna Daddona; Helena Esteban. Thanks to all the strangers who in the difficult moments during excursions promptly helped me… thanks to the "taller mecanico Hermanos Torres" in Ronda; to the café close to the church square in Torre de Moncorvo; and to many others…

I would like to thank Dr. Paula Perez Rubio for the help solving computational problems and thanks to the whole Italian-Hispanic clique at the University of Regensburg for sharing lunch times and more.

Finally, many thanks to my family and to my wife Yu-Mi!

Appendices

Appendix 1: Models selected for the Bayesian analyses in Chapter 2

(a) for cpDNA markers: a transversion model with gamma distribution of substitution rates (TVM + Γ), with freqA = 0.3228, freqC = 0.1072, freqG = 0.1362, freqT = 0.4338, gamma distribution shape parameter α = 0.9142, R[A-C] = 2.2072, R[A-G] = R[C-T] = 1.3164, R[A-T] = 0.5020, R[C-G] = 1.4451, R[G-T] = 1.0000 for *psbA-trnH*, and with freqA = 0.3278, freqC = 0.1623, freqG = 0.1708, freqT = 0.3391, α = 0.8179, R[A-C] = 1.2005, R[A-G] = R[C-T] = 1.1624, R[A-T] = 0.2365, R[C-G] = 0.9246, R[G-T] = 1.0000) for *trnC-petN*; (b) for nrDNA ITS: a symmetrical model (Zharkikh 1994) with gamma (SYM + Γ) with equal base frequencies, α = 0.6384, R[A-C] = 0.6906, R[A-G] = 2.2022, R[A-T] = 1.2016, R[C-G] = 0.1432, R[C-T] = 4.5349, R[G-T] = 1.0000); (c): a Hasegawa-Kishino-Yano model (Hasegawa et al. 1985) for *C16* with gamma (HKY + Γ), freqA = 0.2645, freqC = 0.1685, freqG = 0.1975, freqT = 0.3695, α = 4.0900, Ti/Tv ratio = 1.3002; (d) for *D35*: a Kimura 3-parameter model (Kimura 1981) with unequal base frequencies and invariant sites (K81uf + I), freqA = 0.3156, freqC = 0.1576, freqG = 0.1810, freqT = 0.3458, I = 0.3574, R[A-C] = R[G-T] = 1.0000, R[A-G] = R[C-T] = 3.7684, R[A-T] = R[C-G] = 1.4265)

References:

Zharkikh A. 1994. Estimation of evolutionary distances between nucleotide sequences. – *Journal of Moleuclar Evolution* 39: 315-329.

Hasegawa M, Kishini H, Yano T. 1985. Dating of the human-ape splitting by a molecular clock of mitochondrial DNA. – *Journal of Molecular Evolution* 22: 160-174.

Kimura M. 1981. Estimation of evolutionary distances between homologous nucleotide sequences. – *Proceedings of the National Academy of Sciences, USA* 78: 454-458.

Appendix 2: age estimation for the tribe Anthemideae

To determine the age of the tribe Anthemideae, or more specifically the split between the genera *Ursinia* and *Artemisia* (calibration point used afterwards in the *BEAST analyses for the reconstruction of the accession tree and the estimation of the age of *Castrilanthemum*), we used the 34 OTU *ndhF* alignment used by Oberpieler (2005), with the addition of sequence data for *Artemisia absintium* L. taken from the GeneBank (see the Table A1 for a complete list of the accessions included and relatives accession numbers).

After applying a likelihood ratio (LR) test with the result that the sequences did not evolve in a clock-like manner ($p < 0.0001$), we used the uncorrelated log normal relaxed clock (Drummond et al. 2006) to estimate the age of the tribe Anthemideae. The BEAST.xml input file was produced using BEAUti v1.7.2 (Drummond et al. 2012). Monophyly was enforced for the subset of accessions from all the tribes of the Compositae, excluding those belonging to the tribe Barnadesieae, the most basal tribe of the family. Concerning the nucleotide substitution model, and since we were dealing with a coding gene, we performed analyses using two partition into codon positions (1+2), 3, three partitions (1, 2, 3), and using the nucleotide substitution model chosen by ModelTest, but allowing the parameters to vary normally around a mean value corresponding to the one given by the program, as done for the phylogeny (see materials and methods session).

Two independent analyses were run with BEAST v1.7.2 (Drummond et al. 2012) for 10,000,000 generations sampling every 1,000th generation, for each of the three approaches. All the analyses were run using a personal computer at Regensburg University. To check convergence and determine burn-in values, as well as for checking incongruence between the three different nucleotide substitution models used, the *BEAST runs were analysed in Tracer v1.5 (Rambaut & Drummond 2007). The two independent analyses done for each of the three different approaches were therefore merged using LogCombiner v1.7.2 (Drummond et al. 2012) applying a burn-in period equal to the 10% of the total amount of trees. Finally, a maximum-clade-credibility tree was constructed with TreeAnnotator v1.7.2 (Drummod et al. 2012), using a posterior probability limit set of 0.5.

Four calibration points were used in order to obtain absolute divergence times: The root age for the analysis was calibrated using the newly described “oldest” fossil of Compositae found by Barreda et al. (2012) in North-Western Patagonia, arguing for the divergence age between Mutisioideae and Carduoideae on the one side and Barnadesioideae on the other to be placed in the early Eocene (at least 47.5 Ma). We set therefore a log normally distributed

prior (offset = 47.5 Ma, SD = 1) for the root age, i.e the most recent common ancestor (MRCA) between the accessions belonging to Barnadesieae and the rest of the family.

The oldest fossil of *Ambrosia*-type pollen, for which an age estimate was given by Graham (1996) to lie around 22-35 Ma, was used to calibrate the node connecting Heliantheae s.l. [here represented by *Eupatorium atrorubens* Nicholson (Eupatorieae) and *Madia elegans* D.Don (Madieae)] and Tageteae (represented by *Tagetes erecta* L.). A normally distributed prior (mean = 30 Ma, SD = 3) was therefore chosen for the MRCA of the subset of accessions including *Eupatorium*, *Madia,* and *Tagetes*.

A third calibration point was the crown age of the tribe Cichorieae. Tremetsberger et al. (2012) indicated the Oligocene as an age for the origin of the subtribe, with the 95 % HPD intervals of the crown node of Cichorieae ranging between 26.9 and 38.3 Ma in an unconstrained analysis, and between 24 and 31.2 in a constrained one. We used a normally distributed prior (Mean = 31.0 Ma, SD = 3.1) for the crown age of Cichorieae, i.e. the MRCA of the members of Cichoreae included in the study (*Cichorium* and *Tragopogon*) and members of its sister tribes Liabeae (*Liabum*), Arctotideae (*Arctotis*), and Vernonieae (*Vernonia* and *Stokesia*).

Finally the oldest fossil record of *Artemisia*-type pollen was used to calibrate the node connecting *Artemisia* (as a representative of the subtribe of *Anthemideae* exhibiting the *Artemisia*-type pollen) and the closest genus included in the analysis that does not exhibit the *Artemisia*-type pollen (i.e. *Chrysanthemum*). The prior was therefore log normally distributed (offset = 23.03 Ma, SD = 1) because the earliest records of *Artemisia* type pollen fossils are from the Lower and Upper Oligogene in the provinces of Xinjiang and Qinghai, in North-Eastern China (Wang 2004). Detailed results are shown in Table A2.

Table A2: Prior and posterior distribution of age estimates for the calibration points of the *BEAST analyses of Compositae and the resulting estimate for the age of the tribe Compositae-Anthemideae.

	Prior distribution	Posterior distribution		
		ModelTest values	2 partitions into codon positions	3 partitions into codon positions
Root (Compositae)	LogN: 48.5 (47.59-52.58)	54.77(47.53-77.73)	54.95(47.55-77.75)	54.56(47.52-70.70)
Cichorinae	N: 31 (25.9-36.1)	33.25(27.34-39.03)	33.18(27.37-38.96)	33.28(27.4-38.87)
Ambrosia fossil (Heliantheae s.l.)	N: 30 (25.07-34.93)	25.59(20.1-31.17)	25.59(20.11-31.02)	25.46(20.06-31.19)
Artemisia fossil	LogN: 24.03 (23.22-28.21)	23.62(23.06-25.1)	23.62(23.06-25.12)	23.61(23.06-25.07)
Anthemideae	-	**32.92(27.53-41.43)**	**33.07(27.47-41.91)**	**32.98(27.43-41.91)**

Table A1: List of the accessions (with EMBL/GenBank accession numbers) used in the present study for estimating the age of the tribe Compositae-Anthemidae based on the *ndhF* alignment used by Oberpieler (2005).

Tribe	Taxon	EMBL *nadhF*
Asteroideae		
Anthemideae	*Achillea millefolium* L.	L39442
	Chrysanthemum × *grandiflorum* (Ramat.) Kitam.	L39443
	Santolina chamaecyparissus L.	L39444
	Artemia absintium L.	EU334460
	Ursinia nana DC.	L39441
Anthroismeae	*Blepharispermum zanguebaricum* Oliver & Hiern	L39456
Astereae	*Aster cordifolius* L.	L39449
	Bellis perennis L.	L39446
	Baccharis neglecta Britton	L39448
Calenduleae	*Calendula officinalis* L.	L39439
Gnaphalieae	*Antennaria neodioica* Greene	L39436
Inuleae	*Asteriscus sericeus* Vent.	L39454
	Inula sericea Beck	L39453
	Pluchea sericea Nutt.	L39452
Senecioneae	*Senecio mikanioides* Walp.	L39435
	Syneilesis palmata Maxim.	L39432
Heliantheae alliance		
Coreopsideae	*Fitchia* sp.	L39459
Eupatorieae	*Eupatorium atrorubens* Nicholson	L39376
Madieae	*Madia elegans* D.Don	L39374
Hellenieae	*Psilostrophe gnaphalodes* DC.	L39457
Tageteae	*Tagetes erecta* L.	L39466
Cichorioideae		
Arctotideae	*Arctotis stoechoedifolia* P.J. Bergius	L39425
Cichorieae	*Cichorium intybus* L.	L39390
Liabeae	*Liabum glabrum* Hemsl.	L39421
Vernonieae	*Stokesia laevis* Greene	L39430
	Vernonia mespilifolia Less.	L39427
Carduoideae		
Cardueae	*Centaurea americana* Nutt.	L39416
	Echinops exaltatus Schrad.	L39411
	Tragopogon porrifolius L.	L39391
Mutisioideae		
Barnadesieae	*Barnadesia caryophylla* S.F.Blake	L39394
	Schlechtendalia luzulaefolia Less.	L39395
Gochnatieae	*Gochnatia* sp.	L39397
Mutisieae	*Adenocaulon himalacium* Edgew.	L39401
Nassauvieae	*Trixis californicum* Kellogg	L39406
Stifftieae	*Stifftia chrysantha* Mikan.	L39399

References:

Barreda VD, Palazzesi L, Tellería MC, Katinas L, Crisci JV, Bremer K, Passalia MG, Corsolini R, Rodríguez Brizuela R, Bechis F. 2010. Eocene Patagonia fossils of the daisy family. – *Science*. 329: 1621.

Drummond AJ, Ho SYW, Phillips MJ, Rambaut A. 2006. Relaxed phylogenetics and dating with confidence. – *PLoS Biology* 4: e88. doi:10.1371/journal.pbio.0040088.

Drummond AJ, Suchard MA, Xie D, Rambaut A. 2012. Bayesian phylogenetics with BEAUti and the BEAST 1.7. – *Molecular Biology and Evolution* 29: 1969-1973.

Gernhard T. 2008. The conditioned reconstruction processes. – *Journal of Theoretical Biology* 253: 769-778.

Graham A. 1996. A contribution to the geologic history of the Compositae. In: Hind DJN, Beentje HJ (Eds.). *Proceedings of the International Compositae Conference Kew, 1994,* vol. 1. – Royal Botanic Gardens Kew, London.

Oberprieler C. 2005. Temporal and spatial diversification of Circum-Mediterranean Compositae-Anthemideae. – *Taxon* 54: 951-966.

Rambaut A, Drummond AJ. 2007. Tracer v1.4: MCMC trace analyses tool. Available at: http://beast.bio.ed.ac.uk/Tracer.

Tremetsberger K, Gemeinholzer B, Zetzsche H, Blackmore S, Kilian N, Talavera S. 2012. Divergence time estimation in *Cichorieae* (Asteraceae) using a fossil-calibrated relaxed molecular clock. – *Organisms, Diversity & Evolution* 13: 1-13.

Wang WM. 2004. On the origin and development of *Artemisia* (Asteraceae) in the geological past. – *Botanical Journal of Linnaean Society* 145: 331-336.

Appendix 3: gene trees obtaibned from the Bayesian analyses in Chapter 3

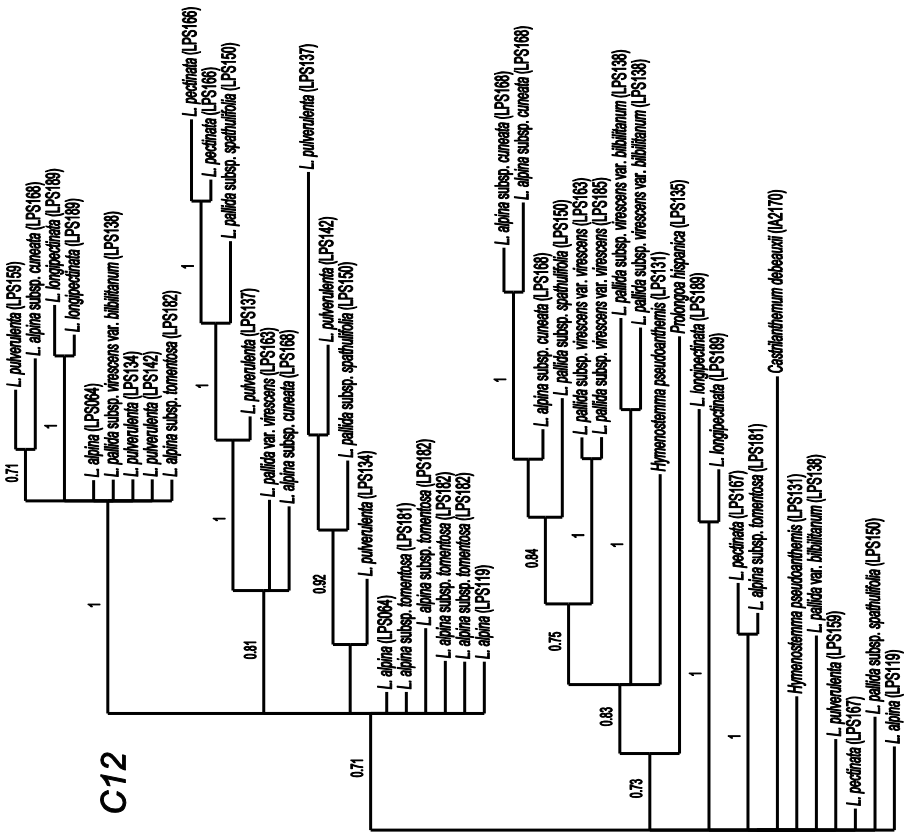
C12
L. pulverulenta (LPS159)
L. alpina subsp. cuneata (LPS168)
L. longipectinata (LPS189)
L. longipectinata (LPS189)
L. alpina (LPS064)
L. pallida subsp. virescens var. bilbilitanum (LPS138)
L. pulverulenta (LPS134)
L. pulverulenta (LPS142)
L. alpina subsp. tomentosa (LPS182)
L. pectinata (LPS166)
L. pectinata (LPS166)
L. pallida subsp. spathulifolia (LPS150)
L. pulverulenta (LPS137)
L. pallida var. virescens (LPS163)
L. alpina subsp. cuneata (LPS168)
L. pulverulenta (LPS137)
L. pulverulenta (LPS142)
L. pallida subsp. spathulifolia (LPS150)
L. pulverulenta (LPS134)
L. alpina (LPS064)
L. alpina subsp. tomentosa (LPS181)
L. alpina subsp. tomentosa (LPS182)
L. alpina subsp. tomentosa (LPS182)
L. alpina (LPS119)
L. alpina subsp. cuneata (LPS168)
L. alpina subsp. cuneata (LPS168)
L. alpina subsp. cuneata (LPS166)
L. pallida subsp. spathulifolia (LPS150)
L. pallida subsp. virescens var. virescens (LPS163)
L. pallida subsp. virescens var. virescens (LPS185)
L. pallida subsp. virescens var. bilbilitanum (LPS138)
L. pallida subsp. virescens var. bilbilitanum (LPS138)
Hymenostemma pseudoanthemis (LPS131)
Prolongoa hispanica (LPS135)
L. longipectinata (LPS189)
L. longipectinata (LPS189)
L. pectinata (LPS167)
L. alpina subsp. tomentosa (LPS181)
Castrilanthemum debeauxii (IA2170)
Hymenostemma pseudoanthemis (LPS131)
L. pallida var. bilbilitanum (LPS138)
L. pulverulenta (LPS159)
L. pectinata (LPS167)
L. pallida subsp. spathulifolia (LPS150)
L. alpina (LPS119)

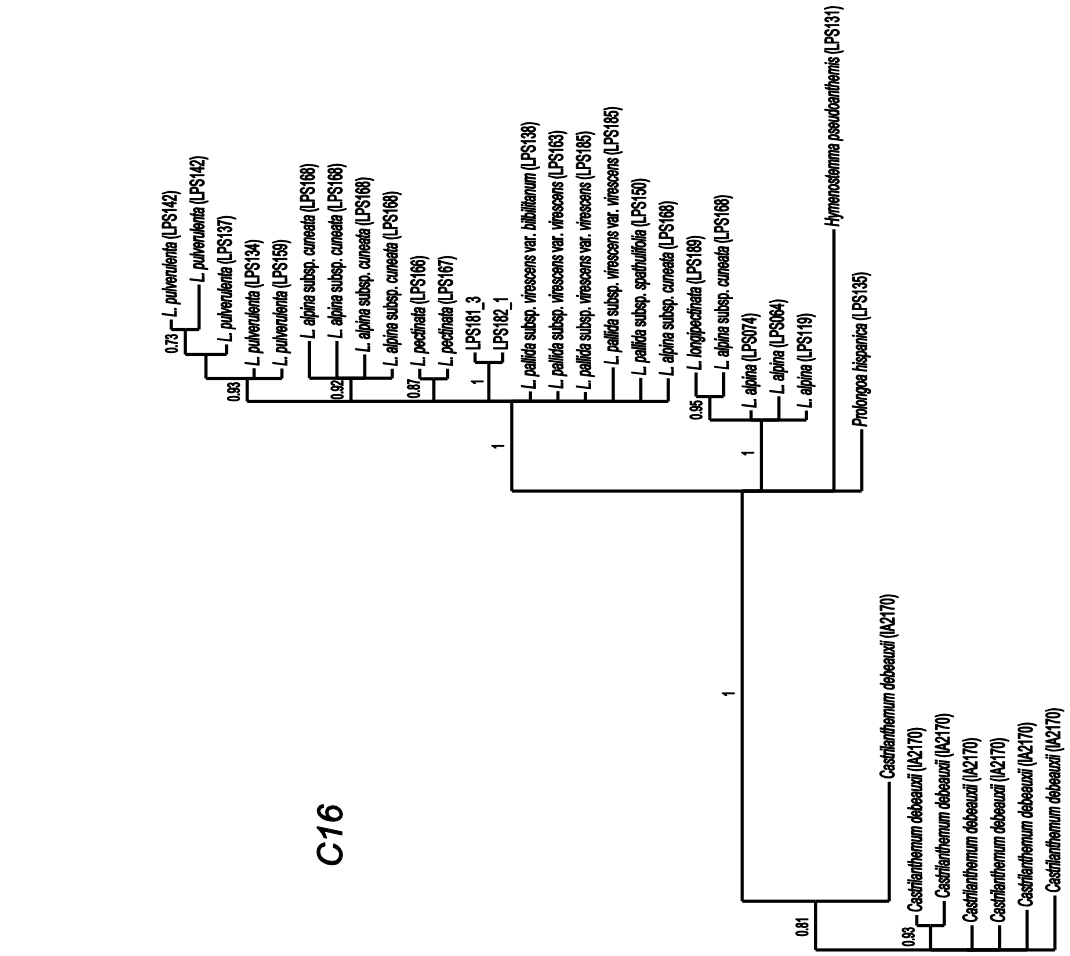
C16
L. pulverulenta (LPS142)
L. pulverulenta (LPS142)
L. pulverulenta (LPS137)
L. pulverulenta (LPS134)
L. pulverulenta (LPS159)
L. alpina subsp. cuneata (LPS168)
L. alpina subsp. cuneata (LPS168)
L. alpina subsp. cuneata (LPS168)
L. alpina subsp. cuneata (LPS168)
L. pectinata (LPS166)
L. pectinata (LPS167)
LPS181_3
LPS182_1
L. pallida subsp. virescens var. bilbilitanum (LPS138)
L. pallida subsp. virescens var. virescens (LPS163)
L. pallida subsp. virescens var. virescens (LPS185)
L. pallida subsp. virescens var. virescens (LPS185)
L. pallida subsp. spathulifolia (LPS150)
L. alpina subsp. cuneata (LPS168)
L. longipectinata (LPS189)
L. alpina subsp. cuneata (LPS168)
L. alpina (LPS074)
L. alpina (LPS064)
L. alpina (LPS119)
Hymenostemma pseudoanthemis (LPS131)
Prolongoa hispanica (LPS135)
Castrilanthemum debeauxii (IA2170)
Castrilanthemum debeauxii (IA2170)
Castrilanthemum debeauxii (IA2170)
Castrilanthemum debeauxii (IA2170)
Castrilanthemum debeauxii (IA2170)
Castrilanthemum debeauxii (IA2170)

cpDNA

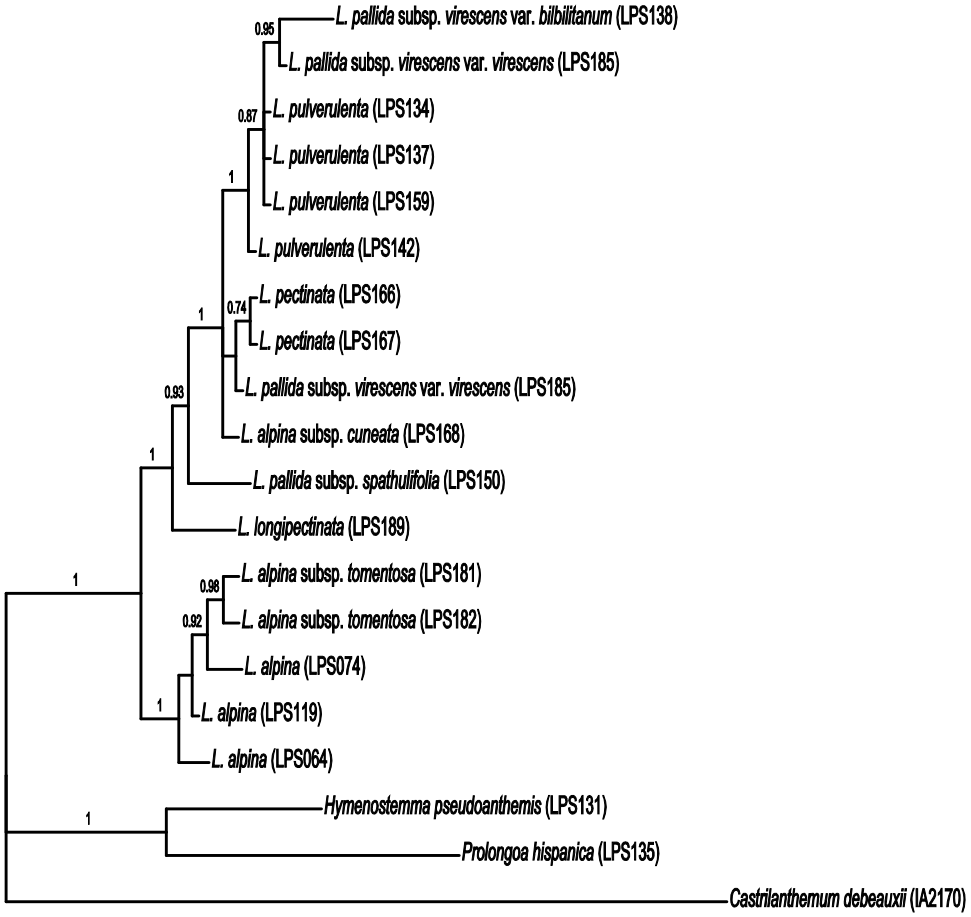
L. pallida subsp. virescens var. bilbilitanum (LPS138)
L. pallida subsp. virescens var. virescens (LPS185)
L. pulverulenta (LPS134)
L. pulverulenta (LPS137)
L. pulverulenta (LPS159)
L. pulverulenta (LPS142)
L. pectinata (LPS166)
L. pectinata (LPS167)
L. pallida subsp. virescens var. virescens (LPS185)
L. alpina subsp. cuneata (LPS168)
L. pallida subsp. spathulifolia (LPS150)
L. longipectinata (LPS189)
L. alpina subsp. tomentosa (LPS181)
L. alpina subsp. tomentosa (LPS182)
L. alpina (LPS074)
L. alpina (LPS119)
L. alpina (LPS064)
Hymenostemma pseudoanthemis (LPS131)
Prolongoa hispanica (LPS135)
Castrilanthemum debeauxii (IA2170)
0.95
0.87
1
1
0.74
0.93
1
1
0.98
0.92
1
1

Appendix 4: localities used for the niche reconstruction analysis

List of presence data used in the niche reconstraction analyses in Chapter 4. Taxa abbreviations are for: **Lalp** = *Leucanthemopsis alpina*; **Lcun** = *L. alpina* subsp. *cuneata*; **Lppa** = *L. pallida* var. *pallida*; **Lpal** = *L. pallida* var. *alpina*; **Lbil** = *L. pallida* subsp. *virescens* var. *bilbilitanum*; **Lvir** = *L. pallida* subsp. *virescens* var. *virescens*; **Lpec** = *L. pectinata*; **Lpul** = *L. pulverulenta*; **LflN** = *L. flaveola* (northern part of the distribution range); **LflS** = *L. flaveola* (southern part of the range). Herbaria abbreviation are for: **B** = herbarium of the Botanical Museum in Berlin-Dahlem; herbarium **MA** = Herbarium of the "Real Jardín Botánico" Madrid; **M** = "Botanische Staatssammlung", Munich; **ST** = personal herbarium of Salvatore Tomasello; **CHO** = personal herbarium of Prof. Dr. Christoph Oberprieler.

Cod.	Longitude	Latitude	Herbar.	Voucher n.	State	Collection Place	Date
Lalp	1.569166667	42.46777778	MA	MA720398	AND	Arroyo de Claror	30/09/2004
Lalp	1.361111111	42.61694444	MA	MA791333	E	Pallars Sobirà	12/09/2009
Lalp	-0.43444444	42.73777778	MA	MA715464	E	Sallent De Gallego	27/06/1999
Lalp	2.270555556	42.43222222	MA	MA778187	E	Portella de Mentet	25/08/2008
Lalp	6.41	45.06305556	MA	MA823273	F	Col du Galibert	20/08/2010
Lalp	1.721111111	42.52861111	MA	MA514084	AND	Puerto del Envalira. Coll Blanc	03/07/1992
Lalp	2.1375	42.36777778	MA	MA458920	E	Collado de Fontalba	10/07/1988
Lalp	-0.59166667	42.77805556	MA	MA488438	E	Aisa	11/09/1990
Lalp	-0.57833333	42.76944444	MA	MA491044	E	Nevero del Aspe	08/08/1975
Lalp	0.634444444	42.61694444	MA	MA569787	E	Aneto	28/08/1990
Lalp	0.818055556	42.59361111	MA	MA618565	E	Collado de Avellaners	29/07/1998
Lalp	1.561944444	42.64972222	MA	MA700299	AND	Port de Siguer	30/08/2002
Lalp	1.420277778	42.54222222	MA	MA705218	AND	Port de Cabus	04/08/2003
Lalp	1.72	42.5575	MA	MA706036	AND	Pic de la Maia	06/08/2003
Lalp	1.420277778	42.54222222	MA	MA707987	AND	Port de Cabus	04/08/2003
Lalp	10.03222222	46.40361111	MA	MA493861	CH	Passo Bernina	18/07/1990
Lalp	20.07583333	49.17222222	B	9341	SK	Zabie Plesa	06/08/1968
Lalp	13.04222222	47.08888889	B		A	Kolm Saigun	18/07/1994
Lalp	13.17138889	47.10222222	B		A	Hüttenkogel	11/07/1988
Lalp	8.033888889	46.25	B		CH	Simplon	
Lalp	10.01555556	46.42972222	B		CH	Piz Lagalb	09/08/1971
Lalp	7.843333333	45.84944444	B		I	Gressoney	26/09/1983
Lalp	11.32166667	46.83916667	B	no.295	I	Jaufenpass	22/06/1957
Lalp	10.72722222	46.2225	B		I	Rifugio Cornisello	14/09/2003
Lalp	6.409722222	45.065	B		F	Col du Galibert	13/07/1970
Lalp	7.149166667	44.20305556	M	Nr. 19821	I	Colle Lombarda	25/08/1964
Lalp	6.954444444	44.66055556	M	Nr. 26382	F	St. Veran	13/08/1979
Lalp	7.978888889	46.07611111	M	Nr. 00-1473	CH	Saal-Almagell	19/07/2000
Lalp	12.09361111	47.11805556	M		A	Zillertal. Plauaner Hutte	15/08/1978
Lalp	11.64333333	47.09472222	M	Nr.34567	A	Tuxer Joch	23/08/1980
Lalp	20.194625	49.19115833	ST	TS1	SK	Visokè Tatry	03/07/2010

Cod.	Longitude	Latitude	Herbar.	Voucher n.	State	Collection Place	Date
Lalp	6.8705	44.98566667	ST	TS11	I	Sestriere	09/07/2010
Lalp	6.978633333	44.68485	ST	TS24	I-F	Colle dell'Agnello	10/07/2010
Lalp	7.360916667	44.11661667	ST	TS26	F	Col De Fenestre	13/07/2010
Lalp	7.150555556	44.2025	ST	TS28	I-F	Col du Lombard	13/07/2010
Lalp	7.191944444	44.19111111	ST	TS30	F	Baisse de Druos	14/07/2010
Lalp	6.807	44.32033333	ST	TS32	F	Col de la Bonette	14/07/2010
Lalp	6.729116667	44.24168333	ST	TS34	F	Pas du Lausson	15/07/2010
Lalp	6.5873	44.3072	ST	TS36	F	Col D'Allos	15/07/2010
Lalp	6.900869444	44.35853889	ST	TS38	I	Tre Vescovi	17/07/2010
Lalp	6.410052778	44.93297778	ST	TS40	F	Glacier Blanc	18/07/2010
Lalp	6.41095	45.06076667	ST	TS42	F	Col du Galibert	18/07/2010
Lalp	5.90565	45.12625	ST	TS43	F	Les Amoreux	20/07/2010
Lalp	6.8829	45.20275	ST	TS45	F	Lac Perrin Superieur	21/07/2010
Lalp	7.031366667	45.41873333	ST	TS47	F	Col de L'Iseran	21/07/2010
Lalp	6.883283333	45.67938333	ST	TS49	F	Piccolo San Bernardo	21/07/2010
Lalp	6.6163	45.38871667	ST	TS51	F	Courchevel	22/07/2010
Lalp	6.885277778	45.90055556	ST	TS53	F	Plan de l'Aiguille	23/07/2010
Lalp	7.451333333	45.59975	ST	TS55	I	Ponton	24/07/2010
Lalp	7.489433333	45.90858333	ST	TS57	I	Bionaz	25/07/2010
Lalp	7.171111111	45.86888889	ST	TS59	I	Gran San Bernardo	25/07/2010
Lalp	7.8457	45.85636667	ST	TS61	I	Staffal	25/07/2010
Lalp	9.170555556	46.49583333	ST	TS63	CH	San Bernardino	26/07/2010
Lalp	7.49455	45.9993	ST	TS67	CH	Arolla	04/08/2010
Lalp	7.483666667	46.21233333	ST	TS69	CH	Alpege …	05/08/2010
Lalp	7.705116667	45.99003333	ST	TS70	CH	Schwarzsee	06/08/2010
Lalp	7.752216667	45.98901667	ST	TS72	CH	Riffelberg	06/08/2010
Lalp	7.771816667	45.98488333	ST	TS74	CH	Gornergrat	06/08/2010
Lalp	7.9444	46.03693333	ST	TS76	CH	Saas Almagell	07/08/2010
Lalp	8.015966667	46.25168333	ST	TS78	CH	Simplonpass	07/08/2010
Lalp	8.3875	46.47694444	ST	TS80	CH	Passo della Novena	08/08/2010
Lalp	8.415277778	46.5725	ST	TS82	CH	Furkapass	08/08/2010
Lalp	8.345555556	46.56194444	ST	TS84	CH	Grimselpass	08/08/2010
Lalp	7.97	46.57805556	ST	TS86	CH	Kleine Scheidegg	09/08/2010
Lalp	8.449444444	46.73027778	ST	TS94	CH	Sustenpass	10/08/2010
Lalp	9.725833333	46.47027778	ST	TS96	CH	Julierpass	12/08/2010
Lalp	10.02527778	46.41055556	ST	TS98	CH	Passo Bernina	12/08/2010
Lalp	9.572966667	46.02658333	ST	Ts100	I	Gerola Alta	13/08/2010
Lalp	10.44722222	46.5325	ST	TS102	I	Passo dello Stelvio	13/08/2010
Lalp	10.68448333	46.47966667	ST	TS104	I	Val Martello	14/08/2010
Lalp	10.3677	45.84321667	ST	TS107	I	Monte Colombine	17/08/2010
Lalp	11.44868333	46.17008333	ST	TS109	I	Passo Maghen	17/08/2010
Lalp	11.78398333	46.28211667	ST	TS111	I	Passo Rolle	18/08/2010
Lalp	11.4615	46.61458333	ST	TS113	I	Rittner Horn	19/08/2010
Lalp	12.19905	46.8876	ST	TS115	I-A	Passo Stalle	20/08/2010
Lalp	11.65845	46.9916	ST	TS117	I-A	Passo di Vizze	20/08/2010
Lalp	11.09638889	46.905	ST	TS119	I-A	Passo di Rombo	21/08/2010
Lalp	10.77756667	46.7673	ST	TS121	I-A	Maso Corto	21/08/2010
Lalp	9.948333333	46.74916667	ST	TS123	CH	Flüelapass	21/08/2010
Lalp	9.620933333	46.76808333	ST	TS125	CH	Arosa	22/08/2010
Lalp	9.265333333	46.87905	ST	TS127	CH	Flims	23/08/2010
Lalp	10.21611111	47.34861111	ST	TS129	D	Fellhorn	24/08/2010

Cod.	Longitude	Latitude	Herbar.	Voucher n.	State	Collection Place	Date
Lalp	9.973166667	47.06751667	ST	TS131	A	Sannigrat	25/08/2010
Lalp	10.09008333	46.91828333	ST	TS133	A	Bielerhöhe	25/08/2010
Lalp	11.03088333	47.2136	ST	TS135	A	Küthai	25/08/2010
Lalp	11.45801667	47.21195	ST	TS137	A	Patscherkofel	26/08/2010
Lalp	12.28361111	47.28083333	ST	TS148	A	Wildkogel	28/08/2010
Lalp	12.38361111	46.7125	ST	TS150	I	Sesto	28/08/2010
Lalp	12.88008333	46.61653333	ST	TS151	A	Rauchkofel	29/08/2010
Lalp	12.84027778	47.08555556	ST	TS157	A	Großglockner	22/09/2010
Lalp	13.09555556	47.10555556	ST	TS159	A	Bad Gastein	23/09/2010
Lalp	13.57138889	47.27	ST	TS161	A	Radstädter Tauerpass	23/09/2010
Lalp	13.57138889	47.27	ST	TS161	A	Radstädter Tauernpass	23/09/2010
Lalp	13.85638889	46.91555556	ST	TS163	A	Kornhock	24/09/2010
Lalp	14.07944444	47.27138889	ST	TS165	A	Sölkpass	24/09/2010
Lalp	14.41388889	47.44	ST	TS167	A	Bösenstein	24/09/2010
Lalp	11.11984444	47.414375	ST	TS169	D	Frauenalp	02/10/2010
Lalp	11.11984444	47.414375	ST	TS169	D	Frauenalp	03/10/2010
Lalp	11.11984444	47.414375	ST	TS169	D	Frauenalp	04/10/2010
Lalp	11.11984444	47.414375	ST	TS169	D	Frauenalp	05/10/2010
Lalp	11.11984444	47.414375	ST	TS169	D	Frauenalp	06/10/2010
Lalp	11.11984444	47.414375	ST	TS169	D	Frauenalp	07/10/2010
Lalp	11.11984444	47.414375	ST	TS169	D	Frauenalp	08/10/2010
Lalp	11.11984444	47.414375	ST	TS169	D	Frauenalp	09/10/2010
Lalp	11.11984444	47.414375	ST	TS169	D	Frauenalp	10/10/2010
Lalp	11.11984444	47.414375	ST	TS169	D	Frauenalp	11/10/2010
Lalp	-0.23611111	42.78891667	ST	TS381	E	Macizo de los Infiernos	27/07/2011
Lalp	-0.06355556	42.70458333	ST	TS388	F	Port de Boucharo	28/07/2011
Lalp	0.138138889	42.92777778	ST	TS389	F	Pic du Midi Bigole	28/07/2011
Lalp	0.453027778	42.63266667	ST	TS391	E	Posets	29/07/2011
Lalp	0.646666667	42.66861111	ST	TS398	E	La Maladeta	29/07/2011
Lalp	0.650222222	42.65777778	ST	TS399	E	La Maladeta	30/07/2011
Lalp	0.820805556	42.57280556	ST	TS400	E	Aigües Tortes	01/08/2011
Lalp	0.983527778	42.59758333	ST	TS401	E	Aigües Tortes	02/08/2011
Lalp	1.420555556	42.54122222	ST	TS402	AND	Port de Cabus	02/08/2011
Lalp	1.479722222	42.62861111	ST	TS404	AND	Port del Rat	03/08/2011
Lalp	1.721027778	42.54302778	ST	TS405	AND	Puerto de Envalira	03/08/2011
Lalp	2.119555556	42.38144444	ST	TS407	E	Puigmal	05/07/2011
Lalp	10.40679444	44.24944722	ST	TS415	I	Monte Prado	22/08/2011
Lalp	22.83844444	45.38844444	ST	M. Galbany 2261	RO	Mt. Retezat	11/07/2011
Lalp	20.13083333	49.15277778	MA	MA820848	SK	Batizovské Pleso	07/06/2010
Lalp	0.644444444	42.67111111	MA	MA200947	E	Subida a la Maladeta	23/07/1975
Lalp	0.455	42.63583333	MA	MA391216	E	Posets	21/07/1987
Lalp	0.0225	42.66861111	MA	MA413611	E	Goriy-Ibon Helado	30/08/1969
Lalp	2.176388889	42.42027778	MA	MA128823	E	Noufont	22/07/1914
Lalp	2.125833333	42.43611111	MA	MA210496	F	Val D'Eyne	26/07/1922
Lalp	2.120833333	42.45527778	M	M1097	F	Cambre D'Aze	25/07/1944
Lalp	24.72861111	45.60805556	M	M5825	RO	Munte Făgăra	August 1964
Lalp	10.38361111	47.39527778	B		D	Laufbacher Eck	15/09/1964
Lalp	19.98138889	49.23055556	B	2787	PL	Zakopane	16/06/1961
Lalp	10.80055556	46.76166667	B		I	Kurzras	01/08/1995
Lalp	10.06555556	46.88388889	B		A	Silvrettastausee	21/09/1986

Cod.	Longitude	Latitude	Herbar.	Voucher n.	State	Collection Place	Date
Lalp	7.913888889	46.14305556	B		CH	Bidermatten	03/08/1970
Lalp	7.780277778	45.89388889	B		I	Monte Bettolina	19/09/1981
Lalp	6.584722222	44.97333333	B		F	Briancon	11/07/1970
Lalp	0.975833333	42.73666667	B		E	Torrent de Barrongueta	31/08/1988
Lalp	11.89222222	46.46361111	M		I	Passo Padon	09/07/1976
Lalp	7.575277778	45.58833333	M	Nr. 19701	I	Pianprato	18/08/1964
Lalp	2.105833333	42.38027778	M	Nr. 26928	F	Puigmale	25/07/1971
Lalp	2.058611111	42.35777778	M	Nr. 26832	F	Col de Ceralps	23/07/1971
Lalp	1.997777778	42.65833333	M	Nr. 27000	F	Porteille d'Orlu	28/07/1971
Lalp	7.449444444	44.10444444	M	Nr. 26312	F	Lac Noir (Tende)	11/08/1970
Lalp	12.71083333	46.93611111	M		A	Hohe Tauern	22/09/1987
Lalp	12.28333333	46.97083333	M	No.309	A	St. Jakob in Defereggen	03/08/1964
Lalp	13.17694444	46.59472222	M	MTB: 9445/11	A	Hochwipfel	12/07/1994
Lalp	24.95833333	45.46083333	M		RO	Mont Papusa et Lespezi	29/06/1963
Lalp	11.10361111	46.75222222	B		I	Rötelspitze	26/09/1985
Lalp	11.26916667	46.73583333	CHO	R. Vogt 17078	I	Hirzer	06/10/2011
Lalp	19.91583333	49.23361111	M	M1960	PL-SK	Cerwonie Wierchy (Tatra)	06/07/1988
Lalp	20.14027778	49.16972222	M		SK	Velická Doliná (Tatra)	02/07/1994
Lalp	20.07833333	49.17305556	M	M494/6	SK	Froschensee-Zabie Plesá	18/07/1931
Lcun	-2.87805556	42.01194444	MA	MA776770	E	Pico de Urbión	15/07/1995
Lcun	-2.84805556	42	MA	MA345705	E	Laguna Nera	08/05/1965
Lcun	-2.87138889	42.01194444	MA	MA128839	E	Urbion	10/07/1935
Lcun	-2.87805556	42.01194444	MA	MA247413	E	Urbion	26/06/1972
Lcun	-2.87805556	42.01194444	M	M9600	E	Pico de Urbión	04/07/1964
Lcun	-2.87666667	42.01105556	ST	TS376	E	Urbión	23/07/2011
Lcun	-2.87138889	42.01194444	MA	MA345706	E	Urbion	01/07/1970
Lcun	-2.87138889	42.01194444	MA	MA128842	E	Urbion	
Lcun	-2.77972222	42.04583333	MA	MA464718	E	Loma de la Revillas	21/07/1976
Lcun	-2.77972222	42.04583333	M	M13685	E	Loma de la Revillas	21/07/1976
Llon	-4.27611111	34.84694444	MA	MA128801	MA	Tizzi Ifri	07/06/1927
Llon	-4.52222222	34.84055556	MA	MA128800	MA	Tidhiguine	06/06/1927
Llon	-4.71777778	34.9675	M	M22098	MA	Bab-Basen	06/04/1967
Llon	-4.51666667	34.86666667	CHO	Oberprieler4016	MA	Djehel Tidirhine	20/06/1992
Lpal	-3.8275	40.98611111	MA	MA743472	E	Pico El Nevero	17/07/1985
Lpal	-3.96972222	40.83416667	MA	MA743477	E	Dos Hermanas (La Granja)	01/07/1990
Lpal	-3.96027778	40.85388889	MA	MA743475	E	Peñalara	24/06/1987
Lpal	-3.96055556	40.83583333	MA	MA594220	E	Valcotos	20/07/1996
Lpal	-3.95638889	40.84944444	MA	MA147663	E	Peñalara	01/07/1924
Lpal	-5.71472222	40.30944444	MA	MA242652	E	Laguna del Trempal	27/10/1979
Lpal	-4.86694444	40.49222222	MA	MA242663	E	Pico del Zapatero	09/07/1978
Lpal	-3.95583333	40.85166667	MA	MA401981	E	Peñalara	07/07/1986
Lpal	-3.83166667	40.82805556	MA	MA440865	E	Puerto de la Morcuera	25/05/1976
Lpal	-5.72944444	40.29416667	MA	MA445801	E	Calvitero. Canderaio	18/07/1980
Lpal	-4.27805556	40.69777778	MA	MA694968	E	El Espinar	14/06/2001
Lpal	-5.74222222	40.30222222	MA	MA242651	E	Hoya Moro. Calderaio	20/07/1979
Lpal	-3.95805556	40.83944444	MA	MA708993	E	Laguna Grande del Peñalara	25/05/2003
Lpal	-3.95444444	40.84972222	MA	MA212525	E	Peñalara	01/08/1932
Lpal	-5.25777778	40.25944444	MA	MA406403	E	Paredes Negras (Gredos)	15/06/1985
Lpal	-5.24611111	40.26861111	MA	MA407298	E	Paredes Negras (Gredos)	15/06/1985
Lpal	-5.26916667	40.25	MA	MA442833	E	Morejón (Gredos)	27/07/1982

Cod.	Longitude	Latitude	Herbar.	Voucher n.	State	Collection Place	Date
Lpal	-5.26944444	40.25916667	MA	MA442849	E	Circo de Gredos	27/07/1982
Lpal	-3.95444444	40.84972222	MA	MA128742	E	Peñalara	06/07/1912
Lpal	-3.95583333	40.84972222	MA	MA128743	E	Peñalara	21/07/1898
Lpal	-5.59722222	40.2225	MA	MA442857	E	Laguna del Barco-Pico de la Cavacha	27/07/1982
Lpal	-4.86694444	40.49222222	MA	MA242662	E	Pico del Zapatero	09/07/1978
Lpal	-4.94194444	40.3075	MA	MA586665	E	Puerto de Serranillos (Gredos)	15/04/1987
Lpal	-3.95638889	40.84944444	M		E	Peñalara	June 1903
Lpal	-5.27972222	40.25194444	M		E	Circo de Gredos	17/07/1997
Lpal	-5.27972222	40.25194444	B		E	Sierra de Gredos	17/07/1997
Lpal	-3.98055556	40.77888889	B		E	Puerto de Navacerrada	19/07/1997
Lpal	-5.18252778	40.25983333	ST	TS332	E	La Mira	12/06/2011
Lpal	-3.9975	40.78194444	ST	TS223	E	Navacerrada	28/04/2011
Lpal	-3.41222222	41.20944444	MA	MA466828	E	Collado de la Quesera	20/05/1989
Lpal	-5.73	40.30416667	MA	MA242647	E	Sierra de Bejar	04/08/1977
Lpal	-3.96	40.83916667	MA	MA442180	E	Cotos-Peñlara	07/09/1983
Lpal	-3.95777778	40.84444444	MA	MA443470	E	Peñlara	18/06/1976
Lpal	-3.95444444	40.84972222	MA	MA147663	E	Peñalara	
Lpal	-3.95444444	40.84972222	MA	MA177553	E	Peñalara	
Lpal	-4.02777778	40.7875	MA	MA128715	E	Navacerrada	06.06.1898
Lpal	-3.96666667	40.78305556	MA	MA378094	E	Las Guarramillas	14/06/1979
Lpal	-4.00083333	40.78805556	MA	MA519333	E	Navacerrada	Juli 82
Lpal	-3.98333333	40.78333333	M	M10867	E	Las Guarramillas	14/06/1979
Lpal	-5.28166667	40.24916667	M	M29696	E	Circo de Gredos	29/08/1974
Lpal	-3.96666667	40.78305556	M	M10867	E	Las Guarramillas	14/06/1979
Lppa	-3.47444444	41.06722222	MA	MA792932	E	Puerto de la Hiruela	26/06/1998
Lppa	-3.66388889	40.87916667	MA	MA789789	E	Valdelmarco	28/06/2009
Lppa	-3.76361111	40.86861111	MA	MA771869	E	Puerto de Canencia	02/09/2007
Lppa	-3.17861111	41.12777778	MA	MA802966	E	Umbralejo	22/06/1986
Lppa	-3.19055556	41.12805556	MA	MA802990	E	Umbralejo	20/06/1986
Lppa	-4.72611111	40.15055556	MA	MA788232	E	Sierra de San Vicente	03/06/1996
Lppa	-3.4725	40.93388889	MA	MA743474	E	El Majalejo	24/05/1986
Lppa	-3.80888889	41.10805556	MA	MA743476	E	Aldelengua de Pedraza	06/06/1987
Lppa	-4.9675	40.39972222	MA	MA446316	E	Hoyocasero	11/05/1985
Lppa	-4.9675	40.39972222	MA	MA446316	E	Hoyocasero	11/05/1985
Lppa	-1.93361111	41.72	MA	MA128728	E	Sierra de Toranzo	09/06/1934
Lppa	-3.16666667	41.11916667	MA	MA217818	E	Umbralejo	
Lppa	-4.81472222	40.33055556	MA	MA242649	E	Puerto de Mijares	01/09/1981
Lppa	-4.51055556	40.62194444	MA	MA242657	E	Puerto de las Pilas	04/06/1980
Lppa	-3.04833333	42.19111111	MA	MA339845	E	Sierra de la Demanda	12/07/1985
Lppa	-4.51055556	40.62194444	MA	MA383940	E	Puerto de las Pilas	04/06/1980
Lppa	-1.83194444	41.69194444	MA	MA468001	E	Sierra del Tablado	28/05/1988
Lppa	-1.90055556	41.69944444	MA	MA484546	E	Sierra de Toranzo	28/05/1988
Lppa	-1.90638889	41.69055556	MA	MA484557	E	Sierra de Toranzo	28/05/1988
Lppa	-3.76361111	40.86861111	MA	MA518905	E	Puerto de Canencia	29/06/1992
Lppa	-1.93027778	41.69055556	MA	MA533669	E	Sierra de Toranzo	01/07/1992
Lppa	-3.84611111	41.15222222	MA	MA562828	E	Arahuetes	26/05/1990
Lppa	-3.84138889	40.79166667	MA	MA648191	E	Peña del Águila	06/06/1999
Lppa	-3.42055556	41.21583333	MA	MA592489	E	Puerto de la Quesera	24/06/1981
Lppa	-1.92694444	41.71583333	MA	MA247507	E	Sierra de Toranzo	02/06/1973
Lppa	-5.29972222	40.42222222	MA	MA208541	E	Puerto de la Peñanegra	23/06/1976

Cod.	Longitude	Latitude	Herbar.	Voucher n.	State	Collection Place	Date
Lppa	-5.04944444	40.30972222	MA	MA128733	E	Puerto del Arenal	July.1918
Lppa	-2.01583333	41.7575	MA	MA128729	E	Sierra del Madero	05/06/1934
Lppa	-2.01583333	41.7575	MA	MA181985	E	Sierra del Madero	05/06/1934
Lppa	-3.77055556	40.81972222	MA	MA518495	E	Miraflores	26/06/1992
Lppa	-3.44166667	40.88333333	MA	MA128719	E	Pontón de la Oliva	01/06/1916
Lppa	-3.03805556	42.19333333	MA	MA421245	E	Necutia (Sierra de la Demanda	31/07/1983
Lppa	-5.275	40.43	MA	MA442856	E	Puerto de la Peñanegra	26/07/1982
Lppa	-5.6225	40.26972222	MA	MA442858	E	Sierra del Barco (Avila)	27/07/1982
Lppa	-3.06027778	42.17305556	MA	MA447453	E	Pico San Lorenzo	15/07/1981
Lppa	-3.06027778	42.16388889	MA	MA531769	E	Sierra de la Demanda	25/06/1991
Lppa	-2.97583333	42.16388889	MA	MA533482	E	Barrancos del Rio Gatón	02/05/1992
Lppa	-2.95138889	42.16388889	MA	MA547359	E	Barrancos Cabrones	30/05/1993
Lppa	-2.95138889	42.18194444	MA	MA547360	E	Collado Blando	05/06/1993
Lppa	-5.16277778	40.23416667	MA	MA653756	E	Nogal del Barranco	31/05/1987
Lppa	-4.02222222	40.755	MA	MA128717	E	El Ventorrillo (Guadarrama)	20/07/1934
Lppa	-3.61722222	40.88333333	MA	MA217820	E	Lozoyuela-La Cabrera	15/11/1976
Lppa	-4.05472222	40.79305556	MA	MA526715	E	Siete Picos (Guadarrama)	27/06/1992
Lppa	-5.80444444	40.13027778	MA	MA217815	E	Sierra de Bernabé (Piornal)	19/11/1980
Lppa	-5.87166667	40.22138889	MA	MA421537	E	Puerto de Honduras (Hervas)	18/07/1981
Lppa	-5.01138889	40.31916667	MA	MA242660	E	Puerto del Pico	17/06/1981
Lppa	-4.625	40.36416667	MA	MA128749	E	Cerro Escusa (Avila)	08/07/1933
Lppa	-5.01138889	40.31916667	MA	MA128752	E	Puerto del Pico	27/06/2028
Lppa	-1.87333333	41.78444444	MA	MA484558	E	Moncayo	14/07/1989
Lppa	-1.80944444	41.73444444	MA	MA544104	E	Moncayo	10/07/1994
Lppa	-2.95166667	42.16333333	MA	MA438816	E	Sierra de Mansilla	28/05/1988
Lppa	-3.05861111	42.17833333	M		E	Sierra de la Demanda	21/07/1997
Lppa	-5.73194444	40.33361111	M		E	Sierra de Caldelario	18/07/1997
Lppa	-4.51055556	40.62194444	M	M11819	E	Puerto de las Pilas	04/06/1980
Lppa	-5.01277778	40.32083333	M		E	Puerto del Pico	10/06/1971
Lppa	-5.71944444	40.33944444	M	M1772	E	Sierra de Caldelario	03/05/1981
Lppa	-4.51055556	40.62194444	M	M5589	E	Puerto de las Pilas	04/06/1980
Lppa	-5.01277778	40.32083333	M	M14120	E	Puerto del Pico	09/07/1986
Lppa	-3.60527778	40.88333333	M		E	Sierra de Cabrera	06/06/1985
Lppa	-3.06027778	42.16388889	M	M15704	E	Pico Gatón	25/06/1991
Lppa	-3.06027778	42.16388889	M	M15704	E	Pico Gatón	25/06/1991
Lppa	-4.51055556	40.62194444	M	M11819	E	Puerto de las Pilas	04/06/1980
Lppa	-5.87166667	40.22138889	B		E	Caceres	16/06/1981
Lppa	-5.73194444	40.33361111	B		E	Sierra de Candelario	18/07/1997
Lppa	-4.65722222	40.5175	ST	TS265	E	Puerto de Parameda	08/05/2011
Lppa	-5.5125	40.2725	ST	TS273	E	Puerto de Tornavacas	08/05/2011
Lppa	-5.17388889	40.25719444	ST	TS333	E	Gredos	12/06/2011
Lppa	-3.06663889	42.18372222	ST	TS364	E	Sierra de la Demanda	18/06/2011
Lppa	-1.93241667	41.71833333	ST	TS367	E	Sierra de Toranzo	19/06/2011
Lppa	-4.83222222	40.31611111	ST	HP20112217	E	Puerto de Mijares	22/04/2011
Lppa	-5.87166667	40.22138889	MA	MA650634	E	Puerto de Honduras (Hervas)	05/05/1994
Lppa	-5.87166667	40.22138889	MA	MA718687	E	Puerto de Honduras (Hervas)	05/05/1994
Lppa	-3.91388889	40.97416667	MA	MA743473	E	Cuenca alta del rio Pirón	03/07/1986
Lppa	-3.81666667	40.9925	MA	MA743471	E	Puerto de Navafria	
Lppa	-5.73583333	40.34277778	MA	MA242661	E	Sierra del Bejar	30/05/1981
Lppa	-1.80972222	41.71638889	MA	MA532546	E	Moncayo	15/05/1990
Lppa	-1.80972222	41.71638889	MA	MA556690	E	Moncayo	01/05/1995

Cod.	Longitude	Latitude	Herbar.	Voucher n.	State	Collection Place	Date
Lppa	-4.18694444	40.71111111	MA	MA177554	E	San Rafael. Segovia	
Lppa	-3.58361111	41.13277778	MA	MA568420	E	Somosierra	10/05/1983
Lppa	-5.75638889	40.26722222	MA	MA128734	E	Sierra de Majarreina	24.06.1863
Lppa	-3.94444444	40.90333333	MA	MA128748	E	Puerto del Reventon	01.06.1893
Lppa	-3.77416667	40.78222222	MA	MA346326	E	Miraflores de la Sierra-Chozas	28/05/1970
Lppa	-4.02777778	40.7875	MA	MA128745	E	Navacerrada	24/06/1928
Lppa	-3.87944444	40.75	MA	MA506093	E	Quebrantaherraduras	15/06/1979
Lppa	-4.15638889	40.60527778	MA	MA128720	E	El Escorial	
Lppa	-3.51444444	40.97305556	MA	MA128723	E	Berzosa	03/06/1918
Lppa	-3.44361111	41.01333333	MA	MA155954	E	Puebla de la Mujer Muerta	
Lppa	-3.99916667	40.78777778	MA	MA160825	E	Navacerrada	22/07/1953
Lppa	-3.59305556	41.10916667	MA	MA173810	E	Robregordo	22/06/1954
Lppa	-4.13138889	40.70666667	MA	MA558090	E	Puerto de los Leones	16/06/1993
Lppa	-4.13138889	40.72138889	MA	MA242658	E	Puerto de los Leones	17/07/1978
Lppa	-3.91388889	40.80416667	MA	MA242664	E	Quebrantaherraduras	15/06/1979
Lppa	-4.13138889	40.72138889	MA	MA242656	E	Puerto de los Leones	17/07/1978
Lppa	-3.99833333	40.78722222	MA	MA128744	E	Navacerrada	Mai 12
Lppa	-5.70138889	40.28527778	MA	MA128753	E	Risco de la Campana (Gredos)	
Lppa	-5.01666667	40.37138889	MA	MA591407	E	Venta Rasquilla (Avila)	07/05/1989
Lppa	-4.92277778	40.27472222	MA	MA588711	E	Garganta Elisa	08/05/1994
Lppa	-5.01666667	40.37138889	MA	MA582023	E	Venta Rasquilla (Avila)	07/05/1989
Lppa	-3.94444444	40.90333333	M	M9573	E	Puerto del Reventon	01.06.1893
Lppa	-4.13138889	40.72138889	M	M9833	E	Puerto de los Leones	17/07/1978
Lppa	-5.01277778	40.32083333	M	M26657	E	Puerto del Pico	01/06/1971
Lppa	-4.03694444	40.73222222	M	M26617	E	Cercedilla-Navacerrada	30/05/1971
Lppa	-1.93638889	41.72277778	M	M7086	E	Monte Toranzo	02/06/1973
Lppa	-4.95222222	40.31222222	M	M1145	E	Puerto de Serranillos (Gredos)	31/07/1970
Lppa	-2.09333333	41.815	M		E	Sierra del Madero	05/06/1934
Lppa	-3.86166667	40.75916667	M	M14659	E	Arroyo de la Chozas	14/05/1989
Lppa	-1.93638889	41.72277778	M	M7086	E	Monte Toranzo	02/06/1973
Lppa	-4.13138889	40.72138889	M	M9833	E	Puerto de los Leones	17/07/1978
Lppa	-5.02333333	40.39111111	M	M79308	E	Venta del Obispo	16/06/1979
Lppa	-3.86166667	40.75916667	M	M14659	E	Arroyo de la Chozas	14/05/1989
Lspa	-2.97722222	37.9025	MA	MA198652	E	Cerro de la Laguna	10/06/1975
Lspa	-2.74944444	37.95611111	MA	MA217821	E	Cueva Parida	21/07/1977
Lspa	-2.42555556	38.52638889	MA	MA217822	E	Puerto de las Crucetillas	01/10/1979
Lspa	-2.87472222	37.89333333	MA	MA217823	E	Nava de San Pedro	05/03/1980
Lspa	-2.97722222	37.9025	MA	MA345462	E	Cerro de la Laguna	10/06/1975
Lspa	-2.96583333	37.84833333	MA	MA444222	E	Sierra del Pozo	23/06/1976
Lspa	-2.97722222	37.9025	MA	MA462193	E	Sierra de Cazorla	22/06/1975
Lspa	-2.78361111	37.92027778	MA	MA462194	E	Sierra de Empanadas	05/06/1976
Lspa	-2.94305556	37.9025	MA	MA462195	E	Fuente del Oso	16/05/1975
Lspa	-2.63416667	38.23527778	MA	MA462196	E	Sierra de Segura	04/05/1985
Lspa	-2.78361111	37.92027778	MA	MA480840	E	Sierra de Empanadas	15/06/1976
Lspa	-2.97722222	37.9025	MA	MA480841	E	Parador del Adelantado (Cazorla)	22/06/1975
Lspa	-2.84055556	37.89333333	MA	MA480842	E	Barranco del Guadalentín	18/06/1975
Lspa	-2.80638889	37.92027778	MA	MA480843	E	Sierra de la Cabrilla	04/07/1975
Lspa	-2.94305556	37.9025	MA	MA480855	E	Fuente del Oso	16/05/1976
Lspa	-2.58861111	38.20805556	MA	MA508192	E	Cerro de Poyo Alto	23/05/1981
Lspa	-2.63444444	38.24416667	MA	MA508196	E	Barranco del rio Madera	10/07/1978
Lspa	-2.55388889	38.28916667	MA	MA508927	E	Calar del Espino	23/05/1979

Cod.	Longitude	Latitude	Herbar.	Voucher n.	State	Collection Place	Date
Lspa	-2.54972222	38.50555556	MA	MA591808	E	Sierra de Alcaraz	22/05/1993
Lspa	-2.35	38.07194444	MA	MA697125	E	Sierra de las Cabras	06/07/2001
Lspa	-2.84055556	37.89333333	MA	MA128776	E	Barranco del Guadalentín	
Lspa	-2.6225	38.29833333	MA	MA508928	E	Fuente de la Zarza	06/06/1980
Lspa	-2.56666667	38.06388889	MA	MA242674	E	La Vidriera. Sierra de Guillimona	20/05/1978
Lspa	-2.84055556	37.90222222	MA	MA480854	E	Los Arenales (Cazorla)	27/05/1976
Lspa	-2.40305556	38.55888889	MA	MA319564	E	Paterna del Madera	04/07/1984
Lspa	-2.42555556	38.52638889	MA	MA538220	E	Puerto de la Crucetillas	26/05/1993
Lspa	-2.4725	38.45694444	M	Vogt3475	E	Calar del Mundo	19/06/1985
Lspa	-2.97722222	37.9025	M	M292	E	Cerro de la Laguna	10/06/1975
Lspa	-2.94330556	37.90686111	ST	TS301	E	Cazorla	20/05/2011
Lspa	-2.45583333	38.46805556	ST	TS316	E	Puerto del Arenal	22/05/2011
Lspa	-2.42541667	38.52713889	ST	TS318	E	Puerto Crucetillas	22/05/2011
Lspa	-2.53333333	38.03055556	ST	TS324	E	Sierra Guillamona	10/06/2011
Lspa	-2.58333333	38.01333333	ST	TS326	E	Sierra Guillamona	10/06/2011
Lspa	-2.56888889	36.94638889	MA	MA217998	E	Sierra Sagra	29/05/1975
Lspa	-2.96111111	37.90388889	MA	MA592488	E	Parador de Cazorla	12/05/1975
Lspa	-2.96111111	37.90388889	MA	MA242665	E	Parador de Cazorla	12/05/1975
Lspa	-2.96111111	37.90388889	MA	MA208647	E	Parador de Cazorla	12/05/1975
Lspa	-2.3825	38.06611111	MA	MA245893	E	Sierra de Taibilla. Las Cabras	17/07/1974
Lspa	-2.51777778	38.50555556	MA	MA128760	E	Sierra de Alcaraz	04/07/1923
Lspa	-2.91694444	37.91388889	M	M25387	E	Cazorla-Parador Nacional	25/05/1969
Lspa	-2.91694444	37.91388889	M	M29189	E	Cazorla-Parador Nacional	17/04/1973
Lspa	-2.49888889	38.19055556	B		E	Marchena	25/06/1988
Lspa	-2.52527778	38.02583333	B		E	Sierra de Guillimona	23/06/1988
Lbil	-0.62833333	40.02805556	MA	MA460500	E	Sierra de la Pina	17/07/1988
Lbil	-0.62833333	40.02805556	MA	MA497809	E	Sierra de Pina	30/06/1988
Lbil	-0.62833333	40.02805556	MA	MA128780	E	Sierra de Pina	29/06/1919
Lbil	-1.33944444	41.32166667	MA	MA247508	E	Puerto de Codos	12/05/1973
Lbil	-1.49194444	41.37083333	MA	MA532930	E	Sierra de Vicort	05/06/1991
Lbil	-1.83305556	40.40777778	MA	MA217826	E	Sierra de San Felipe	05/11/1980
Lbil	-0.91472222	39.08916667	MA	MA128772	E	Caroché (Sierra de Ayora)	04/07/1915
Lbil	-0.62833333	40.02805556	M	M14660	E	Sierra de Pina	30/06/1988
Lbil	-1.33944444	41.32166667	M	M7087	E	Puerto de Codos	12/05/1973
Lbil	-0.62583333	40.02388889	B		E	Sierra de Pina (Castellon)	03/06/1988
Lbil	-1.34083333	41.32005	ST	TS247	E	Sierra del Vicort	01/05/2011
Lbil	-0.62833333	40.02805556	MA	MA465679	E	Sierra de la Pina	28/06/1980
Lbil	-0.39833333	39.92027778	MA	MA128774	E	Sierra d'Espadá	16/05/1908
Lbil	-0.93944444	38.98805556	MA	MA128770	E	Sierra de Ayora	21/06/1906
Lbil	-0.62833333	40.02805556	MA	MA442943	E	Sierra de Pina	30/05/1983
Lbil	-0.41166667	39.92694444	MA	MA348821	E	Sierra d'Espadá	26/05/1947
Lbil	-0.41166667	39.92694444	MA	MA500304	E	Sierra d'Espadá	27/05/1947
Lbil	-1.45416667	41.34	MA	MA128782	E	Sierra de Vicort	06/06/1912
Lbil	-1.59305556	39.87861111	MA	MA443933	E	Villar del Humo	06/06/1976
Lbil	-0.41166667	39.9275	MA	MA128669	E	Sierra d'Espadá	26/05/1947
Lbil	-1.59027778	39.99416667	M	M44171	E	Cañete-Landete	25/05/1988
Lbil	-1.5	41.36666667	M		E	Sierra de Vicort	19/05/1909
Lbil	-1.59027778	39.99416667	M	M44171	E	Cañete-Landete	25/05/1988
Lbil	-1.34527778	41.33	M	M29011	E	Puerto de Aguarón	21/05/1985
Lbil	-0.93944444	38.98805556	M	M4122	E	Sierra de Ayora	June 1891
Lbil	-0.39833333	39.92027778	M		E	Sierra d'Espadá	May1891

Cod.	Longitude	Latitude	Herbar.	Voucher n.	State	Collection Place	Date
Lvir	-3.24583333	42.93472222	MA	MA786958	E	Monte Peñalta	20/04/2006
Lvir	-1.755	40.16666667	MA	MA444292	E	Sierra de Valdemeca	18/07/1974
Lvir	-1.96305556	38.25333333	MA	MA738051	E	Sierra de la Muela	30/04/2006
Lvir	-1.76666667	40.17555556	MA	MA422108	E	Sierra de Valdemeca	22/07/1977
Lvir	-4.76194444	42.835	MA	MA532504	E	Peña Cueto-Peña Fraile	24/05/1990
Lvir	-4.64027778	42.86333333	MA	MA532663	E	Peña Redonda	31/05/1990
Lvir	-2.00888889	40.20777778	MA	MA440795	E	Ciudad Encantada	17/04/1980
Lvir	-2.13194444	40.08888889	MA	MA440796	E	Cuenca	17/04/1980
Lvir	-2.03194444	39.69166667	MA	MA444654	E	Fuente del Pino	
Lvir	-3.03555556	41.00194444	MA	MA525931	E	Alcorto	08/05/1993
Lvir	-1.80805556	40.185	MA	MA440794	E	Beamud	17/04/1980
Lvir	-1.58583333	40.95722222	MA	MA486423	E	Las Cuerlas	31/05/1981
Lvir	-2.835	40.11888889	MA	MA593920	E	Pico del Buitre	18/05/1996
Lvir	-2.82611111	40.18166667	MA	MA577821	E	Pico Altomira	26/05/1996
Lvir	-2.00888889	40.20777778	MA	MA420369	E	Ciudad Encantada	20/05/1974
Lvir	-2.31527778	40.45111111	MA	MA217824	E	Priego	20/09/1979
Lvir	-1.72111111	40.09416667	MA	MA217825	E	Sierra de Valdemeca	06/11/1980
Lvir	-4.75133333	42.84111111	ST	TS361	E	Sierra del Brezo	17/06/2011
Lvir	-3.24777778	42.92916667	MA	Vit77690	E	Monte Peñalta	20/04/2006
Lvir	-1.76083333	40.16861111	MA	MA443027	E	Sierra de Valdemeca	21/07/1979
Lvir	-1.75861111	40.16444444	MA	MA531732	E	Sierra de Valdemeca	15/05/1972
Lvir	-0.50111111	38.76833333	MA	MA128769	E	Sierra Mariola	29/06/1936
Lvir	-0.49888889	38.76972222	MA	MA128771	E	Sierra Mariola	11.6.1896
Lvir	-2.07611111	40.55138889	MA	MA128804	E	El Tobar	12/06/1942
Lvir	-2.4	40.79222222	MA	MA242673	E	Sacecorbo-Ocentejo	17/06/1975
Lvir	-2.4	40.79222222	MA	MA242671	E	Sacecorbo	17/06/1975
Lvir	-2.15388889	40.54361111	MA	MA128942	E	Camino de Carrascosa	16/06/1935
Lvir	-3.19972222	41.21583333	MA	MA500606	E	Galve de Sorbe	01/05/1965
Lvir	-2.07972222	40.555	MA	MA442893	E	Cerro de San Cristobar	16/06/1979
Lvir	-2.23111111	40.69611111	MA	MA442092	E	Villanueva de Alcorcon	July 73
Lvir	-3.19972222	41.21583333	MA	MA239749	E	Galve de Sorbe	01/05/1965
Lvir	-2.07611111	40.55138889	MA	MA128806	E	El Tobar	12/06/1942
Lvir	-1.66361111	39.795	MA	MA442865	E	Cardenete-Villar del Humo	15/05/1978
Lvir	-0.27666667	38.65166667	MA	MA128492	E	Sierra Aitana	19/06/1936
Lvir	-2.41722222	40.8325	M	M14122	E	Sacecorbo	17/06/1975
Lvir	-2.39583333	40.79722222	M	M23539	E	Sacecobo	17/06/1975
Lvir	-2.91055556	41.05583333	M	M23800	E	Pálmaces	06/06/1982
Lvir	-2.91055556	41.05583333	M	M23800	E	Pálmaces	06/06/1982
Lvir	-2.39583333	40.79722222	M	M9835	E	Sacecobo	17/06/1975
Lvir	-1.75	40.16666667	M	M15705	E	Sierra de Valdemeca	15/05/1972
Lvir	-1.75	40.16666667	M	M15705	E	Sierra de Valdemeca	15/05/1972
Lvir	-2.4	40.79222222	B		E	Sacecorbo-Ocentejo	17/06/1975
Lpec	-3.37888889	37.05194444	MA	MA128797	E	Lagunillas	
Lpec	-3.34666667	37.04666667	MA	MA577180	E	Rio Seco. Sierra Nevada	06/07/1990
Lpec	-2.93944444	37.09611111	MA	MA508849	E	Sierra Nevada	19/06/1992
Lpec	-3.37944444	37.05222222	MA	MA446282	E	Lagunillas de la Virgen	25/08/1985
Lpec	-3.38222222	37.06333333	MA	MA443823	E	Los Borreguiles	18/07/1976
Lpec	-3.35972222	37.05472222	MA	MA448220	E	La Veleta	22/07/1984
Lpec	-3.35722222	37.0725	MA	MA452492	E	La Veleta	01/07/1978
Lpec	-3.31444444	37.05916667	MA	MA394513	E	Mulhacen	02/10/1975
Lpec	-3.33527778	37.0575	MA	MA394518	E	Hoya de la Laguna Larga	05/10/1975

Cod.	Longitude	Latitude	Herbar.	Voucher n.	State	Collection Place	Date
Lpec	-3.37222222	37.0625	ST	TS372	E	Veleta	13/07/2011
Lpec	-3.4545	37.01530556	ST	TS374	E	Sierra Nevada	14/07/2011
Lpec	-3.36666667	37.06666667	MA	MA128788	E	Veleta	
Lpec	-3.38722222	37.09638889	MA	MA128789	E	Veleta	23/07/1981
Lpec	-3.40666667	37.03222222	MA	MA128796	E	Valle del Lanjaron	06/08/1930
Lpec	-3.3825	37.06722222	MA	MA680366	E	Barranco del Monachil	30/07/1976
Lpec	-3.37388889	37.06611111	MA	MA449872	E	Subida al Veleta	02/07/1974
Lpec	-3.36972222	37.06416667	MA	MA617178	E	Pico Veleta	12/07/1986
Lpec	-3.38722222	37.06916667	MA	MA242672	E	Los Borreguiles	21/07/1981
Lpec	-3.36944444	37.05694444	MA	MA398235	E	La Veleta	12/07/1986
Lpec	-3.37916667	37.08055556	MA	MA418515	E	Pico Veleta	09/07/1972
Lpec	-3.37916667	37.08055556	MA	MA408845	E	Carretera del Veleta	09/07/1972
Lpec	-3.37194444	37.05333333	MA	MA446283	E	Corral de la Veleta	23/08/1985
Lpec	-3.31888889	37.04083333	MA	MA242670	E	Mulhacen	06/08/1979
Lpec	-3.38694444	37.09555556	MA	MA336986	E	Sierra Nevada.	22/06/1986
Lpec	-3.31166667	36.98777778	M	M23605	E	Sierra Nevada-Capileira	25/09/1987
Lpec	-3.37833333	37.0775	M	M17171	E	Veleta (Sierra Nevada)	08/08/1962
Lpec	-3.31555556	37.03361111	M	M29629	E	Capileira-Veleta	24/08/1974
Lpec	-3.36972222	37.05361111	M	M10012	E	Veleta	23/08/1969
Lpec	-3.38694444	37.09555556	M	M10958	E	Sierra Nevada.	24/07/1969
Lpec	-3.38611111	37.09444444	M	M596	E	Peñon de San Francisco	
Lpec	-3.37833333	37.0775	M		E	La Veleta	
Lpec	-3.38611111	37.09444444	M		E	Peñon de San Francisco	30/07/1930
Lpec	-3.37833333	37.0775	M		E	La Veleta	30.07.1876
Lpec	-2.99861111	37.09444444	B		E	Sierra Nevada. El Chullo	19/06/1988
Lpec	-2.90944444	37.08972222	B		E	Cerro del Almirez	17/03/1988
Lpul	-4.30305556	41.36333333	MA	MA754389	E	Cuellar	18/04/1998
Lpul	-4.29111111	41.35444444	MA	MA754388	E	Cuellar	21/04/1998
Lpul	-4.20583333	41.275	MA	MA754387	E	Cuellar	20/06/1998
Lpul	-4.20583333	41.275	MA	MA754385	E	Cuellar	20/06/1998
Lpul	-4.08638889	41.26722222	MA	MA743464	E	Aguilafuente	18/06/1988
Lpul	-4.08638889	41.26722222	MA	MA743465	E	Aguilafuente	07/05/1988
Lpul	-3.78611111	41.11638889	MA	MA743466	E	Pedraza	01/05/1987
Lpul	-3.80888889	41.03527778	MA	MA743467	E	Puerto de Navafria	11/05/1985
Lpul	-3.80972222	41.11638889	MA	MA743468	E	Aldealengua de Pedraza	13/04/1985
Lpul	-4.08611111	41.24916667	MA	MA756590	E	Aguilafuente	17/04/2002
Lpul	-3.84611111	41.15222222	MA	MA743469	E	Pedraza	30/05/1987
Lpul	-3.93972222	41.02527778	MA	MA743470	E	Sotosalbos	17/05/1986
Lpul	-5.76305556	40.3675	MA	MA784262	E	Llana Alto	01/05/2009
Lpul	-2.22611111	41.00944444	MA	MA754043	E	Ciruelos	06/05/2007
Lpul	-4.0775	40.73583333	MA	MA440824	E	Cercedilla	
Lpul	-5.96916667	39.85888889	MA	Ma443917	E	Serradilla	06/05/1983
Lpul	-3.83111111	40.91805556	MA	MA464717	E	Embalse de la Pinilla	27/03/1980
Lpul	-3.8875	40.69222222	MA	MA506091	E	Cerceda	23/05/1988
Lpul	-3.81861111	40.92	MA	MA381573	E	Pantano de la Pinilla	27/03/1980
Lpul	-4.02722222	40.72722222	MA	MA440572	E	Cerro de la Golondrina	07/05/1977
Lpul	-6.74694444	41.79583333	MA	MA183575	PT	Monte de San Bartolomeu	21/04/1943
Lpul	-3.51305556	41.26222222	MA	MA217810	E	Cereyo de Arriba	07/11/1979
Lpul	-4.41916667	40.65111111	MA	MA217814	E	Casa de la Lancha	09/10/1979
Lpul	-6.7375	40.39444444	MA	MA242668	E	Casillas de Flores	23/05/1981
Lpul	-5.02027778	42.50638889	MA	MA399471	E	Saelices del Rio	10/04/1984

Cod.	Longitude	Latitude	Herbar.	Voucher n.	State	Collection Place	Date
Lpul	-3.605	42.15333333	MA	MA399534	E	Cueva de San Clemente	02/06/1984
Lpul	-3.60805556	41.18055556	MA	MA401990	E	Siguero	30/04/1987
Lpul	-4.82972222	40.52805556	MA	MA440736	E	Siera de Paramera	24/04/1988
Lpul	-1.90611111	41.69944444	MA	MA467999	E	Sierra del Toranzo	28/05/1988
Lpul	-2.33611111	41.97305556	MA	MA468000	E	Puerto de Oncala	21/05/1988
Lpul	-2.33583333	41.98194444	MA	MA532548	E	Puerto de Oncala	17/05/1990
Lpul	-3.51861111	41.95555556	MA	MA532615	E	Tejada	01/05/1990
Lpul	-6.05	41.82	MA	MA650861	E	Valle del Casal	15/05/1996
Lpul	-3.36194444	41.96527778	MA	MA399510	E	Carazo	02/06/1984
Lpul	-3.96361111	39.40333333	MA	MA525763	E	Puerto del Comendador	24/04/1993
Lpul	-3.61833333	41.00944444	MA	MA217811	E	Buitrago-Gadullas	15/11/1979
Lpul	-3.64222222	41.03638889	MA	MA217813	E	Serna del Monte-Gascones	15/11/1979
Lpul	-7.10833333	42.22111111	MA	MA316748	E	Covelo. Viana do Bolo	07/04/1977
Lpul	-6.73777778	40.39111111	M		E	Casillas de Flores	23/05/1981
Lpul	-4.0775	40.73583333	M		E	Cercedillas	May 80
Lpul	-4.19666667	40.55888889	M	M18620	E	Puerto de la Cruz Verde	21/05/1996
Lpul	-4.19666667	40.55888889	M	M18620	E	Puerto de la Cruz Verde	21/05/1996
Lpul	-4.19666667	40.55888889	B		E	Puerto de la Cruz Verde	21/05/1996
Lpul	-3.83111111	40.91805556	B		E	Lozoyuela	27/03/1980
Lpul	-4.0775	40.73583333	B		E	Cercedilla	May 80
Lpul	-3.03527778	41.08194444	B		E	Guadalajara	05/06/1985
Lpul	-4.78060556	41.57130278	ST	TS217	E	Puente Duero	23/04/2011
Lpul	-3.85361111	40.88944444	ST	TS235	E	Rascafria	28/04/2011
Lpul	-4.65722222	40.5175	ST	TS268	E	Puerto de Parameda	08/05/2011
Lpul	-5.16055556	40.5375	ST	TS270	E	Puerto de Villatoro	08/05/2011
Lpul	-6.73272222	40.32336111	ST	TS(01)277	E	El Payo	09/05/2011
Lpul	-6.3925	41.00472222	ST	TS297	E	Vitigudino	11/05/2011
Lpul	-7.09861111	42.11197222	ST	TS336	E	Pixeiros	15/06/2011
Lpul	-6.41055556	41.0025	MA	MA464154	E	Vitigudino	25/04/1989
Lpul	-4.08638889	41.27611111	MA	MA754386	E	Aguilafuente	01/05/1998
Lpul	-3.60111111	41.01138889	MA	MA577490	E	Gandullas	26/03/1990
Lpul	-3.52583333	40.92194444	MA	MA378058	E	Cervera del Buitrago	22/04/1982
Lpul	-5.89944444	39.86638889	MA	MA450238	E	La Herguijuera. Toril	23/03/1978
Lpul	-5.89638889	39.91527778	MA	MA242666	E	Vega del Chiquero.	17/04/1982
Lpul	-5.90583333	39.83861111	MA	MA242667	E	Cuerda del Chiquero	23/03/1978
Lpul	-5.90583333	39.83861111	MA	MA212530	E	Cuerda del Chiquero	23/03/1978
Lpul	-3.33388889	42.27611111	MA	MA440862	E	Villorobe-Pantano de Alrazón	12/05/1977
Lpul	-4.18694444	40.71111111	MA	MA442012	E	San Rafael. Segovia	05/06/1972
Lpul	-4.19861111	40.56388889	MA	MA625979	E	Puerto de la Cruz Verde	21/05/1996
Lpul	-5.97611111	41.31972222	MA	MA205065	E	Fresno del Sazago	02/05/1976
Lpul	-4.72694444	40.13694444	MA	MA257754	E	Real de San Vicente	16/04/1982
Lpul	-7.11027778	42.09222222	MA	MA530665	E	Bouza-Pixeiras	01/05/1993
Lpul	-6.26305556	41.95972222	MA	MA500565	E	Sierra de la Culebra	13/05/1974
Lpul	-4.8725	41.31444444	MA	MA183423	E	Medina del Campo	02/06/1957
Lpul	-3.56972222	42.13833333	MA	MA500091	E	Cuevas de San Clemente	02/06/1984
Lpul	-3.21666667	41.96666667	MA	MA128682	E	Castrillo de la Reina	
Lpul	-4.17472222	41.37972222	MA		E	Frumales	09/04/1982
Lpul	-4.58527778	40.88777778	MA	MA208210	E	Sanchidrian	05/04/1976
Lpul	-5.48916667	40.36805556	MA	MA432078	E	San Lorenzo de Tormes	18/04/1975
Lpul	-3.65666667	41.38194444	MA	MA308918	E	Fresno de la Fuente-Encinar	29/06/1984
Lpul	-4.1	41.23333333	MA	MA128677	E	Aguilafuente	10/06/1944

Cod.	Longitude	Latitude	Herbar.	Voucher n.	State	Collection Place	Date
Lpul	-4.5	41.21666667	MA	MA618956	E	Coca	04/05/1996
Lpul	-3.95	41.33333333	MA	MA494328	E	Navalilla	05/06/1987
Lpul	-3.77583333	41.18583333	MA	MA568419	E	Castroserna de Arriba	17/04/1983
Lpul	-3.7025	41.11527778	MA	MA568418	E	La Dehesa. Arcornes	21/05/1983
Lpul	-3.69611111	41.15	MA	MA568417	E	Pradena	02/06/1984
Lpul	-4.1725	40.71388889	MA	MA406424	E	San Rafael-Gudillos	
Lpul	-4.1725	40.71388889	MA	MA197818	E	San Rafael-Gudillos	16/05/1965
Lpul	-1.67083333	40.84277778	MA	MA542443	E	Campillo- Pobo de Dueñas	17/06/1989
Lpul	-2.83333333	41.08333333	MA	MA239757	E	Rebellosa de Jadraque	01/05/1965
Lpul	-7.10944444	42.22861111	MA	MA440863	E	Covelo. Viana do Bolo	07/04/1977
Lpul	-7.055	42.1625	MA	MA212526	E	San Agostiño-Viana do Bolo	07/04/1977
Lpul	-7.12333333	42.26722222	MA	MA212529	E	Cambela	07/04/1977
Lpul	-7.055	42.1625	MA	MA316760	E	San Agostiño-Viana do Bolo	06/04/1977
Lpul	-7.12333333	42.26722222	MA	MA316743	E	Cambela	07/04/1977
Lpul	-7.10944444	42.22861111	MA	MA212527	E	Covelo. Viana do Bolo	07/04/1977
Lpul	-2.75972222	41.75944444	M		E	Vinuesa	27/04/1973
Lpul	-5.90583333	39.83861111	M	M24198	E	Cuerda del Chiquero	23/03/1978
Lpul	-3.52583333	40.92194444	M	M24199	E	Cervera del Buitrago	22/04/1982
Lpul	-3.81861111	40.92	M	M24200	E	Embalse de la Pinilla	27/03/1980
Lpul	-3.76638889	40.51638889	M	M9574	E	El Pardo	24.04.1854
Lpul	-3.81861111	40.92	M	M13686	E	Embalse de la Pinilla	27/03/1980
Lpul	-3.52583333	40.92194444	M	M10868	E	Cervera del Buitrago	22/04/1982
Lpul	-2.66305556	41.97027778	M	M14766	E	El Royo	23/05/1976
Lpul	-5.04777778	41.46333333	M	M9118	E	Tordesillas	26/04/1974
Lpul	-2.75972222	41.75944444	M	M4123	E	Vinuesa	27/04/1973
Lpul	-5.675	40.47333333	M	M29044	E	Nava de Bejár	09/04/1973
Lpul	-6.9725	40.35861111	M	M27380	PT	Souto do Bispo	29/05/1972
Lpul	-7.42027778	40.71388889	M	M27394	PT	Celorico da Beira	29/05/1972
Lpul	-5.67805556	40.26388889	M	M23098	E	Puerto de Tornavacas-Jerte	05/04/1968
Lpul	-4.42555556	40.68138889	M	M26641	E	Aldea Vieja	01/06/1971
Lpul	-5.95444444	40.48472222	M	M26701	E	Sequeros-Bejar	02/06/1971
Lpul	-4.14027778	40.71	M		E	Puerto de Guadarrama	06/06/1976
LflN	-7.22138889	42.72527778	MA	MA730769	E	Cumbre del Oribio	08/08/2004
LflN	-6.54277778	42.40222222	MA	MA316731	E	Cabeza de la Yegua	09/07/1983
LflN	-6.89694444	42.77111111	MA	MA316758	E	Peñarubia	30/06/1982
LflN	-6.68361111	42.27583333	MA	MA316759	E	Sierra de la Cabrera. La Baña	09/05/1982
LflN	-6.73361111	42.25888889	MA	MA316762	E	Sierra de la Cabrera. La Baña	18/06/1981
LflN	-6.81	42.125	MA	MA386211	E	Ribadelago	27/05/1987
LflN	-6.7975	42.14277778	MA	MA510619	E	San Martin de Castañeda	27/05/1987
LflN	-6.74305556	42.31277778	MA	MA543108	E	Peña Trevinca	29/06/1994
LflN	-7.31722222	42.62	MA	MA546643	E		22/07/1990
LflN	-6.49805556	42.37083333	MA	MA593947	E	Morredero	03/05/1997
LflN	-6.665	43.10388889	MA	MA617179	E	Vega del Horreo	26/02/1990
LflN	-6.7525	42.32305556	MA	MA622255	E	Fonte de Cova	22/05/1991
LflN	-6.51444444	42.26305556	MA	MA652568	E	Iruela	19/04/1992
LflN	-6.60277778	42.44055556	MA	MA316730	E	Pico de la Guiana	30/05/1979
LflN	-6.89694444	42.77111111	MA	MA128706	E	Peña Rubia	
LflN	-6.72119444	42.31241667	ST	TS350	E	Serra do Eixe	15/06/2011
LflN	-6.49972222	42.38861111	ST	TS352	E	Sierra del Taleno	16/06/2011
LflN	-6.71527778	42.31277778	MA	MA756801	E	La Baña	09/06/2005
LflN	-6.38333333	42.33333333	MA	MA316746	E	Sierra del Teleno	14/08/1967

Cod.	Longitude	Latitude	Herbar.	Voucher n.	State	Collection Place	Date
LflN	-6.69666667	42.24888889	MA	MA502683	E	Sierra de Cabrera	26/06/1989
LflN	-6.78277778	42.71888889	MA	MA128786	E	Villar de Acero	21/06/1933
LflN	-6.80361111	42.86333333	MA	MA429963	E	Puerto de Ancares	11/07/1986
LflN	-6.39722222	42.34277778	MA	MA316745	E	Corporales-Teleno	
LflN	-6.48583333	42.19666667	MA	MA316744	E	La Cabrera. Truchillas	06/07/1978
LflN	-7.20111111	42.39694444	MA	MA463785	E	Montefurado	27/03/1987
LflS	-3.77361111	38.44722222	MA	MA783651	E	San Lorenzo de Calatrava	11/05/2008
LflS	-6.24055556	40.28444444	MA	MA718782	E	Puerto del Gamo	04/06/1994
LflS	-6.10361111	39.21694444	MA	MA718357	E	Sierra de Montanchez	24/04/1994
LflS	-4.39861111	38.53777778	MA	MA711833	E	Sierra de Alardia	04/05/1998
LflS	-4.20805556	39.52333333	MA	MA732797	E	Puerto del Robledillo	19/06/2004
LflS	-6.81027778	40.33277778	MA	MA717133	PT	Lajeosa	01/05/1994
LflS	-6.96777778	40.31138889	MA	MA717118	PT	Sabugal	01/05/1994
LflS	-3.79666667	38.42722222	MA	MA783628	E	San Lorenzo de Calatrava	11/05/2008
LflS	-6.77611111	40.24361111	MA	MA727089	E	San Martin de Trevejo	15/05/2005
LflS	-5.76305556	40.3675	MA	MA784261	E	Llana Alto	01/05/2009
LflS	-7.51055556	40.09861111	MA	MA784399	PT	Serra de Guardunha	02/05/2009
LflS	-4.38555556	38.53527778	MA	MA242654	E	Puerto de Niefla	22/04/1980
LflS	-6.79888889	40.32333333	MA	MA242655	E	Navafrias	23/05/1981
LflS	-6.86138889	40.2625	MA	MA378066	E	Puerto de Carrigahonda	05/05/1981
LflS	-4.38555556	38.53527778	MA	MA383939	E	Puerto de Niefla	22/04/1980
LflS	-5.72944444	40.29416667	MA	MA445802	E	Calvitero. Canderaio	18/07/1980
LflS	-4.14666667	38.49166667	MA	MA596887	E	Solana del Pino	16/03/1997
LflS	-4.2375	38.44555556	MA	MA596888	E	Sierra Madera	23/03/1997
LflS	-4.15805556	38.49138889	MA	MA596889	E	Solana del Pino	24/07/1997
LflS	-5.40055556	39.46833333	MA	MA128946	E	Villuercas. Guadalupe	21/06/1948
LflS	-5.40055556	39.46833333	MA	MA128703	E	Villuercas. Guadalupe	23/05/1949
LflS	-6.12388889	39.21472222	MA	MA128787	E	Sierra de Montanchez	03/07/1946
LflS	-5.40055556	39.46833333	MA	MA128736	E	Villuercas. Guadalupe	24/06/1946
LflS	-5.34944444	39.46444444	MA	MA128704	E	El Humilladero. Guadalupe	21/05/1949
LflS	-6.12388889	39.21472222	MA	MA483092	E	Sierra de Montanchez	14/04/1990
LflS	-6.79888889	40.32333333	M		E	Navasfrias	23/05/1981
LflS	-4.51666667	38.56666667	B		E	Almodovar del Campo	31/03/1980
LflS	-6.86138889	40.2625	B		E	Valverde del Fresno	05/05/1981
LflS	-4.38555556	38.53527778	B		E	Brazatortas	22/04/1980
LflS	-6.68685556	40.24583611	ST	TS(01)270	E	Puerto de Peroles	09/05/2011
LflS	-7.21588889	40.335	ST	TS279	PT	Sortelha	09/05/2011
LflS	-7.54944444	40.37277778	ST	TS284	PT	Serra de Estrela	10/05/2011
LflS	-3.82055556	38.49111111	MA	MA713085	E	Hortezuelas	28/03/1998
LflS	-5.38916667	39.47638889	MA	MA706080	E	Las Villuercas-Guadalupe	07/05/2003
LflS	-7.55638889	40.41333333	MA	MA718532	PT	Manteigas	29/04/1994
LflS	-6.68416667	41.20916667	MA	MA518096	E	Salto de la Aldeadavila	
LflS	-6.16972222	40.51138889	MA	MA519063	E	Peña de Francia	
LflS	-6.73666667	40.17027778	MA	MA242653	E	Hoyos	30/03/1972
LflS	-6.22055556	39.85861111	MA	MA341307	E	Mirabel. Sierra Cauclo	04/05/1980
LflS	-5.21444444	39.63972222	MA	MA247424	E	Navatrasierra-Carrascalero	29/04/1968
LflS	-6.98666667	41.16972222	MA	MA643614	PT	Serra de Rebodero	17/04/1996
LflS	-6.98722222	41.16972222	M	M5252	PT	Serra de Rebodero	17/04/1996
LflS	-8.12638889	39.92055556	M		PT	Barragem do Cabril	22/04/1967
LflS	-7.48388889	40.11722222	M		PT	Alcongosta	27/04/1958
LflS	-2.83444444	42.09555556	B	N° 15703	E	Viniegra de Arriba	15/07/1985

Taxon	Sample n.	n. reads expected	B20		C12		C16		D35		Max expected	Allele Mean	Reads Mean
			Reads	Alleles	Reads	Alleles	Reads	Alleles	Reads	Alleles			
Phalacrocarpum oppositifolium	LPS147	33	27	3*		1	7	2		1	2	1.75	17.00
Castrilanthemum debeauxii	IA2170-4	33	29	3*	52	1	13	4*		1	2	2.25	31.33
Hymenostemma pseudoanthemis	LPS131-9	33	50	1	92	2	16	1		1	2	1.25	52.67
Prolongoa hispanica	LPS135-10	33	77	1	75	1	18	2		1	2	1.25	56.67
Leucanthemopsis pulverulenta	LPS134-1	33	35	1	62	2	31	1		1	2	1.25	42.67
L. pulverulenta	LPS137-1	33	43	1	59	2	28	2		2	2	1.75	43.33
L. pulverulenta	LPS141-1	33	30	1	23	2	43	2		2	2	1.75	32.00
L. pulverulenta	LPS142-2	33	25	2	60	2	15	2		2	2	2.00	33.33
L. pulverulenta	LPS145-1	33	25	1	36	2	29	1		2	2	1.50	30.00
L. pulverulenta	LPS149-3	33	42	1	28	2	19	4*		2	2	2.25	29.67
L. pulverulenta	LPS159-1	33	57	2	78	2	36	3*		2	2	2.25	57.00
L. pallida var. pallida	LPS139-1	79	223	4	219	3	140	3		3	4	3.25	194.00
L. pallida var. pallida	LPS143-7	79	143	4	200	3	75	3		4	4	3.50	139.33
L. pallida var. pallida	LPS158-1	79	197	3	151	3	106	4		3	4	3.25	151.33
L. pallida var. pallida	LPS164-1	79	118	3	147	4	87	4		2	4	3.25	117.33
L. pallida var. pallida	LPS165-1	79	76	2	165	4	52	3		3	4	3.00	97.67
L. pallida var. pallida	LPS184	79	213	4	152	3	95	2		4	4	3.25	153.33
L. pallida var. alpina	LPS136-6	79	136	4	230	3	46	4		4	4	3.75	137.33
L. pallida var. alpina	LPS157-3	79	180	4	223	3	62	2		3	4	3.00	155.00
L. pallida subsp. virescens var. bilbilitanum	LPS138-1	33	22	1	80	2	21	2		2	2	1.75	41.00
L. pallida subsp. virescens var. bilbilitanum	LPS052	33	23	1	14	2	26	1		1	2	1.25	21.00
L. pallida subsp. virescens var.virescens	LPS163-2	33	50	1	71	2	20	1		1	2	1.25	47.00
L. pallida subsp. virescens var.virescens	LPS185	33	19	1	45	1	33	1		2	2	1.25	32.33
Leucantemopsis pallida subsp. spathulifolia	LPS150-1	79	71	2	234	4	83	3		4	4	3.25	129.33
Leucantemopsis pallida subsp. spathulifolia	LPS151-4	79	119	3	249	3	98	2		3	4	2.75	155.33
Leucantemopsis pallida subsp. spathulifolia	LPS152-1	79	153	2	195	2	102	3		2	4	2.25	150.00
Leucantemopsis pallida subsp. spathulifolia	LPS153-1	79	114	3	204	3	104	3		4	4	3.25	140.67
Leucantemopsis pallida subsp. spathulifolia	LPS154-1	79	110	3	144	3	84	2		3	4	2.75	112.67
L. flaveola	LPS144-11	79	164	4	230	2	92	3		4	4	3.25	162.00
L. flaveola	LPS146-7	79	124	1	149	3	72	3		2	4	2.25	115.00
L. flaveola	LPS148-1	79	115	3	183	4	93	3		4	4	3.50	130.33
L. flaveola	LPS160-4	79	147	3	170	4	73	3		3	4	3.25	130.00
L. flaveola	LPS161-1	79	130	4	161	4	103	3		4	4	3.75	131.33
L. flaveola	LPS038	79	98	2	251	4	94	2		3	4	2.75	147.67
L. flaveola	LPS039	79	198	1	219	4	74	4		3	4	3.00	163.67
L. pectinata	LPS166-11	3	65	2	57	2	16	1		1	2	1.50	46.00

Taxon	Sample n.	n. reads expected	B20		C12		C16		D35		Max expected	Allele Mean	Reads Mean
			Reads	Alleles	Reads	Alleles	Reads	Alleles	Reads	Alleles			
L. pectinata	LPS167-1	33	66	2	61	2	20	1		2	2	1.75	49.00
L. alpina subsp. tomentosa	LPS181-3	33	59	1	65	2	28	1		1	2	1.25	50.67
L. alpina subsp. tomentosa	LPS182-1	33	65	2	84	4*	25	1		1	2	2.00	58.00
L. alpina subsp. tatra	LPS064-1	33	34	2	51	1	19	1		1	2	1.25	34.67
L. alpina subsp. alpina	LPS074-1	33	51	1	51	1	25	1		1	2	1.00	42.33
L. alpina subsp. Minima	LPS119-7	79	185	2	226	2	80	2		3	4	2.25	163.67
L. alpina subsp. alpina	LPS180-1	79	205	1	150	2	116	3		1	4	1.75	157.00
L. alpina subsp. alpina	LPS173-6	118	195	4	179	4	74	3		4	6	3.75	149.33
L. alpina subsp. alpina	LPS174-5	118	184	3	434	6	119	2		5	6	4.00	245.67
L. alpina subsp. cuneata	LPS168-9	118	251	4	328	6	120	3		5	6	4.50	233.00
L. alpina subsp. cuneata	LPS168-1	118	222	4	266	6	125	2		5	6	4.25	204.33
L. longipectinata	LPS189	118	230	2	437	3	141	3		4	6	3.00	269.33
Leucanthemopsis spec.	LPS186	79	58	2	75	3	85	1		2	4	2.00	72.67

Appendix 6: gene trees obtained from the Bayesian analyses in Chapter 4

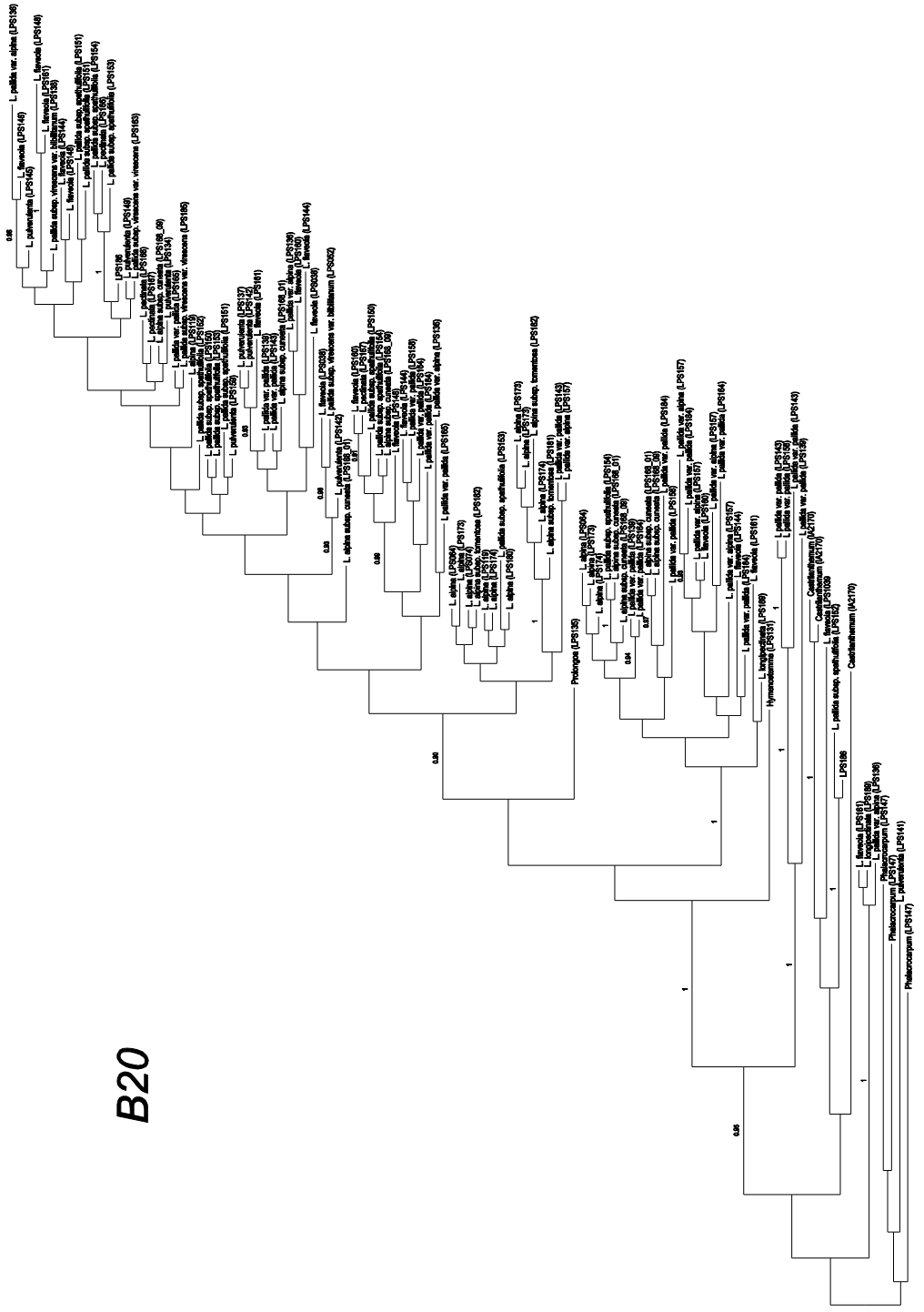


L. flaveola (LPS038)
L. pallida var. pallida (LPS165)
L. pallida subsp. spathulifolia (LPS150)
L. pallida subsp. spathulifolia (LPS153)
L. pulverulenta (LPS142)
L. pallida subsp. spathulifolia (LPS154)
L. pallida var. pallida (LPS164)
L. flaveola (LPS039)
L. alpina subsp. cuneata (LPS168_01)
L. pallida var. pallida (LPS143)
L. pulverulenta (LPS149)
L. flaveola (LPS039)
L. pulverulenta (LPS137)
L. pallida var. pallida (LPS165)
L. flaveola (LPS148)
L. pallida var. alpina (LPS157)
L. pallida var. pallida (LPS143)
L. pulverulenta (LPS134)
L. pallida var. pallida (LPS139)
L. flaveola (LPS146)
L. flaveola (LPS146)
L. alpina (LPS074)
L. alpina subsp. tomentosa (LPS182)
L. alpina (LPS119)
L. alpina subsp. tomentosa (LPS181)
L. alpina subsp. tomentosa (LPS182)
L. alpina subsp. tomentosa (LPS182)
L. pallida var. pallida (LPS158)
L. alpina subsp. cuneata (LPS168_01)
L. pallida var. pallida (LPS139)
L. pallida var. pallida (LPS158)
L. pallida subsp. viridescens var. viridescens (LPS183)
L. pulverulenta (LPS141)
L. pallida var. pallida (LPS158)
L. flaveola (LPS038)
L. pulverulenta (LPS149)
L. alpina subsp. cuneata (LPS168_09)
L. pallida var. pallida (LPS184)
L. flaveola (LPS160)
L. flaveola (LPS161)
L. pallida var. pallida (LPS184)
L. flaveola (LPS161)
L. pulverulenta (LPS141)
L. pulverulenta (LPS145)
L. alpina subsp. cuneata (LPS168_09)
L. flaveola (LPS039)
L. pulverulenta (LPS159)
L. flaveola (LPS146)
L. pallida var. alpina (LPS136)
L. alpina (LPS064)
L. pallida subsp. spathulifolia (LPS153)
L. pallida var. alpina (LPS138)
L. flaveola (LPS144)
L. pallida var. pallida (LPS184)
L. pallida subsp. viridescens var. bilbillanum (LPS052)
L. alpina subsp. tomentosa (LPS182)
L. pulverulenta (LPS134)
L. alpina (LPS180)
L. pulverulenta (LPS142)
L. pallida var. pallida (LPS165)
LPS186
L. longipectinata (LPS189)
L. flaveola (LPS161)
L. flaveola (LPS039)
L. flaveola (LPS148)
L. flaveola (LPS145)
L. flaveola (LPS146)
LPS168_1_5
L. alpina subsp. cuneata (LPS168_01)
L. alpina subsp. cuneata (LPS168_09)
L. pallida var. pallida (LPS139)
L. alpina subsp. cuneata (LPS168_01)
L. flaveola (LPS144)
L. flaveola (LPS160)
L. flaveola (LPS039)
L. flaveola (LPS161)
L. pectinata (LPS169)
L. pectinata (LPS166)
L. pallida subsp. spathulifolia (LPS150)
L. pallida var. alpina (LPS157)
L. pulverulenta (LPS137)
L. pallida var. pallida (LPS184)
L. flaveola (LPS160)
L. pallida subsp. spathulifolia (LPS151)
L. pallida subsp. spathulifolia (LPS154)
L. pallida subsp. spathulifolia (LPS154)
L. pallida subsp. spathulifolia (LPS150)
L. alpina subsp. cuneata (LPS168_01)
L. alpina subsp. cuneata (LPS168_09)
L. pallida var. pallida (LPS143)
L. pallida var. pallida (LPS164)
L. alpina subsp. cuneata (LPS168_01)
L. alpina subsp. cuneata (LPS168_09)
L. pallida var. pallida (LPS164)
L. pallida subsp. spathulifolia (LPS152)
LPS186
L. pallida subsp. spathulifolia (LPS152)
L. pallida subsp. spathulifolia (LPS151)
LPS186
L. pallida subsp. viridescens var. viridescens (LPS183)
L. pallida subsp. viridescens var. viridescens (LPS186)
L. pallida subsp. viridescens var. bilbillanum (LPS052)
L. alpina (LPS174)
L. alpina (LPS174)
L. alpina (LPS173)
Hymenostemma (LPS131)
L. alpina (LPS174)
Prolongoa (LPS135)
L. alpina (LPS119)
L. alpina (LPS174)
L. alpina (LPS180)
L. alpina (LPS173)
L. alpina (LPS173)
L. pectinata (LPS167)
L. pallida subsp. viridescens var. bilbillanum (LPS052)
L. pallida subsp. spathulifolia (LPS152)
L. pallida subsp. spathulifolia (LPS152)
L. pallida subsp. spathulifolia (LPS153)
L. pallida subsp. viridescens var. bilbillanum (LPS138)
L. pulverulenta (LPS145)
L. pulverulenta (LPS159)
L. alpina (LPS173)
L. alpina (LPS174)
L. pallida var. alpina (LPS157)
L. pallida subsp. spathulifolia (LPS150)
L. pallida var. pallida (LPS165)
L. pallida subsp. spathulifolia (LPS151)
L. alpina (LPS174)
Hymenostemma (LPS131)
L. longipectinata (LPS189)
L. longipectinata (LPS189)
L. pallida var. alpina (LPS135)
L. pectinata (LPS167)
L. alpina subsp. tomentosa (LPS181)
L. flaveola (LPS038)
L. flaveola (LPS160)
Castrillanthemum (IA2170)
Phaecrocarpum (LPS147)

C12

C16

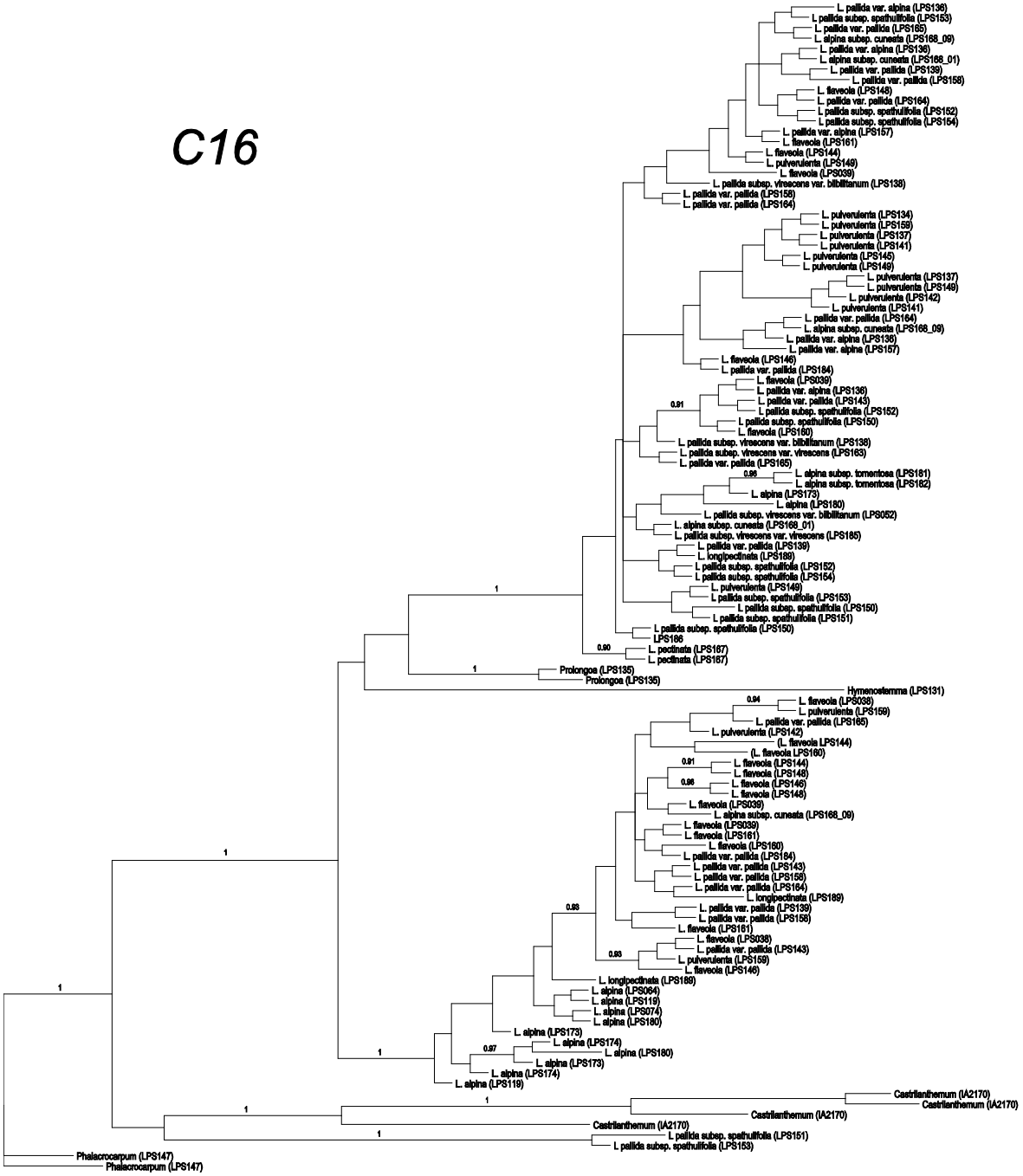
L. pallida var. alpina (LPS136)
L. pallida subsp. spathulifolia (LPS153)
L. pallida var. pallida (LPS165)
L. alpina subsp. cuneata (LPS168_09)
L. pallida var. alpina (LPS136)
L. alpina subsp. cuneata (LPS168_01)
L. pallida var. pallida (LPS139)
L. pallida var. pallida (LPS158)
L. flaveola (LPS148)
L. pallida var. pallida (LPS164)
L. pallida subsp. spathulifolia (LPS152)
L. pallida subsp. spathulifolia (LPS154)
L. pallida var. alpina (LPS157)
L. flaveola (LPS161)
L. flaveola (LPS144)
L. pulverulenta (LPS149)
L. flaveola (LPS039)
L. pallida subsp. virescens var. bilbilitanum (LPS138)
L. pallida var. pallida (LPS155)
L. pallida var. pallida (LPS164)
L. pulverulenta (LPS134)
L. pulverulenta (LPS159)
L. pulverulenta (LPS137)
L. pulverulenta (LPS141)
L. pulverulenta (LPS145)
L. pulverulenta (LPS149)
L. pulverulenta (LPS137)
L. pulverulenta (LPS149)
L. pulverulenta (LPS142)
L. pulverulenta (LPS141)
L. pallida var. pallida (LPS164)
L. alpina subsp. cuneata (LPS168_09)
L. pallida var. alpina (LPS136)
L. pallida var. alpina (LPS157)
L. flaveola (LPS146)
L. pallida var. pallida (LPS184)
L. flaveola (LPS039)
L. pallida var. alpina (LPS136)
L. pallida var. pallida (LPS143)
L. pallida subsp. spathulifolia (LPS152)
L. pallida subsp. spathulifolia (LPS150)
L. flaveola (LPS160)
L. pallida subsp. virescens var. bilbilitanum (LPS138)
L. pallida subsp. virescens var. virescens (LPS163)
L. pallida var. pallida (LPS165)
L. alpina subsp. tomentosa (LPS181)
L. alpina subsp. tomentosa (LPS182)
L. alpina (LPS173)
L. alpina (LPS180)
L. pallida subsp. virescens var. bilbilitanum (LPS052)
L. alpina subsp. cuneata (LPS168_01)
L. pallida subsp. virescens var. virescens (LPS185)
L. pallida var. pallida (LPS139)
L. longipectinata (LPS189)
L. pallida subsp. spathulifolia (LPS152)
L. pallida subsp. spathulifolia (LPS154)
L. pulverulenta (LPS149)
L. pallida subsp. spathulifolia (LPS153)
L. pallida subsp. spathulifolia (LPS150)
L. pallida subsp. spathulifolia (LPS151)
L. pallida subsp. spathulifolia (LPS150)
LPS186
L. pectinata (LPS167)
L. pectinata (LPS167)
Prolongoa (LPS135)
Prolongoa (LPS135)
Hymenostemma (LPS131)
L. flaveola (LPS038)
L. pulverulenta (LPS159)
L. pallida var. pallida (LPS165)
L. pulverulenta (LPS142)
(L. flaveola LPS144)
(L. flaveola LPS160)
L. flaveola (LPS144)
L. flaveola (LPS148)
L. flaveola (LPS146)
L. flaveola (LPS148)
L. flaveola (LPS039)
L. alpina subsp. cuneata (LPS168_09)
L. flaveola (LPS039)
L. flaveola (LPS161)
L. flaveola (LPS160)
L. pallida var. pallida (LPS184)
L. pallida var. pallida (LPS143)
L. pallida var. pallida (LPS158)
L. pallida var. pallida (LPS164)
L. longipectinata (LPS189)
L. pallida var. pallida (LPS139)
L. pallida var. pallida (LPS158)
L. flaveola (LPS161)
L. flaveola (LPS038)
L. pallida var. pallida (LPS143)
L. pulverulenta (LPS159)
L. flaveola (LPS146)
L. longipectinata (LPS189)
L. alpina (LPS064)
L. alpina (LPS119)
L. alpina (LPS074)
L. alpina (LPS180)
L. alpina (LPS173)
L. alpina (LPS174)
L. alpina (LPS180)
L. alpina (LPS173)
L. alpina (LPS174)
L. alpina (LPS119)
Castrillanthemum (IA2170)
Castrillanthemum (IA2170)
Castrillanthemum (IA2170)
L. pallida subsp. spathulifolia (LPS151)
L. pallida subsp. spathulifolia (LPS153)
Phalacrocarpum (LPS147)
Phalacrocarpum (LPS147)
1
0.91
0.96
1
0.90
1
1
0.94
0.91
0.96
0.93
0.93
1
0.97
1
1
1
1

D35

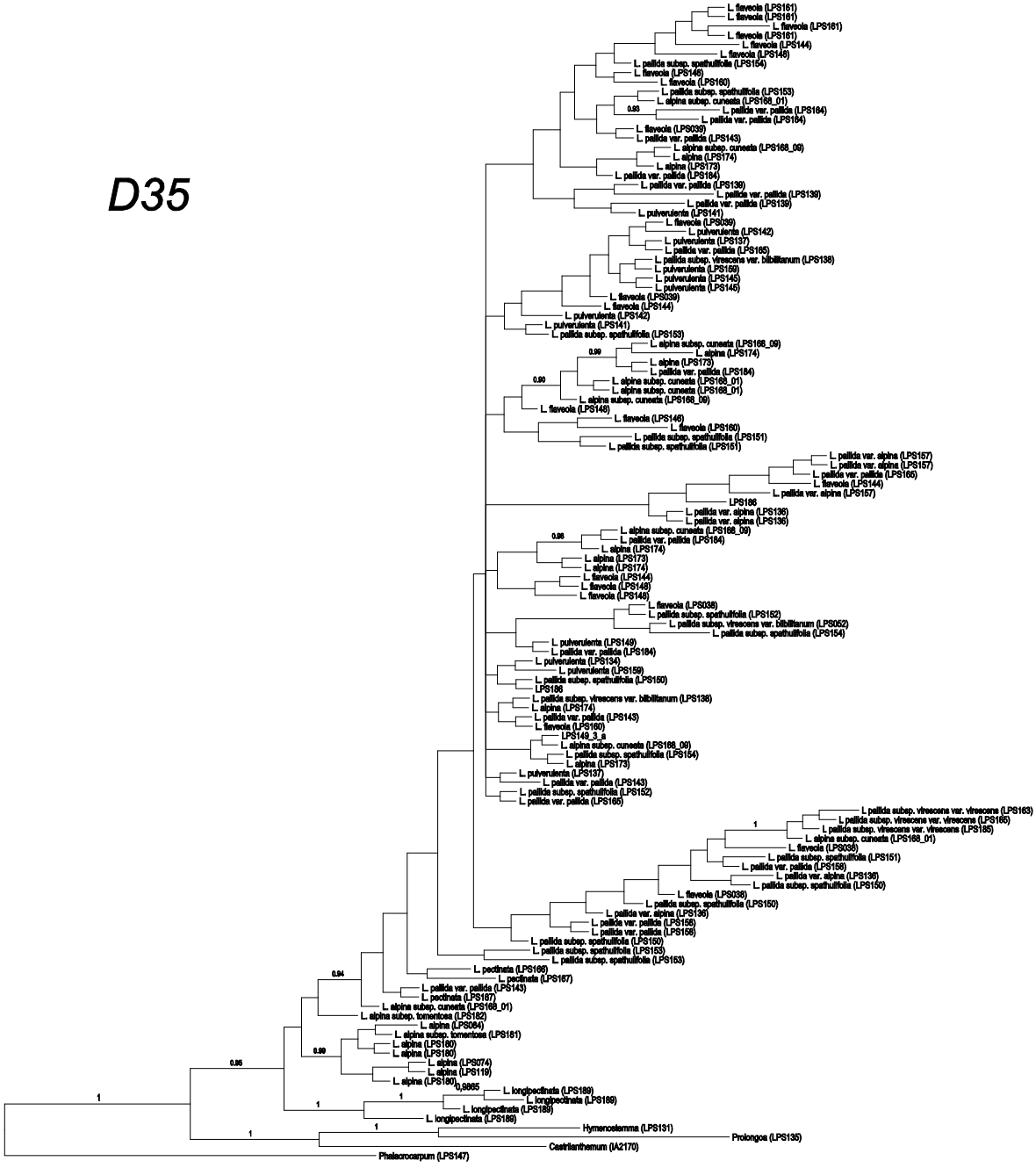
L. flavecola (LPS161)
L. flavecola (LPS161)
L. flavecola (LPS161)
L. flavecola (LPS161)
L. flavecola (LPS144)
L. flavecola (LPS146)
L. pallida subsp. spathulifolia (LPS154)
L. flavecola (LPS146)
L. flavecola (LPS160)
L. pallida subsp. spathulifolia (LPS153)
L. alpina subsp. cuneata (LPS168_01)
0.93
L. pallida var. pallida (LPS164)
L. pallida var. pallida (LPS164)
L. flavecola (LPS039)
L. pallida var. pallida (LPS143)
L. alpina subsp. cuneata (LPS168_09)
L. alpina (LPS174)
L. alpina (LPS173)
L. pallida var. pallida (LPS164)
L. pallida var. pallida (LPS139)
L. pallida var. pallida (LPS139)
L. pallida var. pallida (LPS138)
L. pulverulenta (LPS141)
L. flavecola (LPS039)
L. pulverulenta (LPS142)
L. pulverulenta (LPS137)
L. pallida var. pallida (LPS165)
L. pallida subsp. viridescens var. bibilitanum (LPS138)
L. pulverulenta (LPS159)
L. pulverulenta (LPS145)
L. pulverulenta (LPS145)
L. flavecola (LPS039)
L. flavecola (LPS144)
L. pulverulenta (LPS142)
L. pulverulenta (LPS141)
L. pallida subsp. spathulifolia (LPS153)
L. alpina subsp. cuneata (LPS168_09)
0.99
L. alpina (LPS174)
L. alpina (LPS173)
L. pallida var. pallida (LPS164)
0.99
L. alpina subsp. cuneata (LPS168_01)
L. alpina subsp. cuneata (LPS168_01)
L. alpina subsp. cuneata (LPS168_09)
L. flavecola (LPS148)
L. flavecola (LPS146)
L. flavecola (LPS160)
L. pallida subsp. spathulifolia (LPS151)
L. pallida subsp. spathulifolia (LPS151)
L. pallida var. alpina (LPS157)
L. pallida var. alpina (LPS157)
L. pallida var. pallida (LPS165)
L. flavecola (LPS144)
L. pallida var. alpina (LPS157)
LPS186
L. pallida var. alpina (LPS136)
L. pallida var. alpina (LPS136)
L. alpina subsp. cuneata (LPS168_09)
0.86
L. pallida var. pallida (LPS164)
L. alpina (LPS174)
L. alpina (LPS173)
L. alpina (LPS174)
L. flavecola (LPS144)
L. flavecola (LPS148)
L. flavecola (LPS148)
L. flavecola (LPS038)
L. pallida subsp. spathulifolia (LPS152)
L. pallida subsp. viridescens var. bibilitanum (LPS052)
L. pallida subsp. spathulifolia (LPS154)
L. pulverulenta (LPS149)
L. pallida var. pallida (LPS184)
L. pulverulenta (LPS134)
L. pulverulenta (LPS159)
L. pallida subsp. spathulifolia (LPS150)
LPS186
L. pallida subsp. viridescens var. bibilitanum (LPS136)
L. alpina (LPS174)
L. pallida var. pallida (LPS143)
L. flavecola (LPS160)
LPS149_3_a
L. alpina subsp. cuneata (LPS168_09)
L. pallida subsp. spathulifolia (LPS154)
L. alpina (LPS173)
L. pulverulenta (LPS137)
L. pallida var. pallida (LPS143)
L. pallida subsp. spathulifolia (LPS152)
L. pallida var. pallida (LPS165)
L. pallida subsp. viridescens var. viridescens (LPS163)
1
L. pallida subsp. viridescens var. viridescens (LPS165)
L. pallida subsp. viridescens var. viridescens (LPS165)
L. alpina subsp. cuneata (LPS168_01)
L. flavecola (LPS038)
L. pallida subsp. spathulifolia (LPS151)
L. pallida var. pallida (LPS156)
L. pallida var. alpina (LPS136)
L. pallida subsp. spathulifolia (LPS150)
L. flavecola (LPS038)
L. pallida subsp. spathulifolia (LPS150)
L. pallida var. alpina (LPS136)
L. pallida var. pallida (LPS156)
L. pallida var. pallida (LPS156)
L. pallida subsp. spathulifolia (LPS150)
L. pallida subsp. spathulifolia (LPS153)
L. pallida subsp. spathulifolia (LPS153)
L. pectinata (LPS166)
0.94
L. pectinata (LPS167)
L. pallida var. pallida (LPS143)
L. pectinata (LPS187)
L. alpina subsp. cuneata (LPS168_01)
L. alpina subsp. tomentosa (LPS182)
L. alpina (LPS084)
L. alpina subsp. tomentosa (LPS181)
L. alpina (LPS180)
0.99
L. alpina (LPS180)
0.85
L. alpina (LPS074)
L. alpina (LPS119)
L. alpina (LPS180)
0.9885
L. longipectinata (LPS189)
1
1
L. longipectinata (LPS189)
L. longipectinata (LPS189)
L. longipectinata (LPS189)
1
Hymenostemma (LPS131)
1
Prolongos (LPS135)
Castrilanthemum (IA2170)
Phalacrocarpum (LPS147)

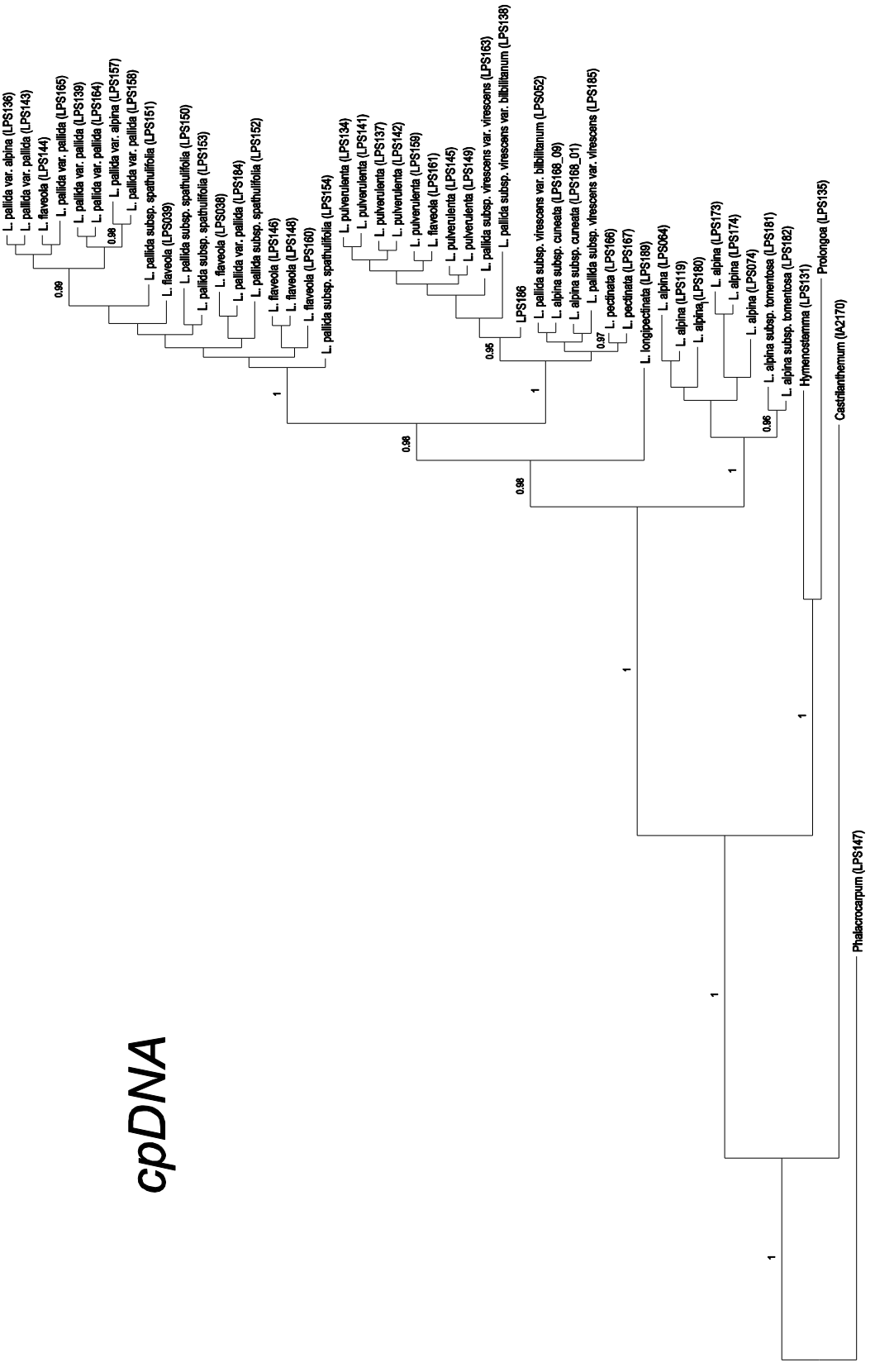
cpDNA
L. pallida var. alpina (LPS136)
L. pallida var. pallida (LPS143)
L. flaveola (LPS144)
L. pallida var. pallida (LPS165)
L. pallida var. pallida (LPS139)
L. pallida var. pallida (LPS164)
L. pallida var. alpina (LPS157)
L. pallida var. pallida (LPS158)
L. pallida subsp. spathulifolia (LPS151)
L. flaveola (LPS039)
L. pallida subsp. spathulifolia (LPS150)
L. pallida subsp. spathulifolia (LPS153)
L. flaveola (LPS038)
L. pallida var. pallida (LPS184)
L. pallida subsp. spathulifolia (LPS152)
L. flaveola (LPS146)
L. flaveola (LPS148)
L. flaveola (LPS160)
L. pallida subsp. spathulifolia (LPS154)
L. pulverulenta (LPS134)
L. pulverulenta (LPS141)
L. pulverulenta (LPS137)
L. pulverulenta (LPS142)
L. pulverulenta (LPS159)
L. flaveola (LPS161)
L. pulverulenta (LPS145)
L. pulverulenta (LPS149)
L. pallida subsp. virescens var. virescens (LPS163)
L. pallida subsp. virescens var. bibilitanum (LPS138)
LPS186
L. pallida subsp. virescens var. bibilitanum (LPS052)
L. alpina subsp. cuneata (LPS168_09)
L. alpina subsp. cuneata (LPS168_01)
L. pallida subsp. virescens var. virescens (LPS185)
L. pectinata (LPS166)
L. pectinata (LPS167)
L. longipectinata (LPS189)
L. alpina (LPS064)
L. alpina (LPS119)
L. alpina (LPS180)
L. alpina (LPS173)
L. alpina (LPS174)
L. alpina (LPS074)
L. alpina subsp. tomentosa (LPS181)
L. alpina subsp. tomentosa (LPS182)
Hymenostemma (LPS131)
Prolongoa (LPS135)
Castrilanthemum (IA2170)
Phalacrocarpum (LPS1447)
0.99
0.98
1
1
0.98
0.95
1
0.97
1
1
1
0.86
1
1
1

Appendix 7: flow cytometric measurements and GenBank numbers

Sample	Petunia Peak	CV (%)	Leucant. Peak	CV (%)	Leucant./ Petunia ratio	Date	Ploidy	Haplotype	*psbA-trnH*	*trnC-petN*
LPS064-1	5.47	2.73	18.33	2.71	3.351	9.11.2012	2*x*	H11		
LPS064-2	5.41	4.27	19.29	3.64	3.566	14.3.2011	2*x*	H11		
LPS064-3	5.08	3.73	18.1	3.57	3.563	14.3.2011	2*x*	H11		
LPS064-4	5.02	3.24	17.72	3.29	3.530	14.3.2011	2*x*			
LPS064-5	5.09	3.6	17.51	4.88	3.440	14.3.2011	2*x*			
LPS065-1	6.33	2.44	36.9	3.37	5.829	6.11.2014	4*x*	H25		
LPS065-2	4.81	4.14	30.09	4.12	6.256	14.3.2011	4*x*	H17		
LPS065-3	5.09	4.64	31.45	6.68	6.179	14.3.2011	4*x*	H25		
LPS065-4	4.97	3.85	30	7.61	6.036	14.3.2011	4*x*			
LPS065-5	4.17	5.22	22.69	9.84	5.441	14.3.2011	4*x*			
LPS066-7	6.16	5.52	38.87	5.36	6.310	2.2.2011	4*x*	H26		
LPS066-1	3.47	4.72	20.79	9.69	5.991	14.3.2011	4*x*	H26		
LPS066-2	6.17	2.51	32.14	5.58	5.209	6.11.2014	4*x*	H26		
LPS066-3	6.17	2.52	33.8	5.41	5.478	6.11.2014	4*x*			
LPS066-4	5.5	3.67	32.02	4.54	5.822	14.3.2011	4*x*			
LPS067-1	5.54	6.57	19.58	7.18	3.534	2.2.2011	2*x*	H1		
LPS067-2	6.18	2.41	19.35	3.37	3.131	6.11.2014	2*x*	H1		
LPS067-3	5.73	4.58	17.77	5.88	3.101	14.3.2011	2*x*	H1		
LPS067-4	5.66	3.14	18.45	3.83	3.260	14.3.2011	2*x*			
LPS067-5	5.54	3.3	18.56	5.23	3.170	14.3.2011	2*x*			
LPS068-6	6.16	2.53	20.41	3.15	3.313	6.11.2014	2*x*	H23		
LPS068-2	4.81	5	14.54	8.99	3.023	14.3.2011	2*x*	H23		
LPS068-3	5.36	3.87	16.45	8.08	3.069	14.3.2011	2*x*	H23		
LPS068-4	5.42	4.16	17.88	4.84	3.299	14.3.2011	2*x*			
LPS068-7	6.17	2.5	19.74	2.51	3.199	6.11.2014	2*x*			
LPS069-1	6.28	6.15	21.46	5.45	3.417	2.2.2011	2*x*	H24		
LPS069-2	5.73	3.69	19.02	4.46	3.319	14.3.2011	2*x*	H24		
LPS069-3	5.99	4.13	27.86	5.36	4.651	14.3.2011	3*x*	H24		
LPS069-4	5.38	3.82	17.35	7.61	3.225	14.3.2011	2*x*			
LPS069-5	5.85	4.28	19.15	5.25	3.274	14.3.2011	2*x*			
LPS070-4	6.02	2.52	18.89	4.06	3.138	6.11.2014	2*x*	H24		
LPS070-1	5.84	3.67	18.52	4.62	3.171	15.3.2011	2*x*	H24		

Sample	Petunia Peak	CV (%)	Leucant. Peak	CV (%)	Leucant./ Petunia ratio	Date	Ploidy	Haplotype	*psbA-trnH*	*trnC-petN*
LPS178-2	5.06	2.5	25.32	2.84	5.004	21.8.2012	4*x*	H36		
LPS178-3	4.88	3.31	23.99	2.58	4.916	21.8.2012	4*x*			
LPS178-4	4.67	3.48	23.19	3.58	4.966	21.8.2012	4*x*			
LPS178-10	5.59	2.86	30.7	4.05	5.492	21.8.2012	4*x*	H36		
LPS179-1	5.53	3.41	29.66	3.56	5.363	21.8.2012	4*x*	H43		
LPS179-2	5.6	2.77	30.09	4	5.373	21.8.2012	4*x*	H43		
LPS179-3	5.59	2.82	29.59	3.65	5.293	21.8.2012	4*x*	H43		
LPS179-4	5.54	3.36	31.35	2.77	5.659	21.8.2012	4*x*			
LPS179-5	5.53	3.4	28.9	3.15	5.226	21.8.2012	4*x*			
LPS179-6	5.31	2.54	29.2	2.58	5.499	31.8.2012	4*x*			
LPS179-7	5.31	2.56	26.77	3.56	5.041	31.8.2012	4*x*			
LPS179-8	5.06	2.53	25.56	4.57	5.051	31.8.2012	4*x*			
LPS179-9	5.07	2.53	27.35	3.39	5.394	31.8.2012	4*x*			
LPS179-10	5.09	2.44	27.83	2.57	5.468	31.8.2012	4*x*			
LPS179-11	4.93	3.87	25.85	4.06	5.243	31.8.2012	4*x*			
LPS179-12	5.25	3.11	29.19	2.59	5.560	31.8.2012	4*x*			
LPS179-13	5.2	2.54	28.53	2.54	5.487	31.8.2012	4*x*			
LPS180-1	5.32	2.58	29.23	2.47	5.494	21.8.2012	4*x*	H43		
LPS180-2	5.18	2.56	28.84	3.17	5.568	21.8.2012	4*x*	H43		
LPS180-3	4.92	2.92	27.2	3.99	5.528	21.8.2012	4*x*	H43		
LPS180-4	5	3.45	27.38	3.49	5.476	21.8.2012	4*x*			
LPS180-5	4.99	3.47	27.7	4.08	5.551	21.8.2012	4*x*			
LPS181-1	5.2	2.59	16.78	3.14	3.227	23.8.2012	2*x*	H46		
LPS181-2	5.46	2.88	17.48	4.16	3.201	23.8.2012	2*x*	H45		
LPS181-3	5.4	3.56	17.7	4.65	3.278	23.8.2012	2*x*	H46	KM589776	KM589793
LPS181-4	5.41	3.54	17.22	3.22	3.183	23.8.2012	2*x*			
LPS181-5	5.15	3.2	16.59	2.6	3.221	23.8.2012	2*x*			
LPS182-1	4.98	3.45	15.44	4.18	3.100	23.8.2012	2*x*	H17		
LPS182-2	5.24	3.19	17.02	2.57	3.248	23.8.2012	2*x*	H36		
LPS182-3	5.07	2.56	16.58	2.58	3.270	23.8.2012	2*x*	H18		
LPS182-4	5.26	3.21	16.84	3.24	3.202	23.8.2012	2*x*			
LPS182-5	5	3.57	16.11	4.18	3.222	23.8.2012	2*x*			

Sample	Petunia Peak	CV (%)	Leucant. Peak	CV (%)	Leucant./ Petunia ratio	Date	Ploidy	Haplotype	*psbA-trnH*	*trnC-petN*
LPS077-2	6.08	3.05	19.69	5.03	3.238	31.1.2012	2*x*	H21		
LPS077-3	5.86	2.76	19.76	2.57	3.372	31.1.2012	2*x*	H21		
LPS077-4	6.03	2.54	19.99	3.07	3.315	31.1.2012	2*x*			
LPS077-5	5.95	3.38	20.43	3.05	3.434	31.1.2012	2*x*			
LPS078-1	5.55	5.98	18.67	5.44	3.364	2.2.2011	2*x*	H17		
LPS078-2	5.86	3.92	20.38	3.08	3.478	31.1.2012	2*x*	H17		
LPS078-3	5.7	3.95	19.66	9.94	3.449	31.1.2012	2*x*	H17		
LPS078-4	5.36	4.08	17.67	4.63	3.297	31.1.2012	2*x*			
LPS078-5	5.52	3.41	17.77	3.4	3.219	31.1.2012	2*x*			
LPS079-1	4.53	8.03	15.54	6.14	3.430	2.2.2011	2*x*	H17		
LPS079-2	5.87	3.95	20.17	3.83	3.436	31.1.2012	2*x*	H28		
LPS079-3	5.54	3.42	18.32	4.07	3.307	31.1.2012	2*x*	H17		
LPS079-4	4.94	4.94	16.22	5.26	3.283	31.1.2012	2*x*			
LPS079-5	5.72	2.8	19.91	4.59	3.481	31.1.2012	2*x*			
LPS080-1	5.58	5.38	20.87	5.25	3.740	2.2.2011	2*x*	H21		
LPS080-2	5.91	3.36	19.94	3.06	3.374	31.1.2012	2*x*	H17		
LPS080-3	5.47	3.92	17.8	5.16	3.254	31.1.2012	2*x*	H22		
LPS080-9	5.14	3.13	17.9	4.06	3.482	31.1.2012	2*x*			
LPS080-10	5.78	4.47	19.31	4.62	3.341	31.1.2012	2*x*			
LPS081-1	5.67	3.19	18.54	3.31	3.270	31.1.2012	2*x*	H17		
LPS081-2	5.55	3.34	18.71	2.81	3.371	31.1.2012	2*x*	H17		
LPS081-3	5.85	2.81	19.43	3.5	3.321	31.1.2012	2*x*			
LPS081-11	5.59	2.79	19.31	4.75	3.454	31.1.2012	2*x*			
LPS081-5	5.57	4.35	18.87	3.96	3.388	4.2.2011	2*x*	H17		
LPS082-1	5.66	2.2	36.02	4.44	6.364	31.1.2012	4*x*	H17		
LPS082-2	5.66	2.15	35.32	3.31	6.240	31.1.2012	4*x*	H17		
LPS082-3	5.66	2.24	34.49	4.41	6.094	31.1.2012	4*x*			
LPS082-4	5.4	3.31	32.6	4.58	6.037	31.1.2012	4*x*			
LPS082-9	6.12	6.02	37.96	5.78	6.203	2.2.2011	4*x*	H1		
LPS083-1	5.3	2.45	33.53	3.2	6.326	31.1.2012	4*x*	H29		
LPS083-2	5.67	2.2	34.31	3.12	6.051	31.1.2012	4*x*	H29		
LPS083-3	5.53	2.23	33.51	3.05	6.060	31.1.2012	4*x*			

Sample	Petunia Peak	CV (%)	Leucant. Peak	CV (%)	Leucant./ Petunia ratio	Date	Ploidy	Haplotype	*psbA-trnH*	*trnC-petN*
LPS083-4	5.59	2.74	33.95	3.7	6.073	31.1.2012	4*x*			
LPS083-8	4.89	6.97	31.92	4.57	6.528	2.2.2011	4*x*	H30		
LPS084-1	6.02	6.19	21.91	4.72	3.640	2.2.2011	2*x*	H17		
LPS084-2	6.03	2.52	20.14	2.59	3.340	16.2.2012	2*x*	H17		
LPS084-3	5.72	2.73	19.93	3.16	3.484	16.2.2012	2*x*	H17		
LPS084-4	6.03	2.5	20.75	4	3.441	16.2.2012	2*x*			
LPS084-5	5.53	3.32	18.1	4.69	3.273	16.2.2012	2*x*			
LPS085-1	5.4	4.4	35.37	4.69	6.550	4.2.2011	4*x*	H1		
LPS085-2	5.86	2.82	36.27	3.34	6.189	16.2.2012	4*x*	H1		
LPS085-3	5.6	1.64	34.69	2.59	6.195	16.2.2012	4*x*			
LPS085-4	5.6	2.75	33.73	3.62	6.023	16.2.2012	4*x*			
LPS085-5	5.91	3.4	35.8	4.01	6.058	16.2.2012	4*x*			
LPS086-1	5.79	2.23	36.89	3.46	6.371	16.2.2012	4*x*	H16		
LPS086-2	5.32	2.52	33.21	3.94	6.242	16.2.2012	4*x*	H13		
LPS086-3	5.66	2.2	34.92	4	6.170	16.2.2012	4*x*			
LPS086-4	5.58	2.79	33.91	5.57	6.077	16.2.2012	4*x*			
LPS086-8	5.09	4.72	31.83	4.61	6.253	4.2.2011	4*x*	H13		
LPS087-1	4.67	6.37	15.78	6.59	3.379	4.2.2011	2*x*	H6		
LPS087-2	5.48	2.78	18.33	3.94	3.345	16.2.2012	2*x*	H1		
LPS087-3	5.58	2.74	18.96	3.43	3.398	16.2.2012	2*x*	H1		
LPS087-4	5.26	1.94	17.7	3.34	3.365	16.2.2012	2*x*			
LPS087-10	5.26	3.12	33.14	5.36	6.300	16.2.2012	4*x*			
LPS087-5	5.07	2.51	16.6	2.53	3.274	31.8.2012	2*x*			
LPS087-6	5.07	2.5	15.97	3.46	3.150	31.8.2012	2*x*			
LPS087-7	5.52	3.46	17.2	3.17	3.116	31.8.2012	2*x*			
LPS087-8	5.31	2.55	17.02	2.57	3.205	31.8.2012	2*x*			
LPS087-9	5.32	2.58	16.77	3.28	3.152	31.8.2012	2*x*			
LPS088-1	5.41	4.42	19.29	4.65	3.566	4.2.2011	2*x*	H28		
LPS088-2	5.73	2.77	19.32	2.78	3.372	16.2.2012	2*x*	H28		
LPS088-3	5.79	2.23	19.39	3.39	3.349	16.2.2012	2*x*			
LPS088-4	5.41	3.43	18.13	3.64	3.351	16.2.2012	2*x*			
LPS088-5	5.48	2.77	18.79	3.96	3.429	16.2.2012	2*x*			

Sample	Petunia Peak	CV (%)	Leucant. Peak	CV (%)	Leucant./ Petunia ratio	Date	Ploidy	Haplotype	*psbA-trnH*	*trnC-petN*
LPS089-1	5.35	4.86	19.03	4.27	3.557	4.2.2011	2*x*	H17		
LPS089-2	5.59	2.74	18.96	3.32	3.392	21.2.2012	2*x*	H17		
LPS089-3	5.86	2.78	19.01	3.38	3.244	21.2.2012	2*x*	H12		
LPS089-4	5.47	2.78	18.29	2.82	3.344	21.2.2012	2*x*			
LPS089-5	5.72	2.82	18.52	3.52	3.238	21.2.2012	2*x*			
LPS090-1	5.4	5.67	35.74	3.98	6.619	4.2.2011	4*x*	H1		
LPS090-2	5.6	1.63	34.35	1.9	6.134	21.2.2012	4*x*	H1		
LPS090-3	5.45	2.78	33.07	2.59	6.068	21.2.2012	4*x*	H17		
LPS090-4	5.14	1.89	32.95	3.99	6.411	21.2.2012	4*x*			
LPS090-5	5.57	2.78	34.25	3.18	6.149	21.2.2012	4*x*			
LPS090-6	5.2	2.57	30.66	4.08	5.896	31.8.2012	4*x*			
LPS090-7	5.19	2.62	30.39	3.52	5.855	31.8.2012	4*x*			
LPS090-8	5.31	2.59	29.67	3.6	5.588	31.8.2012	4*x*			
LPS090-9	5.54	2.21	33.88	2.64	6.116	31.8.2012	4*x*			
LPS090-10	5.48	2.86	32.89	4.12	6.002	31.8.2012	4*x*			
LPS091-1	5.74	2.77	35.29	3.36	6.148	21.2.2012	4*x*	H1		
LPS091-2	5.68	3.29	35.2	3.38	6.197	21.2.2012	4*x*	H1		
LPS091-3	5.52	2.18	33.35	32.27	6.042	21.2.2012	4*x*			
LPS091-4	6.01	2.55	35.66	3.97	5.933	21.2.2012	4*x*			
LPS091-9	5.31	2.54	32.97	3.91	6.209	4.2.2011	4*x*	H1		
LPS092-1	5.21	5.1	18.37	4.69	3.526	4.2.2011	2*x*	H1		
LPS092-2	5.8	3.32	18.74	2.82	3.231	21.2.2012	2*x*	H1		
LPS092-3	5.83	3.79	18.8	3.88	3.225	21.2.2012	2*x*	H1		
LPS092-4	5.66	2.19	18.72	2.8	3.307	21.2.2012	2*x*			
LPS092-5	5.59	2.8	18.56	3.34	3.320	21.2.2012	2*x*			
LPS093-1	5.02	4.48	17.99	4.76	3.584	4.2.2011	2*x*	H17		
LPS093-2	5.33	2.48	17.9	2.8	3.358	21.2.2012	2*x*	H17		
LPS093-3	5.47	2.8	18.58	3.38	3.397	21.2.2012	2*x*	H17		
LPS093-11	5.54	3.21	18.75	3.86	3.384	21.2.2012	2*x*			
LPS093-12	5.13	1.96	17.91	2.81	3.491	21.2.2012	2*x*			
LPS094-1	5.86	2.83	19.21	3.94	3.278	21.2.2012	2*x*	H12		
LPS094-2	5.07	2.53	17.76	3.31	3.503	21.2.2012	2*x*	H5		

Sample	Petunia Peak	CV (%)	Leucant. Peak	CV (%)	Leucant./ Petunia ratio	Date	Ploidy	Haplotype	*psbA-trnH*	*trnC-petN*
LPS094-3	4.61	6.45	16.27	5.86	3.529	4.2.2011	2*x*	H5		
LPS094-4	5.46	2.8	18.13	3.36	3.321	21.2.2012	2*x*			
LPS094-5	5.14	1.95	17.03	2.43	3.313	21.2.2012	2*x*			
LPS095-1	5.25	4.27	18.03	3.67	3.434	4.2.2011	2*x*	H13		
LPS095-2	5.19	2.52	17.75	3.39	3.420	21.2.2012	2*x*	H1		
LPS095-3	4.99	3.34	16.77	3.1	3.361	21.2.2012	2*x*	H12		
LPS095-4	4.83	2.84	16.36	3.42	3.387	21.2.2012	2*x*			
LPS095-5	5.13	1.95	18.31	2.9	3.569	21.2.2012	2*x*			
LPS096-1	4.99	4.59	16.94	5.4	3.395	4.2.2011	2*x*	H1		
LPS096-2	5.74	2.71	19.27	4.07	3.357	28.2.2012	2*x*	H1		
LPS096-3	6.05	2.52	19.97	3.24	3.301	28.2.2012	2*x*	H12		
LPS096-4	5.73	2.77	19.35	3.52	3.377	28.2.2012	2*x*			
LPS096-5	5.88	2.81	19.69	2.54	3.349	28.2.2012	2*x*			
LPS097-1	5.12	7.16	34.17	6.01	6.674	4.2.2011	4*x*	H20		
LPS097-2	5.66	3.31	35.37	3.38	6.249	28.2.2012	4*x*	H19		
LPS097-3	5.48	2.77	33.5	3.22	6.113	28.2.2012	4*x*	H19		
LPS097-4	6.03	2.51	36.82	3.96	6.106	28.2.2012	4*x*			
LPS097-5	5.86	2.79	35.6	3.9	6.075	28.2.2012	4*x*			
LPS098-1	5.04	5.75	18.62	5.22	3.694	4.2.2011	2*x*	H7		
LPS098-2	5.8	3.21	19.17	2.76	3.305	28.2.2012	2*x*	H6		
LPS098-3	5.32	2.52	18.5	2.21	3.477	28.2.2012	2*x*	H8		
LPS098-4	5.32	2.52	18.12	3.38	3.406	28.2.2012	2*x*			
LPS098-5	5.59	2.81	18.99	3.36	3.397	28.2.2012	2*x*			
LPS099-1	5.32	2.53	33.47	3.19	6.291	28.2.2012	4*x*			
LPS099-2	5.14	1.9	32.59	3.35	6.340	28.2.2012	4*x*			
LPS099-3	5.32	2.47	33.5	3.15	6.297	28.2.2012	4*x*			
LPS099-4	5.47	6.17	36.29	4.42	6.634	4.2.2011	4*x*	H15		
LPS099-5	5.25	3.16	32.6	3.38	6.210	28.2.2012	4*x*			
LPS100-1	5.16	5.66	32.84	5	6.364	4.2.2011	4*x*	H32		
LPS100-2	5.43	3.38	32.98	4.2	6.074	28.2.2012	4*x*	H32		
LPS100-3	5.33	2.51	32.47	3.23	6.092	28.2.2012	4*x*	H1		
LPS100-4	5.33	2.48	32.85	4.17	6.163	28.2.2012	4*x*			

Sample	Petunia Peak	CV (%)	Leucant. Peak	CV (%)	Leucant./ Petunia ratio	Date	Ploidy	Haplotype	*psbA-trnH*	*trnC-petN*
LPS100-5	5.19	2.51	31.61	5.47	6.091	28.2.2012	4*x*			
LPS101-1	5.63	5.02	37.06	5.33	6.583	4.2.2011	4*x*	H34		
LPS101-2	5.13	1.88	32.08	2.72	6.253	28.2.2012	4*x*	H32		
LPS101-3	5.32	2.57	33.07	2.46	6.216	28.2.2012	4*x*	H32		
LPS101-4	5.17	2.48	32.09	3.98	6.207	28.2.2012	4*x*			
LPS101-5	5.14	3.16	31	4.67	6.031	28.2.2012	4*x*			
LPS102-1	5.32	2.57	31.54	4.03	5.929	28.2.2012	4*x*	H32		
LPS102-2	5.72	2.72	34.32	3.02	6.000	28.2.2012	4*x*	H32		
LPS102-3	5.42	3.26	32.25	3.96	5.950	28.2.2012	4*x*			
LPS102-4	5.72	2.78	35.89	3.87	6.274	28.2.2012	4*x*			
LPS102-6	5.45	4.97	33.96	3.75	6.231	4.2.2011	4*x*	H32		
LPS103-1	5.57	4.31	36.25	4.37	6.508	4.2.2011	4*x*	H32		
LPS103-2	5.6	2.81	33.62	3.02	6.004	28.2.2012	4*x*	H32		
LPS103-3	5.37	1.9	34.34	3.05	6.395	28.2.2012	4*x*	H32		
LPS103-4	5.41	3.32	34.8	3.83	6.433	28.2.2012	4*x*			
LPS103-5	5.31	2.58	33.84	3.64	6.373	28.2.2012	4*x*			
LPS104-1	5.57	2.72	31.7	3.29	5.691	6.3.2012	4*x*	H32		
LPS104-2	5.61	2.7	32.99	4.04	5.881	6.3.2012	4*x*	H32		
LPS104-3	5.54	2.15	32.63	3.38	5.890	6.3.2012	4*x*			
LPS104-4	5.38	1.91	30.46	5.41	5.662	6.3.2012	4*x*			
LPS104-10	5.29	4.32	33.97	3.58	6.422	4.2.2011	4*x*	H32		
LPS105-1	5.48	2.69	33.81	3.63	6.170	6.3.2012	4*x*	H10		
LPS105-2	5.46	2.81	33.18	4.74	6.077	6.3.2012	4*x*	H10		
LPS105-3	5.59	2.75	35.51	3.8	6.352	6.3.2012	4*x*			
LPS105-4	5.3	2.52	32.92	4.09	6.211	6.3.2012	4*x*			
LPS105-10	5.19	5.07	36.35	4.36	7.004	4.2.2011	4*x*	H1		
LPS106-1	5.53	4.31	19.54	4.19	3.533	4.2.2011	2*x*	H1		
LPS106-2	5.13	1.9	16.98	2.55	3.310	6.3.2012	2*x*	H1		
LPS106-3	5.46	2.78	18.11	3.44	3.317	6.3.2012	2*x*	H1		
LPS106-4	5.33	3.96	17.2	4.73	3.227	6.3.2012	2*x*			
LPS106-5	5.19	2.45	17.25	1.83	3.324	6.3.2012	2*x*			
LPS107-1	5.33	5.06	19.68	4.31	3.692	8.2.2011	2*x*	H1		

Sample	Petunia Peak	CV (%)	Leucant. Peak	CV (%)	Leucant./ Petunia ratio	Date	Ploidy	Haplotype	*psbA-trnH*	*trnC-petN*
LPS107-2	5.07	2.48	16.56	2.45	3.266	6.3.2012	2*x*	H1		
LPS107-3	5.07	2.46	17.21	2.94	3.394	6.3.2012	2*x*	H1		
LPS107-4	4.91	2.69	17.02	2.47	3.466	6.3.2012	2*x*			
LPS107-5	5.13	1.9	17.12	3.04	3.337	6.3.2012	2*x*			
LPS108-1	5.06	2.43	16.87	3.54	3.334	6.3.2012	2*x*	H1		
LPS108-2	5.21	2.45	18.14	3.41	3.482	6.3.2012	2*x*	H1		
LPS108-3	5.25	1.91	17.17	3.32	3.270	6.3.2012	2*x*			
LPS108-4	5.19	2.46	17.92	2.77	3.453	6.3.2012	2*x*			
LPS108-5	5	6.38	20.58	4.44	4.116	8.2.2011	2*x*	H1		
LPS109-1	5.45	3.99	36.36	4.79	6.672	8.2.2011	4*x*	H1		
LPS109-2	5.19	5.19	32.55	3.35	6.272	14.3.2012	4*x*	H1		
LPS109-3	5.3	2.5	33.87	3.67	6.391	14.3.2012	4*x*	H1		
LPS109-4	5.07	2.52	32.21	2.71	6.353	14.3.2012	4*x*			
LPS109-5	5.25	1.92	33.94	3.78	6.465	14.3.2012	4*x*			
LPS110-1	5.55	4.41	35.82	3.96	6.454	8.2.2011	4*x*	H32		
LPS110-2	5.25	2.97	31.63	3.27	6.025	14.3.2012	4*x*	H32		
LPS110-3	5.38	1.96	34.74	3.94	6.457	14.3.2012	4*x*	H33		
LPS110-4	5.2	2.53	31.79	3.36	6.113	14.3.2012	4*x*			
LPS110-5	5.46	2.77	32.84	4.18	6.015	14.3.2012	4*x*			
LPS111-1	5.37	4.03	34.26	6.47	6.380	8.2.2011	4*x*	H32		
LPS111-2	5.12	1.88	29.34	4.09	5.730	14.3.2012	4*x*	H32		
LPS111-3	5.2	2.51	29.37	3.92	5.648	14.3.2012	4*x*	H32		
LPS111-4	5.26	1.93	30.32	3.49	5.764	14.3.2012	4*x*			
LPS111-10	4.98	3.3	28.86	4.62	5.795	14.3.2012	4*x*			
LPS112-1	5.64	6.16	37.13	4.47	6.583	8.2.2011	4*x*	H32		
LPS112-2	5.2	2.48	32.04	3.95	6.162	14.3.2012	4*x*	H32		
LPS112-3	4.94	2.83	29.95	4.04	6.063	14.3.2012	4*x*	H32		
LPS112-4	5.19	2.54	31.44	2.82	6.058	14.3.2012	4*x*			
LPS112-5	5.08	2.47	31.77	3.41	6.254	14.3.2012	4*x*			
LPS113-1	5.9	3.97	37.38	5.25	6.336	8.2.2011	4*x*	H47		
LPS113-2	4.88	2.21	27.33	3.52	5.600	14.3.2012	4*x*	H47		
LPS113-3	5.3	2.49	32.18	4.05	6.072	14.3.2012	4*x*	H32		

Sample	Petunia Peak	CV (%)	Leucant. Peak	CV (%)	Leucant./ Petunia ratio	Date	Ploidy	Haplotype	*psbA-trnH*	*trnC-petN*
LPS113-4	5.25	1.88	31.39	2.77	5.979	14.3.2012	4*x*			
LPS113-5	4.97	3.48	26.98	4.09	5.429	14.3.2012	4*x*			
LPS114-1	5.8	4.52	37.94	4.45	6.541	8.2.2011	4*x*	H7		
LPS114-2	5.37	1.94	31.39	4.09	5.845	14.3.2012	4*x*	H15		
LPS114-3	5.3	2.46	31.38	2.87	5.921	14.3.2012	4*x*	H15		
LPS114-4	5.31	2.45	32.09	2.82	6.043	14.3.2012	4*x*			
LPS114-5	5.32	2.5	33.15	2.5	6.231	14.3.2012	4*x*			
LPS115-1	5.5	3.84	35.4	4.37	6.436	8.2.2011	4*x*	H3		
LPS115-2	4.94	2.75	27.57	5.21	5.581	14.3.2012	4*x*	H3		
LPS115-3	5.4	3.26	30.76	4.01	5.696	14.3.2012	4*x*	H3		
LPS115-4	5.31	2.48	31.21	4.8	5.878	14.3.2012	4*x*			
LPS115-5	5.2	2.45	29.73	3.49	5.717	14.3.2012	4*x*			
LPS116-1	5.36	4.93	32.71	5.69	6.103	8.2.2011	4*x*			
LPS116-2	5.26	3.05	31.48	3.93	5.985	31.7.2012	4*x*	H14		
LPS116-3	5.19	5.51	28.92	3.14	5.572	31.7.2012	4*x*	H16		
LPS116-4	5.19	2.55	30.21	4.8	5.821	31.7.2012	4*x*			
LPS116-5	5.87	2.73	34.08	3.77	5.806	6.11.2014	4*x*			
LPS117-1	5.29	5.99	35.52	5.49	6.715	8.2.2011	4*x*			
LPS117-2	5.58	2.73	31.38	4.02	5.624	31.7.2012	4*x*	H32		
LPS117-3	5.6	2.72	32.42	3.2	5.789	31.7.2012	4*x*	H9		
LPS117-6	5.54	3.31	31.53	4.06	5.691	6.11.2014	4*x*			
LPS117-7	5.85	2.8	32.07	4.08	5.482	6.11.2014	4*x*			
LPS118-1	5.55	4.46	35.3	4.32	6.360	8.2.2011	4*x*	H1		
LPS118-2	5.2	2.57	30.29	4.84	5.825	31.7.2012	4*x*	H1		
LPS118-3	5.13	3.08	29.49	4.82	5.749	31.7.2012	4*x*	H32		
LPS118-4	5.13	1.91	28.1	3.53	5.478	31.7.2012	4*x*			
LPS118-5	5.16	2.52	31.12	3.5	6.031	31.7.2012	4*x*			
LPS119-1	5.06	2.55	29.67	3.49	5.864	21.8.2012	4*x*	H32		
LPS119-2	5.01	1.96	30.34	3.25	6.056	21.8.2012	4*x*	H32		
LPS119-3	4.98	3.51	30.33	3.54	6.090	21.8.2012	4*x*			
LPS119-4	5.12	1.95	31.81	3.44	6.213	21.8.2012	4*x*			
LPS119-7	5.35	3.9	34.25	5.25	6.402	8.2.2011	4*x*	H1		

Sample	Petunia Peak	CV (%)	Leucant. Peak	CV (%)	Leucant./ Petunia ratio	Date	Ploidy	Haplotype	*psbA-trnH*	*trnC-petN*
LPS120-1	5.29	4.24	32.2	4.45	6.087	8.2.2011	4*x*	H4		
LPS120-2	5.04	4.1	25.17	6.86	4.994	1.8.2012	4*x*	H31		
LPS120-3	6.09	3.09	28.95	4.82	4.754	1.8.2012	4*x*	H31		
LPS120-4	6.03	2.53	31.93	6.06	5.295	1.8.2012	4*x*			
LPS120-5	5.86	4.01	27.97	6.37	4.773	1.8.2012	4*x*			
LPS121-1	5.56	5.54	20.19	5.35	3.631	8.2.2011	2*x*	H1		
LPS121-9	5.71	2.74	18.78	2.75	3.289	6.11.2014	2*x*			
LPS121-10	5.46	2.84	17.19	3.26	3.148	6.11.2014	2*x*			
LPS121-4	6.23	1.91	21.04	3.34	3.377	1.8.2012	2*x*			
LPS121-5	6.32	2.59	19.83	4.71	3.138	1.8.2012	2*x*			
LPS122-1	6.63	3.96	35.28	4.88	5.321	8.8.2012	4*x*	H1		
LPS122-2	6.89	3.53	39.82	3.17	5.779	8.8.2012	4*x*	H1		
LPS122-9	6.81	2.77	40.28	2.55	5.915	8.8.2012	4*x*	H2		
LPS122-10	6.96	2.86	39.03	5.4	5.608	8.8.2012	4*x*			
LPS122-4	7.35	2.49	42.96	3.52	5.845	1.8.2012	4*x*			
LPS122-7	5.42	3.39	34.81	5.23	6.423	8.2.2011	4*x*			
LPS123-1	5.59	3.96	35.47	23.26	6.345	8.2.2011	4*x*	H2		
LPS123-2	5.78	3.42	36.02	3.38	6.232	7.8.2012	4*x*	H2		
LPS123-3	5.72	2.88	33.55	3.27	5.865	7.8.2012	4*x*	H2		
LPS123-4	5.81	3.45	37.74	3.46	6.496	7.8.2012	4*x*			
LPS123-5	5.45	2.93	34.68	2.58	6.363	7.8.2012	4*x*			
LPS124-1	5.45	4.31	35.62	2.84	6.536	8.2.2011	4*x*	H1		
LPS124-2	5.41	3.39	32.29	4.11	5.969	7.8.2012	4*x*	H2		
LPS124-3	5.66	2.21	34.3	3.2	6.060	7.8.2012	4*x*	H1		
LPS124-4	5.31	2.66	33.96	3.85	6.395	7.8.2012	4*x*			
LPS124-5	5.37	1.99	31.49	4.12	5.864	7.8.2012	4*x*			
LPS125-1	5.48	3.91	34.52	4.44	6.299	8.2.2011	4*x*	H1		
LPS125-2	5.59	2.81	34.3	3.17	6.136	7.8.2012	4*x*	H1		
LPS125-3	5.46	2.88	33.02	2.67	6.048	7.8.2012	4*x*	H1		
LPS125-4	5.46	2.86	32.9	4.12	6.026	7.8.2012	4*x*			
LPS125-5	5.52	3.47	32.85	4.15	5.951	7.8.2012	4*x*			
LPS126-1	5.42	4.56	35.87	3.73	6.618	8.2.2011	4*x*	H1		

Sample	Petunia Peak	CV (%)	Leucant. Peak	CV (%)	Leucant./ Petunia ratio	Date	Ploidy	Haplotype	*psbA-trnH*	*trnC-petN*
LPS126-7	5.66	4.19	34.73	8.56	6.136	6.11.2014	4*x*	H1		
LPS126-3	4.99	3.39	28.51	2.61	5.713	8.8.2012	4*x*			
LPS126-7	5.13	1.98	31.11	2.33	6.064	8.8.2012	4*x*			
LPS126-10	5.2	2.46	31.86	3.34	6.127	8.8.2012	4*x*			
LPS127-1	5.58	2.9	34.7	2.63	6.219	7.8.2012	4*x*	H1		
LPS127-2	5.45	2.81	32.16	2.83	5.901	7.8.2012	4*x*	H1		
LPS127-3	5.46	2.84	34.22	3.23	6.267	7.8.2012	4*x*			
LPS127-4	5.72	1.64	35.25	3.5	6.163	7.8.2012	4*x*	H1		
LPS128-1	5.3	4.39	33.21	5.26	6.266	8.2.2011	4*x*	H1		
LPS128-2	5.33	2.54	29.7	4.82	5.572	8.8.2012	4*x*	H1		
LPS128-3	5.72	2.85	33.52	3.25	5.860	8.8.2012	4*x*	H1		
LPS128-4	6.01	2.53	34.92	4.18	5.810	8.8.2012	4*x*			
LPS128-5	5.8	3.39	34.76	2.67	5.993	8.8.2012	4*x*			
LPS129-1	4.5	6.82	31.75	6.13	7.056	8.2.2011	4*x*	H32		
LPS129-2	6.23	7.93	37.78	3.43	6.064	8.8.2012	4*x*	H32		
LPS129-3	5.93	3.53	31.07	31.07	5.239	8.8.2012	4*x*	H32		
LPS129-4	6.02	2.53	32.45	3.53	5.390	8.8.2012	4*x*			
LPS129-5	5.87	3.98	34.2	3.17	5.826	8.8.2012	4*x*			
LPS169-1	5.38	1.93	30.01	2.93	5.578	14.8.2012	4*x*	H49		
LPS169-2	5.32	2.56	30.46	3.48	5.726	14.8.2012	4*x*	H49		
LPS169-3	5.54	2.23	30.72	2.93	5.545	14.8.2012	4*x*	H48		
LPS169-4	5.26	1.97	29.54	4.75	5.616	14.8.2012	4*x*			
LPS169-5	5.25	1.92	29.67	4.76	5.651	14.8.2012	4*x*			
LPS170-1	5.33	2.54	28.86	3.18	5.415	14.8.2012	4*x*	H48		
LPS170-2	5.39	1.92	26.55	5.19	4.926	14.8.2012	4*x*	H48		
LPS170-3	5.26	1.91	28.9	3.08	5.494	14.8.2012	4*x*			
LPS170-4	5.2	2.54	27.3	3.46	5.250	14.8.2012	4*x*			
LPS170-9	5.25	1.93	28.15	1.92	5.362	14.8.2012	4*x*	H48		
LPS171-10	5.68	2.17	30.62	4.03	5.391	14.8.2012	4*x*	H39		
LPS171-2	5.61	2.84	31.47	2.88	5.610	14.8.2012	4*x*			
LPS171-3	5.61	2.81	31.08	3.45	5.540	14.8.2012	4*x*			
LPS171-6	5.52	2.21	29.23	2.61	5.295	14.8.2012	4*x*	H42		

Sample	Petunia Peak	CV (%)	Leucant. Peak	CV (%)	Leucant./ Petunia ratio	Date	Ploidy	Haplotype	*psbA-trnH*	*trnC-petN*
LPS171-9	5.72	2.78	30.46	3.48	5.325	14.8.2012	4*x*	H39		
LPS172-1	5.43	3.34	27.84	4.08	5.127	14.8.2012	4*x*	H39		
LPS172-2	5.48	2.81	29.71	3.55	5.422	14.8.2012	4*x*	H41		
LPS172-3	5.64	2.23	29.83	3.39	5.289	14.8.2012	4*x*			
LPS172-4	5.41	3.33	30.47	3.49	5.632	14.8.2012	4*x*			
LPS172-5	5.46	2.83	30.32	3.53	5.553	14.8.2012	4*x*	H38		
LPS173-1	5.14	1.92	40.84	4.68	7.946	16.8.2012	6*x*	H38		
LPS173-2	5.19	2.53	39.34	2.5	7.580	16.8.2012	6*x*	H36		
LPS173-3	5.26	3.16	42.01	3.6	7.987	16.8.2012	6*x*			
LPS173-4	5.19	2.53	39.07	4.2	7.528	16.8.2012	6*x*			
LPS173-6	5.37	1.93	44.01	4.58	8.196	16.8.2012	6*x*	H36		
LPS174-1	5.21	2.47	40.77	3.18	7.825	16.8.2012	6*x*	H38		
LPS174-2	5.12	1.9	40.33	2.51	7.877	16.8.2012	6*x*	H38		
LPS174-3	5.25	1.74	41.26	2.56	7.859	16.8.2012	6*x*			
LPS174-4	5.14	1.86	40.34	3.83	7.848	16.8.2012	6*x*			
LPS174-5	5.06	2.46	40.32	2.5	7.968	16.8.2012	6*x*	H39		
LPS175-1	5.07	1.9	27.67	4.14	5.458	16.8.2012	4*x*	H37		
LPS175-2	5.13	1.9	27.82	2.48	5.423	16.8.2012	4*x*	H37		
LPS175-3	5.14	1.88	27.86	2.55	5.420	16.8.2012	4*x*	H37		
LPS175-4	5.08	2.48	27.59	4.16	5.431	16.8.2012	4*x*			
LPS175-5	5.14	1.9	28.12	3.21	5.471	16.8.2012	4*x*			
LPS176-1	5.13	1.89	28.85	3.11	5.624	16.8.2012	4*x*	H37		
LPS176-2	5.31	2.54	28.78	3.16	5.420	16.8.2012	4*x*			
LPS176-3	5.1	2.43	28.12	3.06	5.514	16.8.2012	4*x*	H37		
LPS176-4	5.2	2.54	28.84	3.24	5.546	16.8.2012	4*x*			
LPS176-7	5.32	2.51	29.22	2.6	5.492	16.8.2012	4*x*	H37		
LPS177-1	4.57	3.45	24.58	4.07	5.379	21.8.2012	4*x*	H40		
LPS177-2	5.13	3.22	28	4.82	5.458	21.8.2012	4*x*	H36		
LPS177-3	5.26	3.07	28.21	3.11	5.363	21.8.2012	4*x*			
LPS177-4	5.31	2.55	28.19	3.29	5.309	21.8.2012	4*x*			
LPS177-6	5.13	3.16	27.38	3.53	5.337	21.8.2012	4*x*	H36		
LPS178-1	5.2	2.52	28.73	3.16	5.525	21.8.2012	4*x*	H36		

Sample	Petunia Peak	CV (%)	Leucant. Peak	CV (%)	Leucant./ Petunia ratio	Date	Ploidy	Haplotype	*psbA-trnH*	*trnC-petN*
LPS178-2	5.06	2.5	25.32	2.84	5.004	21.8.2012	4*x*	H36		
LPS178-3	4.88	3.31	23.99	2.58	4.916	21.8.2012	4*x*			
LPS178-4	4.67	3.48	23.19	3.58	4.966	21.8.2012	4*x*			
LPS178-10	5.59	2.86	30.7	4.05	5.492	21.8.2012	4*x*	H36		
LPS179-1	5.53	3.41	29.66	3.56	5.363	21.8.2012	4*x*	H43		
LPS179-2	5.6	2.77	30.09	4	5.373	21.8.2012	4*x*	H43		
LPS179-3	5.59	2.82	29.59	3.65	5.293	21.8.2012	4*x*	H43		
LPS179-4	5.54	3.36	31.35	2.77	5.659	21.8.2012	4*x*			
LPS179-5	5.53	3.4	28.9	3.15	5.226	21.8.2012	4*x*			
LPS179-6	5.31	2.54	29.2	2.58	5.499	31.8.2012	4*x*			
LPS179-7	5.31	2.56	26.77	3.56	5.041	31.8.2012	4*x*			
LPS179-8	5.06	2.53	25.56	4.57	5.051	31.8.2012	4*x*			
LPS179-9	5.07	2.53	27.35	3.39	5.394	31.8.2012	4*x*			
LPS179-10	5.09	2.44	27.83	2.57	5.468	31.8.2012	4*x*			
LPS179-11	4.93	3.87	25.85	4.06	5.243	31.8.2012	4*x*			
LPS179-12	5.25	3.11	29.19	2.59	5.560	31.8.2012	4*x*			
LPS179-13	5.2	2.54	28.53	2.54	5.487	31.8.2012	4*x*			
LPS180-1	5.32	2.58	29.23	2.47	5.494	21.8.2012	4*x*	H43		
LPS180-2	5.18	2.56	28.84	3.17	5.568	21.8.2012	4*x*	H43		
LPS180-3	4.92	2.92	27.2	3.99	5.528	21.8.2012	4*x*	H43		
LPS180-4	5	3.45	27.38	3.49	5.476	21.8.2012	4*x*			
LPS180-5	4.99	3.47	27.7	4.08	5.551	21.8.2012	4*x*			
LPS181-1	5.2	2.59	16.78	3.14	3.227	23.8.2012	2*x*	H46		
LPS181-2	5.46	2.88	17.48	4.16	3.201	23.8.2012	2*x*	H45		
LPS181-3	5.4	3.56	17.7	4.65	3.278	23.8.2012	2*x*	H46	KM589776	KM589793
LPS181-4	5.41	3.54	17.22	3.22	3.183	23.8.2012	2*x*			
LPS181-5	5.15	3.2	16.59	2.6	3.221	23.8.2012	2*x*			
LPS182-1	4.98	3.45	15.44	4.18	3.100	23.8.2012	2*x*	H17		
LPS182-2	5.24	3.19	17.02	2.57	3.248	23.8.2012	2*x*	H36		
LPS182-3	5.07	2.56	16.58	2.58	3.270	23.8.2012	2*x*	H18		
LPS182-4	5.26	3.21	16.84	3.24	3.202	23.8.2012	2*x*			
LPS182-5	5	3.57	16.11	4.18	3.222	23.8.2012	2*x*			

Sample	Petunia Peak	CV (%)	Leucant. Peak	CV (%)	Leucant./ Petunia ratio	Date	Ploidy	Haplotype	*psbA-trnH*	*trnC-petN*
LPS183-1	5.07	2.6	28.49	2.58	5.619	23.8.2012	4*x*	H1		
LPS183-2	4.99	3.54	27.35	3.5	5.481	23.8.2012	4*x*			
LPS183-3	4.87	3.51	27.37	3.58	5.620	23.8.2012	4*x*			
LPS183-6	4.82	2.92	27.07	2.9	5.616	23.8.2012	4*x*	H1		
LPS183-7	4.93	2.97	27.53	2.02	5.584	23.8.2012	4*x*	H1		
LPS190-1	5.47	2.87	18.95	3.39	3.464	23.8.2012	2*x*	H44		
LPS190-2	5.53	2.22	17.6	3.67	3.183	23.8.2012	2*x*	H44		
LPS190-3	5.26	2.04	16.96	2.64	3.224	23.8.2012	2*x*	H44		
LPS190-4	5.59	2.92	18.49	3.43	3.308	23.8.2012	2*x*			
LPS190-5	5.59	2.88	18.09	3.52	3.236	23.8.2012	2*x*			